Theses and Dissertations | 1. Thesis and Dissertation Collection, all items

1972-03

Holographic interferometry of the flow field between a fin and flat plate.

Heyer, Robert Ward.

Monterey, California. Naval Postgraduate School

HOLOGRAPHIC INTERFEROMETRY OF THE FLOW FIELD BETWEEN A FIN AND FLAT PLATE

Robert Ward Heyer

NAVAL POSTGRADUATE SCHOOL
Monterey, California
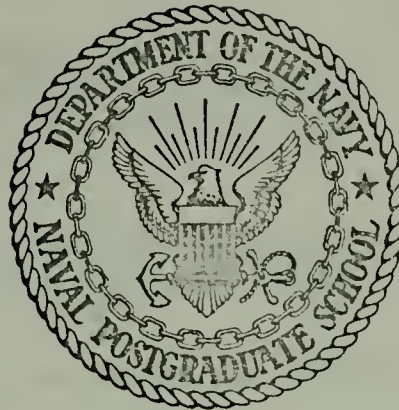
THESIS

Holographic Interferometry of The Flow

Field Between a Fin And Flat Plate

by

Robert Ward Heyer

Thesis Advisor: D. G. Collins

March 1972

Holographic Interferometry of The Flow

Field Between a Fin And Flat Plate

by

Robert Ward Heyer
Lieutenant, United States Navy
B.S.E.E., Duke University, 1964

Submitted in partial fulfillment of the
requirements for the degree of

MASTER OF SCIENCE IN AERONAUTICAL ENGINEERING


from the

NAVAL POSTGRADUATE SCHOOL
March 1972

ABSTRACT

This study was an attempt to map the density field in a fin-flat plate junction three-dimensionally using holographic interferometry. This investigation has extended the density studies by Matulka [12, 13] and Jagota [3, 4] to include, for the first time, interferometric fringe information obtained through a transparent model in supersonic flow. The fringe information was then inverted by a FORTRAN computer program to produce a plot of the density field around the model. The feasibility of the method was demonstrated.

The factors which are thought to have limited the success of the experiment include vibration of the model, fluctuations of the tunnel flow and the fact that the model was somewhat too large in relation to the size of the wind tunnel test section. Schlieren photography was used to look through and around the model and to verify that the same flow was established as was reported by Thomas [23, 24] and Winkelman [26, 27].

The data reduction of holographic interferograms was, for the first time, accomplished using photographic enlargements. This technique is considered to be much easier and more accurate than the one used in the previous investigations. However, the data reduction step, because of the time and labor involved, is considered to be the rate controlling process of the whole analysis.

TABLE OF CONTENTS

ACKNOWLEDGEMENTS

I. INTRODUCTION

The determination of the flow field in the wing-body junction of an aircraft in supersonic flight presents many problems. The typical approach has been to measure the static pressure on the surface using many small pressure taps [23, 24] and to determine the velocity field in the junction using translatable pressure probes [18, 19, 25]. Thomas [23, 24] and Winkelmann [26, 27] used azobenzene and oil-smear tests to view the flow field around a flat plate-fin junction. From the streak patterns on the plate and fin, they were able to illustrate the three-dimensional flow field, although in a partially speculative fashion. This study has attempted to map the density field in a fin-flat plate junction three-dimensionally using holographic interferometry. Although this objective was not fully achieved, the feasibility of the method has been demonstrated.

By using a Q-switched laser with exposure times of about twenty nano-seconds, it was possible to obtain three-dimensional holographic inter-ferograms of the density field in the fin-flat plate junction. From holograms taken at a number of viewing angles the fringe shifts in different planes could be obtained. By integrating this information using a FORTRAN computer program, the density field can be determined. This technique has been previously demonstrated for the flow field of a free jet by Matulka [12, 13] and for the supersonic flow field around a cone at angle of attack by Jagota [3, 4] .

The tests were performed at the Naval Postgraduate School, using the four-inch supersonic wind tunnel.

II. EXPERIMENTAL APPARATUS

A. THE WIND TUNNEL

The investigation was conducted in the Naval Postgraduate School
blowdown-to-atmosphere supersonic wind tunnel. The test section is
four inches by four inches in cross section and six inches long with
two different sets of side walls. The two-inch thick plexiglas side
walls, which have a refraction index of 1.49, present a complete field
of view of the flow from the nozzle throat to aft of the test section
mounting bracket (Figure 1 (a)). The second set of sidewalls used are
aluminum with high quality optical glass portholes located in the test
section area (Figure 1 (b)). The interchangeable nozzle for a test
section Mach number of 2.8 was used for all tests. The nominal run
time is five minutes at Mach 2.8 with the maximum stagnation pressure
of about 105 pounds per square inch.

B. THE HOLOGRAPHIC ARRANGEMENT

The holographic arrangement is illustrated in Figure 2 and shown in
photographs included as Figures 3, 4, and 5. The equipment stand was
rested on a portion of the building floor that was vibrationally isolated.
A Konrad K-1 pulsed ruby laser with a Pockels cell Q-switching unit was
used to produce monochromatic light at a wave length of 6943 Angstroms
and exposure time of twenty nano-seconds. The laser cavity length was
seventy-three cm. giving a coherence length of about ten cm. To main-
tain the laser head and output etalon at a constant temperature of 27.5
degrees centigrade, a Lauda constant temperature circulator Model N was
used. This was controlled by an electronic relay type R-10 coupled with
a Culligan de-ionizer.

Holograms were obtained by routing the reference beam under the wind tunnel and the scene beam through the test section, and intersecting the two beams on the hologram plate at an intersecting angle of approximately 50 degrees. The beam sizes were controlled by translating the concave lenses located between the beam splitter and hologram plate in each beam (Figure 2). The Q-switched laser and optics were aligned using a continuous wave helium-neon laser. For reference purposes, grids were mounted on the outside tunnel walls and aligned using a surveyor's transit. The holographic stand and test section were completely enclosed in a wooden box to enable holograms to be taken in the daylight (Figure 6).

C. THE WIND TUNNEL MODELS

The fin-flat plate models used are shown in Figures 7 (a), (b), (c), and (d). The metal portions of both models were stainless steel. The center section, part of one strake, and all of the other strake of the first model in Figure 7 (a) were made of epoxy while the center section of the second model, Figures 7 (b) and 7 (c), was fabricated from plexiglas. The flat plate grids in both models were etched into the plastic surface and coated with a clear plastic to achieve a smooth surface.

The models were rotated about their sting mounts as shown in Figure 7 (d). Alignment for the desired rotation angle was accomplished by aligning prescribed lines on the sting mount collar with a scribed mark on the sting stand using a surveyor's transit.

III. ANALYTICAL EVALUATION OF THE DENSITY FIELD

A. THE BASIC INTERFEROMETRIC EQUATION

Interferograms are created when two coherent light beams are super-imposed on each other and projected on a viewing screen. The light and dark regions observed correspond to the relative phase difference between the two beams which are caused by a difference in the two optical path lengths. Consider a coherent beam which is split and then recombined on a viewing screen. A difference in optical path lengths of the two beams may be achieved in two ways in order to create an interferogram. The first is to make the physical distance traveled by the two beams different. In a vacuum this path length difference is expressed as $L = c_o \Delta t$ where c_o is the speed of light in a vacuum. The second way is to maintain equal physical path lengths but to have the beams traverse through different media prior to recombining. In this case each light beam will travel at a speed $\frac{c_o}{n}$ where n is the index of refraction for the medium traversed. The optical path length difference then becomes:

$$\Delta L = L (n_2 - n_1) = c_o \Delta t \tag{1}$$

The interference pattern or fringes observed may be expressed as a function of the optical path length difference or

$$g = \frac{\Delta L}{\lambda} \tag{2}$$

where: g = fringe shift

λ = wave length of the light source

ΔL = change in optical path

9

Combining equations (1) and (2), the fringe shift is then

$$g = \frac{L}{\lambda} (n_2 - n_1) \tag{3}$$

The index of refraction is known to be a function of density. Since the speed of light is only slightly less in gases than in a vacuum, the index of refraction could be closely approximated by the series expansion [8]

$$n = 1 + \beta \frac{\rho}{\rho_s} \tag{4}$$

where

β = dimensionless constant related to the Gladstone-Dale

constant by $K = \beta / \rho_s$

ρ_s = reference density of 0° C, 760 mm. Hg.

The variation of with wavelength is small and has a value of 0.000292 for λ = 5893 angstroms.

Considering a fixed difference in the index of refraction between the two beams in Equation (3), then

$$g = \beta \frac{L}{\lambda} \left(\frac{\rho_2 - \rho_\infty}{\rho_s} \right) \tag{5}$$

If the density varies in a beam path, the net change in the optical path length will be the integrated effect along the beam path or

$$g = \frac{\beta}{\lambda \rho_s} \int_o^L (\rho - \rho_\infty) ds = Q \int_o^L f(x,y,z_c) ds \tag{6}$$

where

$$Q = \frac{\beta \rho_\infty}{\lambda \rho_s} \tag{6a}$$

10

$$f(x,y,z_c) = \frac{\rho(x,y\,z_c)}{\rho\infty} - 1 \tag{6b}$$

z_c = a plane of constant Z

ds = incremental distance along the ray

In order to determine the density along the beam path where the fringe shift is known from an interferogram, Equation (6) must be inverted.

B. THE INTEGRAL INVERSION

The integral inversion technique was first reported by C. D. Maldonado et al in 1965 [9, 10, 11]. R.D. Matulka [12, 13] and R. C. Jagota [3, 4] used this method to determine the density variation in an asymmetric free jet and about a cone at angle of attack, respectively. The technique involves representing the function, $f(x,y,z_c)$ in Equation (6) by a complete set of orthogonal functions where the unknown coefficients are evaluated using the orthogonality relationship between the set of functions. The functions are orthogonal over the entire plane and also have the propery of being invariant in form to any rotation of the coordinate system. Figure 8 illustrates the coordinate system for the inversion where x and y are the fixed laboratory coordinates and x' and y' are the coordinates in which the fringe number function is defined. As the view through the test section is varied the primed coordinates are rotated with respect to the fixed coordinates x and y.

The fringe shift expressed in Equation (6) may be written as the transform

$$g(\xi, y, z_c) = f(x,y,z_c) \tag{7}$$

or, inverting the equation, the density function, f, is equal to:

$$f(x, y, z_c) = T^{-1} g(\xi, y, z_c) \tag{8}$$

The density function can be expanded in the following manner using a set of polynomial functions, $U_{m+2k}^{\pm m} (\alpha x, \alpha y)$, and unknown comples coefficients, $C_{m+2k}^{\pm m} (\alpha)$

$$f(x, y, z_c) = \sum_{m=0}^{\infty} \sum_{k=0}^{\infty} \epsilon_m \left[C_{m+2k}^{m}(\alpha) U_{m+2k}^{m}(\alpha x, \alpha y) + C_{m+2k}^{-m}(\alpha) U_{m+2k}^{-m}(\alpha x, \alpha y) \right] \cdot e^{-(\alpha^2 x^2 + \alpha^2 y^2)} \tag{9}$$

where
$$\epsilon_m = \begin{cases} \frac{1}{2} & m = 0 \\ 1 & m = 1, 2, 3, \cdots \end{cases}$$

$$\alpha = \text{arbitrary scale factor}$$

The polynomial functions, $U_{m+2k}^{\pm m} (\alpha x, \alpha y)$, are invariant in form to a rotation of the coordinate system [10, 12, 13]. They also have a Gauss transform which makes them adaptable to the physical situation and to manipulating into the form of Equation (7). The functions are defined as:

$$U_{m+2k}^{\pm m}(\alpha x, \alpha y) = (-1)^k \alpha \left[\frac{k! (\alpha^2 x^2 + \alpha^2 y^2)^m}{\pi (m+k)!} \right]^{\frac{1}{2}} e^{\pm i m \phi} L_k^m (\alpha^2 x^2 + \alpha^2 y^2) \tag{10}$$

where
$$\phi = \tan^{-1}\left(\frac{y}{x}\right) - \frac{\pi}{2} \tag{10a}$$

$$L_k^m = \text{Laguerre polynomial}$$

$$= \sum_{s=0}^{k} \left[\frac{(m+k)!}{(k-s)!(m-s)! s!} \right] \left[(-1)(\alpha^2 x^2 + \alpha^2 y^2) \right]^s \tag{10b}$$

And the Gauss Transform of $U_{m+2k}^{\pm m}$ is:

$$I_{m+2k}^{\pm m}(\alpha y; \xi) = \int_{-\infty}^{\infty} U_{m+2k}^{\pm m}(\alpha x, \alpha y) e^{-\alpha^2 x'^2} dx' = \frac{e^{\pm i m \xi} H_{m+2k}(\alpha y')}{[k! (m+k)!]^{\frac{1}{2}} 2^{m+2k}} \tag{11}$$

where
$$H_{m+2k}(\alpha y') = \text{Hermite polynomials}$$

By applying the transform above to Equation (9), the fringe function in

Equation (7) can be written as:

$$g(\xi, y, z_c) = \sum_{m=0}^{\infty} \sum_{k=0}^{\infty} \frac{\epsilon_m \left[C_{m+2k}^m(\alpha) e^{im\xi} + C_{m+2k}^{-m}(\alpha) e^{-im\xi} \right] H_{m+2k}(\alpha) e^{-\alpha^2 y'^2}}{\left[k!(m+k)! \, 2^{2(m+k)} \right]^{1/2}} \qquad (12)$$

using the following orthogonality relationship on Equation (12)

$$\int_{-\pi}^{\pi} e^{\pm im\xi} e^{\mp in\xi} d\xi \int_{-\infty}^{\infty} H_{m+2k}(\alpha y') H_{n+2\ell}(\alpha y') e^{-\alpha^2 y^2} dy' =$$

$$\frac{2\pi^{3/2}}{\alpha} \left[(m+2k)!(n+2\ell)! \, 2^{m+2k} 2^{n+2\ell} \, \delta_{mn} \delta_{(m+2k)(n+2\ell)} \right] \qquad (13)$$

where δ is the kroneker delta, the expansion coefficients $C_{m+2k}^{\pm m}$, can be determined by:

$$C_{m+2k}^{\pm m}(\alpha) = \frac{\alpha}{2\pi^{3/2}} \left[\frac{(k!(m+k)!)^{1/2}}{(m+2k)!} \right] \int_{-\pi}^{\pi} g(y', \xi, z_c) H_{m+2k}(\alpha y') e^{\mp im\xi} dy' d\xi \qquad (14)$$

Substitution of the coefficients in Equation (14) bact into Equation (9) results in the density variation being expressed as:

$$f(x, y, z_c) = \left(\frac{\alpha}{\pi}\right)^2 \sum_{m=0}^{\infty} \sum_{k=0}^{\infty} \epsilon_m \left[k!(m+k)! \right]^{1/2} e^{-(\alpha^2 x^2 + \alpha^2 y^2)} \cdot$$

$$\text{REAL} \left[\int_{-\pi}^{\pi} \int_{-\infty}^{\infty} g(y', \xi, z_c) e^{-im\xi} H_{m+2k}(\alpha y') dy' d\xi \right] U_{m+2k}^m(\alpha x, \alpha y) \qquad (15)$$

or by inserting Equation (10):

$$f(x, y, z_c) = \left(\frac{\alpha}{\pi}\right)^2 \sum_{m=0}^{\infty} \sum_{k=0}^{\infty} \epsilon_m \frac{(-1)^k k!}{(m+2k)!} (\alpha^2 x^2 + \alpha^2 y^2)^{m/2} L_k^m (\alpha^2 x^2 + \alpha^2 y^2) \cdot$$

$$\left[B_{m+2k}^m(\alpha) \cos(m\phi) + D_{m+2k}^m(\alpha) \sin(m\phi) \right] e^{-(\alpha^2 x^2 + \alpha^2 y^2)} \qquad (16)$$

where:

$$B_{m+2k}^m(\alpha) = \int_{-\pi}^{\pi} \int_{-\infty}^{\infty} g(y', \xi, z_c) \cos(m\xi) H_{m+2k}(\alpha y') dy' d\xi \qquad (17)$$

$$D_{m+2k}^m(\alpha) = \int_{-\pi}^{\pi} \int_{-\infty}^{\infty} g(y', \xi, z_c) \sin(m\xi) H_{m+2k}(\alpha y') dy' d\xi \qquad (18)$$

13

Equations (16), (17), and (18) are the basic equations used to calculate the density distribution from the experimentally determined fringe variations.

C. THE NUMERICAL PROCEDURE

The form of the density distribution in Equations (16), (17), and (18) must be modified in order to input the experimentally determined fringe distribution. First from Figure 8 and Equation (6b) it can be seen that it is only necessary to integrate Equations (17) and (18) over an area where the density is changing from a known density, ρ_∞ . Outside of this region where there is no change in density, the function $f(x,y,z_0) = 0$, i.e. outside the test section. Also since the fringe distribution is taken in small increments over the test area the coefficients, B and D, can be approximated as

$$B^m_{m+2k}(\alpha) = \sum_{i=1}^{I-1} \sum_{j=0}^{J-1} g(\xi_j + \Delta \xi_j, x_i + \Delta x_i) \int_{\xi_j}^{\xi_{j+1}} \cos(m\xi)\,d\xi \int_{x_i}^{x_{i+1}} H_{m+2k}(\alpha x)\,dx \quad (19)$$

$$D^m_{m+2k}(\alpha) = \sum_{i=1}^{I-1} \sum_{j=0}^{J-1} g(\xi_j + \Delta\xi_j, x_i + \Delta x_i) \int_{\xi_j}^{\xi_{j+1}} \sin(m\xi)\,d\xi \int_{x_i}^{x_{i+1}} H_{m+2k}(\alpha x)\,dx \quad (20)$$

The integral of ξ is easily determined and by using the derivative formula for Hermite polynomials the integral of x may be manipulated to yield

$$B^m_{m+2k}(\alpha) = \left[\frac{1}{2\alpha m}\frac{1}{(m+2k+1)}\right] \sum_{i=0}^{I-1} \sum_{j=0}^{J-1} g(\xi_j + \Delta\xi_j, x_i + \Delta x_i) \cdot$$

$$\left[\sin(m\xi_{j+1}) - \sin(m\xi_j)\right]\left[H_{m+2k+1}(\alpha x_{i+1}) - H_{m+2k+1}(\alpha x_i)\right] \quad (21)$$

$$D^m_{m+2k}(\alpha) = -\left[\frac{1}{2\alpha m(m+2k+1)}\right] \sum_{i=0}^{I-1} \sum_{j=0}^{J-1} g(\xi_j + \Delta\xi_j, x_i + \Delta x_i) \cdot \quad (22)$$

$$\left[\cos(m\xi_{j+1}) - \cos(m\xi_j)\right]\left[H_{m+2k+1}(\alpha x_{i+1}) - H_{m+2k+1}(\alpha x_i)\right]$$

In the computation of the density function from Equation (16), obtaining the infinite summations experimentally is not plausible or

possible. It has been demonstrated that by using a finite number of terms and by adjusting the values of $\Delta \xi$, Δx and α, it is possible to obtain the density distribution with very good accuracy [3, 4, 12, 13]. Equation (16) then becomes:

$$\rho(x,y,z_c) = \left(\frac{\alpha}{\pi}\right)^2 \sum_{k=0}^{K} \sum_{m=0}^{M} \epsilon_m (-1)^k \left[\frac{k!}{(m+2k)!}\right] (\alpha^2 x^2 + \alpha^2 y^2) \cdot$$

$$L_k^m (\alpha^2 x^2 + \alpha^2 y^2) \left[B_{m+2k}^m (\alpha) \cos(m\phi) + D_{m+2k}^m (\alpha) \sin(m\phi)\right] \cdot$$

$$e^{-(\alpha^2 x^2 + \alpha^2 y^2)}$$

(23)

IV. EXPERIMENTAL PROCEDURE

A. LABORATORY TECHNIQUES

The analysis of a free jet by Matulka [12, 13] illustrated how holographic interferometry can be used to obtain a complete three dimensional plot of the density within a moving transparent flow field. Jagota [3, 4] in his study of a cone at angle of attack in supersonic flow went one step further by introducing an opaque object into an assumed steady state flow field and describing the density field three-dimensionally.

This investigation has attempted to determine the three-dimensional density field around a transparent object in a supersonic flow field by passing a light beam through the object. Specifically the interest was to describe the flow field existing in the junction of a fin-root inter-section.

1. Model Considerations

In order to obtain uniform flow around the fin-root area, a model of the form shown in Figure 9 was selected. The flat plate has a knife

edge and is intended to remain at zero degrees angle of attack so as
to establish the flow conditions illustrated. The fin edges were made
circular in order to approach flow conditions similar to those estab-
lished in Winkelmann's [26, 27] investigation. Plastic and metal strakes
were added on the model sides so as to maintain two-dimensional flow as
well as to add strength to the flat plate. In the first model constructed
(Figure 7(a)), maximum visibility of the plastic fin-flat plate center
section was achieved by bolting the leading edge and aft plate together
through the plastic center section. Due to model flexure, this design
was found to be unsuitable and the second model in Figures 7(b) and 7(c)
was constructed. The model was made from a single piece of stainless
steel. The model rigidity was satisfactory but unfortunately the strength-
ening borders around the plastic center section reduced the holographic
visibility somewhat.

Since the wind tunnel blocks were fixed, it was possible to make
multiple test runs with the same flow conditions over the model provided
supersonic flow had been established over the model.

2. Holographic Techniques

In order to obtain holographic interferograms it was necessary to
ensure that the optical path lengths of the scene and reference beams
remained approximately equal. Since the ruby laser is believed to have
a coherency length of approximately ten centimeters, the equality of
lengths is far less critical than in the classical Mach-Zehner inter-
ferometric approach. Consequently a string was used in the experiment
to trace the reference beam and then adjust the scene beam. This method
kept the two beam lengths within one centimeter of each other. Since the
scene beam traversed approximately 4.5 inches of plastic tunnel walls and

16

grids which the reference beam did not, it was necessary to compensate by making the scene beam physically 2.25 inches shorter than the reference beam. The reference beam varied in length from 61 inches to 68 inches during the experimentation.

To determine the fringe/density field, finite fringe interferograms were made by three different techniques. In the direct fin-root flow approach the diffuser plate was part of the model. Either the mirror, M_5, in Figure 2 or the hologram plate holder was translated between the no-flow exposure and the flow-established exposure. In the total model flow method the diffuser plate was located between scene beam lens, L_3, and the test section (See Figure 2) and it was translated horizontally or vertically. Translations were varied from .001 inches to .006 inches with the translation distance of .003 inches yielding the best fringe separation.

Most of the holograms taken using basically the holographic arrangement shown in Figure 2 gave well-defined fringe patterns. In order to improve upon the fringe definition, a variety of techniques was attempted. The transverse mode selector was varied from 1.0 mm. to 2.5 mm. in increments of 0.5 mm. to determine the best lighting of the model. The hologram plate holder was rotated horizontally to various positions. These positions varied between being perpendicular to the scene beam to being perpendicular to the bisection of the angle between the scene and reference beams. Polarization plates were added in both the scene and reference beams between the test section and hologram plate in the scene beam and between the last mirror, M_4, and the hologram plate in the reference beam. A one-quarter wave plate was also placed between the first lens, L_1, and the beam splitter as recommended by Okayama and Emori [14].

17

The holograms were taken using 4" x 5" Agfa-Gavaert 8E-75 holo-
gram plates. The developing process involved:

1. Five minutes in Kodak D-19 developer

2. Thirty seconds in an acetic acid stop bath

3. Five minutes in standard fixer

4. Five minutes in a flowing water bath

5. One minute emersion in Kodak Photo Flo wetting agent

6. Drying using blowing cool air

a. Direct Fin-Root Flow Method

Since the flow field in the fin-root junction is assumed to
be identical on either side of the fin, then it is only necessary to
determine the density on one side of the fin. To accomplish this it is
necessary to obtain holograms for 180° of view as shown in Figure 10.
The holograms for the views from 0° to 90° can be obtained by using a
frosted fin and flat plate as shown in Figure 11. The advantage of
having the frosted plate as part of the model is that the fringe/density
information obtained by the interferogram is believed to be only for the
area between the fin-root intersection to the tunnel wall vice the whole
test section, but this was not verified. In order to obtain the fringe
information for angles greater than 90° but less than 180° the fin
would be exchanged for one containing a stainless steel reflective sur-
face. The scene beam would then enter the test area from the viewing
port below the tunnel and be reflected to the hologram plate as shown
in Figure 12.

b. Total Model Flow Method

In this method the diffuser plate was located in the scene
beam outside the test section as shown in Figure 14 and the flat plate

center section and fin were made of optically clear plexiglas. By translating the diffuser plate between exposures of the hologram, an interferogram of the whole density field in the test section about the model was obtained. From Figure 13 it can be seen that due to symmetry only 90° of view was required to obtain the density field. This makes it much easier experimentally to take the holograms than the previous method described.

3. Schlieren Analysis

A standard Schlieren knife-edge system was used to verify the establishment of the supersonic flow network around the model as shown in Figure 9. Photographs were also taken of the flow with the model at 0° and 90° rotation in order to compare the fin shock conditions with those obtained by Winkelmann [26, 27].

B. PHOTOGRAPHIC TECHNIQUES

By illuminating the holograms with a helium-neon laser beam which has a wave length of 6328 Angstroms, the original scene was reconstructed. Since the original scene beam and the reconstructed beam were of different wave lengths, there is actually a small distortion in the reconstructed scene but of neglectable effect because the hologram plate emulsion in the development process also shrinks.

The typical method for reconstructing the scene is to illuminate the hologram as illustrated in Figure 15. The diffuse glass used in the construction of the hologram appears to act as an infinite light source of non-parallel rays which illuminates the scene. If a small aperture is positioned at the focal plane of the imaging lense, an almost parallel set of rays may then be selected as shown in Figure 16. A third method

illustrated in Figure 17 uses a small diameter conjugate beam to illuminate the hologram. A large depth of field is achieved because the narrow beam acts as an aperture. This effect was of considerable advantage since it enabled both the front and rear grids, the model, and the fringe patterns to be simultaneously projected on the screen. The best photographs were obtained by focusing on the plane of the fringes.

C. DATA REDUCTION

Photographic interferograms were obtained by illuminating the hologram scene with a thin laser beam and using a camera with a viewing screen located in the film plane as shown in Figure 15. The line of sight in the plane desired was achieved by translating the hologram until common points on the front and rear grids were aligned. The camera, with the aperture set wide open at 7.7, was then adjusted to give the best focus on the fringe plane. The best photographic results were achieved by using an exposure time of 1/10 second with Polaroid Type 55 P/N film.

It was felt that the density field could be well defined three-dimensionally along the fin if the density fields were determined in four planes perpendicular to the Z-axis and equally spaced along the fin as shown in Figure 18. In obtaining the fringe data across a constant Z-plane it would be necessary to take six photographs per rotation angle, aligned at appropriate intervals down the y' axis, and then graphically mate the fringe data to form one complete set. The six photos across the field were felt necessary because the optical path length from the model to the hologram plate varied for those points not on the aligned plane.

The fringe shift reduction was accomplished using two different techniques. The first was to project the negative, using a photo enlarger,

onto a sheet of paper and trace out the fringe pattern, model surfaces and grid lines. The light fringes were traced out since it was much easier to judge their center line. From the fringe lines forward of the fin in the region of uniform flow one fringe line which appeared the straightest and compatible with most others was selected as the bench mark. A straight line was then drawn over that fringe and extended past the aligned Z plane (i.e. y' axis). Lines parallel to the bench mark line were then drawn likewise over the remaining fringe lines. The fringe displacements were then read relative to the lines drawn at the points of intersection of the fringes with the y' axis. The radius of the inversion circle was selected so that the fin-root intersection was the origin and the fin tip was the 100 percent point.

In the second technique an enlarged positive photograph was made from the negative. Again one fringe line in the uniform flow region just forward of the fin which appeared to be parallel with the majority of the fringes was selected as the bench mark. The remaining fringes were likewise traced over with lines parallel to the first. The fringe displacements were then measured relative to the lines drawn. For further details see Appendix A.

The locations at which reference lines crossed the y' axis in both techniques above were further adjusted to account for the tunnel wall refraction displacement as shown in Figure 19 and computed by a computer program in Appendix B. Once these corrections were made, the radial variation of the fringe number could then be plotted for the various y' alignment planes and a smooth curve drawn through the data points. The fringe number at 201 equidistant points across the field can then be obtained for input into the computer program, HOLOFER, in MODE 3. For

further details on how to use the computer program, HOLOFER, see Appen-
dix C. Once the data from all the rotation angles of the model have
been put into the computer program, the program will then calculate the
density field across the inversion circle for that Z-plane. After the
density has been calculated for all four Z-planes in Figure 18, a three-
dimensional plot of the density field can be made by connecting points
of equal density across the fin.

V. EXPERIMENTAL RESULTS AND DISCUSSION

The initial attempts to establish uniform flow over the flat plate
shown in Figure 7(a) were unsuccessful due to model vibration and flexure.
Movement of the model sting within its holder and flexure of the model
plastic center section allowed the model leading edge to establish a lit-
tle over 1° angle of attack upward when flow was established. Due to
various modifications made in attempts to eliminate the vibration, the
sting finally fractured.

In an attempt to eliminate these problems, the second model shown in
Figures 7(b) and 7(c) was made of a single piece of stainless steel and
the sting was mated to its holder to within .001 inches. The model center
section was made of poured epoxy and the strakes were both made of stain-
less steel with plexiglas inserts. The model rotation about the sting
was reduced to approximately 0.3° angle of attack upward. Due to the
vibration in passing through the transonic range and a weak glue seal
between the metal strakes and plexiglas inserts, the inserts were found
to break loose. They were subsequently removed and not replaced.

In order to determine the flow field using the direct fin-root approach,
the epoxy fin and model center section were frosted on one side using fine

emery paper (see Figure 20). Holograms were taken of the model at rotation angles of 0°, 12°, 45° and 90° using the holographic arrangement in Figure 2 excluding the diffuser plate between lens, L_3, and the test section. The mirror, M_5, was translated in various directions from towards to parallel to the test section between the exposures without flow and with flow established. Fringe patterns were obtained around the model, but only at 0° and 12° rotation could any fringe patterns be observed across the fin. It was found that the fin fringe pattern appeared to remain almost unchanged no matter how or how much the mirror, M_5, was translated while the fringe around the model changed appropriately. For instance, in Figure 21 the mirror was not translated and in Figure 22 the mirror was translated .006 inches horizontally parallel to the tunnel.

Since fringes could not be observed across the flat plate at 45° and 90°, it was felt that the epoxy center section might be too imperfect optically. Consequently double-exposed holograms were taken with no flow through the test section and various translation distances from 0 to .005 inches. The fringe patterns were excellent across the whole model and their spacing decreased according to the increase in the translation of M_5. Next the diffuser plate in the scene beam in Figure 2 was inserted with the model at 0° rotation angle and translated between no flow and flow exposures of the hologram. The fringes about the model were of excellent quality but the double diffusion of the scene beam through the model caused all fringe patterns on the model (fin) to disappear.

It was felt at this point that the fringe pattern obtained across the fin was caused by the movement of the model to an angle of attack and possibly by model vibration, although none was observed visually. The

lack of any fringes across the flat plate center section is not well understood but is believed to be caused by vibration of the model.

Since it was not possible to obtain acceptable interferograms with the diffuser plate as part of the model due to model motion, it was felt that the effect of minor model movements could be eliminated by using an optically clear model and an external translating diffuser plate. Therefore the fin and model center sections were replaced with optically clear plexiglas. With these changes it was found that the flat-plate leading-edge angle of attack had been reduced to approximately 0.1°.

Initially double-exposure holograms were taken using the arrangement in Figure 2 and translating the diffuser horizontally. At 0° model rotation the holographic interferograms were excellent. But as observed in Figure 23 it would be extremely difficult to determine the fringe change across the fin since no free stream reference fringes were available, due to the flat plate leading edge Prandtl-Meyer expansion and fin shock intersecting the tunnel top just above the fin. With a larger tunnel or smaller model this would be an excellent technique.

The diffuser plate was then translated vertically between exposures and excellent horizontal fringe patterns were obtained as shown in Figure 24. The model was then rotated to $22\frac{1}{2}^{\circ}$ and the same holographic technique was used. Excellent fringe patterns were obtained above and below the flat plate center section. Fringe patterns across the flat plate center section and fin in this area were very light and usable interferograms could not be photographed with the polaroid camera. In an attempt to improve on the fringe quality, polarizer plates were inserted in the reference beam between the mirror, M_4, and the hologram plate and in the scene beam between the lens, L_3, and the diffuser plate in order to ensure

polarization of both beams. No significant improvement could be noticed and they were subsequently removed. A one-quarter wave polarizer plate was then placed between the lens, L_1 and the beam splitter in order to utilize circularly polarized light for the reference and scene beams. Okayama and Emori [14] found that their image resolution improved considerably; however, with this particular arrangement little to no improvement in the fringe resolution was observed and the approach was abandoned.

The transverse mode selector was then varied from 2.0 mm. to 1.5 mm. and later to 1.0 mm. in an effort to improve the coherency length of the laser light and consequently the image resolution. Due to the decrease in output light intensity, up to six exposures were taken during a run with flow established. Image and fringe definition were not found to increase possibly due to model vibration which was not visible to the eye.

The model was rotated to 45° and $67\frac{1}{2}^{\circ}$ and double exposure holograms were taken with a 2.5 mm. transverse mode selector. There were no observable fringe patterns in any portion of the test section. Consequently it was believed that supersonic flow was not established due to tunnel blockage caused by the shock wave from the model and by slight model vibrations in passing through the transonic range. In the transition to supersonic flow, the model leading edge would sometimes flex as much as 0.2° depending upon the transition time.

The test section walls were changed from the total plexiglas side walls shown in Figure 1(a) to the aluminum walls with the optical quality glass port holes (Figure 1(b)). The better quality glass would hopefully improve the viewing and the port holes made the model much more accessible. The metal strakes were also removed from the model since they appeared to have a minimal effect on the flow, were an interference optically,

25

and appeared to add very little structurally. Flow tests were run and the model was found to attain an angle of attack of about 0.14^o upward when flow was established at Mach 2.84. The angle of attack was tolerable, however the model also maintained a visible high frequency vibration of about $\pm$ 0.05^o. Double exposure holograms were taken with the model at 0° rotation and fringes could only be observed forward of the Prandtl-Meyer expansion on the top of the model and forward of the flat plate leading edge shock on the bottom. The tunnel seals were found to leak and were replaced and resealed. The same angle of attack and high frequency model vibration still persisted. Double exposure holograms were again taken and a very faint fringe pattern was observed across the model. In reproducing the scene when aligned along a constant Z-plane passing through the fin, it was impossible to photograph the fringe pattern across the fin because of a bad speckle effect. Double exposure holograms were made at model rotation angles of 45° and 90° without and with flow. The holograms taken without flow gave excellent fringe patterns across the model however no fringes could be observed with flow.

At this point a knife edge Schlieren system was set up to determine just what the flow conditions were in the tunnel and around the model. The first runs were made at a model rotation angle of 90° and presented the shock knee in front of the fin (Figures 25(a) and 25 (b)) which was pointed out by Thomas [23, 24] and Winkelman [26, 27]. Due to the model vibration, the shock extending out from the shock knee was observed to flutter about $\pm\frac{1}{2}$ cm.

The model was then rotated back to 0° and Schlieren photographs were taken as shown in Figure 26. During all but one of the runs at this rotation angle, the model would pitch up approximately 0.14^o angle of attack and continue to vibrate about $\pm$ 0.05^o at a high frequency when

flow was established. The plate leading edge shock and fin shock appeared quite fuzzy and light. Due to oil from the tunnel supply reservoir mixing in the flow, a light oil smear pattern can be observed across the fin in Figure 26. During one run, which could not be duplicated, the model pitched up as flow was established but did not vibrate. The plate shock and Prandtl-Meyer waves, fin shock system, and tunnel Mach lines became very distinct and well defined as seen in Figure 27. The schematic of the Schlieren photographs in Figure 28 points out the cause for the various flow lines observed. The non-uniformity of the free stream caused by tunnel leakage can be easily seen. Consequently the experimental work was discontinued due to tunnel conditions and time considerations.

It was felt at this point that if the holographic interferogram taken of the clear plexiglas fin at 0° rotation angle could be reduced to useful data for the computer program then the holographic method would be to a certain extent verified even though the actual density field could not yet be determined.

In obtaining interferograms from the hologram, the reconstruction technique shown in Figure 15 was used. The plane of constant Z across the model to be reduced was chosen to be the forward most vertical grid line crossing the fin. It should be pointed out that in order to simplify the hologram alignment process, all four reduction planes across the model should have been scribed on the exterior grids. The three photographic points across the Z plane on the y' axis were, for convenience, chosen to be where horizontal exterior grid lines crossed the y' axis on the fin. Five interferogram photographs were taken at points A, B, and C as shown in Figure 29. Photographs 2 and 5 were taken using a Kodak Wratten Gelatin Filter N.D. 2.0 placed in the reconstruction beam in order to reduce the

27

beam intensity and increase the fringe definition. These two photographs were also used to provide a check on the consistency of the reduction process.

All five negatives were blown up on the photo enlarger in the dark room and the plate, fin, grid lines and fringes were traced out on a sheet of white paper as shown in Figures 30-34. It was very difficult to trace the fringes in the region of the fin tip and fin root due to the photographic resolution and the fin tip shadow. Also fringes were not visible in the region of the fin leading edge shock. Consequently, connecting the fringe in front of the fin to the correct fringe on the fin was a best guess effort. Typical of the problem was that fringe lines in two of the drawings were initially improperly connected across the fin leading edge shock. After being checked against the photograph negatives, the fringes were reconnected and the data taken correlated well with the data from other drawings. The fringes in the fin root area were extremely light in some photographs which made it quite difficult to determine their centerline crossing the y' axis. Another point of difficulty was determing the location of the top and bottom of the fin. An error in drawing here will have an effect later when the fringe locations are normalized with respect to the fin height.

Enlarged positives were then made from the negatives as shown in Figures 35-39 to see if the data accuracy could be improved by eliminating the difficulties of tracing the fringes in the dark room. This method also made it possible usually to reassess the assumed path of the fringe lines at a later time if the data did no appear to correlate properly. The same problems of locating the fringe lines in the region of the fin tip and of connecting the fringe lines across the fin shock are readily apparent in the figures.

28

To obtain the fringe change across the fin one of the straightest fringes in the free stream region which paralleled the majority of other free stream fringes was selected. A straight line was drawn through its centerline and extended to cross the y' axis. The other free stream reference lines were then drawn parallel to the first and adjusted so as to best follow the centerline of the selected fringe. This method actually averages the free stream conditions and is only valid if the free stream is essentially uniform. Since it was not possible to obtain in the photographs the free stream fringe pattern forward of the leading edge Prandtl-Meyer expansion for the lower fin region, the fringe reference lines in photo enlargements were drawn over the fringes just prior to the fin shock. In order to adjust them to free stream conditions their location was moved downward a distance equal to 1.1 times the average fringe interval for that photograph. The figure 1.1 was observed in all the enlarged photographs to be the approximate fringe change across the Prandtl-Meyer expansion. In the drawings (Figures 30-34), fringe reference lines for the lower fringes (generally $y' \leq .8$) were initially aligned along the straightest portion of the fringe prior to intercepting the fin shock. By comparing the reference line location on the drawing with the fringe pattern in the photographic enlargements the reference line location and fringe change were adjusted by an appropriate portion or all of the 1.1 fringe change caused by the Prandtl-Meyer expansion. All of the reference lines were then corrected for the tunnel wall and grid plastic parrallax shown in Figure 19 and computed in Appendix B. The reference fringe locations were then normalized with respect to the wing height and the fringe numbers calculated by dividing the fringe change by the average fringe interval. For further details and calculations see Appendix A.

The data obtained for alignment points A and C by the two different reduction processes are plotted in Figures 40-43. The data obtained from the photo enlargements aligned at point C and shown in Figure 43 gave the best data agreement between two photographs. The worst data agreement was obtained from the reduction of the drawings aligned at the same point. The inconsistency in the data was probably caused by connecting the wrong fringe lines across the fin leading edge shock. The data fluctuations and discrepencies between the curves in the figures could have been caused by a number of things. It could have been caused, for instance, by not drawing the fringe reference line parallel to or exactly on the free stream fringe center line or slightly missing the fringe center as it crosses the y' axis or by misconnecting fringe lines across the fin shock as was illustrated in Figure 42. Fringe location errors could be caused by misdrawing the fin tip and root lines as was mentioned earlier. Another contributer would be measurement errors.

To analyze these sources for error, first consider that the typical fin size in the drawings and photo enlargements averaged about 2.5 inches high and 2.75 inches wide and that the fringe spacing averaged about 0.10 inches. All measurements were taken using a ruler graduated in 0.01 inches and readings were made to the nearest .005 inches. Since the average difference between the data points and curves ran around $\frac{1}{4}$ fringe, some figures were calculated to determine what measurement errors could produce this fringe error. It was found that an error of .025 inches in alignment of the fringe reference line with the free stream fringe center line and/or fringe center line crossing the y' axis could produce $\frac{1}{4}$ fringe error. This fringe error will also occur if the fringe reference line differs from the free stream center line by more than 1.4° when drawn 1 inch from the y' axis or by more than 0.36° when drawn 4 inches from the

y' axis. A difference of .01 inches in the average fringe interval could also produce a ¼-fringe error; however, this is not too likely since it is an average of fifteen to twenty-five intervals. By comparing the actual height-to-width ratio with those found in all the drawings and photo enlargements it was found that average error was around 2% or a distance of .02 on the y'-axis.

In order to compare the interferogram negative quality and the two different reduction techniques, a plot of the data for each negative was made as shown in Figures 44-48. Photographs 1 and 3 in Figures 44 and 46 gave the smoothest curves indicating the highest interferogram resolution. Photograph 5 (Figure 48) gave the worst dispersion indicating poor interferogram resolution; yet looking at the enlargement in Figure 39, the fringe line contrast is very good. In comparing Figures 40-48 it appears that the reduction technique using the photographic enlargements gave the most consistent data. This technique also provides a much easier and faster recheck on the proper tracing of fringe lines because it is extremely difficult and tedious to duplicate the fringe pattern to the same scale over the drawings using the photo-enlarger in the dark room.

All the data obtained by either method for one alignment point were then plotted in Figures 49 and 50 in order to observe the dispersion. A fringe number dispersion of about 0.6 fringes was observed in the data taken from the negatives aligned at point A and a dispersion of about 0.8 fringes for the data about point C. The dispersion is attributable to the inaccuracies in the drawings, to the photographic quality of the interferograms, and to the inaccuracies in correcting the lower fringe reference lines to free stream conditions. The last point is based upon the increased dispersion between the fin tip and fin root data.

31

Figures 51 and 52 show an integrated curve of the fringe change across the wing as determined by each reduction method. In constructing the curve, the data from the three aligned points was plotted so as to just overlap each other. These two curves were then compared in Figure 53. The maximum variation in the fringe number is about ½ a fringe but the variations in the location of the fringe maximums and minimums average about 0.1 inches on the fin. The location difference is probably due to improper drawing of the fringe reference lines compounded with not being able to measure the wing height accurately. Due to the inaccuracies introduced in tracing the negative and then reducing the data it is felt that the photo enlargement method is the more accurate reduction method.

With fringe data from only one field of view, the density field, obviously, could not be obtained. It was felt useful to consider the flow field axisymmetric in order to exercise the computer program and to provide a check on the program's ability to handle these particular curve shapes. Fringe data at 101 equidistant points across the fin from $0 \leqslant Y' \leqslant 1.0$ was obtained from Figure 53 for both curves and fed in HOLOFER in Mode 3 for the axisymmetric case. For further details on HOLOFER see Appendix C. The scale factor, α, in Equation 9 was then varied from 0.2 to 2.5 and a value to 1.0 was determined to yield the most accurate density solutions. This value was verified by feeding the function data, $(\rho/\rho_\infty -1)$, calculated by Mode 3 back into the program in Mode 1 and comparing the fringe data calculated with the original fringe data obtained from Figure 53.

The density distribution for both the drawing and photographic reduction cases is plotted in Figure 54. The density as Y' approaches zero actually goes as the drawn lines even though the points indicate a dip.

Matulka [12, 13] pointed out that the computer program accuracy does not converge at the origin. The large variations of the density curves at values of $Y' > 0.8$ are caused by the program trying to adapt to a step or shock wave type function at $Y' = 1.0$. If the remainder of the fringe data in Figure 53 for values of $Y' > 1.0$ had been included as input data the density curves would have smoothed out. This shock wave step function effect was demonstrated and analyzed by Matulka [12, 13].

The low values of density for the photographic data curve around $Y' = 0.38$ were unexpected but not surprising. First, the photographic fringe data curve is more extreme than the drawing fringe data curve and second, the density curves are not true values anyway since the field was considered axisymmetric and this is not the case in reality.

In general the density curves are felt to be reasonable under the assumed conditions. Consequently it is believed that the computer program could very easily and accurately handle a complete analysis of the flow field around the fin-flat plate.

In completing the analysis there are some data reduction problems which would have been encountered in reducing the interferograms at other model rotation angles which merit discussion. With no model rotation, adjusting the fringe reference lines close to the fin root to account for the leading edge Prandtl-Meyer expansion was relatively easy. However, when the model is rotated, the fringe shift across the Prandtl-Meyer expansion can no longer be considered a constant and it will be very difficult to adjust the fringe lines at lower values of Y' to free stream conditions. The best solution would be to increase the scene beam diameter and/or reduce the model size in order to photograph the free stream fringe lines forward of the plate leading edge. The free

33

stream lines could be connected to the appropriate fringe lines forward of the fin and this would eliminate the numerical correction and increase the fringe data accuracy.

Also at the rotated angles, fringe information will not be available for portions of the reduction plane due to shadows cast by the model sides as shown in Figure 55. In the lower portion of the hologram the fringe curve can be connected with a smooth line because the density field in that portion should be essentially constant. Care must be taken in completing the curve, though, since this information will be used in the integration of other rotation angles. The fringe curve in the upper portion must also be completed carefully but should be easier since the shadow will be smaller. For this particular model it was calculated that for angles greater than 46.6° the upper shadow would not penetrate the fin.

There are two more problems to be coped with which do not have apparent solutions at this time. The first has to do with the superimposing of fringe information from different locations onto one scene beam line as illustrated in Figure 56. In case I the superimposing of the fringe change in Region A onto that in Region C and locating the fringe reference line at point C' is tolerable because the density field in Region A should be fairly constant and uniform. However in case II where the fringe change in all three regions are superimposed and located at point C'', the answer is not readily apparent. If the plate and fin were of equal thicknesses then points A'' and C'' would be the same and the error would be somewhat reduced. If, in addition, the thicknesses were made as thin as structurally possible, the error would be reduced to a minimum. Also it might be possible to integrate the model geometry into the computer program but this has not been attempted.

34

With the model at rotation angles between 0° and 90° scene beam defraction at the fin root and tip areas would also present problems as seen in Figure 57. A minimization of the problem could again be achieved by minimizing the fin and plate thicknesses.

VI. CONCLUSIONS AND RECOMMENDATIONS

The investigation, although not totally successful, has demonstrated the feasibility of using holographic interferometry to determine the flow field around a transparent model by looking through the model. The problems of model vibration and movement, of superimposing different fringe information on one beam, and of scene beam divergence through the fin root and tip regions must still be solved. The model vibrations and rotation to an angle of attack are attributable to the tunnel pressure fluctuations caused by tunnel leaks and to possible movement of the sting holder. It is felt that all three problems could be decreased to neglectable effects by reducing the overall model size and by incorporating the model geometry into the computer program.

The basic holographic arrangement was found to work quite well for this type of experiment. The holograms were generally high quality except when unfavorable tunnel flow conditions existed. The use of circularly polarized light recommended by Okayama and Emori [14] did not increase the hologram resolution appreciably but the method merits further considerations because of their excellent results.

The data reduction process was found to be the rate-controlling step in the investigation due to the time and labor involved. Reducing the data from enlarged photographs of the interferogram saved some time and appeared to increase the data accuracy. The data scatter of ± 1/8 fringe

was considered acceptable considering the fringe resolution in the holo-
grams. It was felt that this could be reduced by using either a larger
tunnel or a smaller model. With either of the changes it would be pos-
sible either to use the free stream fringe pattern forward of the model
as the reference conditions across the whole model or to use a vertical
fringe pattern, since the leading edge Prandtl-Meyer expansion and fin
shock would not block out the free stream fringes above the fin. It
appears that the use of vertical fringes would also considerably reduce
the data reduction time.

With the use of Schlieren the flow network described by both Thomas
[23, 24] and Winkelmann [26, 27] was verified to exist. From the top
view (90° model rotation) the fin shock and its fluctuations were ob-
served and photographed through the flat plate plastic center section.

The computer program, HOLOFER, was found to be quite capable of
handling the type of flow field fringe data which would be generated in
a complete analysis of this type. As pointed out before it is believed
that the program should be modified to incorporate the model geometry.
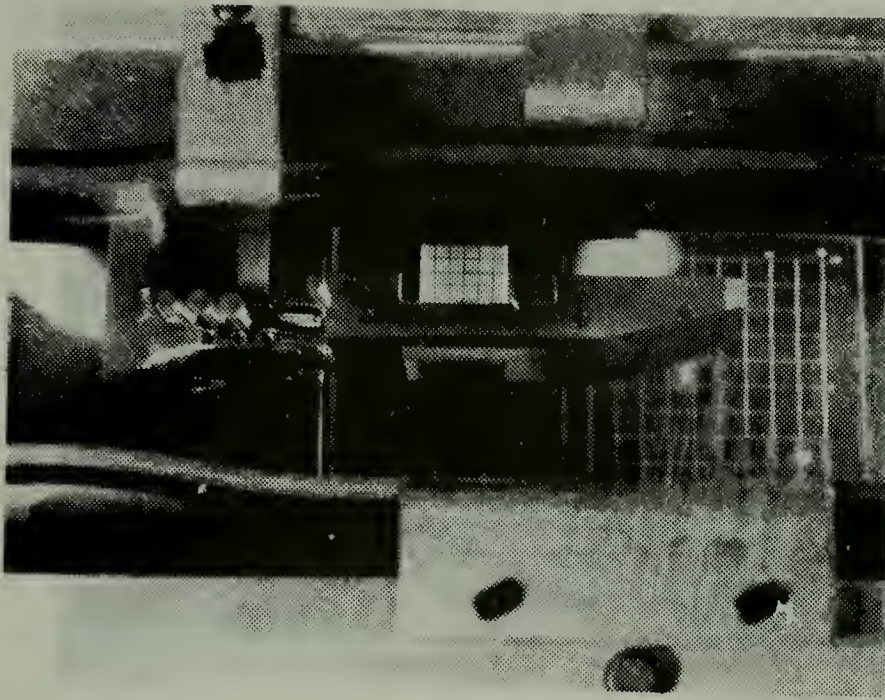
Figure 1(a). Wind Tunnel Test Section with Clear Plastic Side Walls
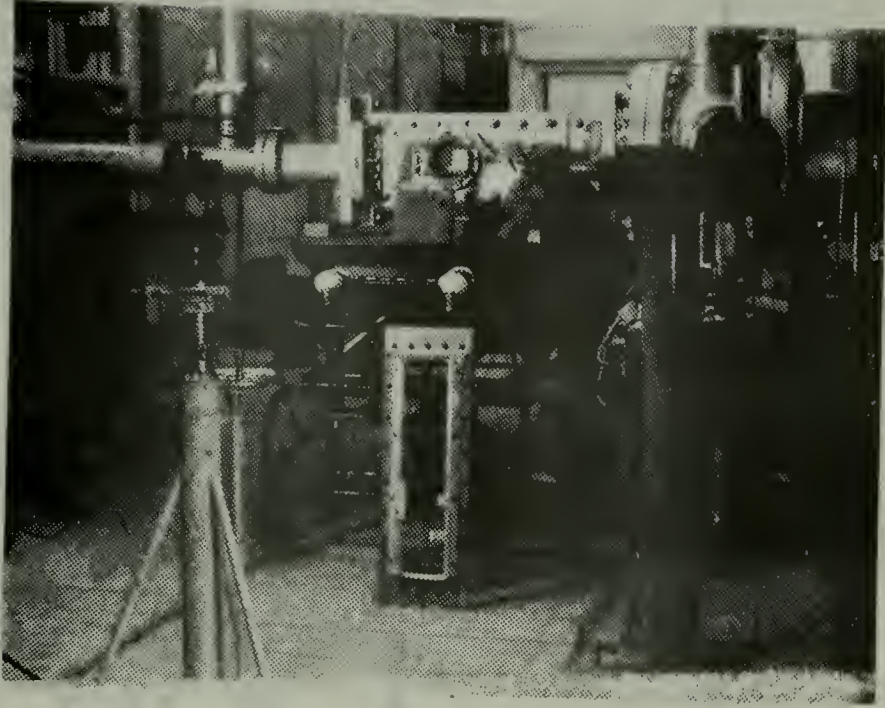
Figure 1(b). Wind Tunnel Test Section with Aluminum Side Walls
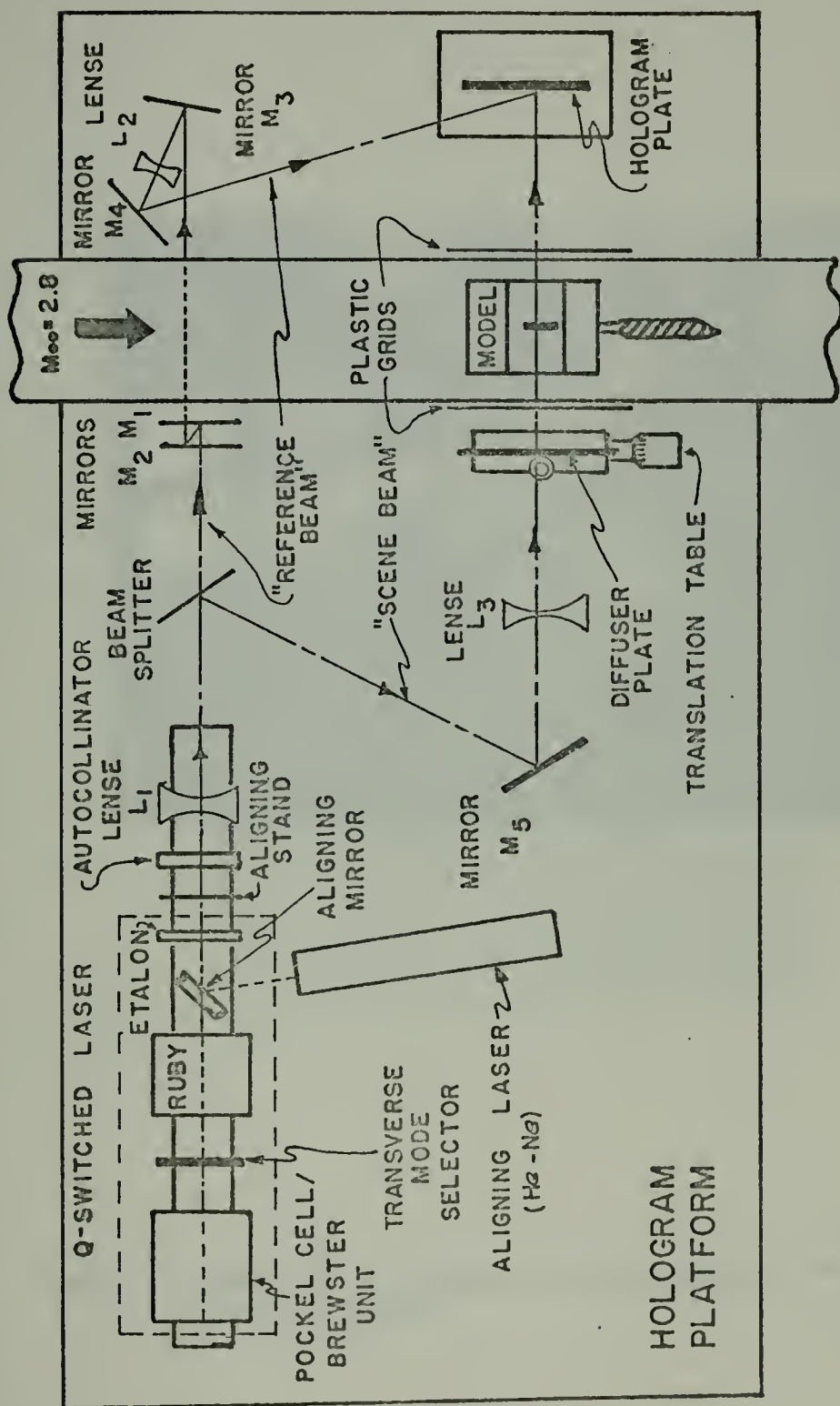
Figure 2. Schematic Representation of the Holographic Arrangement
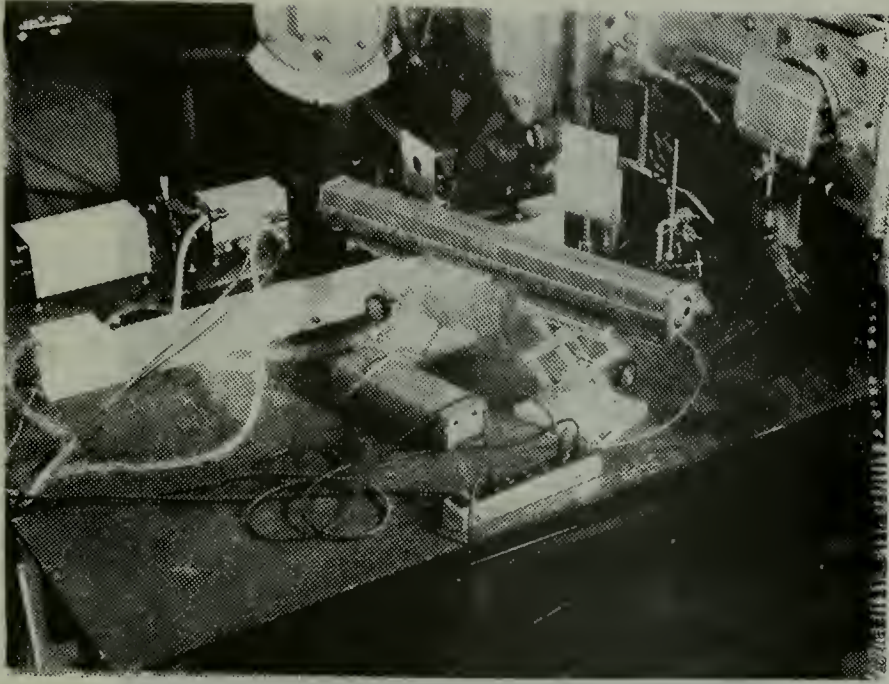
Figure 3. Holographic Arrangement Including the Laser Cooling and Aligning Equipment

Городской общественный самоуправление. Общий вид.
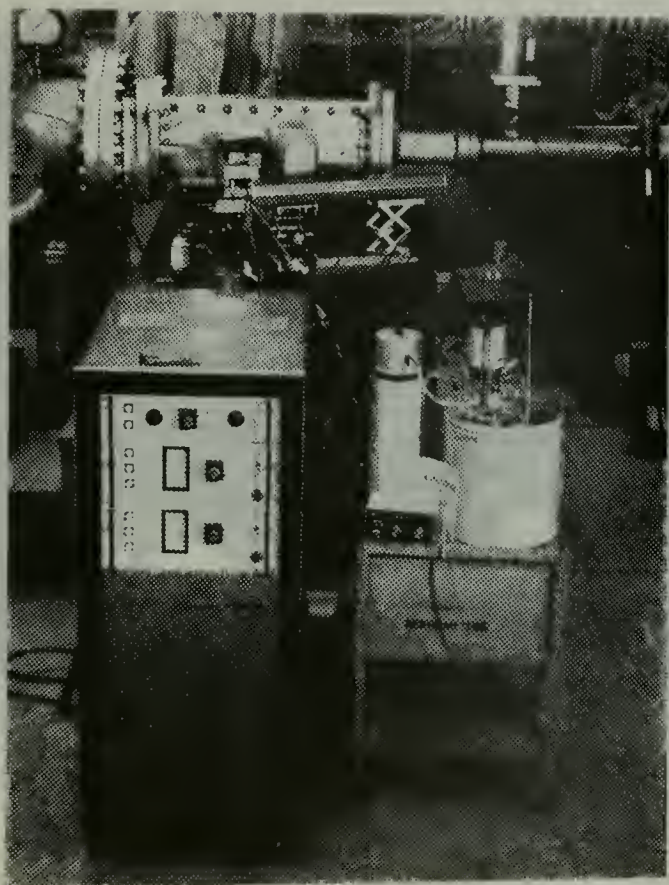
Figure 4.   Ruby Laser Power Supply and Cooling Unit
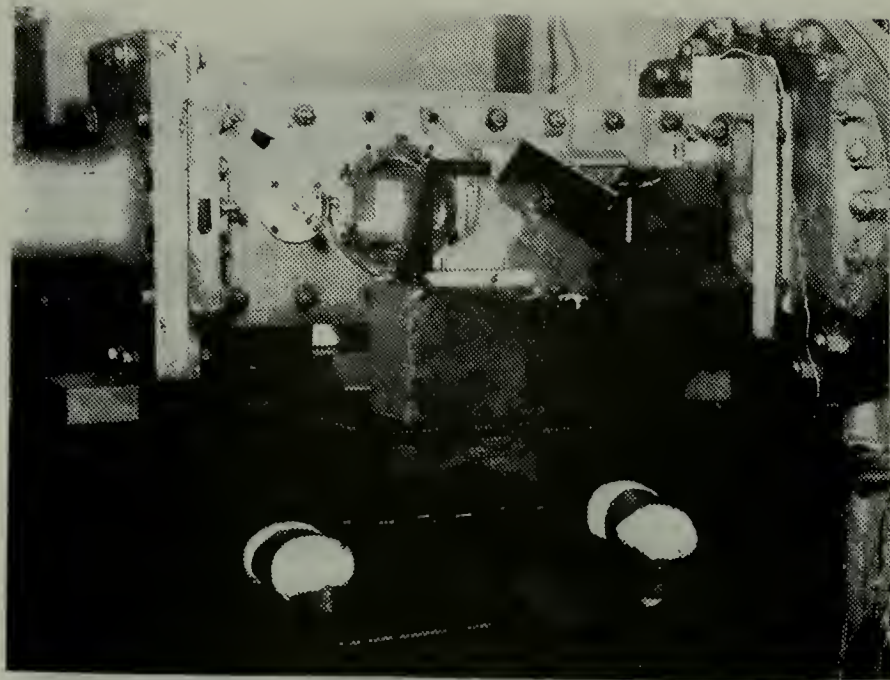
Figure 5. Hologram Plate Holder and Mirrors on the Reverse Side
of the Wind Tunnel
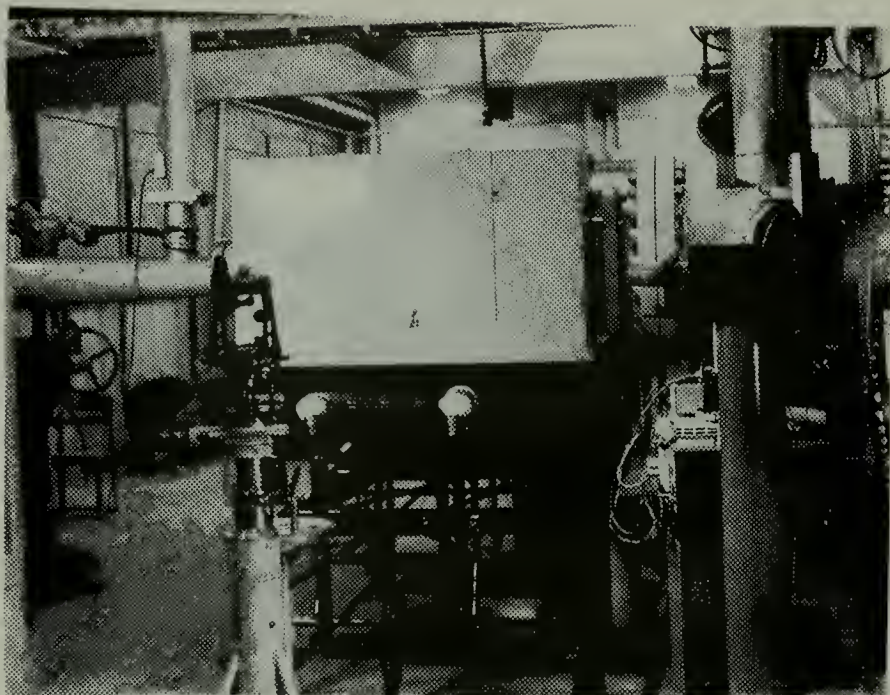
Figure 6. Hologram Platform Box Cover for Daylight Photography

43
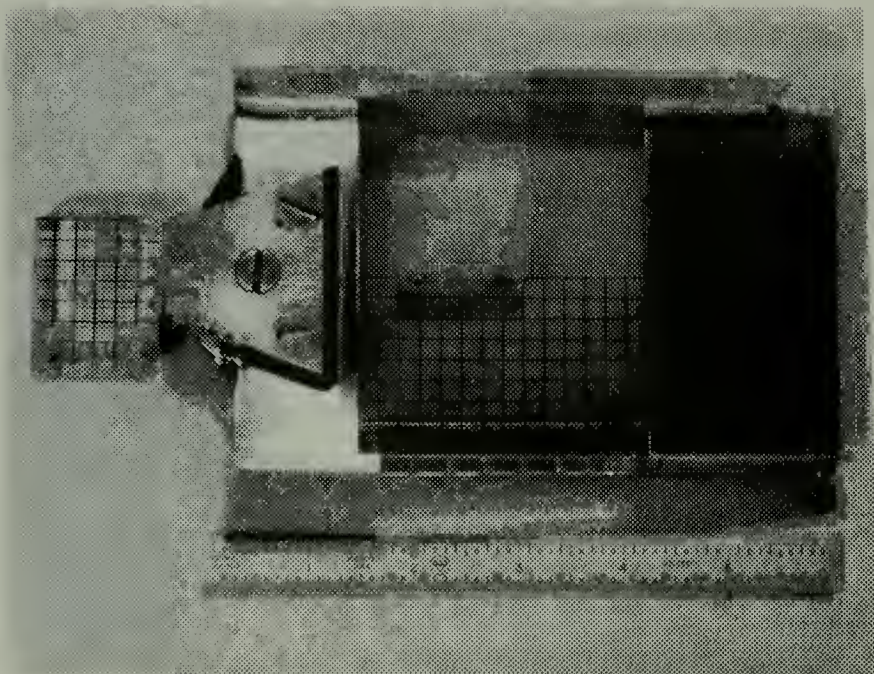
Figure 7(a). Initial Fin-Flat Plate Model Used in the Experiment
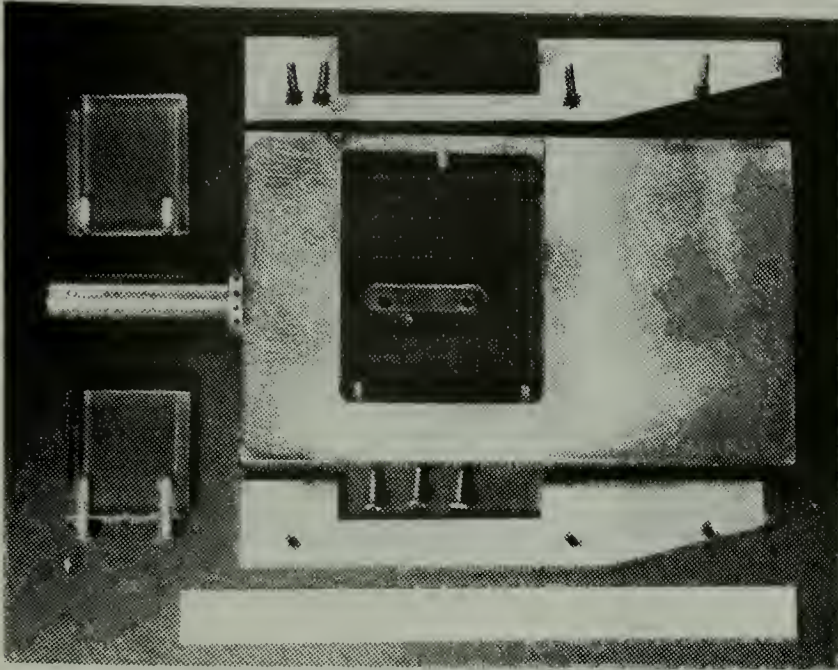
Figure 7(b). Second Fin-Flat Plate Model Used in the Experiment

Figure 7(c). Details of the Second Fin-Flat Plate Model

46
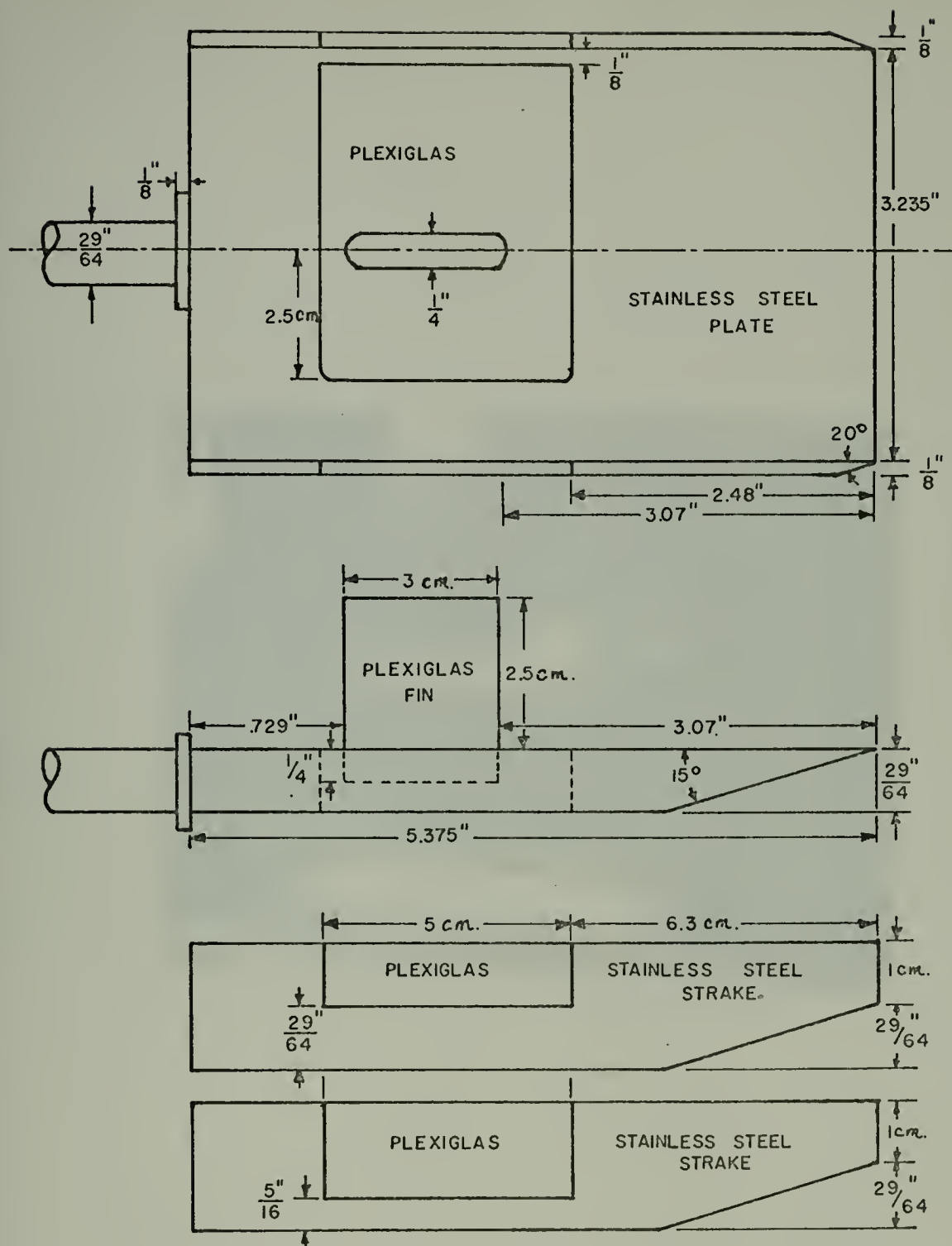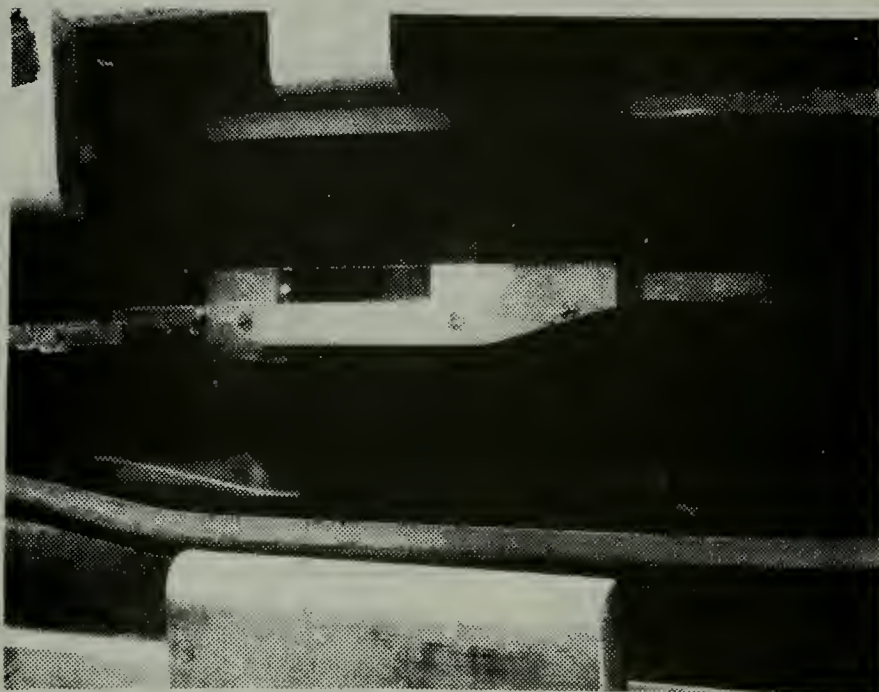
Figure 7(d). Model Mounting in the Wind Tunnel Test Section
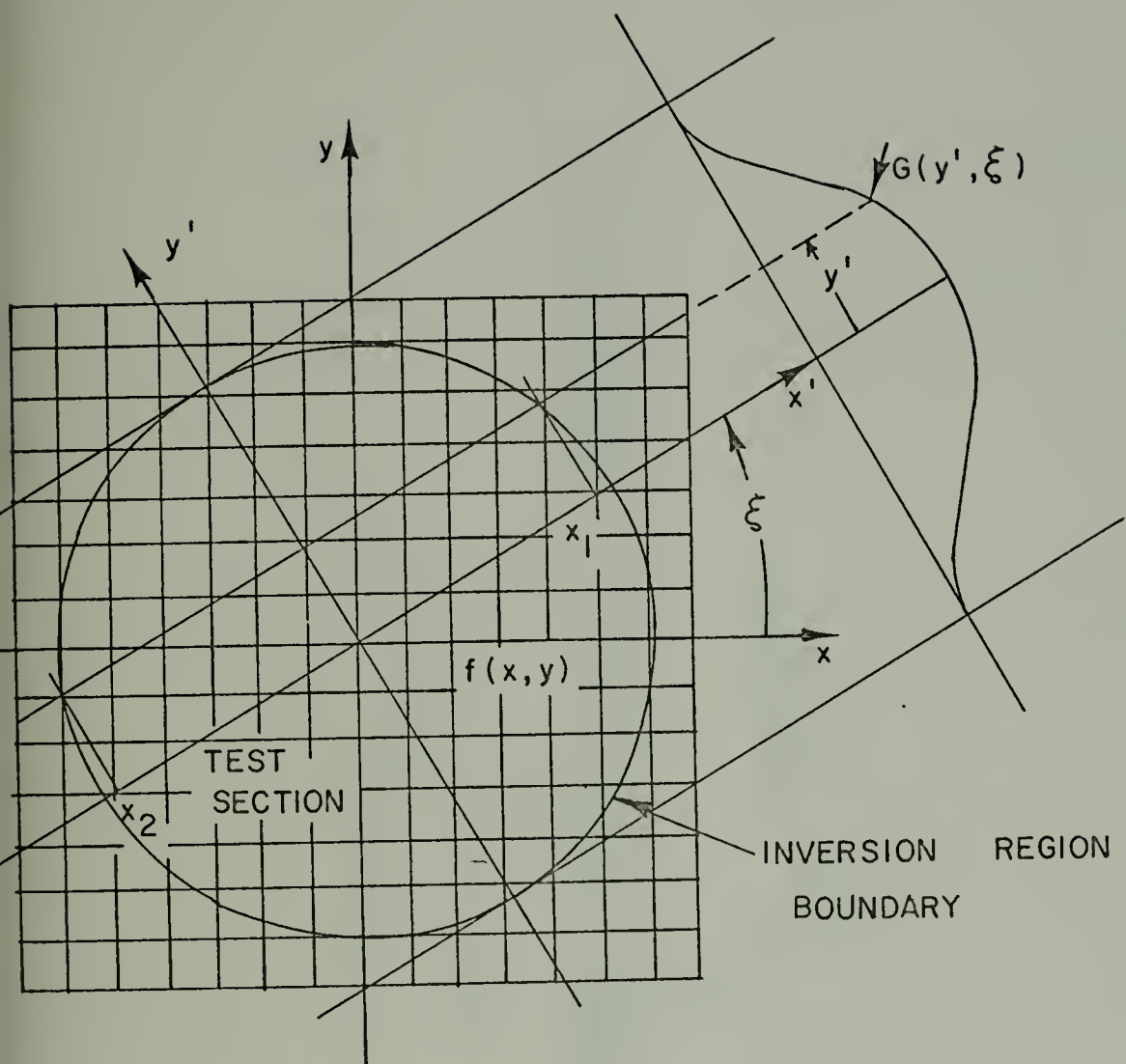
FIGURE 8. CO-ORDINATE SYSTEM USED FOR THE INVERSION
OF FRINGE NUMBER TO DENSITY
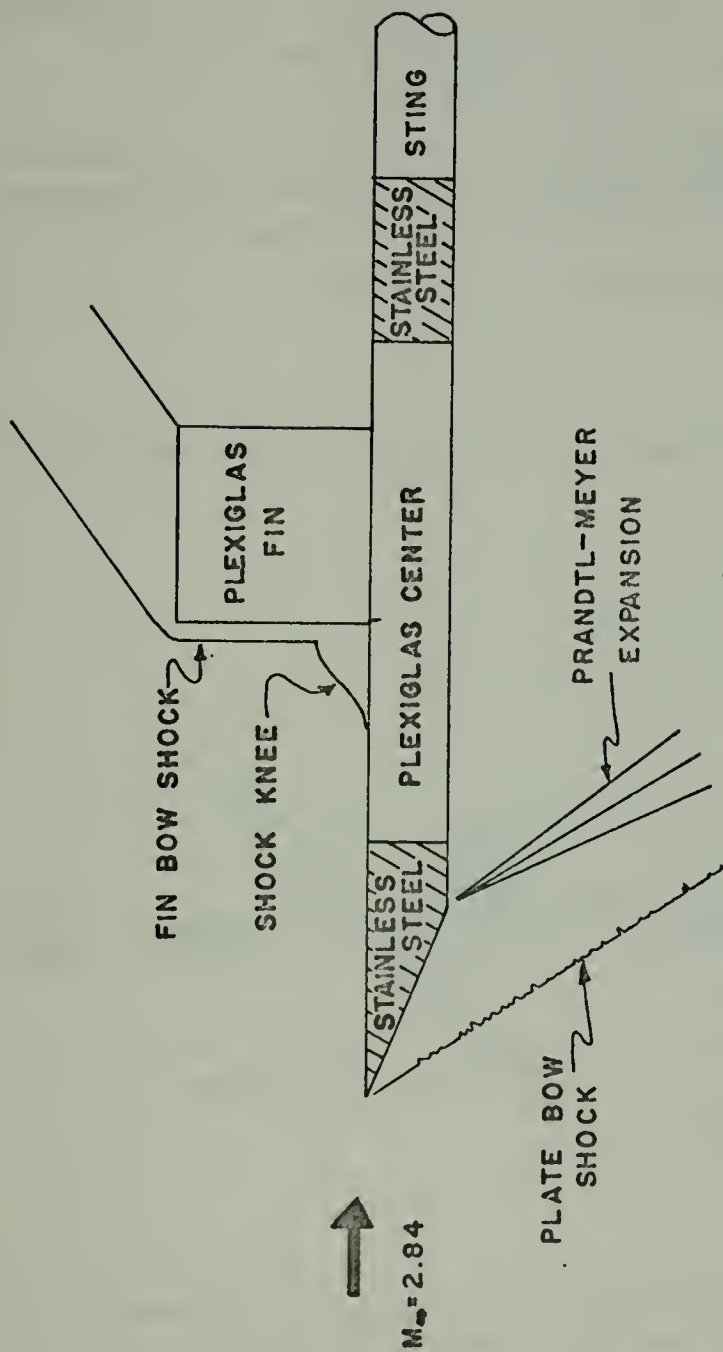
Figure 9. Schematic of the Desired Model Flow Network

49
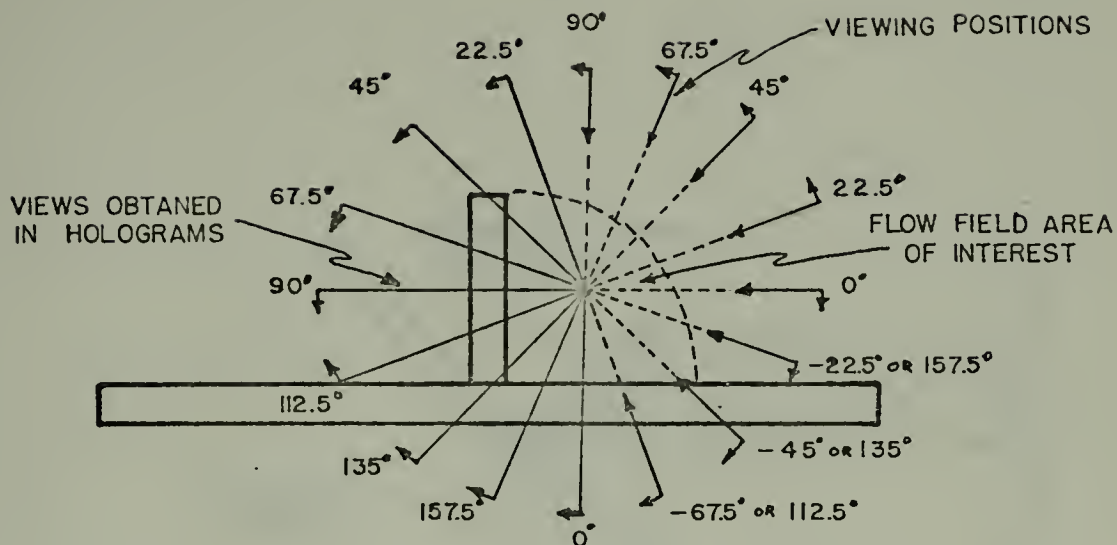
Figure 10. Desired Holographic Views in the Direct Fin-Root Method
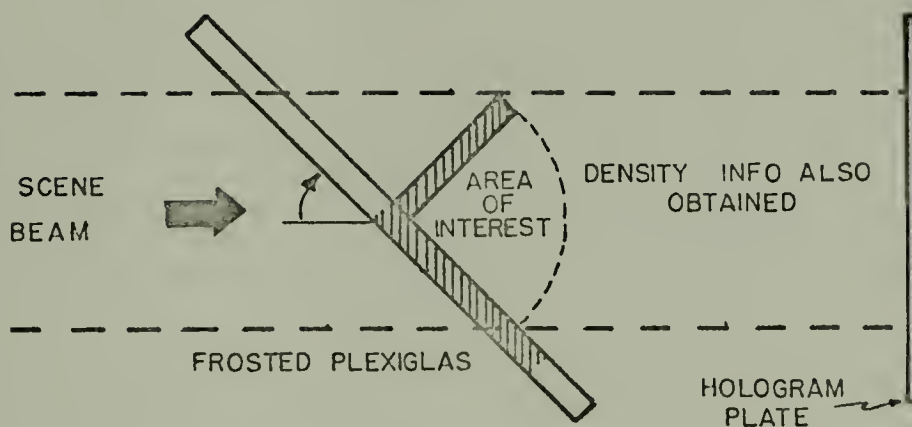
Figure 11. Schematic of the Model Used to Obtain Holographic Views
Between 0° and 90° in the Direct Fin-Root Method
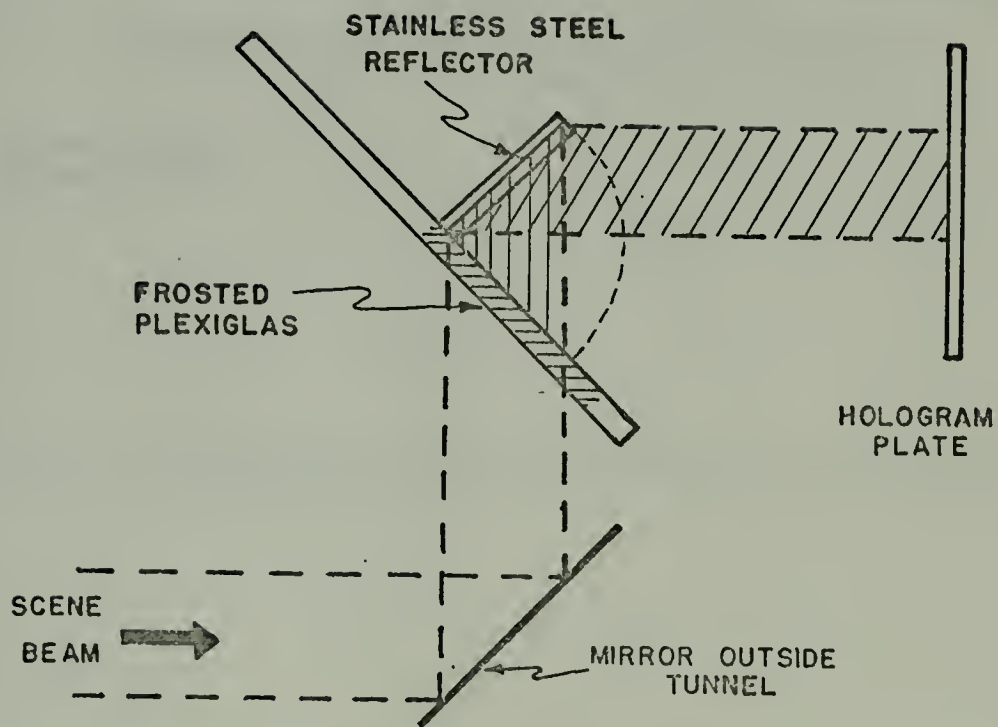
Figure 12.   Schematic of the Model Used to Obtain Holographic Views
Between 90° and 180° in the Direct Fin-Root Method

51
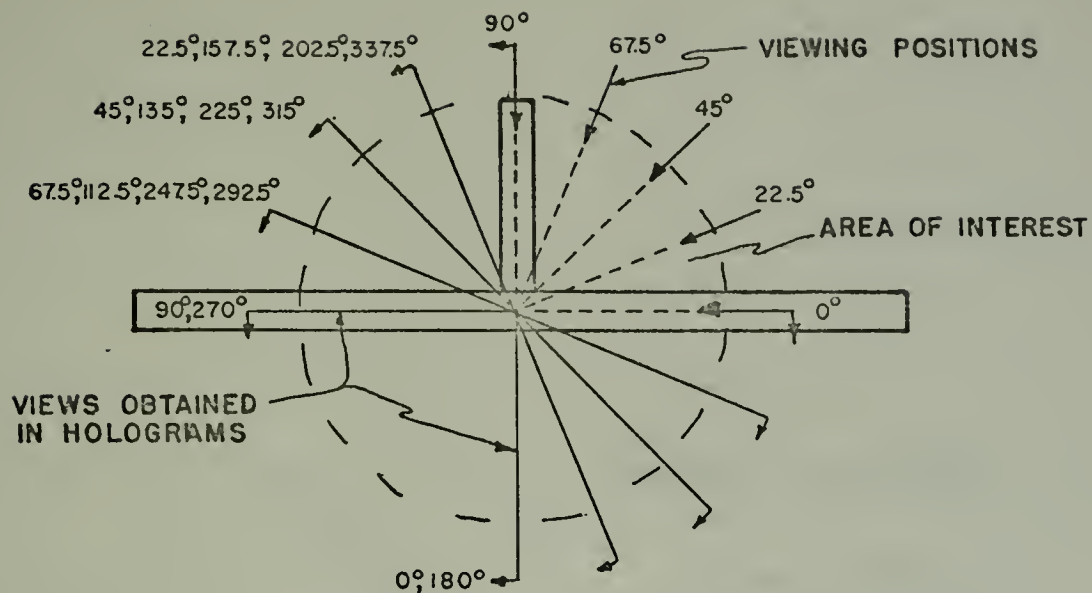
Figure 13. Holographic Viewing Angles Required in the Total Model Flow Method
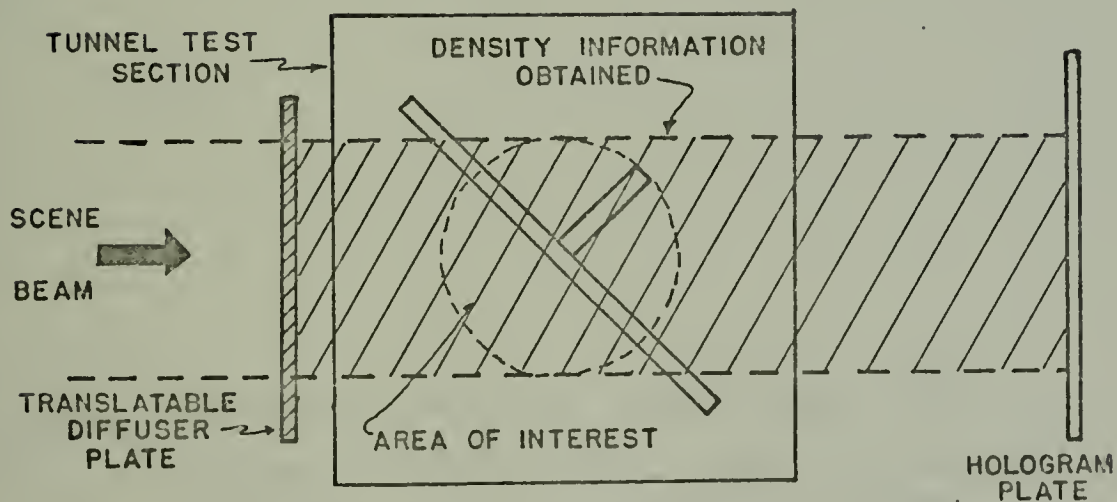
Figure 14. Schematic of the Technique Used to Obtain Holograms in the Total Model Flow Method
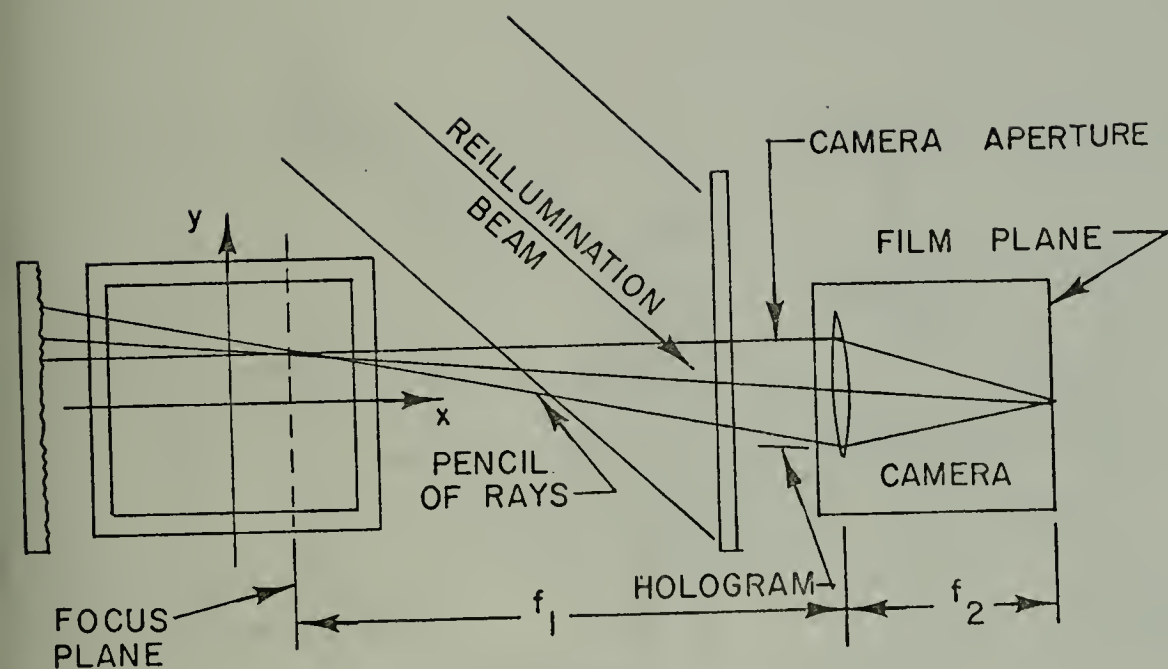
FIGURE 15. EFFECT OF APERTURE SIZE FOCUS PLANE
POSITION ON THE PENCIL SIZE OF RAYS ABOUT
A LINE OF SIGHT RECORDED BY CAMERA
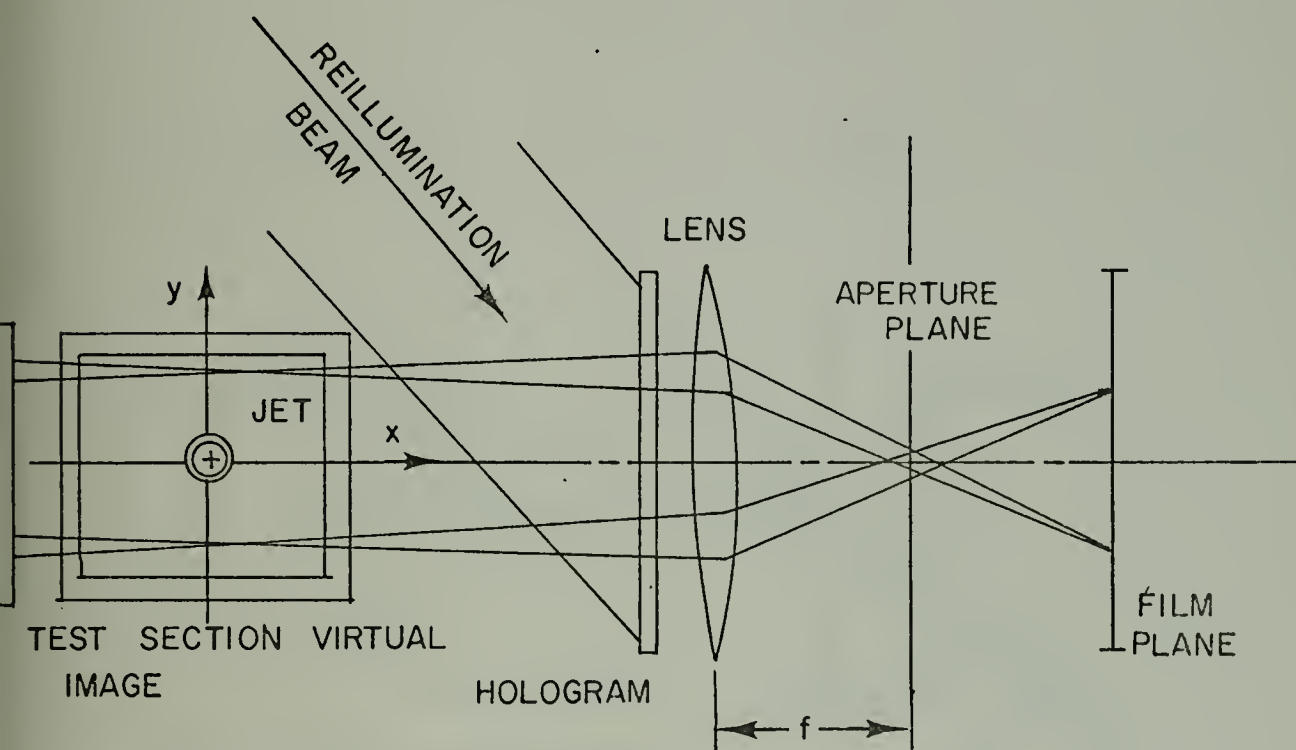
FIGURE 16. SPATIAL FILTERING TECHNIQUE FOR SELECTING
PHOTOGRAPH OF CONSTANT ANGLE LINES OF
LIGHT
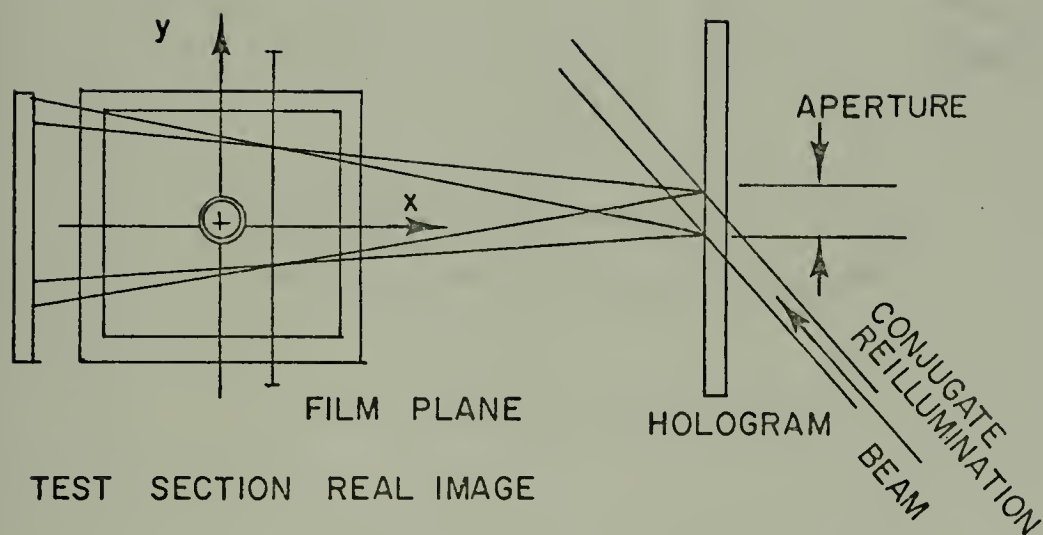
FIGURE 17. LENSLESS PHOTOGRAPHIC TECHNIQUE USING A
CONJUGATE REFERENCE BEAM OF SMALL DIAMETER

CONSTANT Z REDUCTION
PLANES

EXTERIOR GRID LINE
PLANES USED AS
REDUCTION
PLANES

Y'

1.0

$M_\infty = 2.84$

Z' 1.19   0

-1.0
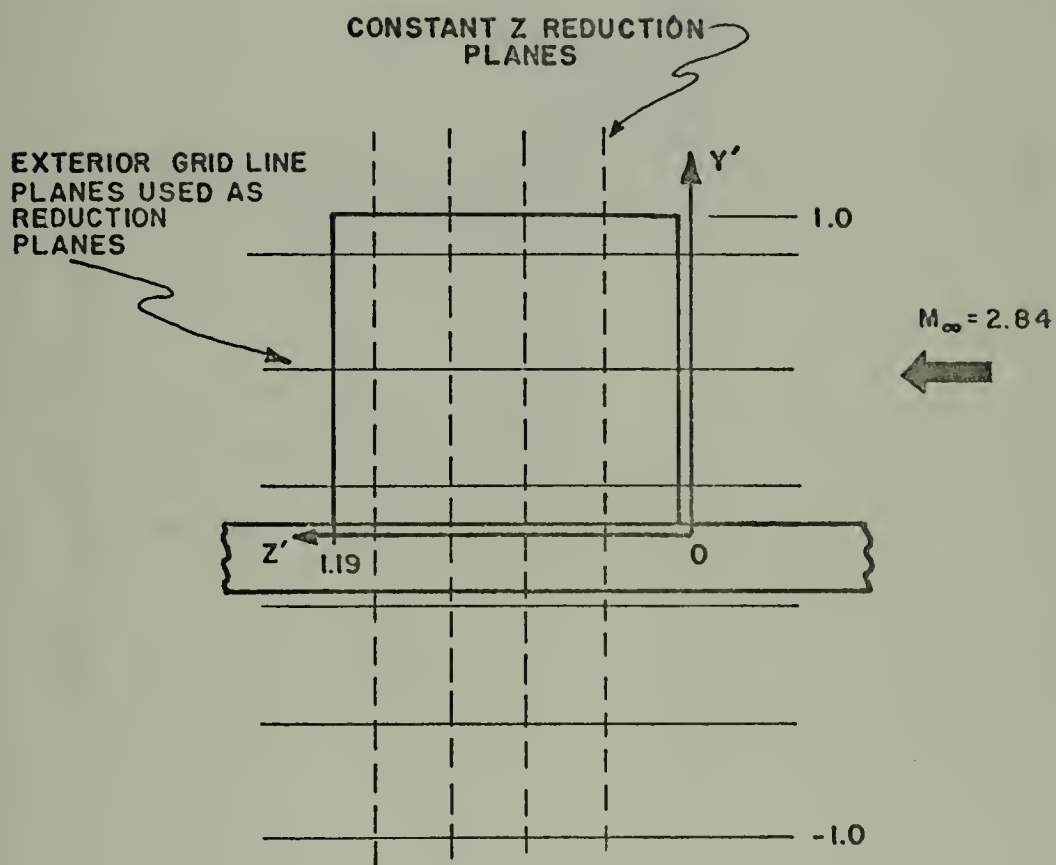
Figure 18.   Data Reduction Planes Desired to Describe the Density
Field Down the Fin

Figure 19. Schematic of the Refraction Displacement in the Photographs of Points Not Located on the Aligned Axis Caused by the Plastic Grid and Tunnel Wall
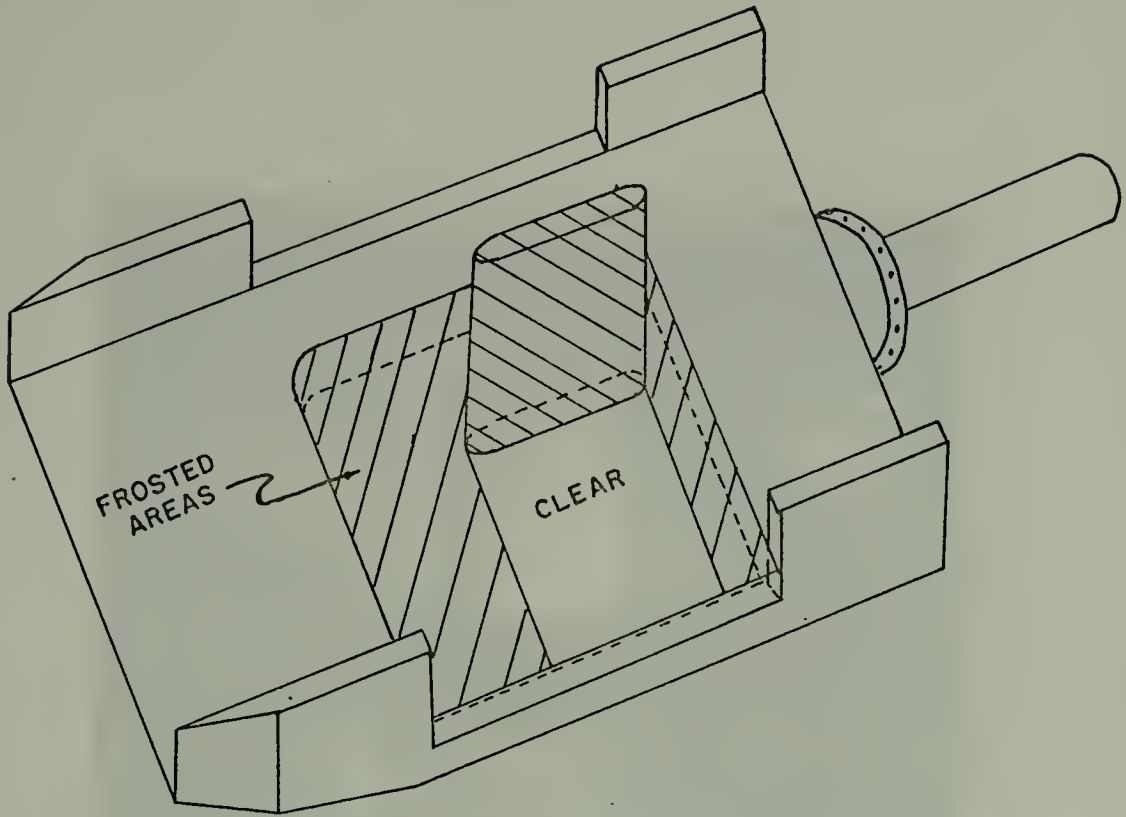
Figure 20. Schematic of the Diffused Plastic Portion of the Model
Required in the Direct Fin Flow Method
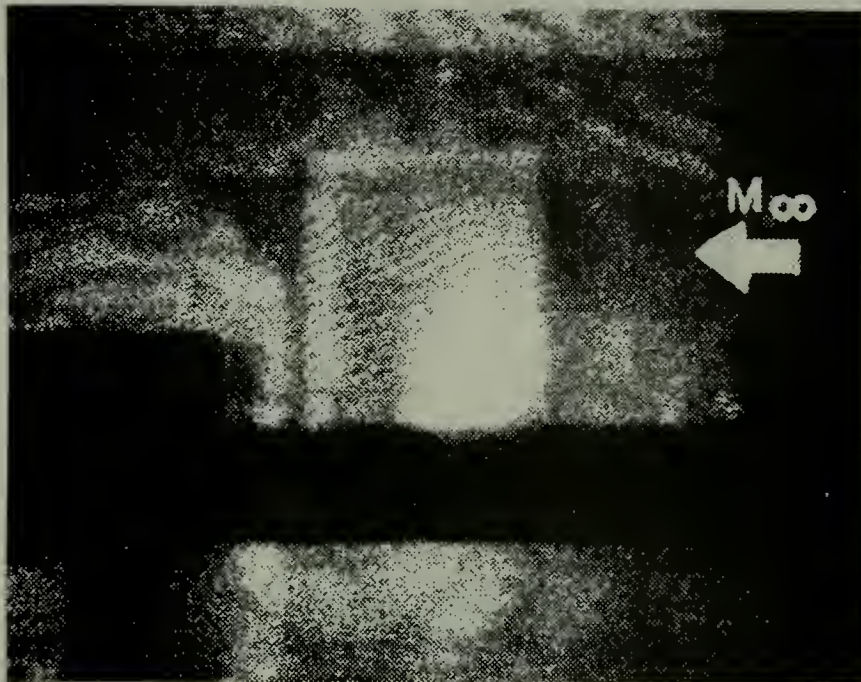
Figure 21. Interferogram Obtained in the Direct Fin Flow Method with the Model at $0°$ Rotation, Mach 2.84 and no Translation of Mirror, M_5
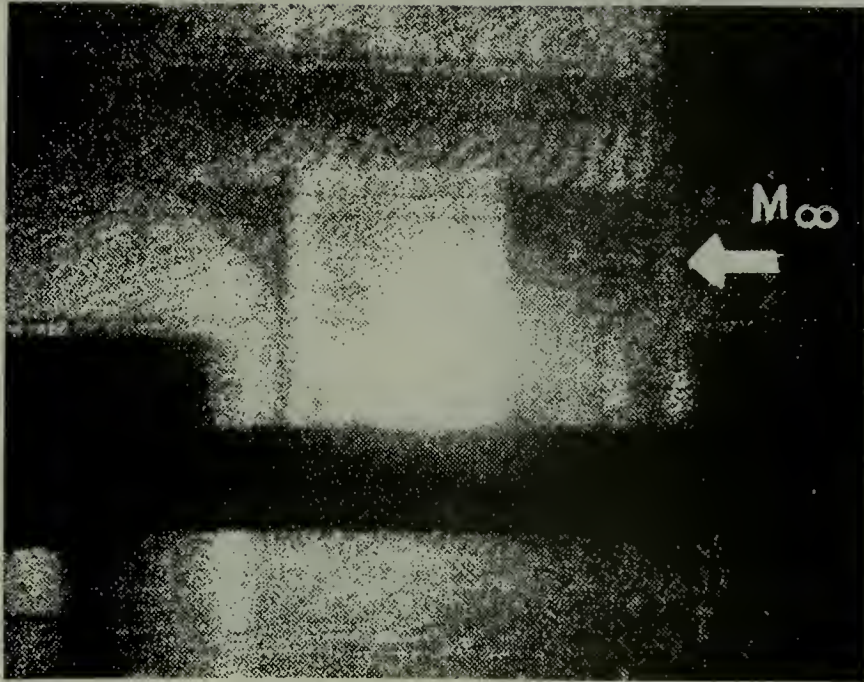
Figure 22. Interferogram Obtained in the Direct Fin Flow Method with
the Model at 0° Rotation, Mach 2.84 and a .006 inches
Translation of Mirror, M_5, Parallel to the Test Section
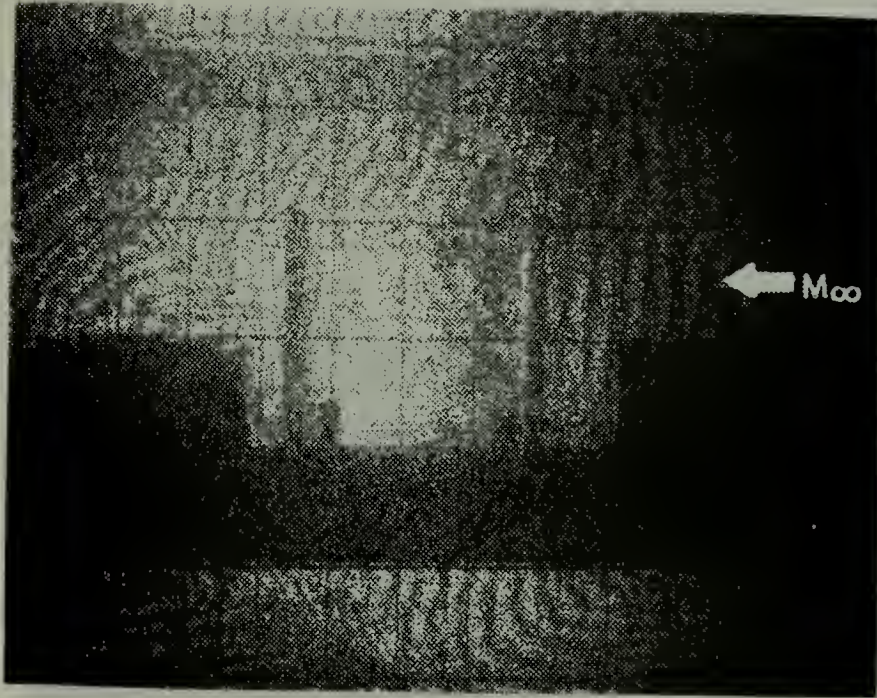
Figure 23. Interferogram Obtained in the Total Flow Method with the
Clear Plexiglas Fin Model at 0° Rotation, Mach 2.84 and
a .0015 inches Horizontal Translation of the Diffuser
Plate Parallel to the Test Section

Figure 24. Interferogram Obtained in the Total Flow Method with the
Clear Plexiglas Fin Model at 0° Rotation, Mach 2.84 and
a .0045 Vertical Translation of the Diffuser Plate
Parallel to the Test Section

Figure 25(a).   Illustration of the Shock Network Around the Fin at
Mach 2.84 with a 90° Model Rotation Angle Using a
Horizontal Knife Edge Schlieren System
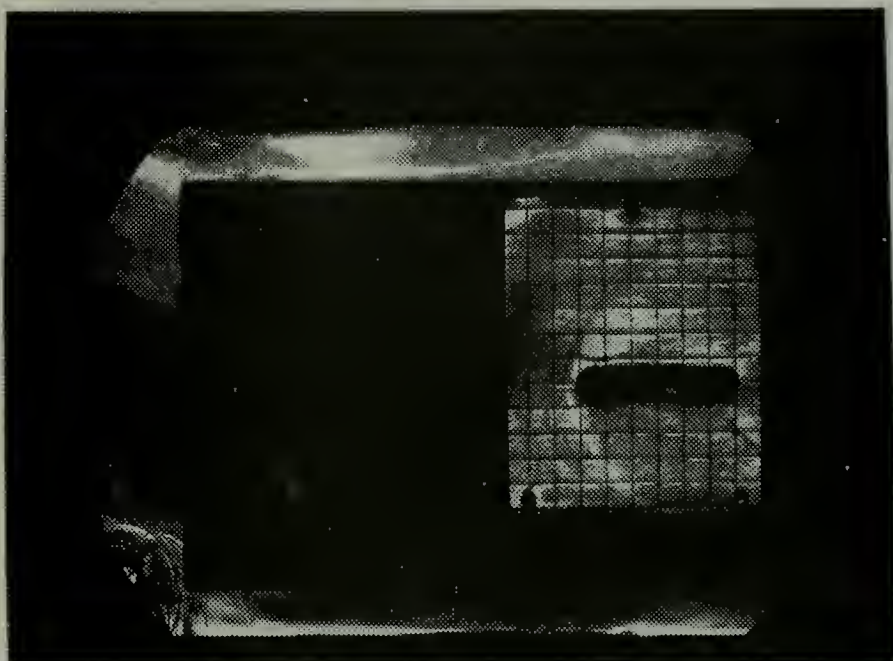
Figure 25(b). Illustration of the Shock Network Around the Fin at
Mach 2.84 with a 90° Model Rotation Angle Using a
Vertical Knife Edge Schlieren System
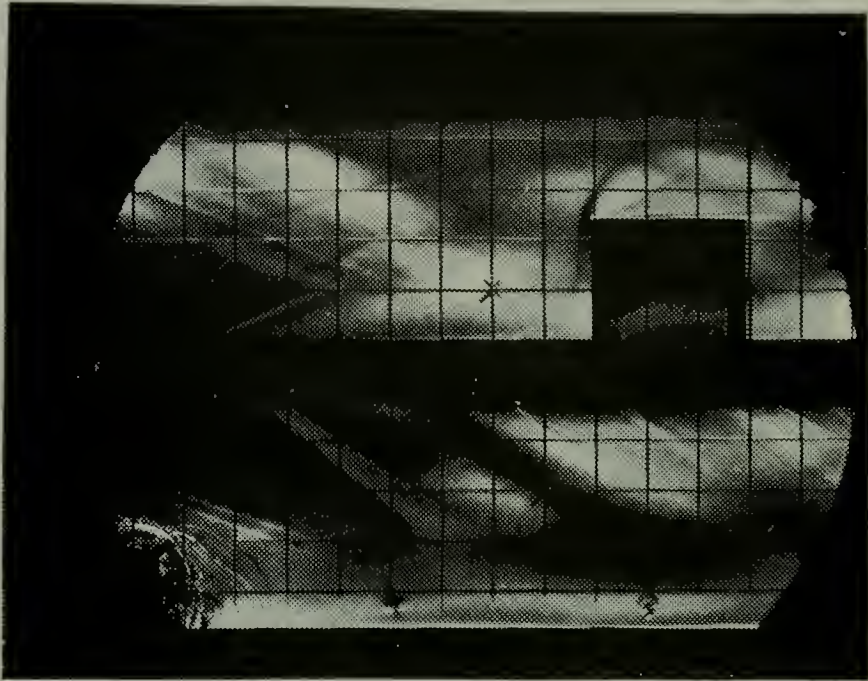
Figure 26. Illustration of the Model Flow Network at Mach 2.84, 0°
Model Rotation and a Plate Vibration of ±.05 Angle of
Attack Using a Schlieren System
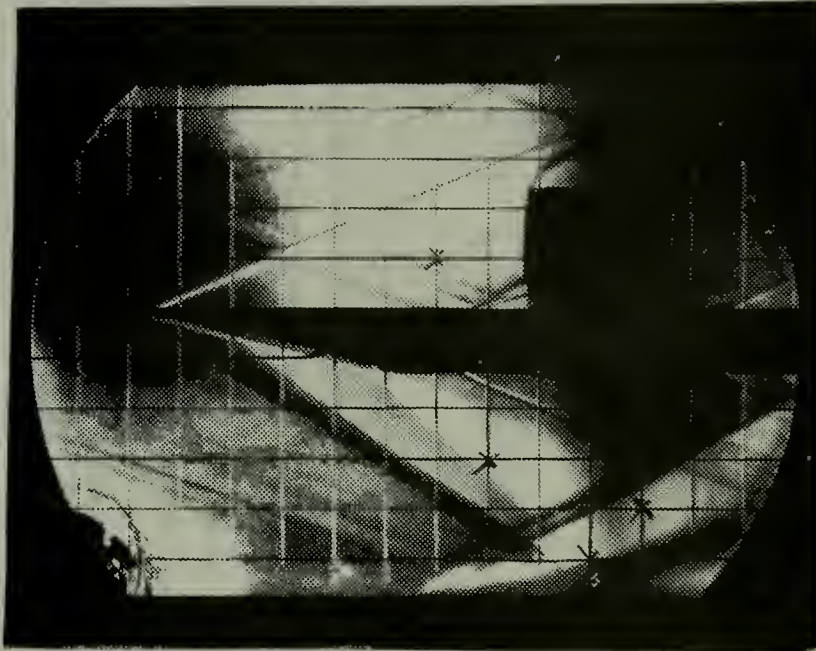
Figure 27.   Illustration of the Model Flow Network at Mach 2.84, 0°
Model Rotation and No Plate Vibration Using a Schlieren
System
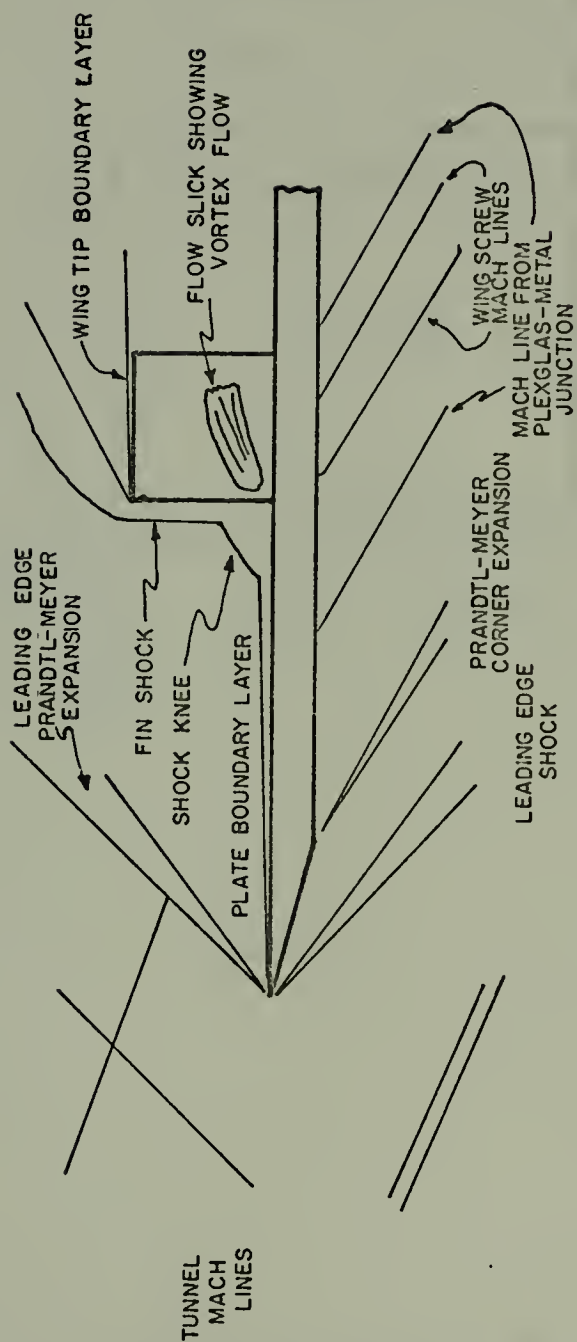
Figure 28. Schematic of the Flow Observed in the Schlieren Photographs

The diagram labels include: TUNNEL MACH LINES, LEADING EDGE PRANDTL-MEYER EXPANSION, FIN SHOCK, SHOCK KNEE, PLATE BOUNDARY LAYER, WING TIP BOUNDARY LAYER, FLOW SLICK SHOWING VORTEX FLOW, WING SCREW MACH LINES, MACH LINE FROM PLEXGLAS-METAL JUNCTION, PRANDTL-MEYER CORNER EXPANSION, LEADING EDGE SHOCK
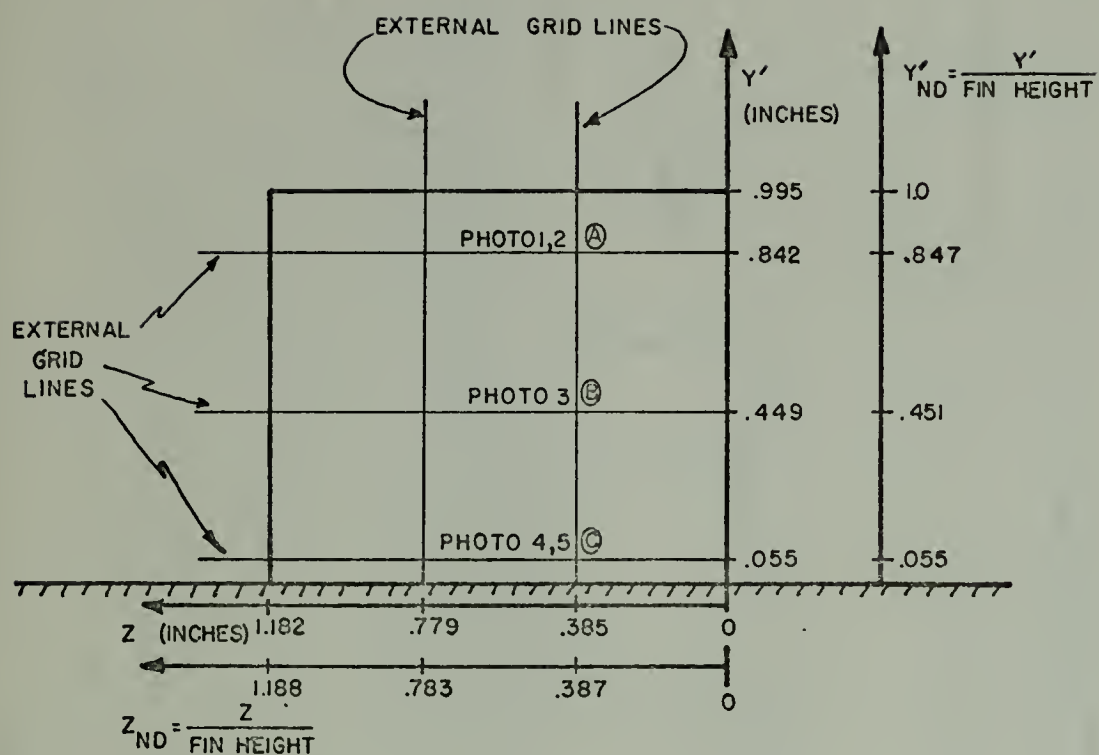
Figure 29. Schematic of the Fin at 0° Rotation Showing the Locations of the External Grid Lines and of the Interferogram Photographic Points
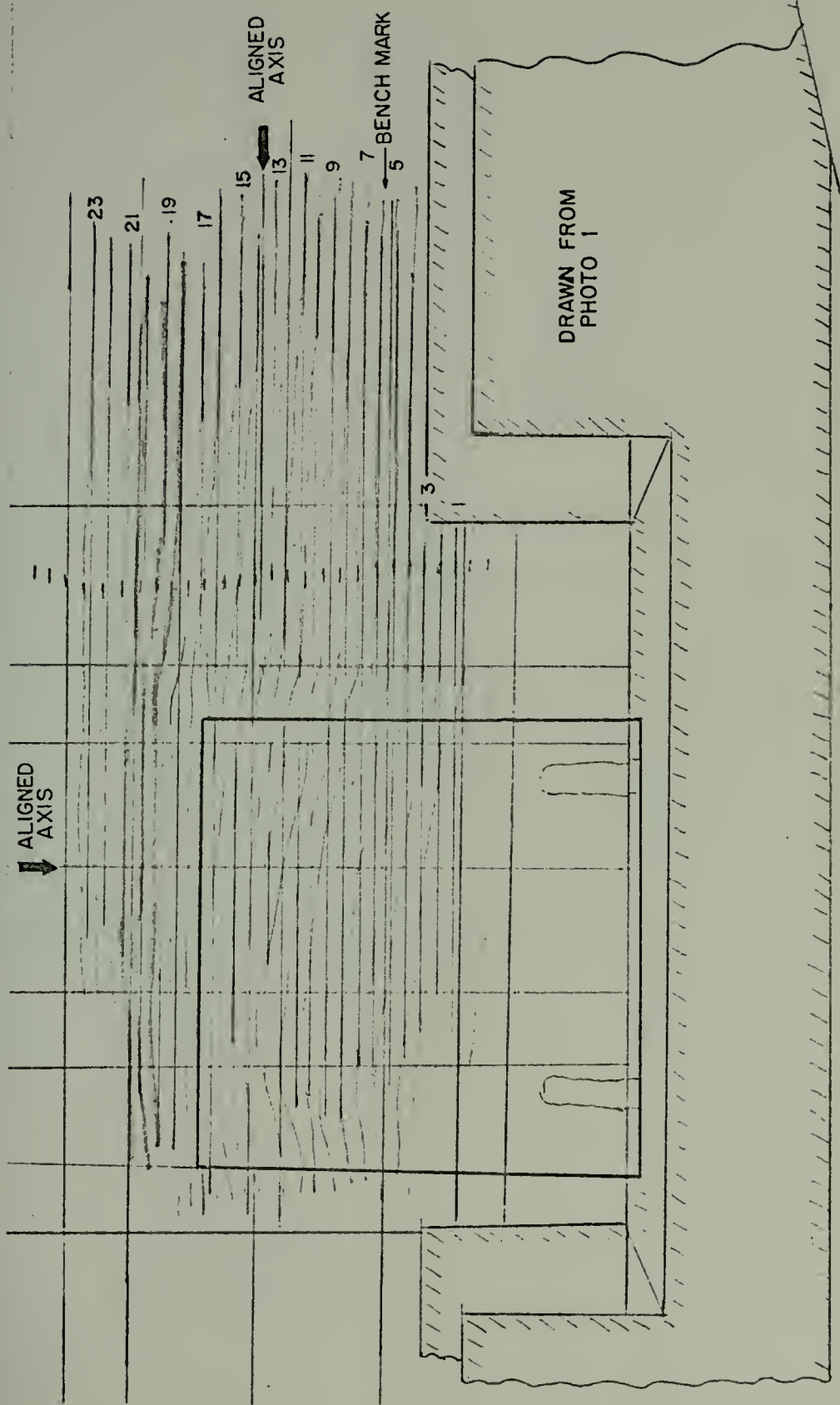
Figure 30. Actual Drawing and Data Reduction of Interferogram Photograph 1 Aligned at Z = 0.387, Y' = 0.847 for Mach 2.84 and 0° Model Rotation Angle
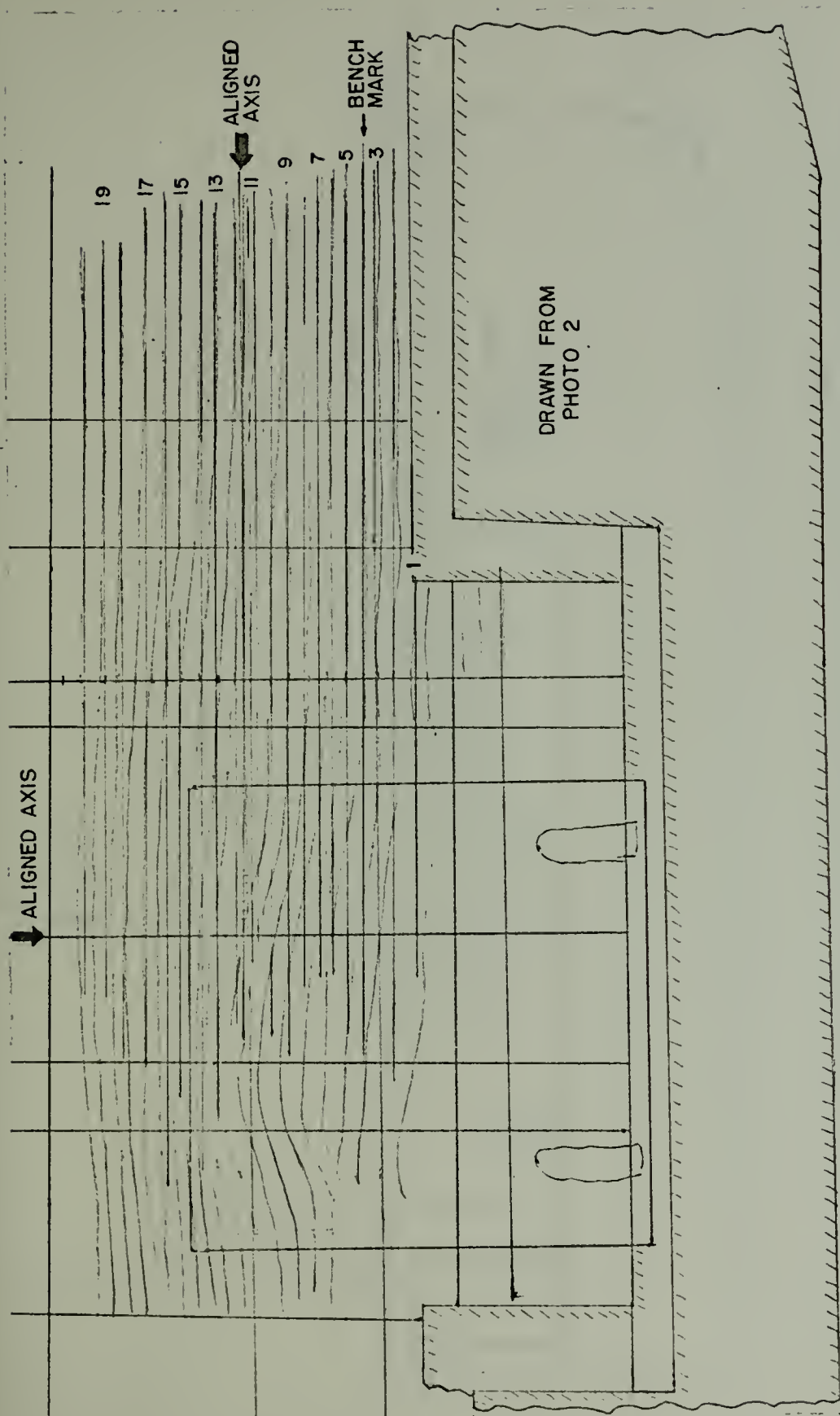
Figure 31. Actual Drawing and Data Reduction of Interferogram Photograph 2 Aligned at Z = 0.387, Y' = 0.847 for Mach 2.84 and 0° Model Rotation Angle
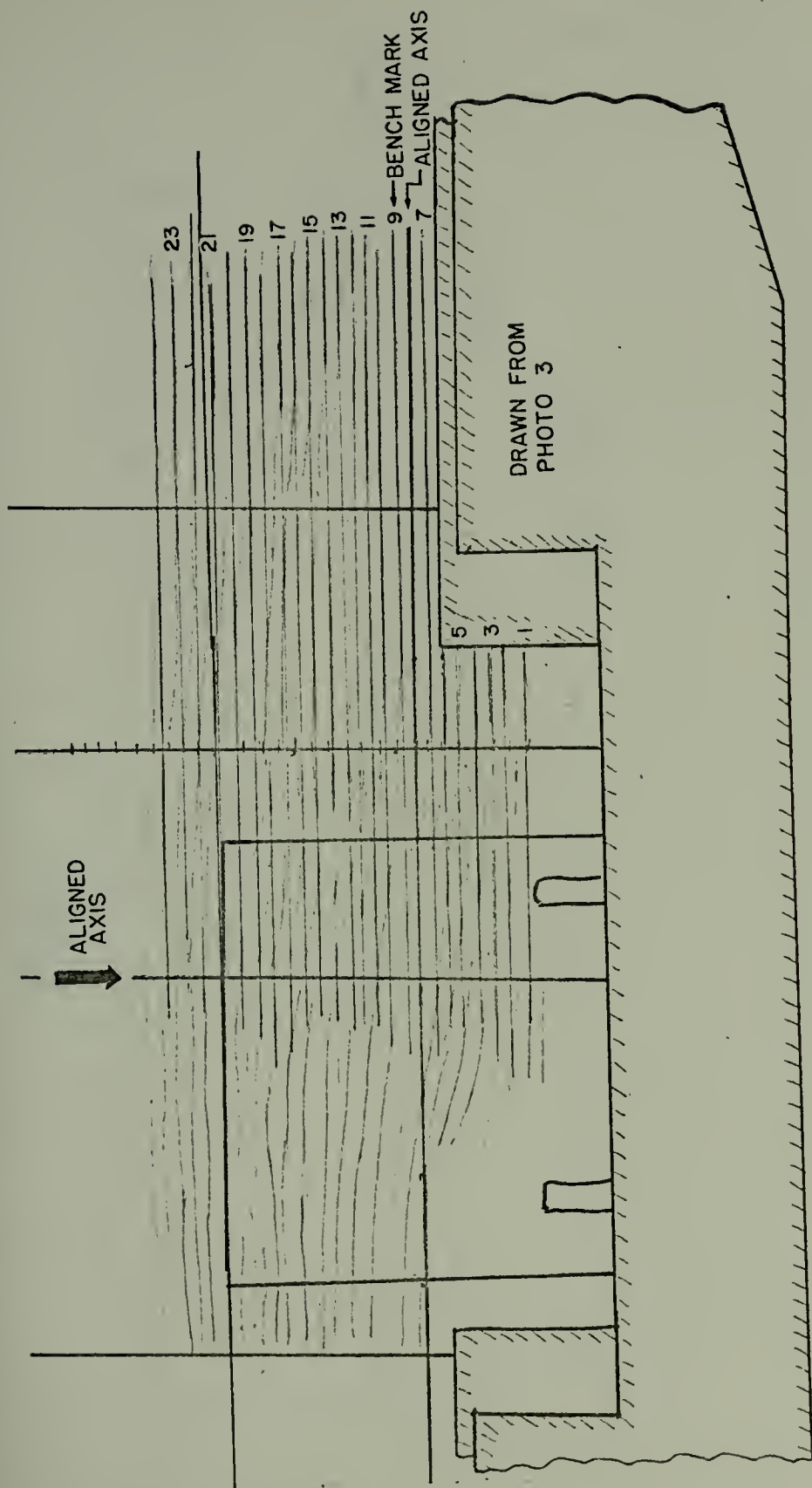
Figure 32. Actual Drawing and Data Reduction of Interferogram Photograph 3 Aligned at Z = 0.381, Y' = 0.451 for Mach 2.84 and 0° Model Rotation Angle

71
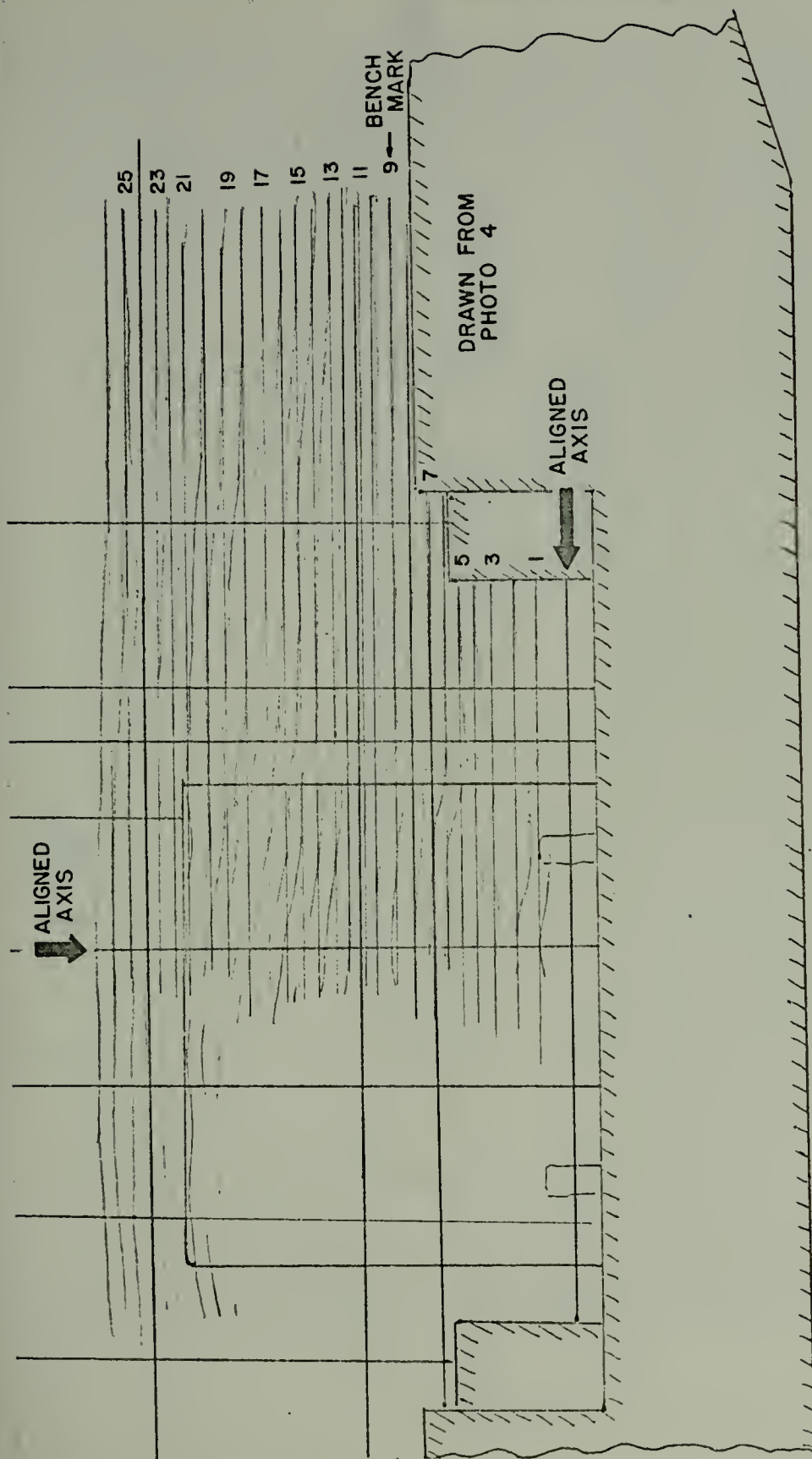
Figure 33. Actual Drawing and Data Reduction of Interferogram Photograph 4 Aligned at Z = 0.387, Y' = 0.055 for Mach 2.84 and 0° Model Rotation Angle
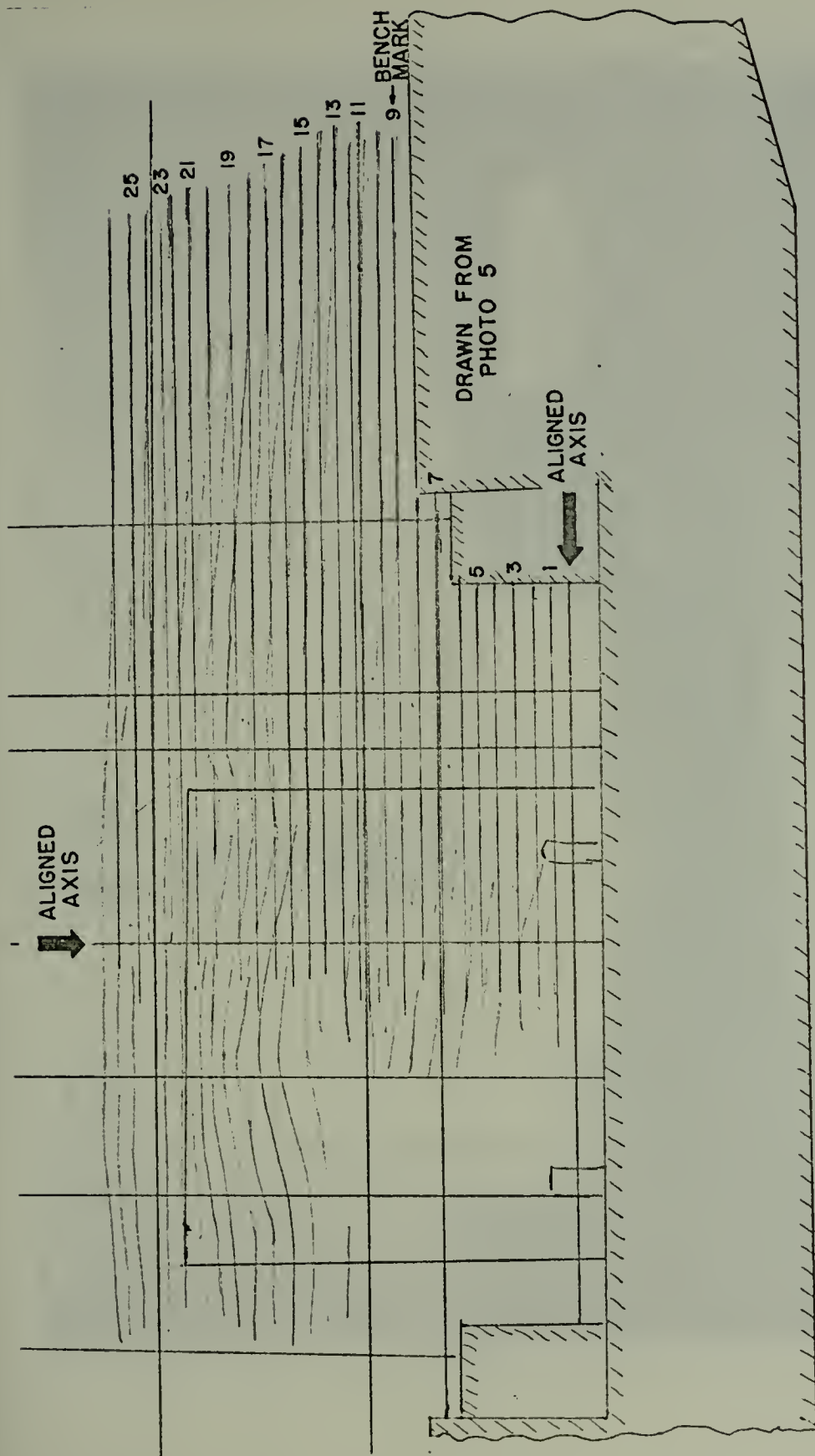
Figure 34. Actual Drawing and Data Reduction of Interferogram Photograph 5 Aligned at Z = 0.387, Y' = 0.055 for Mach 2.84 and 0° Model Rotation Angle

73
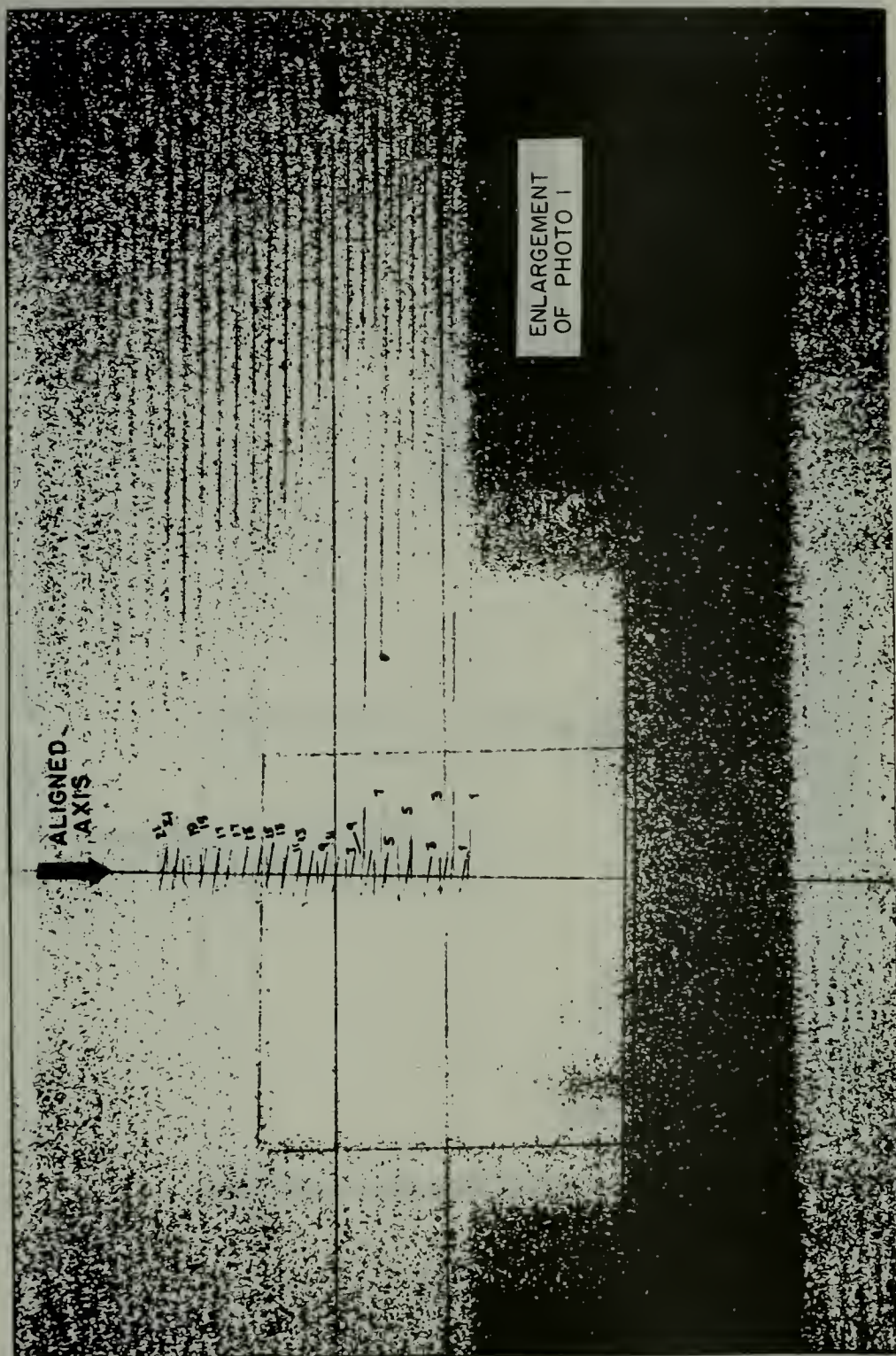
Figure 35. Actual Enlarged Photograph Used for the Data Reduction of Interferogram Photograph 1
Aligned at Z = 0.387, Y' = 0.847 for Mach 2.84 and $0°$ Model Rotation Angle
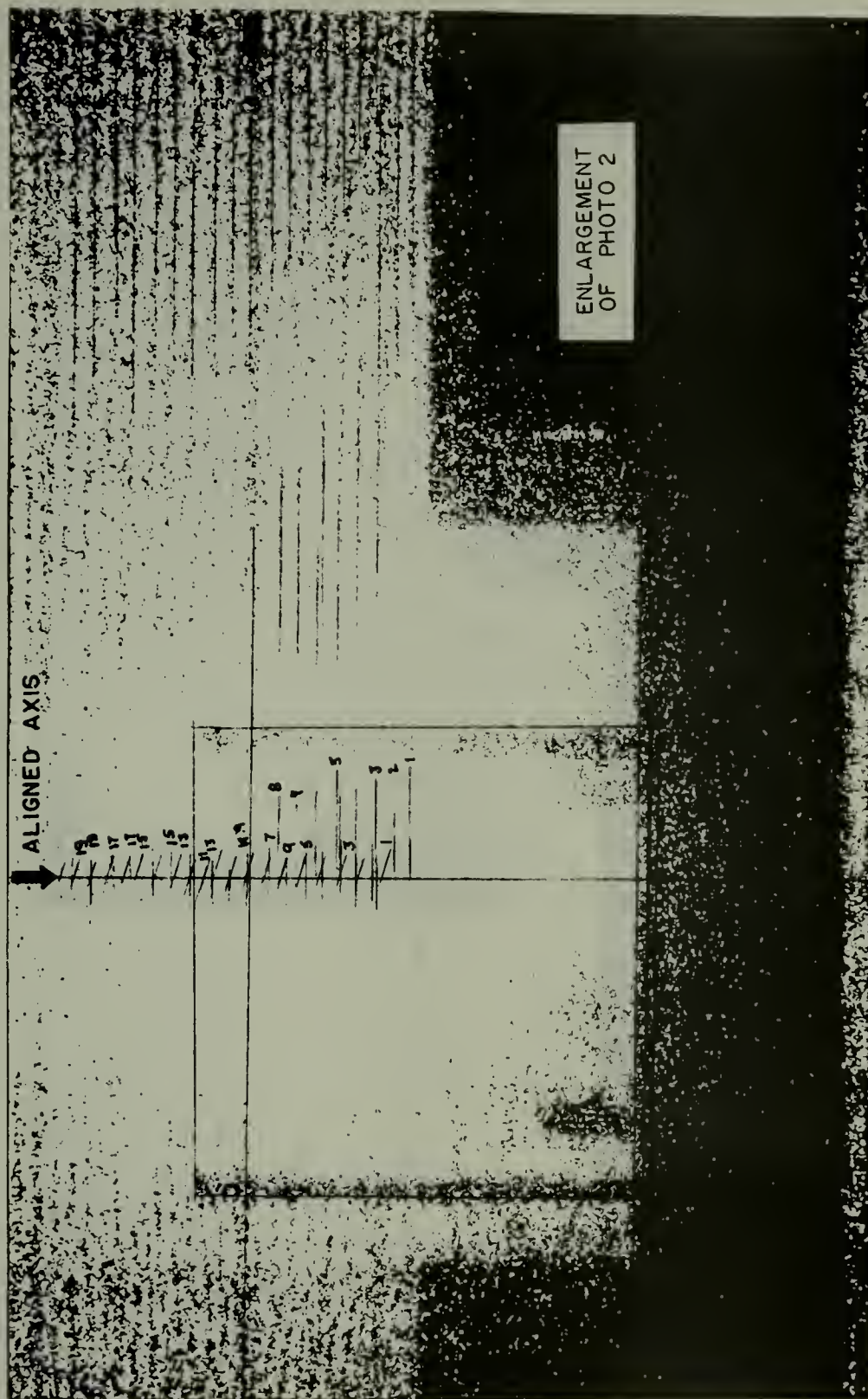
Figure 36. Actual Enlarged Photograph Used for the Data Reduction of Interferogram Photograph 2
Aligned at Z = 0.387, Y' = 0.847 for Mach 2.84 and 0° Model Rotation Angle
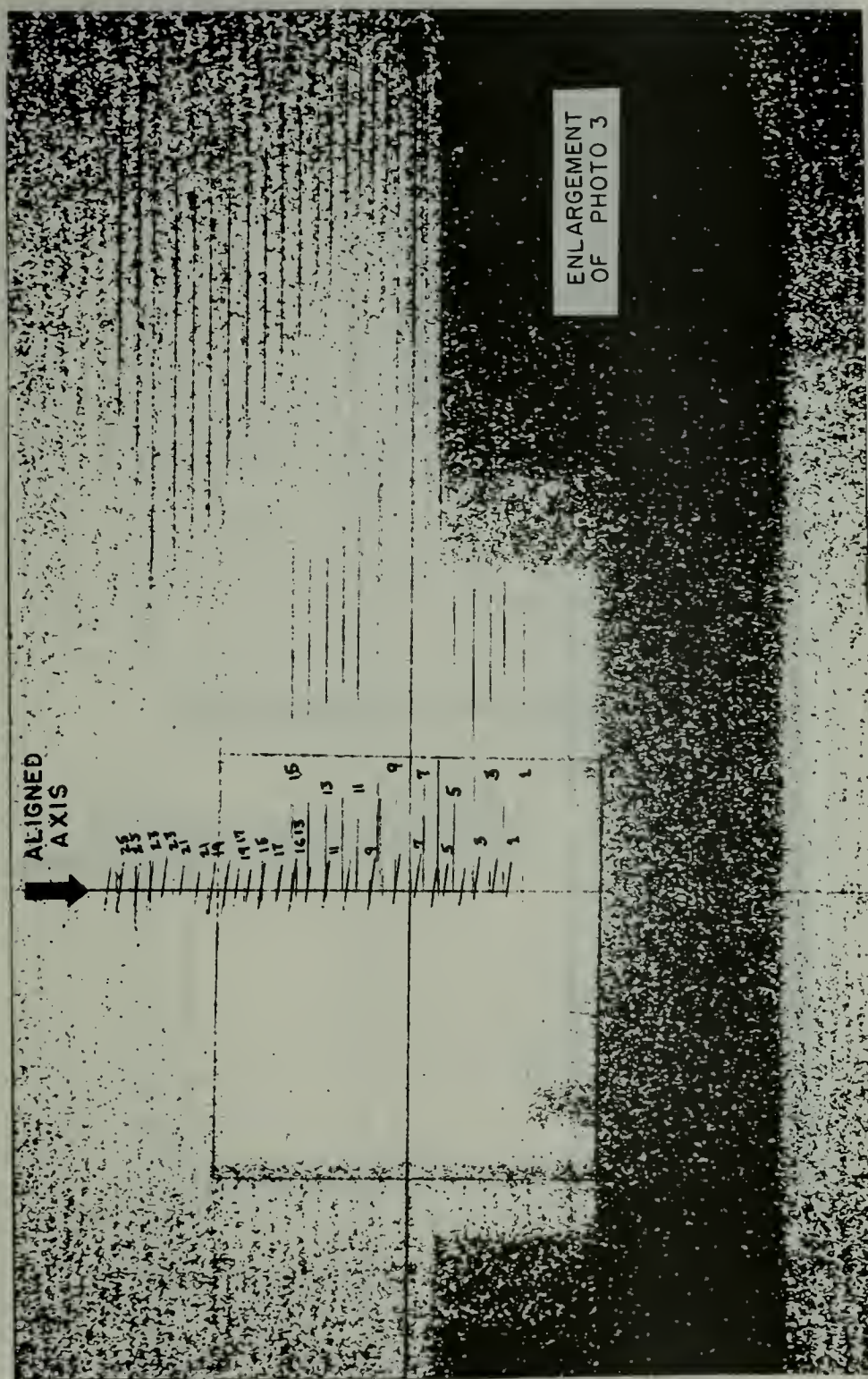
Figure 37. Actual Enlarged Photograph Used for the Data Reduction of Interferogram Photograph 3
Aligned at Z = 0.387, Y' = 0.451 for Mach 2.84 and 0 Model Rotation Angle

76

Figure 38. Actual Enlarged Photograph Used for the Data Reduction of Interferogram Photograph 4 Aligned at Z = 0.387, Y' = 0.055 for Mach 2.84 and 0° Model Rotation Angle
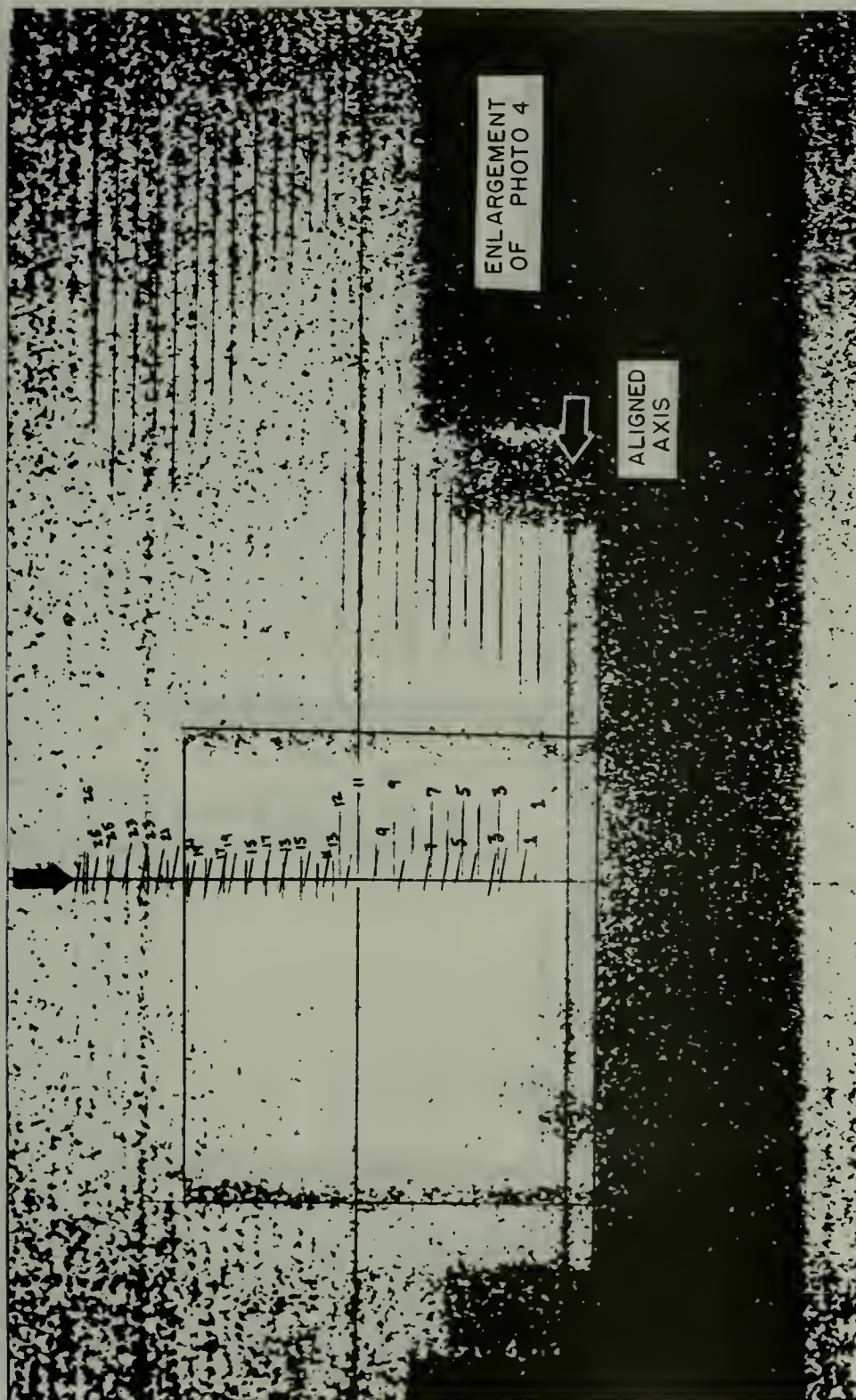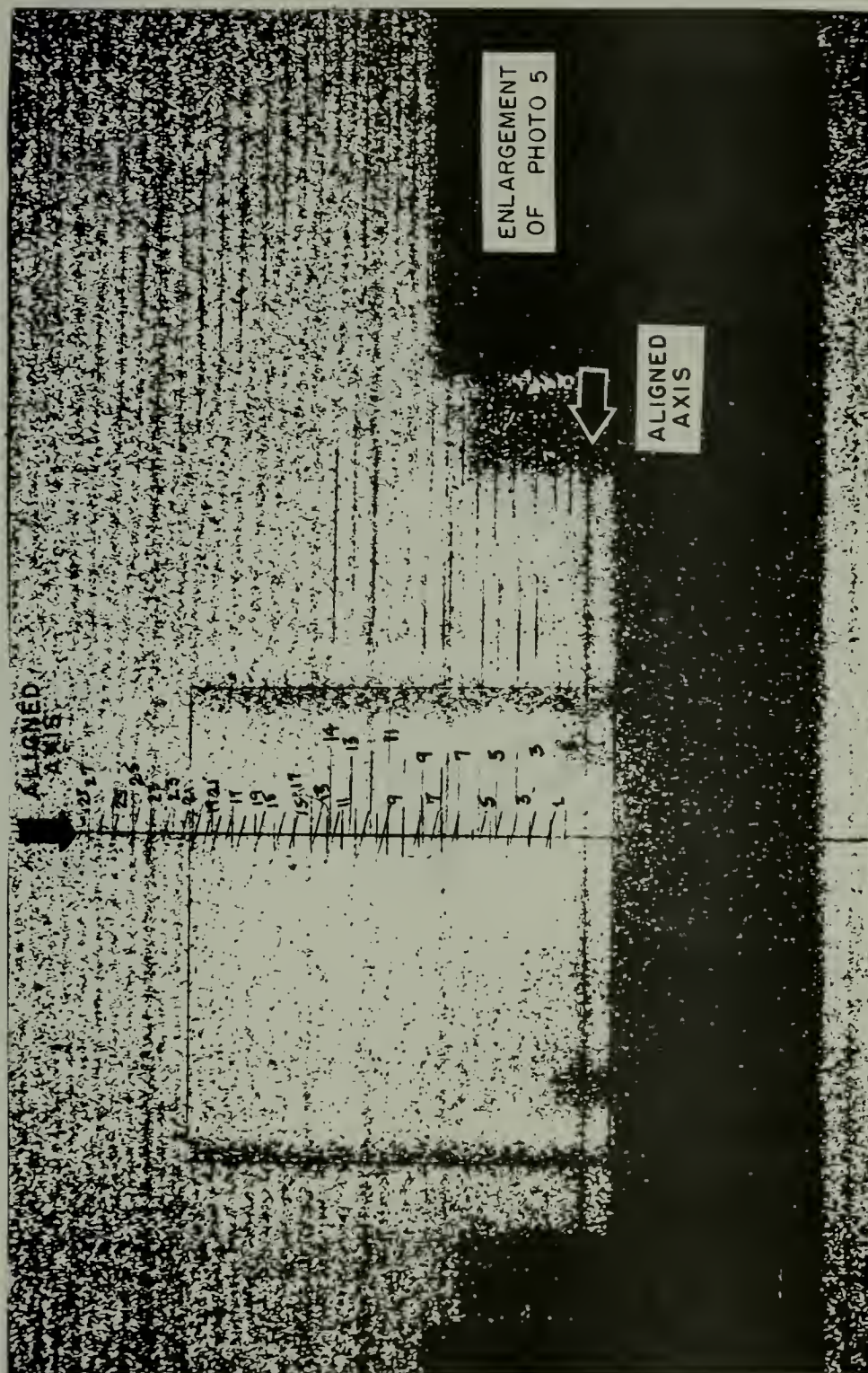
Figure 39. Actual Enlarged Photograph Used for the Data Reduction of Interferogram Photograph 5 Aligned at Z = 0.387, Y' = 0.055 for Mach 2.84 and 0° Model Rotation Angle

Figure 40. Comparison of Fringe Data Obtained from Drawings of
Interferogram Photographs 1 and 2 Aligned at Y' = 0.847

Figure 41. Comparison of Fringe Data Obtained from Photographic
Enlargements of Interferogram Photographs 1 and 2 Aligned
at Y' = 0.847
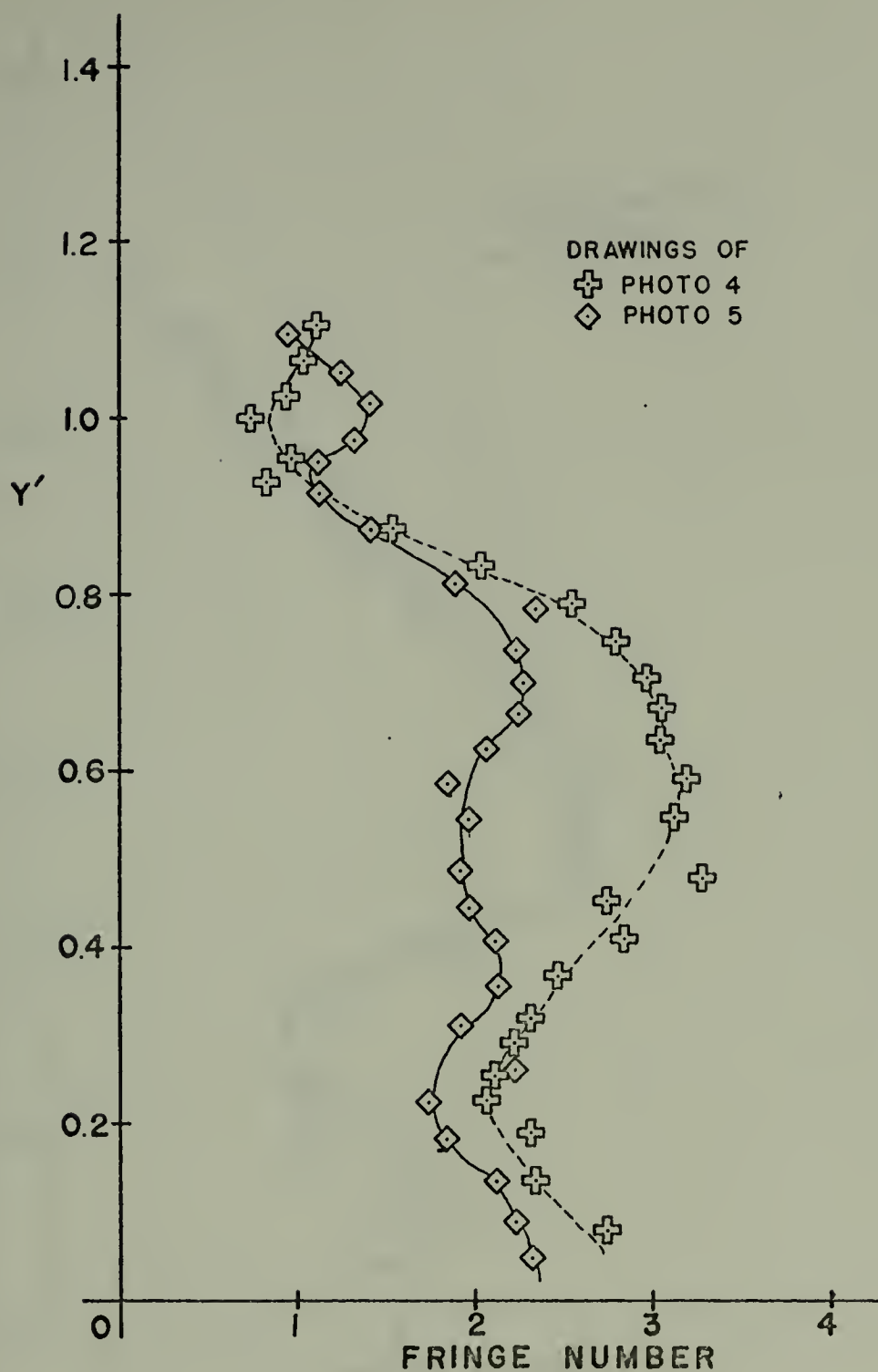
Figure 42.   Comparison of Fringe Data Obtained from Drawings of
Interferogram Photographs 4 and 5 Aligned at Y' = 0.055
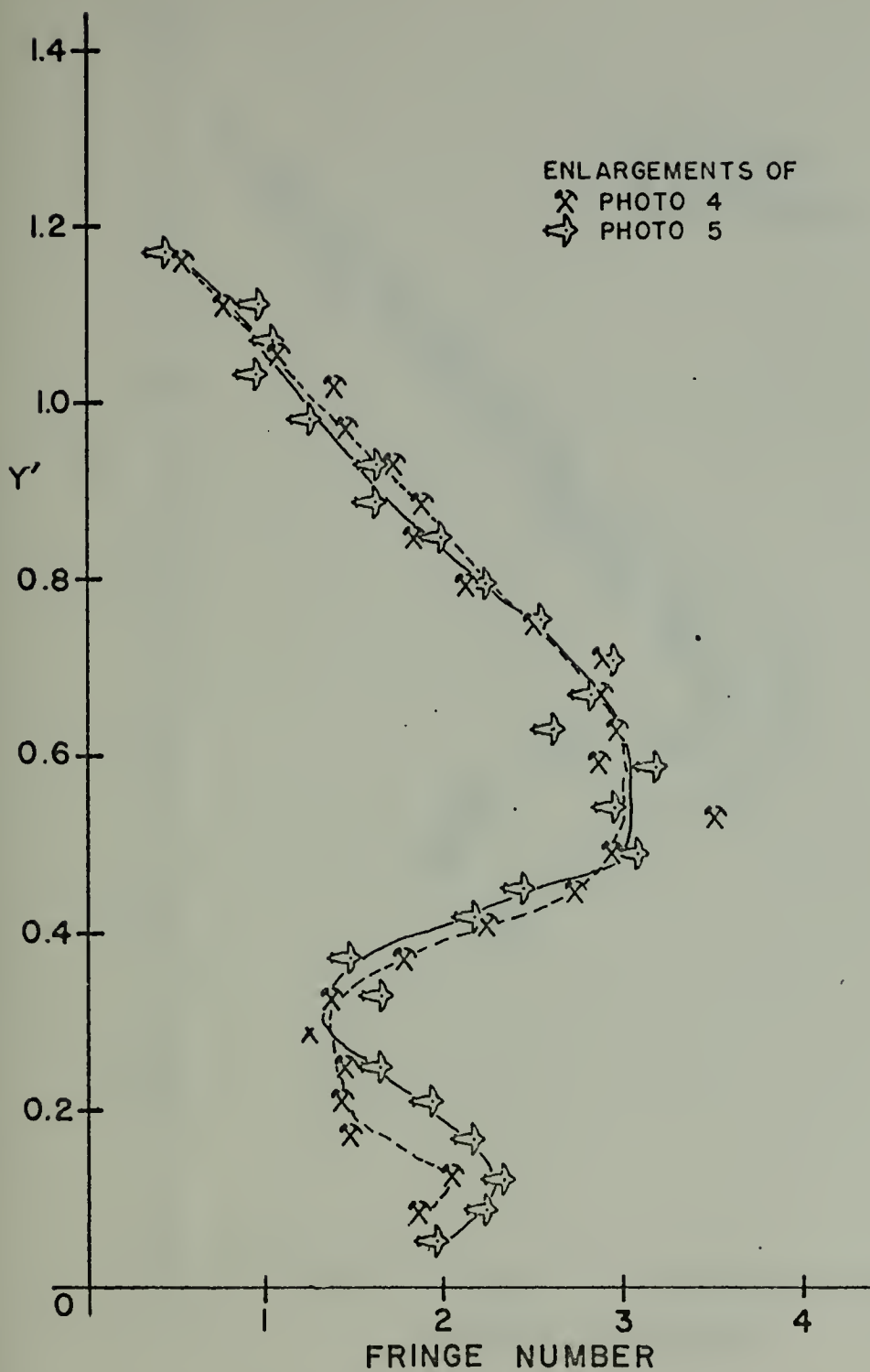
Figure 43. Comparison of Fringe Data Obtained from Photographic
Enlargements of Interferogram Photographs 4 and 5 Aligned
at Y' = 0.055
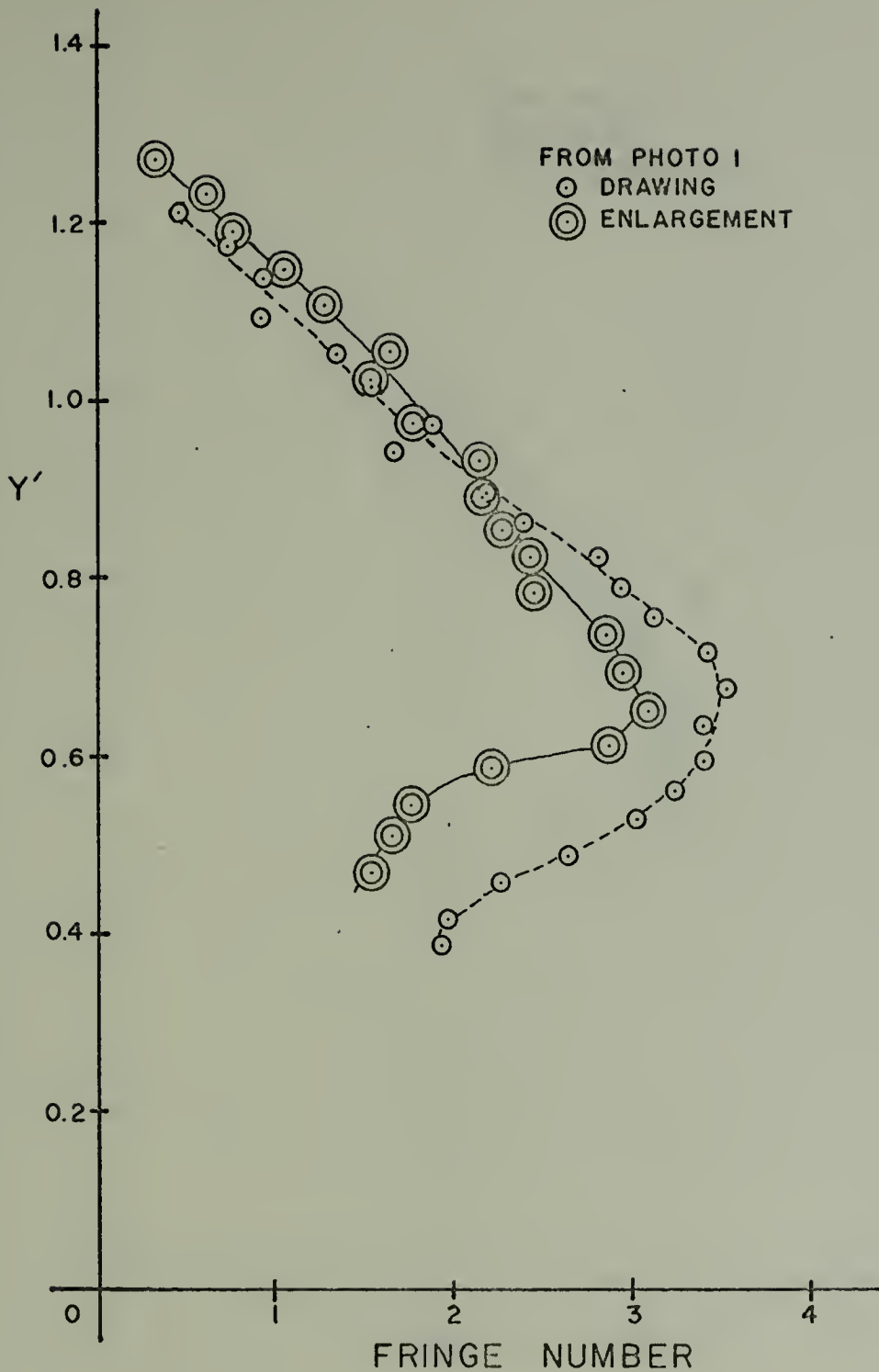
Figure 44. Comparison of Fringe Data Obtained from the Drawing and
Photographic Enlargement of Interferogram Photograph 1
Aligned at Y' = 0.847
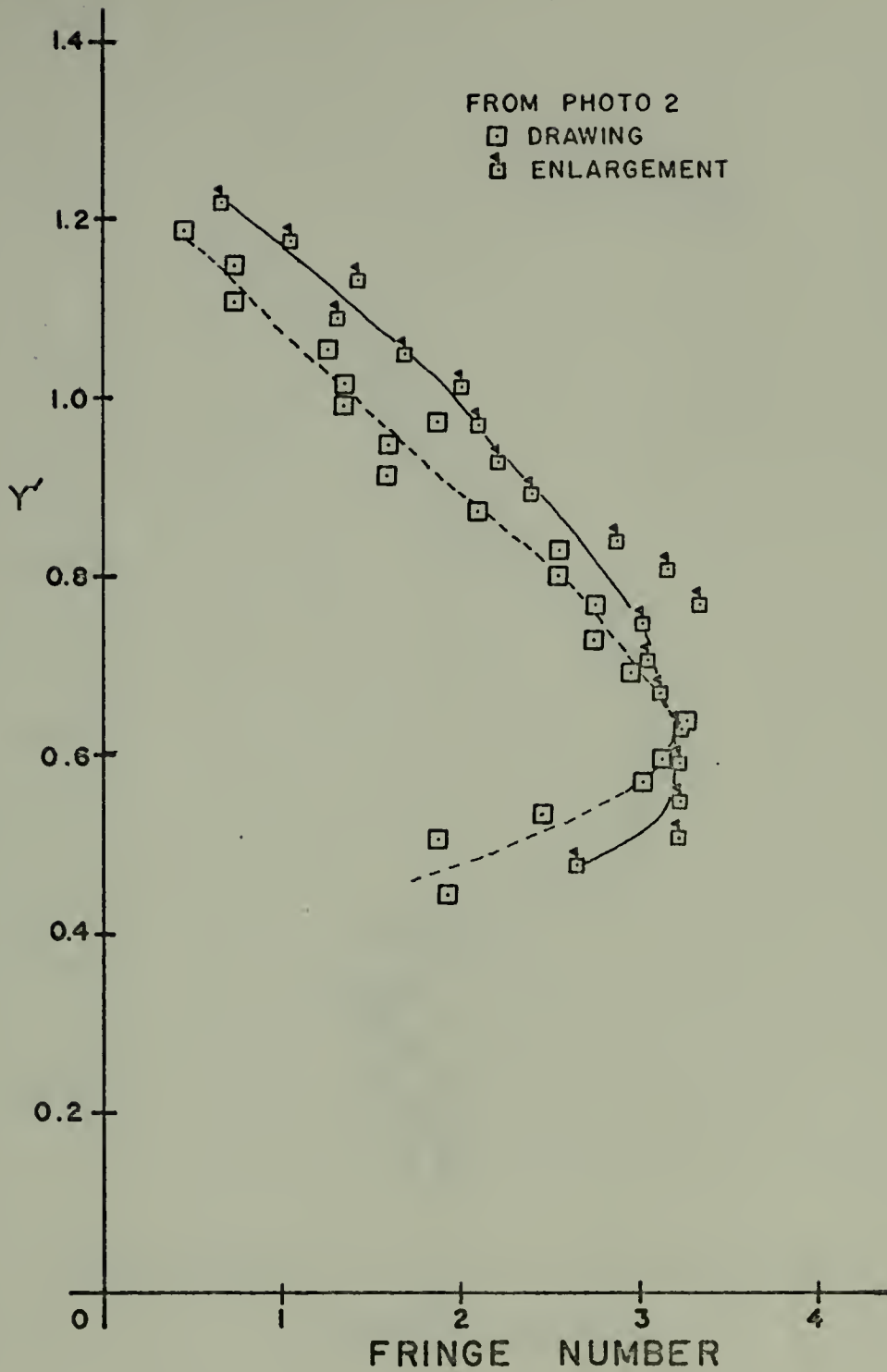
Figure 45. Comparison of Fringe Data Obtained from the Drawing and Photographic Enlargement of Interferogram Photograph 2 Aligned at Y' = 0.847
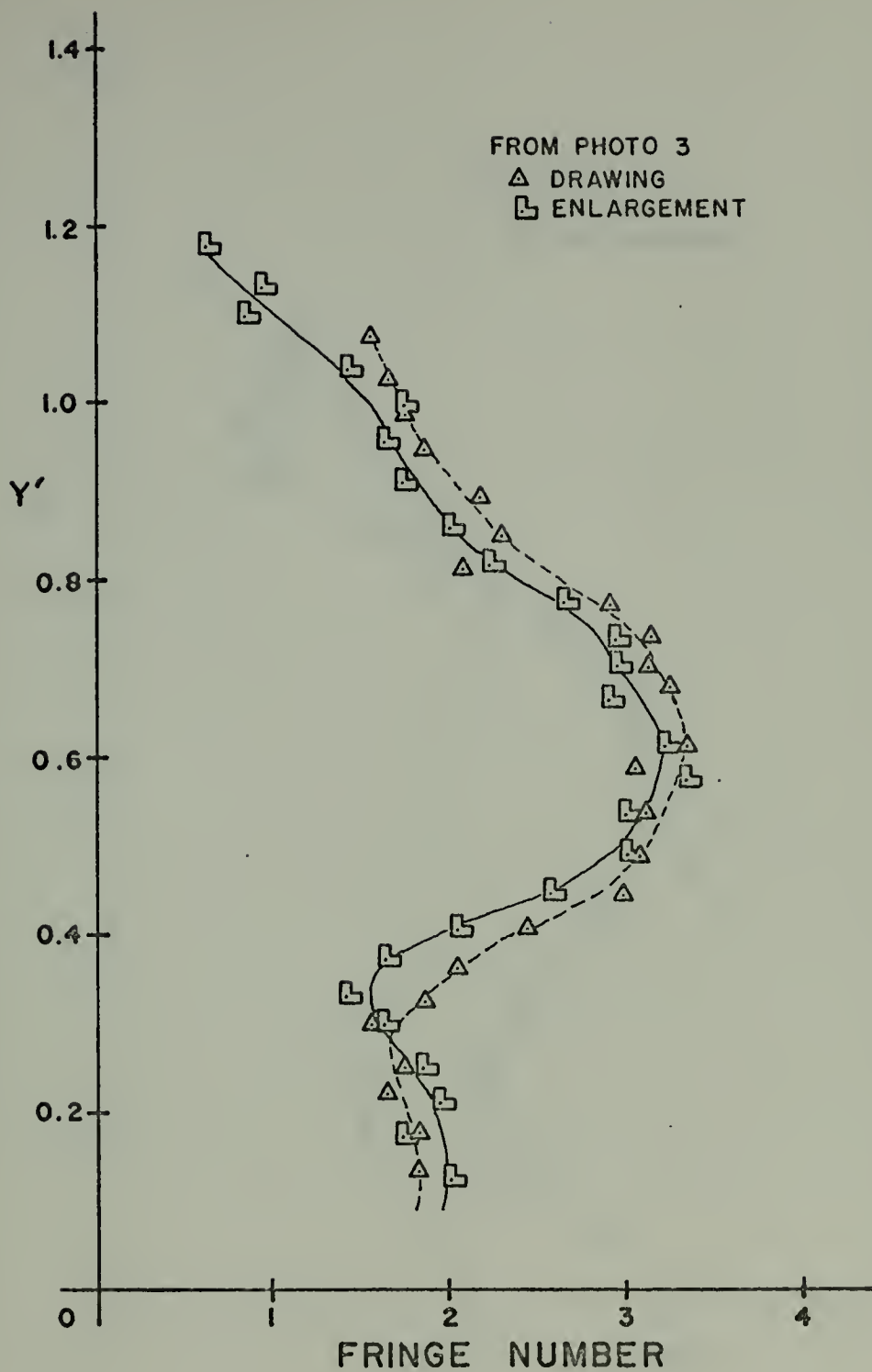
Figure 46.   Comparison of Fringe Data Obtained from the Drawing and
Photographic Enlargement of Interferogram Photograph 3
Aligned at Y' = 0.451

85
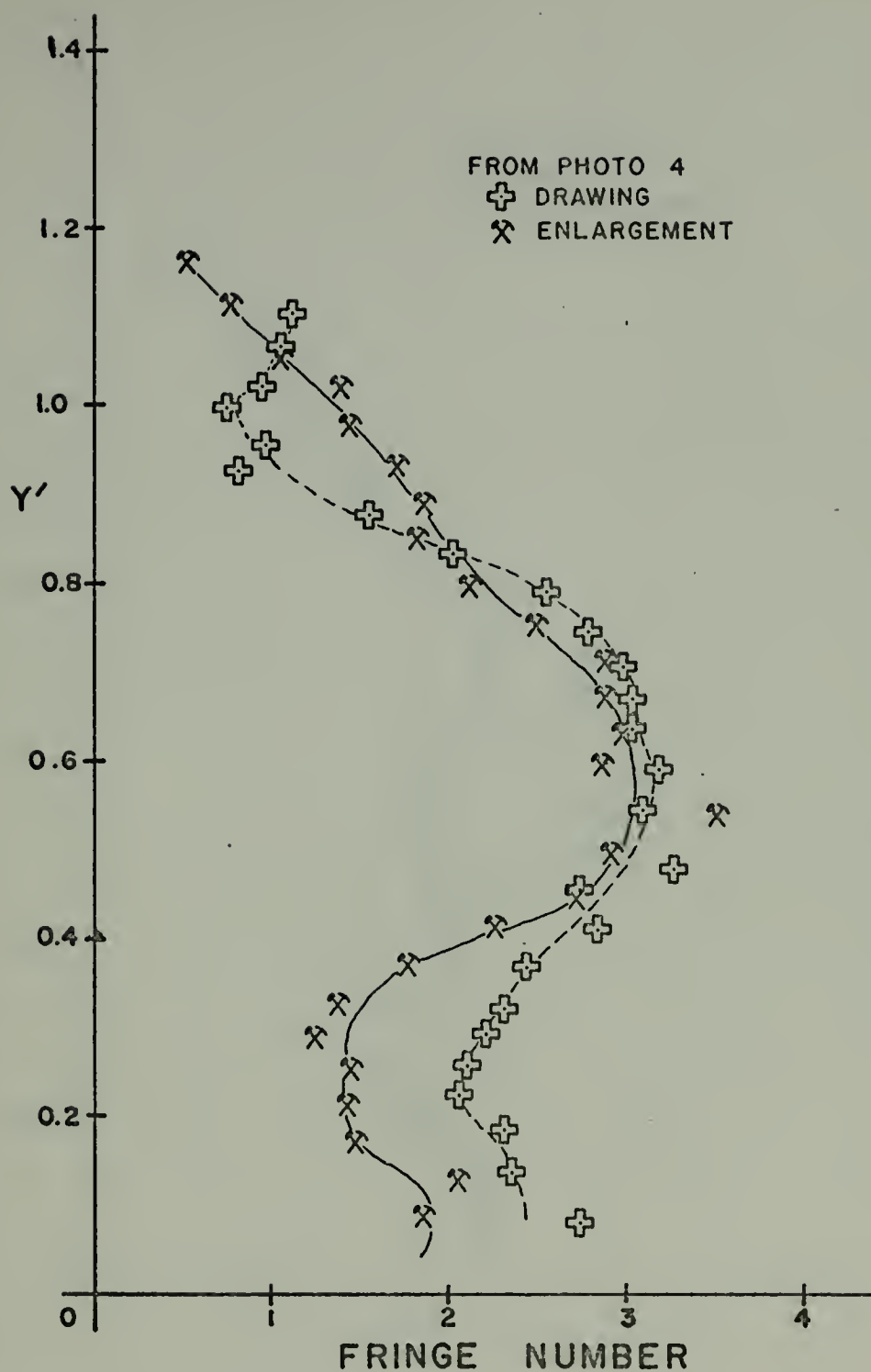
Figure 47. Comparison of Fringe Data Obtained from the Drawing and Photographic Enlargement of Interferogram Photograph 4 Aligned at Y' = 0.055
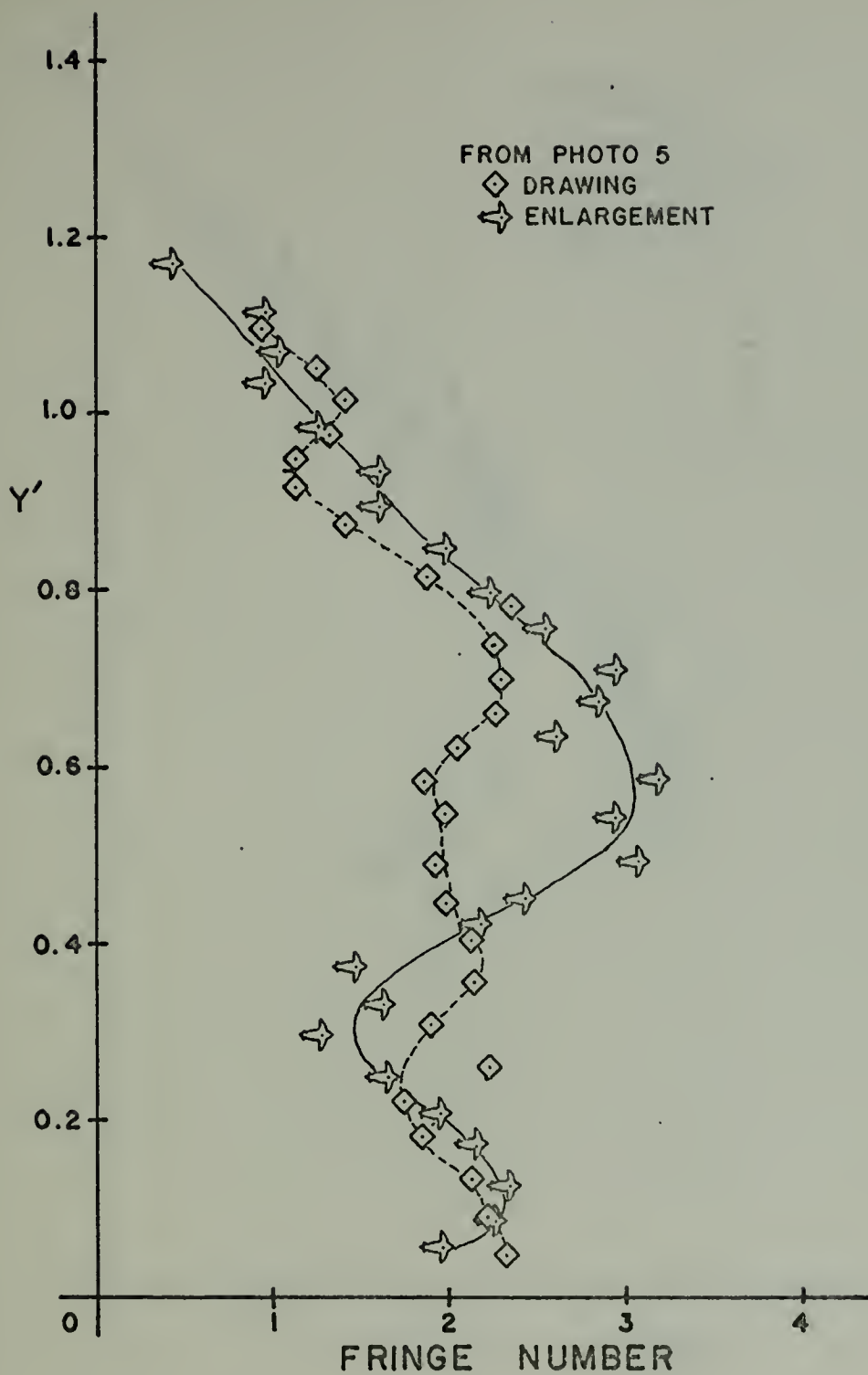
Figure 48. Comparison of Fringe Data Obtained from the Drawing and Photographic Enlargement of Interferogram Photograph 5 Aligned at Y' = 0.055
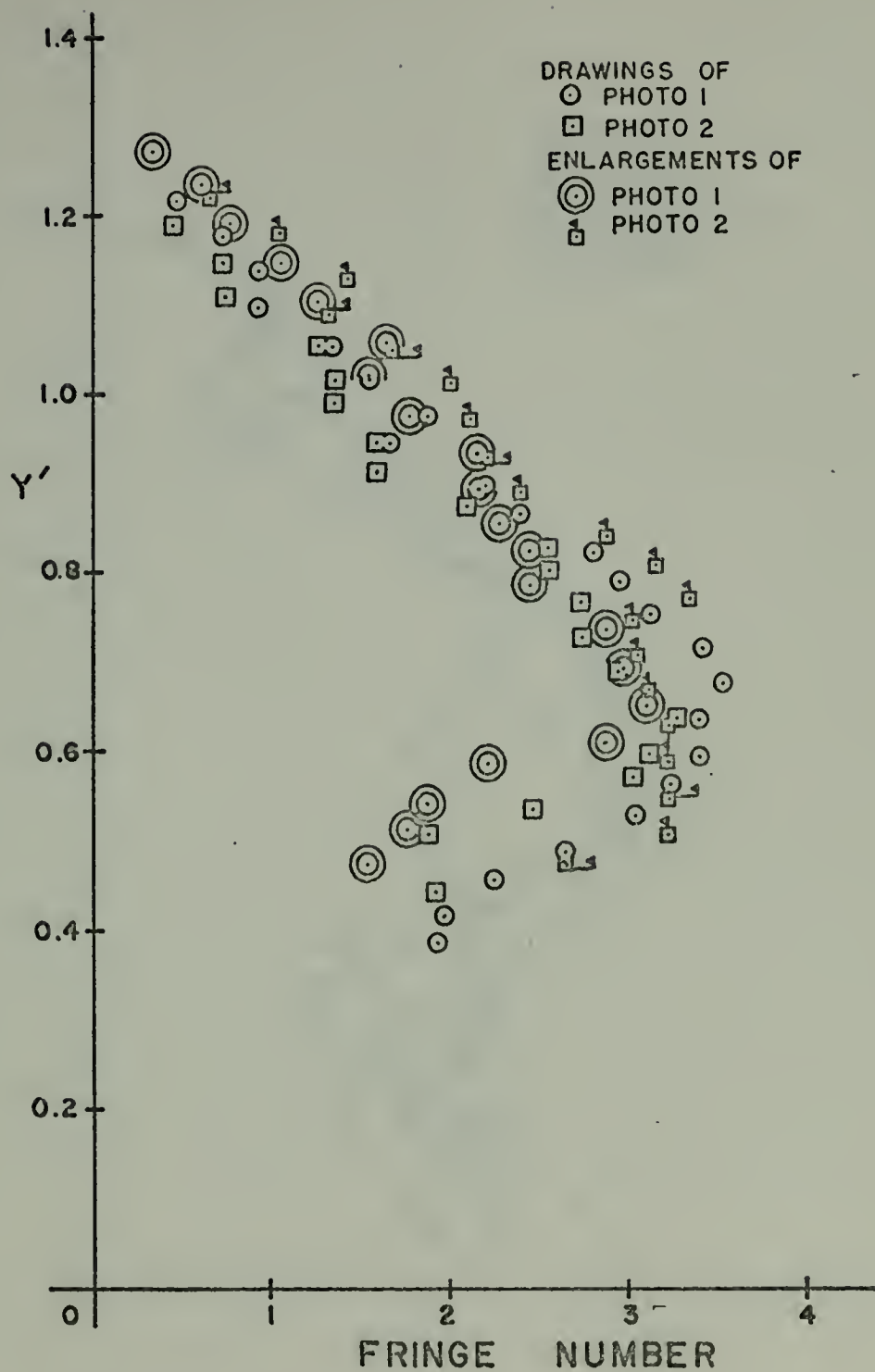
Figure 49. Comparison of Fringe Data Obtained from the Drawings and Photographic Enlargements of Interferogram Photographs 1 and 2 Aligned at Y' = 0.847
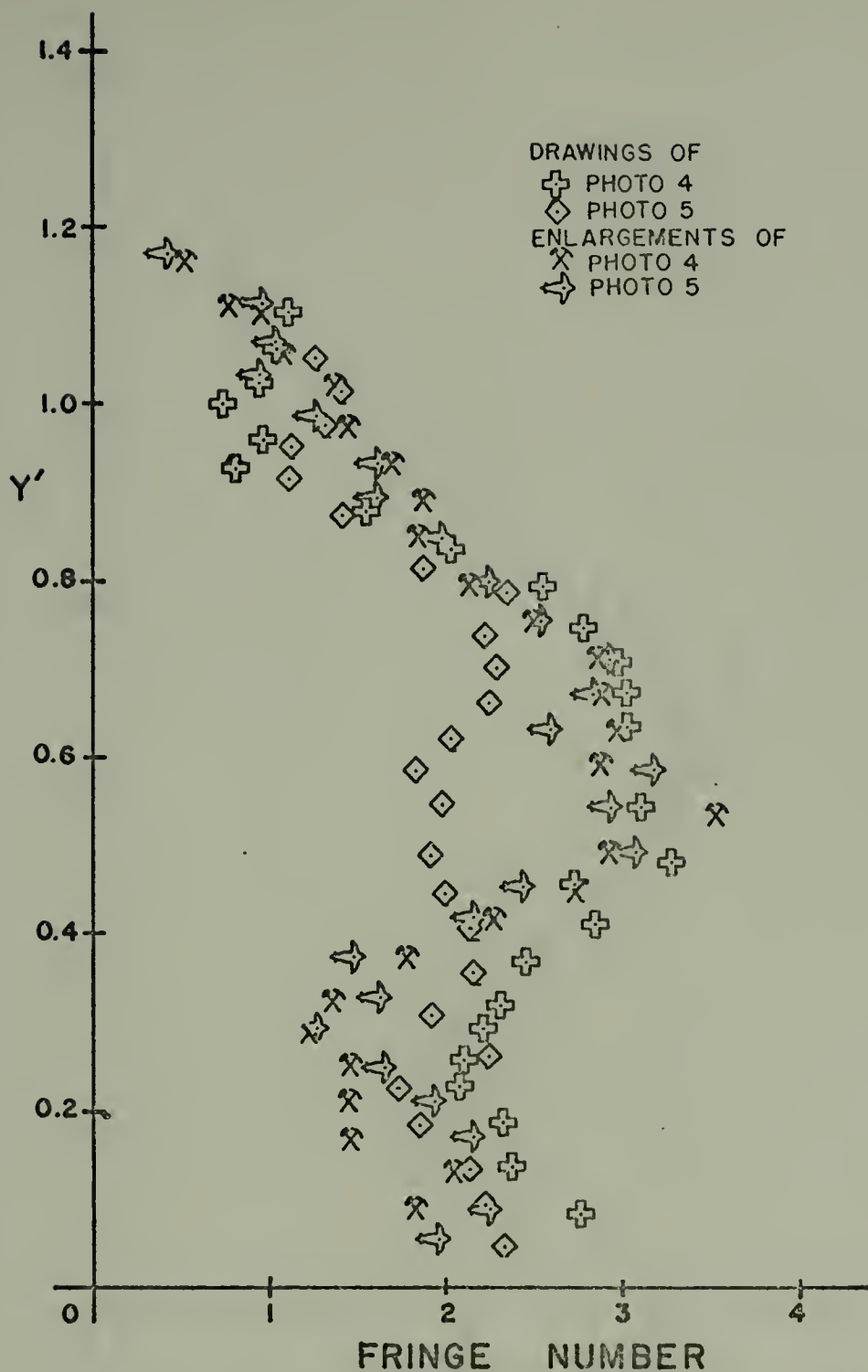
Figure 50. Comparison of Fringe Data Obtained from the Drawings and Photographic Enlargements of Interferogram Photographs 4 and 5 Aligned at Y' = 0.055
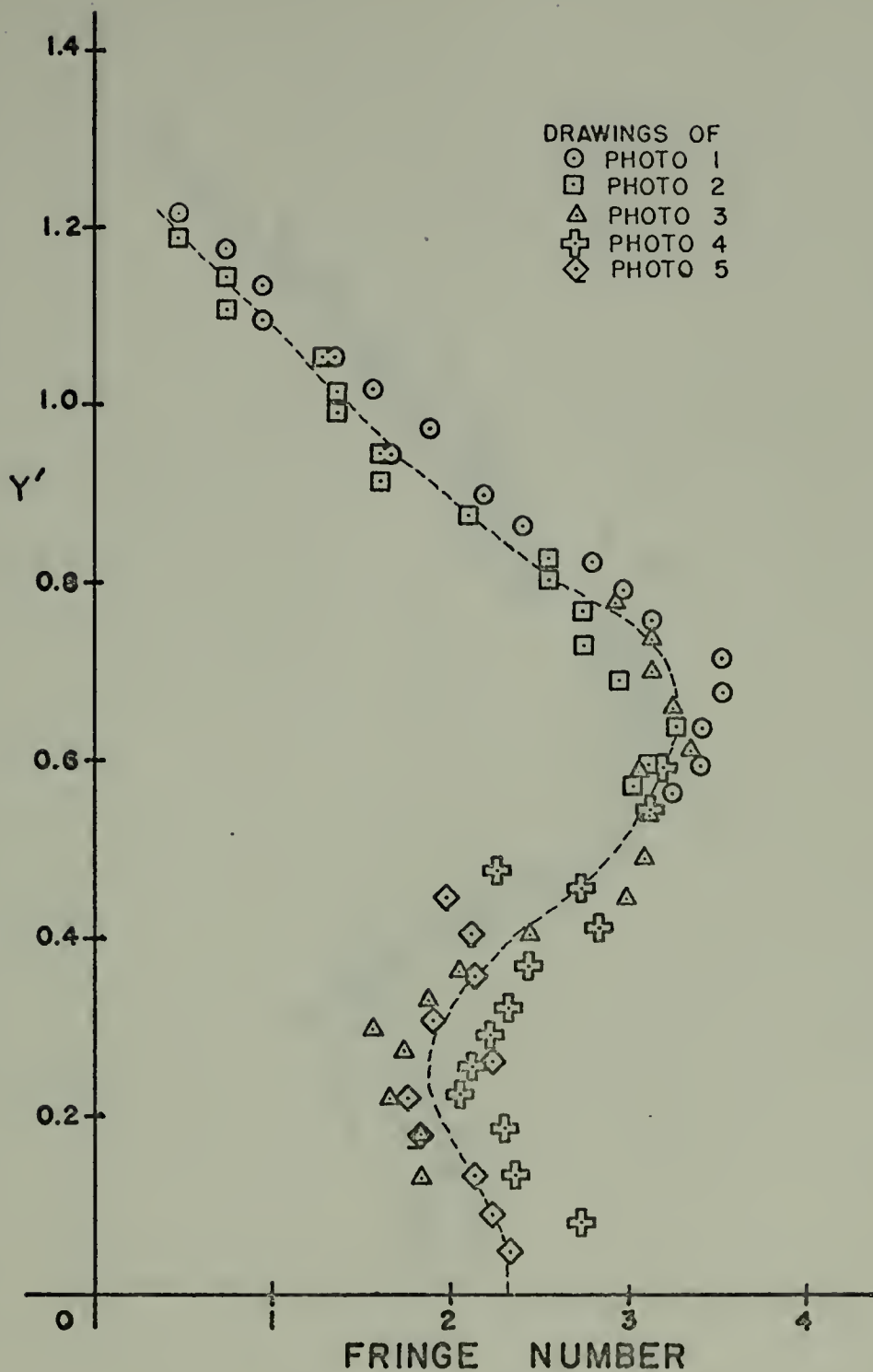
Figure 51. Fringe Number Across the Fin in the Z = 0.387 Plane for δ = 0°, Mach 2.84 as Determined from the Drawings of the Interferogram Photographs
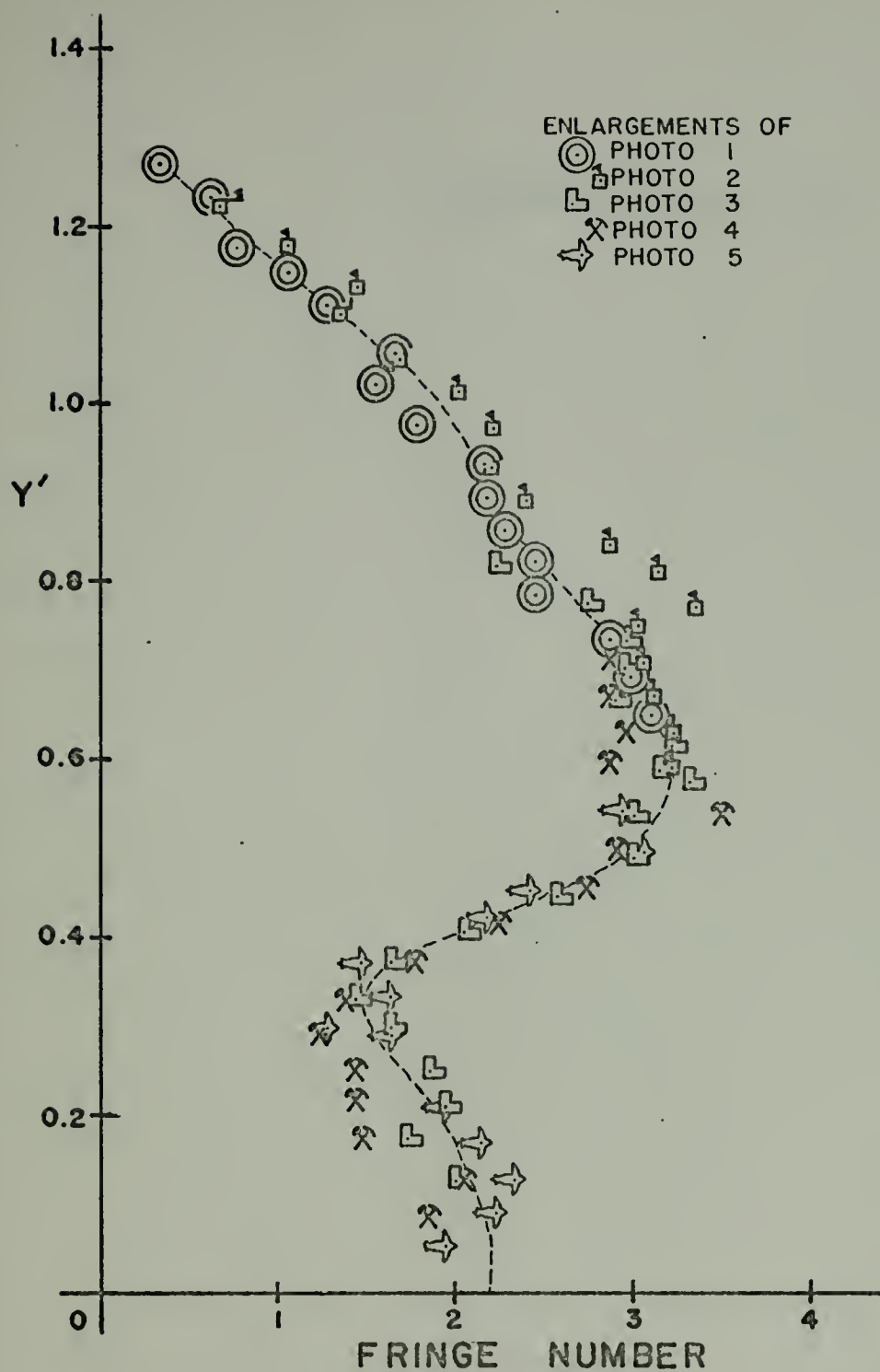
Figure 52. Fringe Number Across the Fin in the Z = 0.387 Plane for
§ = 0°, Mach 2.84 as Determined from the Photographic
Enlargements of the Interferogram Photographs

91
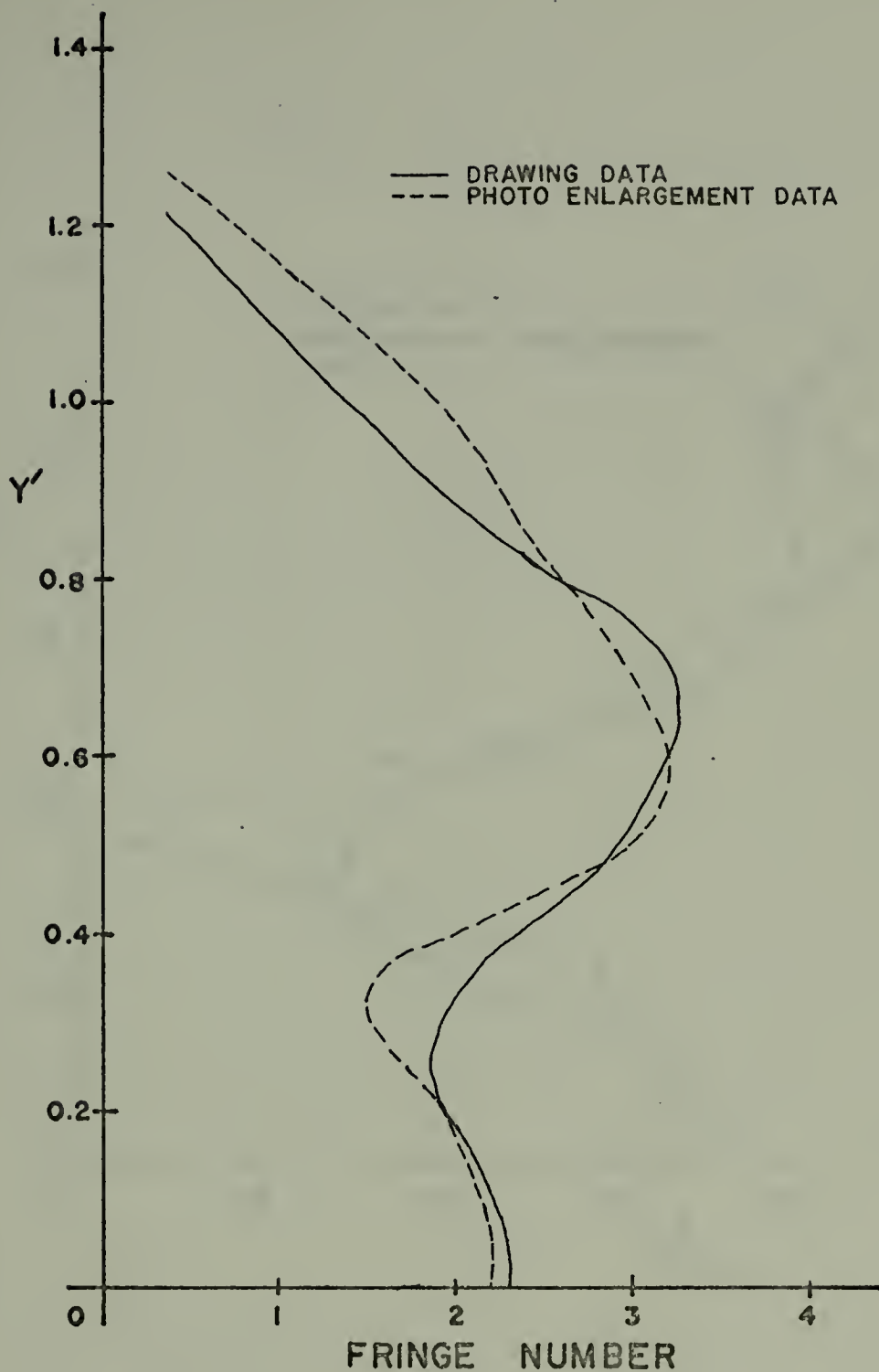
Figure 53.   Comparison of the Fringe Numbers Across the Fin in the
Z = 0.387 Plane for ξ = 0°, Mach 2.84 as Determined
from the Drawings and Photographic Enlargements of the
Interferogram Photographs
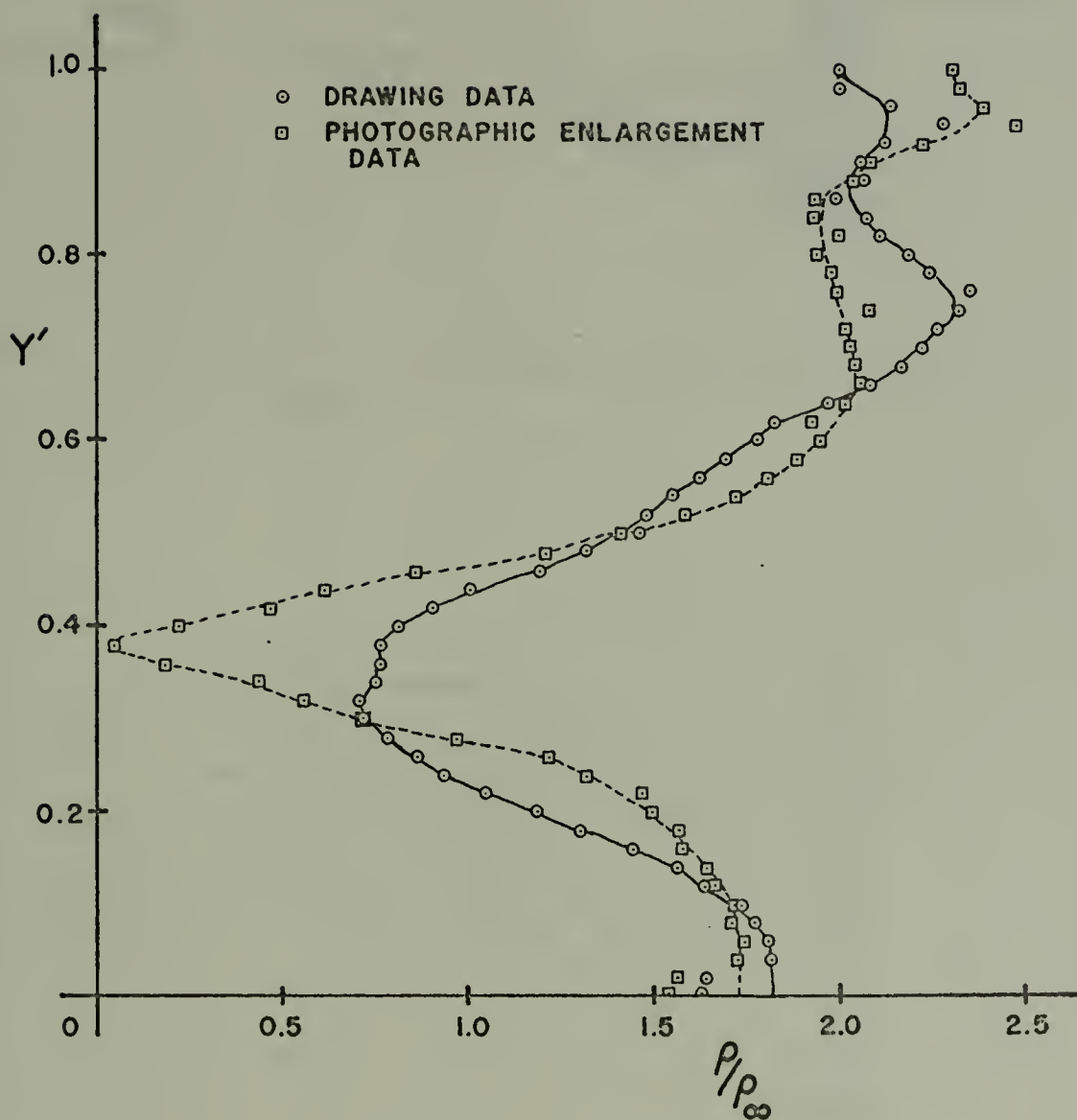
Figure 54. Comparison of the Density Distributions Calculated by HOLOVLR for an Axisymmetric Case

93
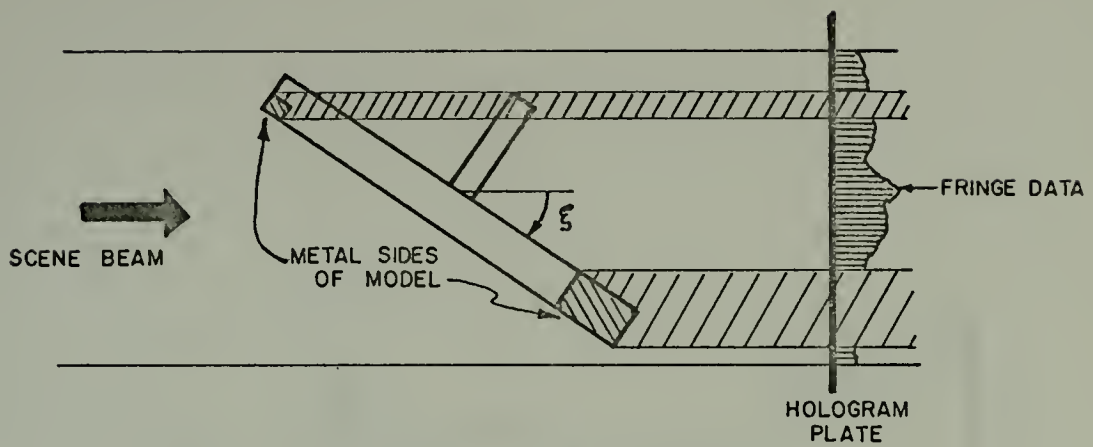
Figure 55. Schematic of the Model Center Section Rotated to Illustrate the Loss of Fringe Information Due to Model Shadows on the Hologram
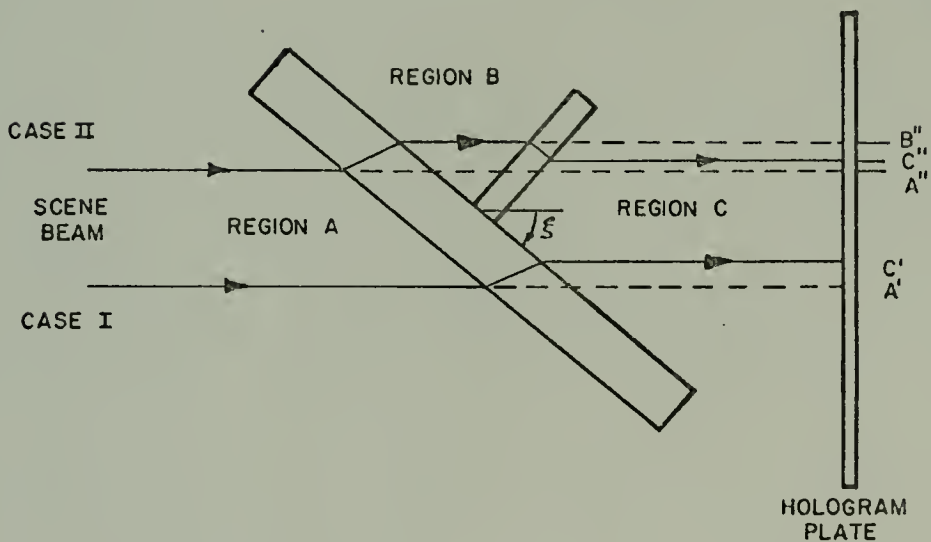
Figure 56. Schematic Illustrating the Problem of Different Fringe Information Being Superimposed on One Beam Caused by the Model Plastic
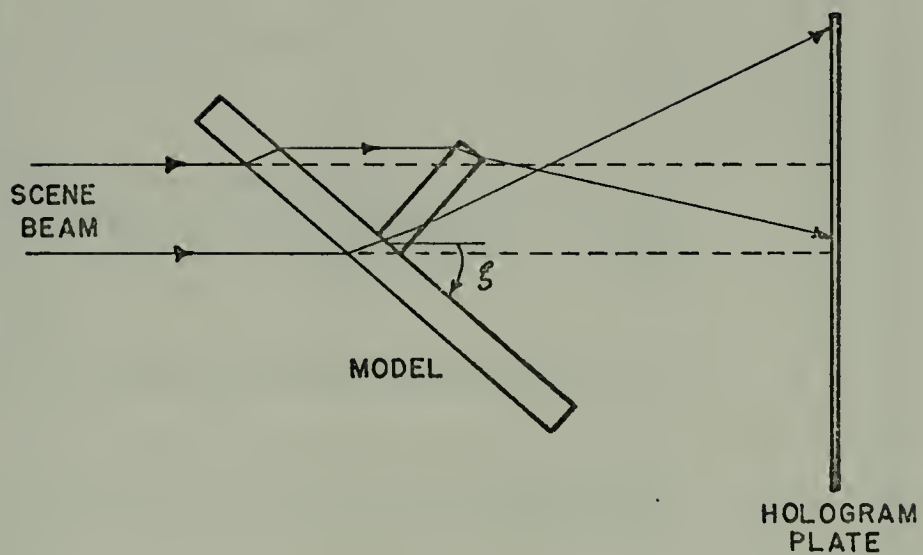
Figure 52. Schematic Illustrating the Scene Beam Refraction in the Fin Root and Tip Areas

Table I. Tabulation of Fringe Shift Data Taken From the Drawing of Photo 4

Line No.	Distance Above Aligned Plane			Y' $\odot = \odot + .055$	Fringe Location (inches) $\odot$	Fringe Change $f = \odot - \odot$	Fringe Number $g = \frac{f}{h}$	Amount of 1.1 Fringe Correction Required	Corrected Values	
	Measured (inches)	Normalized $\odot$ wing height	Corrected Distance from Tables						Y'	g
1	.190	.075	.071	.126	.360	.170	1.641	1.1	.081	2.74
2	.330	.131	.124	.179	.460	.130	1.255	1.1	.134	2.36
3	.465	.185	.176	.231	.590	.125	1.208	1.1	.186	2.31
4	.570	.226	.215	.270	.670	.100	.965	1.1	.225	2.07
5	.660	.262	.249	.304	.765	.105	1.013	1.1	.259	2.11
6	.745	.296	.281	.336	.860	.115	1.110	1.1	.291	2.21
7	.825	.327	.311	.366	.950	.125	1.208	1.1	.321	2.31
8	.950	.377	.358	.413	1.090	.140	1.352	1.1	.368	2.45
9	1.060	.421	.400	.455	1.240	.180	1.737	1.1	.410	2.84
10	1.180	.468	.445	.500	1.350	.170	1.641	1.1	.455	2.74
11	1.245	.494	.469	.524	1.500	.255	2.172	1.1	.479	3.27
12	1.350	.536	.509	.564	1.620	.270	2.607	.5	.543	3.11
13	1.430	.567	.539	.594	1.750	.320	3.090	.1	.590	3.19
14	1.533	.609	.579	.634	1.850	.315	3.041	0.	.634	3.04
15	1.625	.649	.617	.672	1.940	.315	3.041	0.	.672	3.04
16	1.720	.683	.649	.704	2.030	.310	2.994	0.	.704	2.99
17	1.830	.726	.690	.745	2.120	.290	2.800	0.	.745	2.80
18	1.955	.776	.737	.792	2.220	.265	2.560	0.	.792	2.56
19	2.080	.825	.783	.838	2.290	.210	2.028	0.	.838	2.03
20	2.180	.865	.821	.876	2.340	.160	1.545	0.	.876	1.55
21	2.315	.919	.872	.927	2.400	.085	.820	0.	.927	.82
22	2.400	.952	.904	.959	2.500	.100	.965	0.	.959	.97
23	2.500	.992	.942	.997	2.580	.080	.772	0.	.997	.77
24	2.570	1.020	.969	1.024	2.670	.100	.965	0.	1.024	.97
25	2.680	1.063	1.009	1.064	2.790	.110	1.062	0.	1.064	1.06
26	2.780	1.103	1.048	1.103	2.885	.115	1.110	0.	1.103	1.11

Wing height = 2.52 inches

Wing length = 2.92 inches

Average fringe interval = .1036 inches

	Distance Above Aligned Plane							
Line No.	Measured (inches) ①	Corrected to Free Stream (inches) ②	Normalized ② / (wing height)	Corrected Distance from Tables ③	Y' ④ = ③ + .055	Fringe Location (inches) ⑤	Fringe Change f = ⑤ - ④	Fringe Number g = f/b
1	.190*	.076	.032	.030	.085	.270	.194	1.867
2	.290*	.176	.073	.069	.124	.390	.214	2.050
3	.410*	.296	.123	.117	.172	.450	.154	1.482
4	.525*	.411	.171	.162	.217	.560	.149	1.434
5	.615*	.501	.208	.198	.253	.650	.149	1.434
6	.710*	.596	.247	.235	.290	.725	.129	1.242
7	.800*	.686	.285	.271	.326	.830	.144	1.386
8	.910*	.796	.330	.314	.369	.980	.184	1.771
9	1.020*	.906	.376	.357	.412	1.140	.234	2.252
10	1.120*	1.006	.417	.396	.451	1.290	.284	2.738
11	1.230*	1.116	.463	.440	.495	1.420	.304	2.926
12	1.330*	1.216	.505	.480	.535	1.580	.364	3.503
13	1.370	1.370	.568	.540	.595	1.670	.300	2.887
14	1.460	1.460	.606	.576	.631	1.770	.310	2.984
15	1.560	1.560	.647	.615	.670	1.860	.300	2.887
16	1.660	1.660	.689	.655	.710	1.960	.300	2.887
17	1.760	1.760	.730	.694	.749	2.020	.260	2.502
18	1.880	1.880	.780	.741	.796	2.100	.220	2.117
19	2.000	2.000	.830	.788	.843	2.190	.190	1.829
20	2.110	2.110	.876	.832	.887	2.305	.195	1.877
21	2.220	2.220	.921	.875	.930	2.390	.170	1.704
22	2.330	2.330	.967	.919	.974	2.480	.150	1.444
23	2.445	2.445	1.015	.964	1.019	2.590	.145	1.396
24	2.570	2.570	1.066	1.013	1.068	2.680	.110	1.059
25	2.680	2.680	1.112	1.056	1.111	2.760	.080	.770
26	2.805	2.805	1.164	1.106	1.161	2.860	.055	.529

* Locations to be corrected to free stream conditions

Table II. Tabulation of Fringe Shift Data Taken From the Photographic Enlargement of Photo 4

REDUCTION OF AN INTERFEROGRAM TO OBTAIN FRINGE SHIFT DATA

The fringe shift reduction process was accomplished using two techniques. The first involved projecting the interferogram negative onto a sheet of white paper using a photo-enlarger. The light fringes offered the best contrast and were therefore traced out in Figures 30-34. In each drawing it was necessary to begin tracing the fringes above the fin and work towards the fin root since the transition across the fin tip determined the correct connection of the fringes across the fin leading edge shock. In order to determine the fringe change, one fringe line in the free stream region forward of the fin which appeared the straightest and paralleled the majority of other fringe lines was selected. A straight line, called the fringe reference line, was drawn over its centerline and extended to cross the y' axis. The remaining reference lines were then drawn parallel to the first and along the centerlines of the remaining free stream fringes. In reducing the drawings it was not realized until later that the free stream fringe patterns before and after the plate leading edge Prandtl-Meyer expansion differed considerably. This effect was taken into account later.

A ruler scaled to 0.01 inches was then placed along the y' axis and the distances of the fringes and reference lines above and below the aligned y' plane were then recorded in Table I for Photograph 4. The fin width and length were then measured and the average values were recorded. The average fringe interval was determined by measuring the distance between the first and last fringes used and dividing by the number of intervals. The fringe change was found by subtracting the fringe crossing

point. The fringe number was calculated by dividing the change by the average fringe interval. The reference line location was then normalized with respect to the measured fin height. Since the actual fin height was very close to one inch, the above number was considered to be the number of inches above or below the aligned plane. Thus the table computing the tunnel wall and grid refraction displacements in Appendix B could be entered to determine the actual reference line location with respect to the aligned plane of the drawing (see Figure 29). The locations were then converted to the y' axis system by adding the normalized location of the aligned plane. After realizing that not all the reference lines were referenced to the free stream density forward of the plate leading edge, the enlarged photographs (Figures 35-39) were checked against the drawings. It was found that the Prandtl-Meyer expansion caused a fringe number change of approximately 1.1. Consequently each reference line in the drawing was compared with the enlarged photograph and an appropriate percentage of the 1.1 fringe number was used as a correction (see Table I). The calculated fringe numbers had the correction fringe number added to them while the y' locations were corrected by

$$y'corr = y'orig - \frac{(1.1 \text{ Fringe no.}) \times (\text{Fringe Interval})}{(\text{Fin Height})} \qquad (A-1)$$

The second reduction technique was to use enlarged photographs made from the interferogram negatives to obtain the fringe change. The fringe lines were first traced over lightly with a pencil and then verified against the other photographs to ensure correct tracing. A datum fringe reference line was chosen as before and drawn. The remaining reference lines for the upper free stream fringe lines forward of the Prandtl-Meyer expansion were then drawn parallel to the datum. When it became impossible

99

to use fringe lines forward of the expansion, the reference lines were then drawn along the centerline of the fringes between the expansion and the fin. The same ruler was used to obtain the fringe crossing points, the reference crossing points, fin measurements, and the average fringe interval and they were recorded in Table 2. The reference line crossing points were then corrected to free stream conditions, using a 1.1 Fringe number correction for those referenced to the pattern between the expansion and fin leading edge. The fringe number and reference fin locations were calculated as before. This method was considered more accurate because the reference lines and fringe lines could easily be rechecked for accuracy and corrected in the event that a fringe line was traced incorrectly or a reference line was misaligned. The accuracy was directly proportional to the hologram resolution which was not true for the drawings since the reference lines are drawn parallel to hand-drawn fringe lines.

APPENDIX B

CALCULATION OF TUNNEL WALL AND GRID PLASTIC REFRACTION CORRECTION

In the interferogram photographs used to obtain the fringe change,
every point off the alignment axis will be slightly distorted due to the
plastic tunnel wall and grid. This effect is illustrated in Figure 19.
From Snells Law of Refraction, the angles of incidence and refraction are
related by

$$\sin \alpha = n \sin \beta \qquad \text{(B-1)}$$

where n is the index of refraction between plastic and air. Then can be
written

$$\beta = \sin^{-1} \left(\frac{\sin \alpha}{n} \right) \qquad \text{(B-2)}$$

Since the tunnel wall and grid have the same index of refraction, they
can be considered on material with thickness $t = ab$ in Figure 19. Then
consider the height bd which can be written

$$bd = t \tan \alpha \qquad \text{(B-3)}$$

The beam displacement, Δy, is then

$$\Delta Y = bd - bc = t \tan \alpha - t \tan \beta \qquad \text{(B-4)}$$

but $\tan \alpha$ is

$$\tan \alpha = \frac{Y_{observed}}{L} \qquad \text{(B-5)}$$

Combining Equation (B-2), (B-4), and (B-5) the beam displacement becomes

$$\Delta Y = t \left[\frac{Y_{observed}}{L} - \tan \left[\sin^{-1} \left(\frac{\sin \alpha}{n} \right) \right] \right] \qquad \text{(B-6)}$$

The true location of the observed point is then

$$Y_{true} = Y_{observed} - \Delta Y \qquad \text{(B-7)}$$

101

A FORTRAN computer program was written to generate a table giving the true locations versus the observed locations. In the program the constants and variables from the above equations were defined as

$$Y_{observed} \quad = \quad Y$$

$$Y_{true} \quad = \quad YTRUE$$

$$\Delta Y \quad = \quad DY$$

$$\alpha \quad = \quad ALFA$$

$$L \quad = \quad L$$

$$n \quad = \quad N$$

Since the computer cannot calculate Equations (B-2) and (B-6) as written, they were constructed by parts using such letters as AA, AB, etc. The program and tables are included in the next few pages.

```
C     **************************************************************
C     **                                                        **
C     **    THIS PROGRAM COMPUTES THE CORRECTION FOR THE        **
C     **    OFF AXIS TUNNEL WALL PARALLAX. THE FOLLOWING        **
C     **    INPUT PARAMETERS ARE REQUIRED:                      **
C     **    L = DISTANCE FROM HOLOGRAM PLANE TO THE MODEL       **
C     **        CENTER LINE                                     **
C     **    N = INDEX OF REFRACTION FOR TUNNEL WALL             **
C     **    T = THICKNESS OF TUNNEL AND GRID PLEXIGLAS          **
C     **    Y = OBSERVED DISTANCE OF THE POINT IN THE           **
C     **        PHOTOGRAPH FROM THE ALIGNED POINT               **
C     **    YTRUE = TRUE DISTANCE FROM ALIGNED POINT TO         **
C     **            THE POINT ON THE MODEL PLANE                **
C     **    YMAX = MAXIMUM DISTANCE OF INTEREST FROM THE        **
C     **           ALIGNED POINT                                **
C     **                                                        **
C     **************************************************************
C
      REAL*4 L,N
C
C         INPUT PARAMETERS
C
      L=15.0
      N=1.5
      T=2.25
      YMAX=2.5
      PI=3.141593
C
C         OUTPUT FORMAT
C
      WRITE(6,100)L,N,T
  100 FORMAT('1',T25,'THE FOLLOWING TABLE IS TO ACCOUNT FOR'
     1' THE PARALLAX'/T25,'ERROR IN VIEWING THE MODEL '
     2'THROUGH GLASS WALLS AT'/T25,'ANY OTHER POINT THAN '
     3'AT THE ALIGNMENT POINT. INPUT'/T25,'PARAMETERS ARE:'
     4/T35,'(1) L = ',F6.3,' INCHES'/T35,'(2) N = ',F6.3,
     5' INCHES'/T35,'(3) T = ',F6.3,' INCHES')
      WRITE(6,110)
  110 FORMAT(' ',T24,'OBSERVED',T40,'TRUE',T54,'ERROR',T70,
     1'RAY'/T24,'DISTANCE',T38,'DISTANCE',T69,'ANGLE'/T24,
     2'(INCHES)',T38,'(INCHES)',T53,'(INCHES)',T67,
     3'(DEGREES)'/)
C
C         CALCULATIONS
C
      Y=0.0
   10 DO 15 I=1,2000
      AA=Y/L
      AB=ATAN(AA)
      ALFA=AB*180.0/PI
      AC=SIN(AB)/N
      BETA=ARSIN(AC)
      AD=TAN(BETA)
      DY=T*(AA-AD)
      YTRUE=Y-DY
C
      WRITE(6,200)Y,YTRUE,DY,ALFA
  200 FORMAT(' ',T24,F7.4,T38,F7.4,T53,F8.6,T67,F8.4)
      IF(MOD(I,10).EQ.0)WRITE(6,201)
  201 FORMAT(' ')
      IF(MOD(I,60).EQ.0)GO TO 11
      GO TO 12
   11 WRITE(6,202)
  202 FORMAT('1')
      WRITE(6,110)
   12 Y=.002*FLOAT(I)
      IF(Y.GE.YMAX)GO TO 20
   15 CONTINUE
   20 STOP
      END
```

THE FOLLOWING TABLE IS TO ACCOUNT FOR THE PARALLAX
ERROR IN VIEWING THE MODEL THROUGH GLASS WALLS AT
ANY OTHER POINT THAN AT THE ALIGNMENT POINT. INPUT
PARAMETERS ARE:
                (1) L = 15.000 INCHES
                (2) N =   1.500 INCHES
                (3) T =   2.250 INCHES

OBSERVED DISTANCE (INCHES)	TRUE DISTANCE (INCHES)	ERROR (INCHES)	RAY ANGLE (DEGREES)
0.0	0.0	0.0	0.0
0.0020	0.0019	0.000100	0.0076
0.0040	0.0038	0.000200	0.0153
0.0060	0.0057	0.000300	0.0229
0.C080	0.0076	0.000400	0.0306
0.0100	0.0095	0.000500	0.0382
0.0120	0.0114	0.000600	0.0458
0.0140	0.0133	0.000700	0.0535
0.0160	0.0152	0.000800	0.0611
0.0180	0.0171	0.000900	0.0688
0.0200	0.0190	0.001000	0.0764
0.0220	0.0209	0.001100	0.0840
0.0240	0.0228	0.001200	0.0917
0.0260	0.0247	0.001300	0.0993
0.0280	0.0266	0.001400	0.1070
0.0300	0.0285	0.001500	0.1146
0.0320	0.0304	0.001600	0.1222
0.0340	0.0323	0.001700	0.1299
0.0360	0.0342	0.001800	0.1375
0.0380	0.0361	0.001900	0.1451
0.0400	0.0380	0.002000	0.1528
0.0420	0.0399	0.002100	0.1604
0.0440	0.0418	0.002200	0.1681
0.0460	0.0437	0.002300	0.1757
0.0480	0.0456	0.002400	0.1833
0.0500	0.0475	0.002500	0.1910
0.0520	0.0494	0.002600	0.1986
0.0540	0.0513	0.002700	0.2063
0.0560	0.0532	0.002800	0.2139
0.0580	0.0551	0.002900	0.2215
0.0600	0.0570	0.003000	0.2292
0.0620	0.0589	0.003100	0.2368
0.0640	0.0608	0.003200	0.2445
0.0660	0.0627	0.003300	0.2521
0.0680	0.0646	0.003400	0.2597
0.0700	0.0665	0.003500	0.2674
0.C720	0.0684	0.003600	0.2750
0.C740	0.0703	0.003700	0.2827
0.C760	0.0722	0.003800	0.2903
0.0780	0.0741	0.003900	0.2979
0.0800	0.0760	0.004000	0.3056
0.0820	0.0779	0.004100	0.3132
0.C840	0.0798	0.004200	0.3209
0.C860	0.0817	0.004300	0.3285
0.0880	0.0836	0.004400	0.3361
0.0900	0.0855	0.004500	0.3438
0.0920	0.0874	0.004600	0.3514
0.0940	0.0893	0.004700	0.3590
0.C960	0.0912	0.004800	0.3667
0.0980	0.0931	0.004900	0.3743
0.1000	0.0950	0.005000	0.3820
0.1020	0.0969	0.005100	0.3896
0.1040	0.0988	0.005200	0.3972
0.1060	0.1007	0.005300	0.4049
0.1C80	0.1026	0.005400	0.4125
0.1100	0.1045	0.005500	0.4202
0.1120	0.1064	0.005600	0.4278
0.1140	0.1083	0.005700	0.4354
0.1160	0.11C2	0.005800	0.4431
0.1180	0.1121	0.005900	0.4507

OBSERVED DISTANCE (INCHES)	TRUE DISTANCE (INCHES)	ERROR (INCHES)	RAY ANGLE (DEGREES)
0.1200	0.1140	0.006000	0.4584
0.1220	0.1159	0.006100	0.4660
0.1240	0.1178	0.006200	0.4736
0.1260	0.1197	0.006300	0.4813
0.1280	0.1216	0.006400	0.4889
0.1300	0.1235	0.006500	0.4966
0.1320	0.1254	0.006600	0.5042
0.1340	0.1273	0.006700	0.5118
0.1360	0.1292	0.006800	0.5195
0.1380	0.1311	0.006900	0.5271
0.1400	0.1330	0.007000	0.5347
0.1420	0.1349	0.007100	0.5424
0.1440	0.1368	0.007200	0.5500
0.1460	0.1387	0.007300	0.5577
0.1480	0.1406	0.007400	0.5653
0.1500	0.1425	0.007500	0.5729
0.1520	0.1444	0.007600	0.5806
0.1540	0.1463	0.007700	0.5882
0.1560	0.1482	0.007800	0.5959
0.1580	0.1501	0.007901	0.6035
0.1600	0.1520	0.008001	0.6111
0.1620	0.1539	0.008101	0.6188
0.1640	0.1558	0.008201	0.6264
0.1660	0.1577	0.008301	0.6340
0.1680	0.1596	0.008401	0.6417
0.1700	0.1615	0.008501	0.6493
0.1720	0.1634	0.008601	0.6570
0.1740	0.1653	0.008701	0.6646
0.1760	0.1672	0.008801	0.6722
0.1780	0.1691	0.008901	0.6799
0.1800	0.1710	0.009001	0.6875
0.1820	0.1729	0.009101	0.6952
0.1840	0.1748	0.009201	0.7028
0.1860	0.1767	0.009301	0.7104
0.1880	0.1786	0.009401	0.7181
0.1900	0.1805	0.009501	0.7257
0.1920	0.1824	0.009601	0.7333
0.1940	0.1843	0.009701	0.7410
0.1960	0.1862	0.009801	0.7486
0.1980	0.1881	0.009901	0.7563
0.2000	0.1900	0.010001	0.7639
0.2020	0.1919	0.010101	0.7715
0.2040	0.1938	0.010201	0.7792
0.2060	0.1957	0.010301	0.7868
0.2080	0.1976	0.010401	0.7944
0.2100	0.1995	0.010501	0.8021
0.2120	0.2014	0.010601	0.8097
0.2140	0.2033	0.010701	0.8174
0.2160	0.2052	0.010801	0.8250
0.2180	0.2071	0.010901	0.8326
0.2200	0.2090	0.011001	0.8403
0.2220	0.2109	0.011101	0.8479
0.2240	0.2128	0.011201	0.8556
0.2260	0.2147	0.011301	0.8632
0.2280	0.2166	0.011401	0.8708
0.2300	0.2185	0.011502	0.8785
0.2320	0.2204	0.011602	0.8861
0.2340	0.2223	0.011702	0.8937
0.2360	0.2242	0.011802	0.9014
0.2380	0.2261	0.011902	0.9090

OBSERVED DISTANCE (INCHES)	TRUE DISTANCE (INCHES)	ERROR (INCHES)	RAY ANGLE (DEGREES)
0.2400	0.2280	0.012002	0.9167
0.2420	0.2299	0.012102	0.9243
0.2440	0.2318	0.012202	0.9319
0.2460	0.2337	0.012302	0.9396
0.2480	0.2356	0.012402	0.9472
0.2500	0.2375	0.012502	0.9548
0.2520	0.2394	0.012602	0.9625
0.2540	0.2413	0.012702	0.9701
0.2560	0.2432	0.012802	0.9778
0.2580	0.2451	0.012902	0.9854
0.2600	0.2470	0.013002	0.9930
0.2620	0.2489	0.013102	1.0007
0.2640	0.2508	0.013202	1.0083
0.2660	0.2527	0.013302	1.0159
0.2680	0.2546	0.013402	1.0236
0.2700	0.2565	0.013502	1.0312
0.2720	0.2584	0.013602	1.0388
0.2740	0.2603	0.013703	1.0465
0.2760	0.2622	0.013803	1.0541
0.2780	0.2641	0.013903	1.0618
0.2800	0.2660	0.014003	1.0694
0.2820	0.2679	0.014103	1.0770
0.2840	0.2698	0.014203	1.0847
0.2860	0.2717	0.014303	1.0923
0.2880	0.2736	0.014403	1.0999
0.2900	0.2755	0.014503	1.1076
0.2920	0.2774	0.014603	1.1152
0.2940	0.2793	0.014703	1.1229
0.2960	0.2812	0.014803	1.1305
0.2980	0.2831	0.014903	1.1381
0.3000	0.2850	0.015003	1.1458
0.3020	0.2869	0.015103	1.1534
0.3040	0.2888	0.015203	1.1610
0.3060	0.2907	0.015304	1.1687
0.3080	0.2926	0.015404	1.1763
0.3100	0.2945	0.015504	1.1839
0.3120	0.2964	0.015604	1.1916
0.3140	0.2983	0.015704	1.1992
0.3160	0.3002	0.015804	1.2069
0.3180	0.3021	0.015904	1.2145
0.3200	0.3040	0.016004	1.2221
0.3220	0.3059	0.016104	1.2298
0.3240	0.3078	0.016204	1.2374
0.3260	0.3097	0.016304	1.2450
0.3280	0.3116	0.016404	1.2527
0.3300	0.3135	0.016504	1.2603
0.3320	0.3154	0.016605	1.2679
0.3340	0.3173	0.016705	1.2756
0.3360	0.3192	0.016805	1.2832
0.3380	0.3211	0.016905	1.2908
0.3400	0.3230	0.017005	1.2985
0.3420	0.3249	0.017105	1.3061
0.3440	0.3268	0.017205	1.3138
0.3460	0.3287	0.017305	1.3214
0.3480	0.3306	0.017405	1.3290
0.3500	0.3325	0.017505	1.3367
0.3520	0.3344	0.017605	1.3443
0.3540	0.3363	0.017705	1.3519
0.3560	0.3382	0.017806	1.3596
0.3580	0.3401	0.017906	1.3672

OBSERVED DISTANCE (INCHES)	TRUE DISTANCE (INCHES)	ERROR (INCHES)	RAY ANGLE (DEGREES)
0.3600	0.3420	0.018006	1.3748
0.3620	0.3439	0.018106	1.3825
0.3640	0.3458	0.018206	1.3901
0.3660	0.3477	0.018306	1.3977
0.3680	0.3496	0.018406	1.4054
0.3700	0.3515	0.018506	1.4130
0.3720	0.3534	0.018606	1.4206
0.3740	0.3553	0.018706	1.4283
0.3760	0.3572	0.018807	1.4359
0.3780	0.3591	0.018907	1.4435
0.3800	0.3610	0.019007	1.4512
0.3820	0.3629	0.019107	1.4588
0.3840	0.3648	0.019207	1.4665
0.3860	0.3667	0.019307	1.4741
0.3880	0.3686	0.019407	1.4817
0.3900	0.3705	0.019507	1.4894
0.3920	0.3724	0.019607	1.4970
0.3940	0.3743	0.019708	1.5046
0.3960	0.3762	0.019808	1.5123
0.3980	0.3781	0.019908	1.5199
0.4000	0.3800	0.020008	1.5275
0.4020	0.3819	0.020108	1.5352
0.4040	0.3838	0.020208	1.5428
0.4060	0.3857	0.020308	1.5504
0.4080	0.3876	0.020408	1.5581
0.4100	0.3895	0.020509	1.5657
0.4120	0.3914	0.020609	1.5733
0.4140	0.3933	0.020709	1.5810
0.4160	0.3952	0.020809	1.5886
0.4180	0.3971	0.020909	1.5962
0.4200	0.3990	0.021009	1.6039
0.4220	0.4009	0.021109	1.6115
0.4240	0.4028	0.021209	1.6191
0.4260	0.4047	0.021310	1.6268
0.4280	0.4066	0.021410	1.6344
0.4300	0.4085	0.021510	1.6420
0.4320	0.4104	0.021610	1.6497
0.4340	0.4123	0.021710	1.6573
0.4360	0.4142	0.021810	1.6649
0.4380	0.4161	0.021910	1.6726
0.4400	0.4180	0.022011	1.6802
0.4420	0.4199	0.022111	1.6878
0.4440	0.4218	0.022211	1.6955
0.4460	0.4237	0.022311	1.7031
0.4480	0.4256	0.022411	1.7107
0.4500	0.4275	0.022511	1.7184
0.4520	0.4294	0.022611	1.7260
0.4540	0.4313	0.022712	1.7336
0.4560	0.4332	0.022812	1.7413
0.4580	0.4351	0.022912	1.7489
0.4600	0.4370	0.023012	1.7565
0.4620	0.4389	0.023112	1.7642
0.4640	0.4408	0.023212	1.7718
0.4660	0.4427	0.023312	1.7794
0.4680	0.4446	0.023413	1.7870
0.4700	0.4465	0.023513	1.7947
0.4720	0.4484	0.023613	1.8023
0.4740	0.4503	0.023713	1.8099
0.4760	0.4522	0.023813	1.8176
0.4780	0.4541	0.023913	1.8252

OBSERVED DISTANCE (INCHES)	TRUE DISTANCE (INCHES)	ERROR (INCHES)	RAY ANGLE (DEGREES)
0.4800	0.4560	0.024014	1.8328
0.4820	0.4579	0.024114	1.8405
0.4840	0.4598	0.024214	1.8481
0.4860	0.4617	0.024314	1.8557
0.4880	0.4636	0.024414	1.8634
0.4900	0.4655	0.024515	1.8710
0.4920	0.4674	0.024615	1.8786
0.4940	0.4693	0.024715	1.8863
0.4960	0.4712	0.024815	1.8939
0.4980	0.4731	0.024915	1.9015
0.5000	0.4750	0.025015	1.9092
0.5020	0.4769	0.025116	1.9168
0.5040	0.4788	0.025216	1.9244
0.5060	0.4807	0.025316	1.9320
0.5080	0.4826	0.025416	1.9397
0.5100	0.4845	0.025516	1.9473
0.5120	0.4864	0.025617	1.9549
0.5140	0.4883	0.025717	1.9626
0.5160	0.4902	0.025817	1.9702
0.5180	0.4921	0.025917	1.9778
0.5200	0.4940	0.026017	1.9855
0.5220	0.4959	0.026118	1.9931
0.5240	0.4978	0.026218	2.0007
0.5260	0.4997	0.026318	2.0083
0.5280	0.5016	0.026418	2.0160
0.5300	0.5035	0.026518	2.0236
0.5320	0.5054	0.026619	2.0312
0.5340	0.5073	0.026719	2.0389
0.5360	0.5092	0.026819	2.0465
0.5380	0.5111	0.026919	2.0541
0.5400	0.5130	0.027019	2.0618
0.5420	0.5149	0.027120	2.0694
0.5440	0.5168	0.027220	2.0770
0.5460	0.5187	0.027320	2.0846
0.5480	0.5206	0.027420	2.0923
0.5500	0.5225	0.027521	2.0999
0.5520	0.5244	0.027621	2.1075
0.5540	0.5263	0.027721	2.1152
0.5560	0.5282	0.027821	2.1228
0.5580	0.5301	0.027921	2.1304
0.5600	0.5320	0.028022	2.1380
0.5620	0.5339	0.028122	2.1457
0.5640	0.5358	0.028222	2.1533
0.5660	0.5377	0.028322	2.1609
0.5680	0.5396	0.028423	2.1686
0.5700	0.5415	0.028523	2.1762
0.5720	0.5434	0.028623	2.1838
0.5740	0.5453	0.028723	2.1914
0.5760	0.5472	0.028824	2.1991
0.5780	0.5491	0.028924	2.2067
0.5800	0.5510	0.029024	2.2143
0.5820	0.5529	0.029124	2.2220
0.5840	0.5548	0.029225	2.2296
0.5860	0.5567	0.029325	2.2372
0.5880	0.5586	0.029425	2.2448
0.5900	0.5605	0.029525	2.2525
0.5920	0.5624	0.029626	2.2601
0.5940	0.5643	0.029726	2.2677
0.5960	0.5662	0.029826	2.2754
0.5980	0.5681	0.029926	2.2830

OBSERVED DISTANCE (INCHES)	TRUE DISTANCE (INCHES)	ERROR (INCHES)	RAY ANGLE (DEGREES)
0.6000	0.5700	0.030027	2.2906
0.6020	0.5719	0.030127	2.2982
0.6040	0.5738	0.030227	2.3059
0.6060	0.5757	0.030327	2.3135
0.6080	0.5776	0.030428	2.3211
0.6100	0.5795	0.030528	2.3287
0.6120	0.5814	0.030628	2.3364
0.6140	0.5833	0.030729	2.3440
0.6160	0.5852	0.030829	2.3516
0.6180	0.5871	0.030929	2.3593
0.6200	0.5890	0.031029	2.3669
0.6220	0.5909	0.031130	2.3745
0.6240	0.5928	0.031230	2.3821
0.6260	0.5947	0.031330	2.3898
0.6280	0.5966	0.031431	2.3974
0.6300	0.5985	0.031531	2.4050
0.6320	0.6004	0.031631	2.4126
0.6340	0.6023	0.031731	2.4203
0.6360	0.6042	0.031832	2.4279
0.6380	0.6061	0.031932	2.4355
0.6400	0.6080	0.032032	2.4431
0.6420	0.6099	0.032133	2.4508
0.6440	0.6118	0.032233	2.4584
0.6460	0.6137	0.032333	2.4660
0.6480	0.6156	0.032434	2.4736
0.6500	0.6175	0.032534	2.4813
0.6520	0.6194	0.032634	2.4889
0.6540	0.6213	0.032735	2.4965
0.6560	0.6232	0.032835	2.5041
0.6580	0.6251	0.032935	2.5118
0.6600	0.6270	0.033035	2.5194
0.6620	0.6289	0.033136	2.5270
0.6640	0.6308	0.033236	2.5346
0.6660	0.6327	0.033336	2.5423
0.6680	0.6346	0.033437	2.5499
0.6700	0.6365	0.033537	2.5575
0.6720	0.6384	0.033637	2.5651
0.6740	0.6403	0.033738	2.5728
0.6760	0.6422	0.033838	2.5804
0.6780	0.6441	0.033938	2.5880
0.6800	0.6460	0.034039	2.5956
0.6820	0.6479	0.034139	2.6033
0.6840	0.6498	0.034239	2.6109
0.6860	0.6517	0.034340	2.6185
0.6880	0.6536	0.034440	2.6261
0.6900	0.6555	0.034541	2.6337
0.6920	0.6574	0.034641	2.6414
0.6940	0.6593	0.034741	2.6490
0.6960	0.6612	0.034842	2.6566
0.6980	0.6631	0.034942	2.6642
0.7000	0.6650	0.035042	2.6719
0.7020	0.6669	0.035143	2.6795
0.7040	0.6688	0.035243	2.6871
0.7060	0.6707	0.035343	2.6947
0.7080	0.6726	0.035444	2.7024
0.7100	0.6745	0.035544	2.7100
0.7120	0.6764	0.035645	2.7176
0.7140	0.6783	0.035745	2.7252
0.7160	0.6802	0.035845	2.7328
0.7180	0.6821	0.035946	2.7405

OBSERVED DISTANCE (INCHES)	TRUE DISTANCE (INCHES)	ERROR (INCHES)	RAY ANGLE (DEGREES)
0.7200	0.6840	0.036046	2.7481
0.7220	0.6859	0.036146	2.7557
0.7240	0.6878	0.036247	2.7633
0.7260	0.6897	0.036347	2.7710
0.7280	0.6916	0.036448	2.7786
0.7300	0.6935	0.036548	2.7862
0.7320	0.6954	0.036648	2.7938
0.7340	0.6973	0.036749	2.8014
0.7360	0.6992	0.036849	2.8091
0.7380	0.7011	0.036950	2.8167
0.7400	0.7029	0.037050	2.8243
0.7420	0.7048	0.037150	2.8319
0.7440	0.7067	0.037251	2.8395
0.7460	0.7086	0.037351	2.8472
0.7480	0.7105	0.037452	2.8548
0.7500	0.7124	0.037552	2.8624
0.7520	0.7143	0.037652	2.8700
0.7540	0.7162	0.037753	2.8776
0.7560	0.7181	0.037853	2.8853
0.7580	0.7200	0.037954	2.8929
0.7600	0.7219	0.038054	2.9005
0.7620	0.7238	0.038155	2.9081
0.7640	0.7257	0.038255	2.9157
0.7660	0.7276	0.038355	2.9234
0.7680	0.7295	0.038456	2.9310
0.7700	0.7314	0.038556	2.9386
0.7720	0.7333	0.038657	2.9462
0.7740	0.7352	0.038757	2.9538
0.7760	0.7371	0.038858	2.9615
0.7780	0.7390	0.038958	2.9691
0.7800	0.7409	0.039059	2.9767
0.7820	0.7428	0.039159	2.9843
0.7840	0.7447	0.039259	2.9919
0.7860	0.7466	0.039360	2.9996
0.7880	0.7485	0.039460	3.0072
0.7900	0.7504	0.039561	3.0148
0.7920	0.7523	0.039661	3.0224
0.7940	0.7542	0.039762	3.0300
0.7960	0.7561	0.039862	3.0376
0.7980	0.7580	0.039963	3.0453
0.8000	0.7599	0.040063	3.0529
0.8020	0.7618	0.040164	3.0605
0.8040	0.7637	0.040264	3.0681
0.8060	0.7656	0.040365	3.0757
0.8080	0.7675	0.040465	3.0834
0.8100	0.7694	0.040566	3.0910
0.8120	0.7713	0.040666	3.0986
0.8140	0.7732	0.040767	3.1062
0.8160	0.7751	0.040867	3.1138
0.8180	0.7770	0.040968	3.1214
0.8200	0.7789	0.041068	3.1291
0.8220	0.7808	0.041169	3.1367
0.8240	0.7827	0.041269	3.1443
0.8260	0.7846	0.041369	3.1519
0.8280	0.7865	0.041470	3.1595
0.8300	0.7884	0.041570	3.1671
0.8320	0.7903	0.041671	3.1748
0.8340	0.7922	0.041772	3.1824
0.8360	0.7941	0.041872	3.1900
0.8380	0.7960	0.041973	3.1976

OBSERVED DISTANCE (INCHES)	TRUE DISTANCE (INCHES)	ERROR (INCHES)	RAY ANGLE (DEGREES)
0.8400	0.7979	0.042073	3.2052
0.8420	0.7998	0.042174	3.2128
0.8440	0.8017	0.042274	3.2204
0.8460	0.8036	0.042375	3.2281
0.8480	0.8055	0.042475	3.2357
0.8500	0.8074	0.042576	3.2433
0.8520	0.8093	0.042676	3.2509
0.8540	0.8112	0.042777	3.2585
0.8560	0.8131	0.042877	3.2661
0.8580	0.8150	0.042978	3.2738
0.8600	0.8169	0.043078	3.2814
0.8620	0.8188	0.043179	3.2890
0.8640	0.8207	0.043280	3.2966
0.8660	0.8226	0.043380	3.3042
0.8680	0.8245	0.043481	3.3118
0.8700	0.8264	0.043581	3.3194
0.8720	0.8283	0.043682	3.3270
0.8740	0.8302	0.043782	3.3347
0.8760	0.8321	0.043883	3.3423
0.8780	0.8340	0.043983	3.3499
0.8800	0.8359	0.044084	3.3575
0.8820	0.8378	0.044185	3.3651
0.8840	0.8397	0.044285	3.3727
0.8860	0.8416	0.044386	3.3803
0.8880	0.8435	0.044486	3.3880
0.8900	0.8454	0.044587	3.3956
0.8920	0.8473	0.044688	3.4032
0.8940	0.8492	0.044788	3.4108
0.8960	0.8511	0.044889	3.4184
0.8980	0.8530	0.044989	3.4260
0.9000	0.8549	0.045090	3.4336
0.9020	0.8568	0.045190	3.4412
0.9040	0.8587	0.045291	3.4489
0.9060	0.8606	0.045392	3.4565
0.9080	0.8625	0.045492	3.4641
0.9100	0.8644	0.045593	3.4717
0.9120	0.8663	0.045693	3.4793
0.9140	0.8682	0.045794	3.4869
0.9160	0.8701	0.045895	3.4945
0.9180	0.8720	0.045995	3.5021
0.9200	0.8739	0.046096	3.5097
0.9220	0.8758	0.046197	3.5174
0.9240	0.8777	0.046297	3.5250
0.9260	0.8796	0.046398	3.5326
0.9280	0.8815	0.046499	3.5402
0.9300	0.8834	0.046599	3.5478
0.9320	0.8853	0.046700	3.5554
0.9340	0.8872	0.046800	3.5630
0.9360	0.8891	0.046901	3.5706
0.9380	0.8910	0.047002	3.5782
0.9400	0.8929	0.047102	3.5858
0.9420	0.8948	0.047203	3.5935
0.9440	0.8967	0.047304	3.6011
0.9460	0.8986	0.047404	3.6087
0.9480	0.9005	0.047505	3.6163
0.9500	0.9024	0.047606	3.6239
0.9520	0.9043	0.047706	3.6315
0.9540	0.9062	0.047807	3.6391
0.9560	0.9081	0.047908	3.6467
0.9580	0.9100	0.048009	3.6543

OBSERVED DISTANCE (INCHES)	TRUE DISTANCE (INCHES)	ERROR (INCHES)	RAY ANGLE (DEGREES)
0.9600	0.9119	0.048109	3.6619
0.9620	0.9138	0.048210	3.6695
0.9640	0.9157	0.048310	3.6771
0.9660	0.9176	0.048411	3.6848
0.9680	0.9195	0.048512	3.6924
0.9700	0.9214	0.048613	3.7000
0.9720	0.9233	0.048713	3.7076
0.9740	0.9252	0.048814	3.7152
0.9760	0.9271	0.048915	3.7228
0.9780	0.9290	0.049015	3.7304
0.9800	0.9309	0.049116	3.7380
0.9820	0.9328	0.049217	3.7456
0.9840	0.9347	0.049318	3.7532
0.9860	0.9366	0.049418	3.7608
0.9880	0.9385	0.049519	3.7684
0.9900	0.9404	0.049620	3.7760
0.9920	0.9423	0.049720	3.7836
0.9940	0.9442	0.049821	3.7913
0.9960	0.9461	0.049922	3.7989
0.9980	0.9480	0.050023	3.8065
1.0000	0.9499	0.050123	3.8141
1.0020	0.9518	0.050224	3.8217
1.0040	0.9537	0.050325	3.8293
1.0060	0.9556	0.050426	3.8369
1.0080	0.9575	0.050526	3.8445
1.0100	0.9594	0.050627	3.8521
1.0120	0.9613	0.050728	3.8597
1.0140	0.9632	0.050829	3.8673
1.0160	0.9651	0.050929	3.8749
1.0180	0.9670	0.051030	3.8825
1.0200	0.9689	0.051131	3.8901
1.0220	0.9708	0.051232	3.8977
1.0240	0.9727	0.051332	3.9053
1.0260	0.9746	0.051433	3.9129
1.0280	0.9765	0.051534	3.9205
1.0300	0.9784	0.051635	3.9281
1.0320	0.9803	0.051735	3.9357
1.0340	0.9822	0.051836	3.9433
1.0360	0.9841	0.051937	3.9509
1.0380	0.9860	0.052038	3.9586
1.0400	0.9879	0.052139	3.9662
1.0420	0.9898	0.052240	3.9738
1.0440	0.9917	0.052340	3.9814
1.0460	0.9936	0.052441	3.9890
1.0480	0.9955	0.052542	3.9966
1.0500	0.9974	0.052643	4.0042
1.0520	0.9993	0.052743	4.0118
1.0540	1.0012	0.052844	4.0194
1.0560	1.0031	0.052945	4.0270
1.0580	1.0050	0.053046	4.0346
1.0600	1.0069	0.053147	4.0422
1.0620	1.0088	0.053248	4.0498
1.0640	1.0107	0.053348	4.0574
1.0660	1.0125	0.053449	4.0650
1.0680	1.0144	0.053550	4.0726
1.0700	1.0163	0.053651	4.0802
1.0720	1.0182	0.053752	4.0878
1.0740	1.0201	0.053853	4.0954
1.0760	1.0220	0.053953	4.1030
1.0780	1.0239	0.054054	4.1106

OBSERVED DISTANCE (INCHES)	TRUE DISTANCE (INCHES)	ERROR (INCHES)	RAY ANGLE (DEGREES)
1.0800	1.0258	0.054155	4.1182
1.0820	1.0277	0.054256	4.1258
1.0840	1.0296	0.054357	4.1334
1.0860	1.0315	0.054458	4.1410
1.0880	1.0334	0.054559	4.1486
1.0900	1.0353	0.054660	4.1562
1.0920	1.0372	0.054760	4.1638
1.0940	1.0391	0.054861	4.1714
1.0960	1.0410	0.054962	4.1790
1.0980	1.0429	0.055063	4.1866
1.1000	1.0448	0.055164	4.1942
1.1020	1.0467	0.055265	4.2018
1.1040	1.0486	0.055366	4.2094
1.1060	1.0505	0.055467	4.2170
1.1080	1.0524	0.055568	4.2246
1.1100	1.0543	0.055668	4.2322
1.1120	1.0562	0.055769	4.2398
1.1140	1.0581	0.055870	4.2474
1.1160	1.0600	0.055971	4.2550
1.1180	1.0619	0.056072	4.2626
1.1200	1.0638	0.056173	4.2702
1.1220	1.0657	0.056274	4.2778
1.1240	1.0676	0.056375	4.2854
1.1260	1.0695	0.056476	4.2929
1.1280	1.0714	0.056577	4.3005
1.1300	1.0733	0.056678	4.3081
1.1320	1.0752	0.056779	4.3157
1.1340	1.0771	0.056880	4.3233
1.1360	1.0790	0.056981	4.3309
1.1380	1.0809	0.057082	4.3385
1.1400	1.0828	0.057183	4.3461
1.1420	1.0847	0.057284	4.3537
1.1440	1.0866	0.057385	4.3613
1.1460	1.0885	0.057486	4.3689
1.1480	1.0904	0.057586	4.3765
1.1500	1.0923	0.057687	4.3841
1.1520	1.0942	0.057788	4.3917
1.1540	1.0961	0.057889	4.3993
1.1560	1.0980	0.057990	4.4069
1.1580	1.0999	0.058091	4.4145
1.1600	1.1018	0.058192	4.4221
1.1620	1.1037	0.058293	4.4297
1.1640	1.1056	0.058394	4.4373
1.1660	1.1075	0.058495	4.4448
1.1680	1.1094	0.058596	4.4524
1.1700	1.1113	0.058697	4.4600
1.1720	1.1132	0.058798	4.4676
1.1740	1.1151	0.058899	4.4752
1.1760	1.1170	0.059000	4.4828
1.1780	1.1189	0.059101	4.4904
1.1800	1.1208	0.059202	4.4980
1.1820	1.1227	0.059303	4.5056
1.1840	1.1246	0.059404	4.5132
1.1860	1.1265	0.059506	4.5208
1.1880	1.1284	0.059607	4.5284
1.1900	1.1303	0.059708	4.5360
1.1920	1.1322	0.059809	4.5436
1.1940	1.1341	0.059910	4.5511
1.1960	1.1360	0.060011	4.5587
1.1980	1.1379	0.060112	4.5663

OBSERVED DISTANCE (INCHES)	TRUE DISTANCE (INCHES)	ERROR (INCHES)	RAY ANGLE (DEGREES)
1.2000	1.1398	0.060213	4.5739
1.2020	1.1417	0.060314	4.5815
1.2040	1.1436	0.060415	4.5891
1.2060	1.1455	0.060516	4.5967
1.2080	1.1474	0.060617	4.6043
1.2100	1.1493	0.060718	4.6119
1.2120	1.1512	0.060819	4.6195
1.2140	1.1531	0.060920	4.6270
1.2160	1.1550	0.061021	4.6346
1.2180	1.1569	0.061123	4.6422
1.2200	1.1588	0.061224	4.6498
1.2220	1.1607	0.061325	4.6574
1.2240	1.1626	0.061426	4.6650
1.2260	1.1645	0.061527	4.6726
1.2280	1.1664	0.061628	4.6802
1.2300	1.1683	0.061729	4.6878
1.2320	1.1702	0.061830	4.6954
1.2340	1.1721	0.061931	4.7029
1.2360	1.1740	0.062032	4.7105
1.2380	1.1759	0.062134	4.7181
1.2400	1.1778	0.062235	4.7257
1.2420	1.1797	0.062336	4.7333
1.2440	1.1816	0.062437	4.7409
1.2460	1.1835	0.062538	4.7485
1.2480	1.1854	0.062639	4.7560
1.2500	1.1873	0.062740	4.7636
1.2520	1.1892	0.062842	4.7712
1.2540	1.1911	0.062943	4.7788
1.2560	1.1930	0.063044	4.7864
1.2580	1.1949	0.063145	4.7940
1.2600	1.1968	0.063246	4.8016
1.2620	1.1987	0.063348	4.8092
1.2640	1.2006	0.063448	4.8167
1.2660	1.2024	0.063550	4.8243
1.2680	1.2043	0.063651	4.8319
1.2700	1.2062	0.063752	4.8395
1.2720	1.2081	0.063854	4.8471
1.2740	1.2100	0.063955	4.8547
1.2760	1.2119	0.064056	4.8622
1.2780	1.2138	0.064157	4.8698
1.2800	1.2157	0.064258	4.8774
1.2820	1.2176	0.064360	4.8850
1.2840	1.2195	0.064461	4.8926
1.2860	1.2214	0.064562	4.9002
1.2880	1.2233	0.064663	4.9078
1.2900	1.2252	0.064764	4.9153
1.2920	1.2271	0.064865	4.9229
1.2940	1.2290	0.064967	4.9305
1.2960	1.2309	0.065068	4.9381
1.2980	1.2328	0.065169	4.9457
1.3000	1.2347	0.065270	4.9533
1.3020	1.2366	0.065372	4.9608
1.3040	1.2385	0.065473	4.9684
1.3060	1.2404	0.065574	4.9760
1.3080	1.2423	0.065675	4.9836
1.3100	1.2442	0.065777	4.9912
1.3120	1.2461	0.065878	4.9987
1.3140	1.2480	0.065979	5.0063
1.3160	1.2499	0.066081	5.0139
1.3180	1.2518	0.066182	5.0215

OBSERVED DISTANCE (INCHES)	TRUE DISTANCE (INCHES)	ERROR (INCHES)	RAY ANGLE (DEGREES)
1.3200	1.2537	0.066283	5.0291
1.3220	1.2556	0.066384	5.0366
1.3240	1.2575	0.066486	5.0442
1.3260	1.2594	0.066587	5.0518
1.3280	1.2613	0.066688	5.0594
1.3300	1.2632	0.066789	5.0670
1.3320	1.2651	0.066891	5.0745
1.3340	1.2670	0.066992	5.0821
1.3360	1.2689	0.067093	5.0897
1.3380	1.2708	0.067195	5.0973
1.3400	1.2727	0.067296	5.1049
1.3420	1.2746	0.067398	5.1124
1.3440	1.2765	0.067499	5.1200
1.3460	1.2784	0.067600	5.1276
1.3480	1.2803	0.067701	5.1352
1.3500	1.2822	0.067803	5.1428
1.3520	1.2841	0.067904	5.1503
1.3540	1.2860	0.068005	5.1579
1.3560	1.2879	0.068107	5.1655
1.3580	1.2898	0.068208	5.1731
1.3600	1.2917	0.068309	5.1806
1.3620	1.2936	0.068411	5.1882
1.3640	1.2955	0.068512	5.1958
1.3660	1.2974	0.068614	5.2034
1.3680	1.2993	0.068715	5.2110
1.3700	1.3012	0.068816	5.2185
1.3720	1.3031	0.068918	5.2261
1.3740	1.3050	0.069019	5.2337
1.3760	1.3069	0.069121	5.2413
1.3780	1.3088	0.069222	5.2488
1.3800	1.3107	0.069323	5.2564
1.3820	1.3126	0.069425	5.2640
1.3840	1.3145	0.069526	5.2716
1.3860	1.3164	0.069628	5.2791
1.3880	1.3183	0.069729	5.2867
1.3900	1.3202	0.069830	5.2943
1.3920	1.3221	0.069932	5.3019
1.3940	1.3240	0.070033	5.3094
1.3960	1.3259	0.070135	5.3170
1.3980	1.3278	0.070236	5.3246
1.4000	1.3297	0.070338	5.3322
1.4020	1.3316	0.070439	5.3397
1.4040	1.3335	0.070540	5.3473
1.4060	1.3354	0.070642	5.3549
1.4080	1.3373	0.070743	5.3624
1.4100	1.3392	0.070845	5.3700
1.4120	1.3411	0.070946	5.3776
1.4140	1.3430	0.071048	5.3852
1.4160	1.3448	0.071149	5.3927
1.4180	1.3467	0.071251	5.4003
1.4200	1.3486	0.071352	5.4079
1.4220	1.3505	0.071454	5.4154
1.4240	1.3524	0.071555	5.4230
1.4260	1.3543	0.071657	5.4306
1.4280	1.3562	0.071758	5.4382
1.4300	1.3581	0.071860	5.4457
1.4320	1.3600	0.071961	5.4533
1.4340	1.3619	0.072063	5.4609
1.4360	1.3638	0.072164	5.4684
1.4380	1.3657	0.072266	5.4760

OBSERVED DISTANCE (INCHES)	TRUE DISTANCE (INCHES)	ERROR (INCHES)	RAY ANGLE (DEGREES)
1.4400	1.3676	0.072367	5.4836
1.4420	1.3695	0.072469	5.4912
1.4440	1.3714	0.072571	5.4987
1.4460	1.3733	0.072672	5.5063
1.4480	1.3752	0.072774	5.5139
1.4500	1.3771	0.072875	5.5214
1.4520	1.3790	0.072977	5.5290
1.4540	1.3809	0.073078	5.5366
1.4560	1.3828	0.073180	5.5441
1.4580	1.3847	0.073281	5.5517
1.4600	1.3866	0.073383	5.5593
1.4620	1.3885	0.073484	5.5668
1.4640	1.3904	0.073586	5.5744
1.4660	1.3923	0.073687	5.5820
1.4680	1.3942	0.073789	5.5895
1.4700	1.3961	0.073891	5.5971
1.4720	1.3980	0.073992	5.6047
1.4740	1.3999	0.074094	5.6122
1.4760	1.4018	0.074196	5.6198
1.4780	1.4037	0.074297	5.6274
1.4800	1.4056	0.074399	5.6349
1.4820	1.4075	0.074500	5.6425
1.4840	1.4094	0.074602	5.6501
1.4860	1.4113	0.074704	5.6576
1.4880	1.4132	0.074805	5.6652
1.4900	1.4151	0.074907	5.6728
1.4920	1.4170	0.075009	5.6803
1.4940	1.4189	0.075110	5.6879
1.4960	1.4208	0.075212	5.6955
1.4980	1.4227	0.075314	5.7030
1.5000	1.4246	0.075415	5.7106
1.5020	1.4265	0.075517	5.7182
1.5040	1.4284	0.075618	5.7257
1.5060	1.4303	0.075720	5.7333
1.5080	1.4322	0.075822	5.7408
1.5100	1.4341	0.075923	5.7484
1.5120	1.4360	0.076025	5.7560
1.5140	1.4379	0.076127	5.7635
1.5160	1.4398	0.076229	5.7711
1.5180	1.4417	0.076330	5.7787
1.5200	1.4436	0.076432	5.7862
1.5220	1.4455	0.076534	5.7938
1.5240	1.4474	0.076635	5.8013
1.5260	1.4493	0.076737	5.8089
1.5280	1.4512	0.076839	5.8165
1.5300	1.4531	0.076940	5.8240
1.5320	1.4550	0.077042	5.8316
1.5340	1.4569	0.077144	5.8391
1.5360	1.4588	0.077246	5.8467
1.5380	1.4607	0.077347	5.8543
1.5400	1.4625	0.077449	5.8618
1.5420	1.4644	0.077551	5.8694
1.5440	1.4663	0.077653	5.8769
1.5460	1.4682	0.077754	5.8845
1.5480	1.4701	0.077856	5.8921
1.5500	1.4720	0.077958	5.8996
1.5520	1.4739	0.078060	5.9072
1.5540	1.4758	0.078161	5.9147
1.5560	1.4777	0.078263	5.9223
1.5580	1.4796	0.078365	5.9299

OBSERVED DISTANCE (INCHES)	TRUE DISTANCE (INCHES)	ERROR (INCHES)	RAY ANGLE (DEGREES)
1.5600	1.4815	0.078467	5.9374
1.5620	1.4834	0.078568	5.9450
1.5640	1.4853	0.078670	5.9525
1.5660	1.4872	0.078772	5.9601
1.5680	1.4891	0.078874	5.9676
1.5700	1.4910	0.078976	5.9752
1.5720	1.4929	0.079078	5.9827
1.5740	1.4948	0.079179	5.9903
1.5760	1.4967	0.079281	5.9979
1.5780	1.4986	0.079383	6.0054
1.5800	1.5005	0.079485	6.0130
1.5820	1.5024	0.079587	6.0205
1.5840	1.5043	0.079689	6.0281
1.5860	1.5062	0.079790	6.0356
1.5880	1.5081	0.079892	6.0432
1.5900	1.5100	0.079994	6.0508
1.5920	1.5119	0.080096	6.0583
1.5940	1.5138	0.080198	6.0659
1.5960	1.5157	0.080300	6.0734
1.5980	1.5176	0.080402	6.0810
1.6000	1.5195	0.080503	6.0885
1.6020	1.5214	0.080605	6.0961
1.6040	1.5233	0.080707	6.1036
1.6060	1.5252	0.080809	6.1112
1.6080	1.5271	0.080911	6.1187
1.6100	1.5290	0.081013	6.1263
1.6120	1.5309	0.081115	6.1338
1.6140	1.5328	0.081217	6.1414
1.6160	1.5347	0.081319	6.1489
1.6180	1.5366	0.081421	6.1565
1.6200	1.5385	0.081523	6.1640
1.6220	1.5404	0.081624	6.1716
1.6240	1.5423	0.081726	6.1791
1.6260	1.5442	0.081828	6.1867
1.6280	1.5461	0.081930	6.1942
1.6300	1.5480	0.082032	6.2018
1.6320	1.5499	0.082134	6.2093
1.6340	1.5518	0.082236	6.2169
1.6360	1.5537	0.082338	6.2244
1.6380	1.5556	0.082440	6.2320
1.6400	1.5575	0.082542	6.2395
1.6420	1.5594	0.082644	6.2471
1.6440	1.5613	0.082746	6.2546
1.6460	1.5632	0.082848	6.2622
1.6480	1.5650	0.082950	6.2697
1.6500	1.5669	0.083052	6.2773
1.6520	1.5688	0.083154	6.2848
1.6540	1.5707	0.083256	6.2924
1.6560	1.5726	0.083358	6.2999
1.6580	1.5745	0.083460	6.3075
1.6600	1.5764	0.083562	6.3150
1.6620	1.5783	0.083664	6.3226
1.6640	1.5802	0.083766	6.3301
1.6660	1.5821	0.083868	6.3377
1.6680	1.5840	0.083970	6.3452
1.6700	1.5859	0.084072	6.3528
1.6720	1.5878	0.084174	6.3603
1.6740	1.5897	0.084276	6.3679
1.6760	1.5916	0.084378	6.3754
1.6780	1.5935	0.084480	6.3829

OBSERVED DISTANCE (INCHES)	TRUE DISTANCE (INCHES)	ERROR (INCHES)	RAY ANGLE (DEGREES)
1.6800	1.5954	0.084583	6.3905
1.6820	1.5973	0.084685	6.3980
1.6840	1.5992	0.084787	6.4056
1.6860	1.6011	0.084889	6.4131
1.6880	1.6030	0.084991	6.4207
1.6900	1.6049	0.085093	6.4282
1.6920	1.6068	0.085195	6.4358
1.6940	1.6087	0.085297	6.4433
1.6960	1.6106	0.085399	6.4508
1.6980	1.6125	0.085501	6.4584
1.7000	1.6144	0.085603	6.4659
1.7020	1.6163	0.085706	6.4735
1.7040	1.6182	0.085808	6.4810
1.7060	1.6201	0.085910	6.4886
1.7080	1.6220	0.086012	6.4961
1.7100	1.6239	0.086114	6.5036
1.7120	1.6258	0.086216	6.5112
1.7140	1.6277	0.086318	6.5187
1.7160	1.6296	0.086421	6.5263
1.7180	1.6315	0.086523	6.5338
1.7200	1.6334	0.086625	6.5413
1.7220	1.6353	0.086727	6.5489
1.7240	1.6372	0.086829	6.5564
1.7260	1.6391	0.086932	6.5640
1.7280	1.6410	0.087034	6.5715
1.7300	1.6429	0.087136	6.5790
1.7320	1.6448	0.087238	6.5866
1.7340	1.6467	0.087340	6.5941
1.7360	1.6486	0.087443	6.6017
1.7380	1.6505	0.087545	6.6092
1.7400	1.6524	0.087647	6.6167
1.7420	1.6543	0.087749	6.6243
1.7440	1.6561	0.087851	6.6318
1.7460	1.6580	0.087954	6.6393
1.7480	1.6599	0.088056	6.6469
1.7500	1.6618	0.088158	6.6544
1.7520	1.6637	0.088260	6.6620
1.7540	1.6656	0.088363	6.6695
1.7560	1.6675	0.088465	6.6770
1.7580	1.6694	0.088567	6.6846
1.7600	1.6713	0.088669	6.6921
1.7620	1.6732	0.088772	6.6996
1.7640	1.6751	0.088874	6.7072
1.7660	1.6770	0.088976	6.7147
1.7680	1.6789	0.089079	6.7222
1.7700	1.6808	0.089181	6.7298
1.7720	1.6827	0.089283	6.7373
1.7740	1.6846	0.089385	6.7448
1.7760	1.6865	0.089488	6.7524
1.7780	1.6884	0.089590	6.7599
1.7800	1.6903	0.089692	6.7674
1.7820	1.6922	0.089795	6.7750
1.7840	1.6941	0.089897	6.7825
1.7860	1.6960	0.089999	6.7900
1.7880	1.6979	0.090102	6.7976
1.7900	1.6998	0.090204	6.8051
1.7920	1.7017	0.090306	6.8126
1.7940	1.7036	0.090409	6.8202
1.7960	1.7055	0.090511	6.8277
1.7980	1.7074	0.090613	6.8352

OBSERVED DISTANCE (INCHES)	TRUE DISTANCE (INCHES)	ERROR (INCHES)	RAY ANGLE (DEGREES)
1.8000	1.7093	0.090716	6.8428
1.8020	1.7112	0.090818	6.8503
1.8040	1.7131	0.090921	6.8578
1.8060	1.7150	0.091023	6.8654
1.8080	1.7169	0.091125	6.8729
1.8100	1.7188	0.091228	6.8804
1.8120	1.7207	0.091330	6.8879
1.8140	1.7226	0.091433	6.8955
1.8160	1.7245	0.091535	6.9030
1.8180	1.7264	0.091637	6.9105
1.8200	1.7283	0.091740	6.9181
1.8220	1.7302	0.091842	6.9256
1.8240	1.7321	0.091945	6.9331
1.8260	1.7340	0.092047	6.9406
1.8280	1.7358	0.092150	6.9482
1.8300	1.7377	0.092252	6.9557
1.8320	1.7396	0.092355	6.9632
1.8340	1.7415	0.092457	6.9708
1.8360	1.7434	0.092559	6.9783
1.8380	1.7453	0.092662	6.9858
1.8400	1.7472	0.092764	6.9933
1.8420	1.7491	0.092867	7.0009
1.8440	1.7510	0.092969	7.0084
1.8460	1.7529	0.093072	7.0159
1.8480	1.7548	0.093174	7.0234
1.8500	1.7567	0.093277	7.0310
1.8520	1.7586	0.093379	7.0385
1.8540	1.7605	0.093482	7.0460
1.8560	1.7624	0.093584	7.0535
1.8580	1.7643	0.093687	7.0611
1.8600	1.7662	0.093790	7.0686
1.8620	1.7681	0.093892	7.0761
1.8640	1.7700	0.093995	7.0836
1.8660	1.7719	0.094097	7.0912
1.8680	1.7738	0.094200	7.0987
1.8700	1.7757	0.094302	7.1062
1.8720	1.7776	0.094405	7.1137
1.8740	1.7795	0.094507	7.1213
1.8760	1.7814	0.094610	7.1288
1.8780	1.7833	0.094713	7.1363
1.8800	1.7852	0.094815	7.1438
1.8820	1.7871	0.094918	7.1513
1.8840	1.7890	0.095020	7.1589
1.8860	1.7909	0.095123	7.1664
1.8880	1.7928	0.095226	7.1739
1.8900	1.7947	0.095328	7.1814
1.8920	1.7966	0.095431	7.1889
1.8940	1.7985	0.095533	7.1965
1.8960	1.8004	0.095636	7.2040
1.8980	1.8023	0.095739	7.2115
1.9000	1.8042	0.095841	7.2190
1.9020	1.8061	0.095944	7.2265
1.9040	1.8080	0.096047	7.2340
1.9060	1.8098	0.096149	7.2416
1.9080	1.8117	0.096252	7.2491
1.9100	1.8136	0.096355	7.2566
1.9120	1.8155	0.096457	7.2641
1.9140	1.8174	0.096560	7.2716
1.9160	1.8193	0.096663	7.2792
1.9180	1.8212	0.096765	7.2867

OBSERVED DISTANCE (INCHES)	TRUE DISTANCE (INCHES)	ERROR (INCHES)	RAY ANGLE (DEGREES)
1.9200	1.8231	0.096868	7.2942
1.9220	1.8250	0.096971	7.3017
1.9240	1.8269	0.097073	7.3092
1.9260	1.8288	0.097176	7.3167
1.9280	1.8307	0.097279	7.3242
1.9300	1.8326	0.097382	7.3318
1.9320	1.8345	0.097484	7.3393
1.9340	1.8364	0.097587	7.3468
1.9360	1.8383	0.097690	7.3543
1.9380	1.8402	0.097793	7.3618
1.9400	1.8421	0.097895	7.3693
1.9420	1.8440	0.097998	7.3769
1.9440	1.8459	0.098101	7.3844
1.9460	1.8478	0.098204	7.3919
1.9480	1.8497	0.098306	7.3994
1.9500	1.8516	0.098409	7.4069
1.9520	1.8535	0.098512	7.4144
1.9540	1.8554	0.098615	7.4219
1.9560	1.8573	0.098718	7.4294
1.9580	1.8592	0.098820	7.4370
1.9600	1.8611	0.098923	7.4445
1.9620	1.8630	0.099026	7.4520
1.9640	1.8649	0.099129	7.4595
1.9660	1.8668	0.099232	7.4670
1.9680	1.8687	0.099335	7.4745
1.9700	1.8706	0.099437	7.4820
1.9720	1.8725	0.099540	7.4895
1.9740	1.8744	0.099643	7.4970
1.9760	1.8763	0.099746	7.5045
1.9780	1.8782	0.099849	7.5121
1.9800	1.8800	0.099952	7.5196
1.9820	1.8819	0.100054	7.5271
1.9840	1.8838	0.100157	7.5346
1.9860	1.8857	0.100260	7.5421
1.9880	1.8876	0.100363	7.5496
1.9900	1.8895	0.100466	7.5571
1.9920	1.8914	0.100569	7.5646
1.9940	1.8933	0.100672	7.5721
1.9960	1.8952	0.100775	7.5796
1.9980	1.8971	0.100878	7.5871
2.0000	1.8990	0.100981	7.5946
2.0020	1.9009	0.101084	7.6021
2.0040	1.9028	0.101186	7.6096
2.0060	1.9047	0.101289	7.6172
2.0080	1.9066	0.101392	7.6247
2.0100	1.9085	0.101495	7.6322
2.0120	1.9104	0.101598	7.6397
2.0140	1.9123	0.101701	7.6472
2.0160	1.9142	0.101804	7.6547
2.0180	1.9161	0.101907	7.6622
2.0200	1.9180	0.102010	7.6697
2.0220	1.9199	0.102113	7.6772
2.0240	1.9218	0.102216	7.6847
2.0260	1.9237	0.102319	7.6922
2.0280	1.9256	0.102422	7.6997
2.0300	1.9275	0.102525	7.7072
2.0320	1.9294	0.102628	7.7147
2.0340	1.9313	0.102731	7.7222
2.0360	1.9332	0.102834	7.7297
2.0380	1.9351	0.102937	7.7372

OBSERVED DISTANCE (INCHES)	TRUE DISTANCE (INCHES)	ERROR (INCHES)	RAY ANGLE (DEGREES)
2.0400	1.9370	0.103040	7.7447
2.0420	1.9389	0.103143	7.7522
2.0440	1.9408	0.103246	7.7597
2.0460	1.9426	0.103349	7.7672
2.0480	1.9445	0.103453	7.7747
2.0500	1.9464	0.103556	7.7822
2.0520	1.9483	0.103659	7.7897
2.0540	1.9502	0.103762	7.7972
2.0560	1.9521	0.103865	7.8047
2.0580	1.9540	0.103968	7.8122
2.0600	1.9559	0.104071	7.8197
2.0620	1.9578	0.104174	7.8272
2.0640	1.9597	0.104277	7.8347
2.0660	1.9616	0.104380	7.8422
2.0680	1.9635	0.104483	7.8497
2.0700	1.9654	0.104587	7.8572
2.0720	1.9673	0.104690	7.8647
2.0740	1.9692	0.104793	7.8722
2.0760	1.9711	0.104896	7.8797
2.0780	1.9730	0.104999	7.8872
2.0800	1.9749	0.105102	7.8947
2.0820	1.9768	0.105205	7.9022
2.0840	1.9787	0.105309	7.9097
2.0860	1.9806	0.105412	7.9172
2.0880	1.9825	0.105515	7.9246
2.0900	1.9844	0.105618	7.9321
2.0920	1.9863	0.105721	7.9396
2.0940	1.9882	0.105825	7.9471
2.0960	1.9901	0.105928	7.9546
2.0980	1.9920	0.106031	7.9621
2.1000	1.9939	0.106134	7.9696
2.1020	1.9958	0.106238	7.9771
2.1040	1.9977	0.106341	7.9846
2.1060	1.9996	0.106444	7.9921
2.1080	2.0015	0.106547	7.9996
2.1100	2.0033	0.106650	8.0071
2.1120	2.0052	0.106754	8.0146
2.1140	2.0071	0.106857	8.0220
2.1160	2.0090	0.106960	8.0295
2.1180	2.0109	0.107064	8.0370
2.1200	2.0128	0.107167	8.0445
2.1220	2.0147	0.107270	8.0520
2.1240	2.0166	0.107374	8.0595
2.1260	2.0185	0.107477	8.0670
2.1280	2.0204	0.107580	8.0745
2.1300	2.0223	0.107683	8.0820
2.1320	2.0242	0.107787	8.0894
2.1340	2.0261	0.107890	8.0969
2.1360	2.0280	0.107993	8.1044
2.1380	2.0299	0.108097	8.1119
2.1400	2.0318	0.108200	8.1194
2.1420	2.0337	0.108303	8.1269
2.1440	2.0356	0.108407	8.1344
2.1460	2.0375	0.108510	8.1419
2.1480	2.0394	0.108613	8.1493
2.1500	2.0413	0.108717	8.1568
2.1520	2.0432	0.108820	8.1643
2.1540	2.0451	0.108924	8.1718
2.1560	2.0470	0.109027	8.1793
2.1580	2.0489	0.109131	8.1868

OBSERVED DISTANCE (INCHES)	TRUE DISTANCE (INCHES)	ERROR (INCHES)	RAY ANGLE (DEGREES)
2.1600	2.0508	0.109234	8.1943
2.1620	2.0527	0.109337	8.2017
2.1640	2.0546	0.109441	8.2092
2.1660	2.0565	0.109544	8.2167
2.1680	2.0584	0.109647	8.2242
2.1700	2.0602	0.109751	8.2317
2.1720	2.0621	0.109854	8.2392
2.1740	2.0640	0.109958	8.2466
2.1760	2.0659	0.110061	8.2541
2.1780	2.0678	0.110165	8.2616
2.1800	2.0697	0.110268	8.2691
2.1820	2.0716	0.110372	8.2766
2.1840	2.0735	0.110475	8.2840
2.1860	2.0754	0.110579	8.2915
2.1880	2.0773	0.110682	8.2990
2.1900	2.0792	0.110786	8.3065
2.1920	2.0811	0.110889	8.3140
2.1940	2.0830	0.110993	8.3214
2.1960	2.0849	0.111096	8.3289
2.1980	2.0868	0.111200	8.3364
2.2000	2.0887	0.111303	8.3439
2.2020	2.0906	0.111407	8.3514
2.2040	2.0925	0.111510	8.3588
2.2060	2.0944	0.111614	8.3663
2.2080	2.0963	0.111717	8.3738
2.2100	2.0982	0.111821	8.3813
2.2120	2.1001	0.111924	8.3887
2.2140	2.1020	0.112028	8.3962
2.2160	2.1039	0.112131	8.4037
2.2180	2.1058	0.112235	8.4112
2.2200	2.1077	0.112339	8.4187
2.2220	2.1096	0.112442	8.4261
2.2240	2.1115	0.112546	8.4336
2.2260	2.1133	0.112650	8.4411
2.2280	2.1152	0.112753	8.4486
2.2300	2.1171	0.112857	8.4560
2.2320	2.1190	0.112960	8.4635
2.2340	2.1209	0.113064	8.4710
2.2360	2.1228	0.113168	8.4784
2.2380	2.1247	0.113271	8.4859
2.2400	2.1266	0.113375	8.4934
2.2420	2.1285	0.113479	8.5009
2.2440	2.1304	0.113582	8.5083
2.2460	2.1323	0.113686	8.5158
2.2480	2.1342	0.113790	8.5233
2.2500	2.1361	0.113893	8.5308
2.2520	2.1380	0.113997	8.5382
2.2540	2.1399	0.114101	8.5457
2.2560	2.1418	0.114205	8.5532
2.2580	2.1437	0.114308	8.5606
2.2600	2.1456	0.114412	8.5681
2.2620	2.1475	0.114516	8.5756
2.2640	2.1494	0.114620	8.5830
2.2660	2.1513	0.114723	8.5905
2.2680	2.1532	0.114827	8.5980
2.2700	2.1551	0.114931	8.6055
2.2720	2.1570	0.115034	8.6129
2.2740	2.1589	0.115138	8.6204
2.2760	2.1608	0.115242	8.6279
2.2780	2.1627	0.115346	8.6353

OBSERVED DISTANCE (INCHES)	TRUE DISTANCE (INCHES)	ERROR (INCHES)	RAY ANGLE (DEGREES)
2.2800	2.1645	0.115450	8.6428
2.2820	2.1664	0.115553	8.6503
2.2840	2.1683	0.115657	8.6577
2.2860	2.1702	0.115761	8.6652
2.2880	2.1721	0.115865	8.6727
2.2900	2.1740	0.115969	8.6801
2.2920	2.1759	0.116072	8.6876
2.2940	2.1778	0.116176	8.6951
2.2960	2.1797	0.116280	8.7025
2.2980	2.1816	0.116384	8.7100
2.3000	2.1835	0.116488	8.7174
2.3020	2.1854	0.116592	8.7249
2.3040	2.1873	0.116695	8.7324
2.3060	2.1892	0.116799	8.7398
2.3080	2.1911	0.116903	8.7473
2.3100	2.1930	0.117007	8.7548
2.3120	2.1949	0.117111	8.7622
2.3140	2.1968	0.117215	8.7697
2.3160	2.1987	0.117319	8.7772
2.3180	2.2006	0.117423	8.7846
2.3200	2.2025	0.117527	8.7921
2.3220	2.2044	0.117631	8.7995
2.3240	2.2063	0.117735	8.8070
2.3260	2.2082	0.117839	8.8145
2.3280	2.2101	0.117942	8.8219
2.3300	2.2120	0.118046	8.8294
2.3320	2.2138	0.118150	8.8368
2.3340	2.2157	0.118254	8.8443
2.3360	2.2176	0.118358	8.8518
2.3380	2.2195	0.118462	8.8592
2.3400	2.2214	0.118566	8.8667
2.3420	2.2233	0.118670	8.8741
2.3440	2.2252	0.118774	8.8816
2.3460	2.2271	0.118878	8.8890
2.3480	2.2290	0.118982	8.8965
2.3500	2.2309	0.119086	8.9040
2.3520	2.2328	0.119190	8.9114
2.3540	2.2347	0.119294	8.9189
2.3560	2.2366	0.119398	8.9263
2.3580	2.2385	0.119502	8.9338
2.3600	2.2404	0.119606	8.9412
2.3620	2.2423	0.119711	8.9487
2.3640	2.2442	0.119815	8.9561
2.3660	2.2461	0.119919	8.9636
2.3680	2.2480	0.120023	8.9711
2.3700	2.2499	0.120127	8.9785
2.3720	2.2518	0.120231	8.9860
2.3740	2.2537	0.120335	8.9934
2.3760	2.2556	0.120439	9.0009
2.3780	2.2575	0.120543	9.0083
2.3800	2.2594	0.120647	9.0158
2.3820	2.2612	0.120751	9.0232
2.3840	2.2631	0.120856	9.0307
2.3860	2.2650	0.120960	9.0381
2.3880	2.2669	0.121064	9.0456
2.3900	2.2688	0.121168	9.0530
2.3920	2.2707	0.121272	9.0605
2.3940	2.2726	0.121376	9.0679
2.3960	2.2745	0.121480	9.0754
2.3980	2.2764	0.121585	9.0828

OBSERVED DISTANCE (INCHES)	TRUE DISTANCE (INCHES)	ERROR (INCHES)	RAY ANGLE (DEGREES)
2.4000	2.2783	0.121689	9.0903
2.4020	2.2802	0.121793	9.0977
2.4040	2.2821	0.121897	9.1052
2.4060	2.2840	0.122001	9.1126
2.4080	2.2859	0.122106	9.1201
2.4100	2.2878	0.122210	9.1275
2.4120	2.2897	0.122314	9.1350
2.4140	2.2916	0.122418	9.1424
2.4160	2.2935	0.122523	9.1498
2.4180	2.2954	0.122627	9.1573
2.4200	2.2973	0.122731	9.1647
2.4220	2.2992	0.122835	9.1722
2.4240	2.3011	0.122940	9.1796
2.4260	2.3030	0.123044	9.1871
2.4280	2.3049	0.123148	9.1945
2.4300	2.3067	0.123253	9.2020
2.4320	2.3086	0.123357	9.2094
2.4340	2.3105	0.123461	9.2168
2.4360	2.3124	0.123565	9.2243
2.4380	2.3143	0.123670	9.2317
2.4400	2.3162	0.123774	9.2392
2.4420	2.3181	0.123879	9.2466
2.4440	2.3200	0.123983	9.2541
2.4460	2.3219	0.124087	9.2615
2.4480	2.3238	0.124191	9.2689
2.4500	2.3257	0.124296	9.2764
2.4520	2.3276	0.124400	9.2838
2.4540	2.3295	0.124505	9.2913
2.4560	2.3314	0.124609	9.2987
2.4580	2.3333	0.124713	9.3061
2.4600	2.3352	0.124818	9.3136
2.4620	2.3371	0.124922	9.3210
2.4640	2.3390	0.125027	9.3285
2.4660	2.3409	0.125131	9.3359
2.4680	2.3428	0.125235	9.3433
2.4700	2.3447	0.125340	9.3508
2.4720	2.3466	0.125444	9.3582
2.4740	2.3484	0.125549	9.3657
2.4760	2.3503	0.125653	9.3731
2.4780	2.3522	0.125758	9.3805
2.4800	2.3541	0.125862	9.3880
2.4820	2.3560	0.125967	9.3954
2.4840	2.3579	0.126071	9.4028
2.4860	2.3598	0.126176	9.4103
2.4880	2.3617	0.126280	9.4177
2.4900	2.3636	0.126385	9.4251
2.4920	2.3655	0.126489	9.4326
2.4940	2.3674	0.126594	9.4400
2.4960	2.3693	0.126698	9.4474
2.4980	2.3712	0.126803	9.4549
2.5000	2.3731	0.126907	9.4623

APPENDIX C

APPLICATION OF COMPUTER PROGRAM "HOLOFER"

The computer program is an adptation of the inversion first proposed
by C. D. Maldonado [9, 10, 11] and is designed to invert fringe numbers
across a field to the density field. It can be operated in three dif-
ferent modes as described below:

(a) Mode 1

Mode 1 is utilized as a self-test of the computer program. It
can either generate its own input density field using Subroutine FUNCT
or read in a density field through Subroutine FREAD. The program then
generates the fringe array and inverts the array back to the original
density field. This mode was utilized in the present investigation to
determine the value of the scale factor, α , required to obtain the
correct density across the fin.

(b) Mode 2

This mode reads in irregularly spaced fringe data and generates
the fringe array at regular intervals across the field using Subroutine
SHEET. By specifying NCODE = 1, the fringe array can be generated by one
of the functions in Subroutine FUNCT. Mode 2 was not utilized .

(c) Mode 3

Mode 3 reads in the fringe data at regularly spaced intervals and
inverts the array to density data across the field. The Subroutine GARRAY
calls Subroutine READ to read in the fringe data. The first two cards
preceeding the fringe data provide the program with the fringe field size,
location, and symmetry.

The following parameters were used in considering the symmetric field case:

PARAMETER	INPUT
NOF	Run Number
IMAX	201
JMAX	1
ISYM	101
JSYM	1
IMS	2
JMS	100
Z	0.387
XO	0.0
YO	0.0
PHISYM	0.0

References [3] and [12] contain further details and applications of the computer program. A print-out of the program is included in the next few pages of this appendix.

```fortran
C     *************HOLOVERT******************************************       CAL00001C
C     *************************************************************       CAL000020
C     HOLOVERT INVERTS THE FIELD AT AN ARRAY OF POINTS IN A VARIABLE      CAL000030
C     COORDINATE SYSTEM. IT SURVEYS NPTS POINTS EACH FOR A SET OF NLINS   CAL000040
C     LINES ACROSS THE FIELD.                                            CAL000050
                                                                          CAL000060
      COMMON IMAX,JMAX,IIMX,JJMX,ALPHA,SIZE,EPS,MODE,BOX,SD,IX,Z         CAL000070
      COMMON /TAB/ INDEX,KEXTRA,MEXTRA,KLIMIT,MLIMIT,KOUT,MOUT           CAL000080
      COMMON /TAB2/ IPT,KPT,BND,NPTS,NLINS,RHOINF,RLAMDA,BETA            CAL000090
      COMMON /OUT/ XP,THEO,CALC,ERR,RHO,CA,FA                            CAL000100
      COMMON /EQPARA/ A,B,C,D,E,P,Q,S,T,U,V,W,RO,RA,NO,NA,NOF,NAF        CAL000110
      COMMON /SYM/ ISYM,JSYM,MSYM,FCU,IMS,JMS,QSYM                       CAL000120
      COMMON /IO/ CMS,IN1,IN2,IN4                                        CAL000130
      DATA BL,PL,ST,EX,OH,SC,DH,BR/1H ,1H+,1H*,1HX,1HO,1H:,1H-,1H|/      CAL000140
      DIMENSION RB(7),TL(62),RO(101),RA(101)                            CAL000150
C                                                                        CAL000160
      DIMENSION G(5151),GA(5151),H(202,5),SCF(73,6),BDA(4000)            CAL000170
      DIMENSION THEO(51,11),CALC(51,11),ERR(51),RHO(51)                 CAL000180
      DIMENSION CA(51),FA(51),AR(42),XP(51),YP(51)                      CAL000190
      CMS=0.                                                            CAL000200
C                                                                        CAL000220
      REWIND 3                                                          CAL000230
      IN1=5                                                             CAL000240
      IN2=5                                                             CAL000250
      IN4=5                                                             CAL000260
      IF(CMS.NE.1.) GO TO 20                                            CAL000270
      IN1=1                                                             CAL000280
      IN2=2                                                             CAL000290
      IN4=4                                                             CAL000300
      IF(CMS.EQ.1.) REWIND 4                                            CAL000310
   20 READ(IN4,89) (AR(I),I=1,42)                                       CAL000320
      IMAX=AR(1)                                                        CAL000330
      JMAX=AR(2)*2.                                                     CAL000340
      IF(JMAX.LE.0) JMAX=1                                              CAL000350
      KLIMIT=AR(3)                                                      CAL000360
      MLIMIT=AR(4)                                                      CAL000370
      KEXTRA=AR(5)                                                      CAL000380
      MEXTRA=AR(6)                                                      CAL000390
      JSYM=AR(14)                                                       CAL000400
      ALPHA=AR(7)                                                       CAL000410
      SIZE=AR(8)                                                        CAL000420
      EPS=AR(9)                                                         CAL000430
      MODE=AR(13)                                                       CAL000440
      DGN=AR(17)                                                        CAL000450
      RHOINF=AR(10)                                                     CAL000460
      RLAMDA=AR(11)*1.E-8                                               CAL000470
      BETA=AR(12)
```

127

```
      NPTS=AR(15)                                                        CAL00480
      NLINS=AR(16)                                                       CAL00490
      SD=AR(18)                                                          CAL00500
      PHIZ=AR(19)                                                        CAL00510
      DELPHI=AR(20)                                                      CAL00520
      YPZERO=AR(21)                                                      CAL00530
      YPRNG=AR(22)                                                       CAL00540
      XPZERO=AR(23)                                                      CAL00550
      XPRNG=AR(24)                                                       CAL00560
      NOF=AR(25)                                                         CAL00570
      NAF=AR(26)                                                         CAL00580
      IPT=AR(27)                                                         CAL00590
      KPT=AR(28)                                                         CAL00600
      LPT=AR(29)                                                         CAL00610
      BND=AR(30)                                                         CAL00620
      A=AR(31)                                                           CAL00630
      B=AR(32)                                                           CAL00640
      C=AR(33)                                                           CAL00650
      D=AR(34)                                                           CAL00660
      E=AR(35)                                                           CAL00670
      P=AR(37)                                                           CAL00680
      S=AR(38)                                                           CAL00690
      T=AR(39)                                                           CAL00700
      U=AR(40)                                                           CAL00710
      V=AR(41)                                                           CAL00720
      W=AR(42)                                                           CAL00730
      Q=AR(42)                                                           CAL00740
      WRITE(6,90)
      WRITE(6,98)
      WRITE(6,91)
      WRITE(6,92)
      WRITE(6,93)
      WRITE(6,94)
      WRITE(6,95)
      WRITE(6,96)
      WRITE(6,97)
      WRITE(6,98)
   90 FORMAT(/////,5X,'INPUT PARAMETERS FOR THIS RUN ARE :',///)
   91 FORMAT(/5X,'* KLIMIT * MLIMIT * KEXTRA * JMAX/2 * IMAX *
     1 MEXTRA */3X,6F10.0)                                               SET00310
   92 FORMAT(/5X,'* RHO-INF * LAMBDA * EPS. * SIZE *',                   SET00340
     1 /3X,'* ALPHA',F11.6,2X,F8.7,F9.1,F11.6)                          SET
   93 FORMAT(/5X,'* POINTS * LINES * DIAGNOS * SYM. *',                  SET00360
     1 /2X,'* MODE',2F10.0,F10.3)
   94 FORMAT(/5X,'* DELPHI * YPZERO * XPZERO * PHIZERO *',               SET
     1 /2X,'* STD.DEV',5F10.0,F10.3)
   95 FORMAT(/5X,'* YPRANGE * XPRANGE * GARRAY * GRAPH * LIN PRT *',     SET00400
     1 /2X,'* ADD FUN * TST FUN * MAP BND',6F10.0)
```

```
96  FORMAT (/5X,'**  A  *  B  *  C  *  D  *  E  *',SET00420
   1  P**'/4X,6F10.3)
97  FORMAT (/5X,'**  S  *  T  *  U  *  V  *  W  *',SET00440
   1  Q**'/4X,6F10.3)
98  FORMAT (/3X,75A1)
    IF (DGN.GE.4) WRITE (6,89) (AR(I),I=1,42)
    NNN=2
    IF (MODE.LT.0) NNN=1
    IF (MODE.GT.5) NNN=3
    IF (MODE.GT.5) MODE=MODE-10
    NGP=0
    IF (KLIMIT.LT.KEXTRA) KEXTRA=KLIMIT
    IF (MLIMIT.LT.MEXTRA) MEXTRA=MLIMIT
    IF (IPT.LT.0) NGP=IPT
    IF (IPT.LT.0) IPT=-IPT
    ISYM=2.-(FLOAT(JSYM)/2.-FLOAT(JSYM/2))*2.
    IF (JSYM.EQ.0) ISYM=1
    IF (JSYM.GT.JMAX) ISYM=2
    IF (ISYM.EQ.1) JMAX=((JMAX+1)/2)*2
    RJMX=JMAX
    MSYM=JSYM
    IF ((MSYM.EQ.0).OR.(MSYM.GT.JMAX)) MSYM=1
    FCU=ISYM*JSYM*JMAX
    IF ((JSYM.GT.JMAX).OR.(JSYM.EQ.0)) FCU=JMAX
    QSYM=FCU/RJMX
    IMS=(IMAX+ISYM-1)/ISYM
    JMS=JMAX
    IF (ISYM.EQ.1) JMS=(JMAX/2+1)/2
    IF (JSYM.EQ.0) JMS=JMAX/2
    MODE=ABS(AR(13))
    XO=0.
    YO=0.
    ZD=0.
    PHISYM=0.
    HS=SIZE/2.
    RHOS=1.286
    BOX=RHOINF*BETA/RHOS/RLAMDA
    RPTS=NPTS
    XPR=0.
    IF (NPTS.GT.1) XPR=XPRNG/(RPTS-1.)/2.
    XPM=-XPR
    PIE=3.14159265358979793
    MONE=1
    WRITE (6,58) IMAX,JMAX,IMS,JMS,ISYM,JSYM,JSYM,MSYM,QSYM,FCU
   1  58 FORMAT(3X,7I5,2F7.3/)
    NTWO=2
    IX=IMAX+JMAX
```

```
      NF=IN1
      IF((MODE.EQ.1.).AND.(NOF.EQ.8).AND.(DGN.GE.1.)) WRITE (6,69)
      IF((MODE.EQ.1).AND.(NOF.EQ.8)) CALL FREAD (NO,RO,NF,ZD)
      Z=ZD
      IF(DGN.GE.1.) WRITE (6,68)
      CALL GARRAY (G,GA,NOF,DGN,MONE,XO,YO,PHISYM)
      LM=1
      IF((LPT.EQ.0).AND.(BND.EQ.0)) LM=0
      IIMX=IMAX+1
      JJMX=JMAX+1
      IJMX=IMAX*JMAX
      NBD=1
      IF(JSYM.EQ.0) NBD=2
      KBD=KLIMIT*NBD
      DO 15 IJ=1,IJMX
   15 GA(IJ)=0.
      NF=IN2
      IF((NAF.EQ.8).AND.(DGN.GE.1.)) WRITE (6,69)
      IF((NAF.EQ.8) CALL FREAD (NA,RA,NF,ZD)
      MST=MODE
      MODE=1
      IF((DGN.GE.1.) WRITE (6,68)
      IF(NAF.NE.0) CALL GARRAY (GA,G,NAF,DGN,NTWO,XO,YO,PHISYM)
      MODE=MST
      DO 6 IJ=1,IJMX
    6 G(IJ)=G(IJ)+GA(IJ)
      RLINS=NLINS
      IF(NAF.EQ.8) WRITE (6,88) NA,(RA(L),L=1,NA)
      IF(NOF.EQ.8) WRITE (6,87) NO,(RO(I),I=1,NO)
      IF(LM.EQ.0) GO TO 14
      RB(1)=1.2.7
      DO 1 I=2,7
    1 RB(I)=RB(I-1)+.5
      TPIE=2.*PIE
      MPIE=0.-PIE
      DYP=0.
      DXP=0.
      IF((NLINS.GT.1) DYP=YPRNG/(RLINS-1.)
      IF((NPTS.GT.1) DXP=XPRNG/(RPTS-1.)
      IF((NNN.EQ.2).AND.(DGN.GE.1.) WRITE (6,64)
      IF(NNN.EQ.2)CALL BDGEN (G,H,SCF,DGN,NBD,BDA,KBD)
      DO 5 J=1,NLINS
      IF(DGN.GE.1.) WRITE (6,67) J
      RJM=J-1
      PHI=PHIZ+DELPHI*RJM
      YP(J)=YPZERO+DYP*RJM
      PSI=(PHI+90.)*PIE/180.
```

```
      TAU=PSI-PHISYM
      IF(LPT.EQ.0) GO TO 9
      IF(LPT.LE.1) WRITE(6,78) (ST,I=1,124)
      IF(LPT.GT.1) WRITE(6,74) (ST,I=1,95)
      IF((CMS.EQ.1.).AND.(LPT.GT.1)) READ (5,79) ZZ
      WRITE(6,86) Z,PHI,YP(J)
      WRITE(6,85)
      WRITE(6,76)
      IF(MODE.EQ.1) WRITE(6,83) (RB(I),I=1,7)
      IF(MODE.GT.1) WRITE(6,80) (RB(I),I=1,7)
      WRITE(6,81) (DH,I=1,54),(PL,II=1,13)
      IC=0
      DO 3 I=1,NPTS
      RIM=I-1
      THEO(I,J)=0.
      CA(I,J)=0.
      ERR(I,J)=0.
      CALC(I,J)=0.
      RHO(I)=XPZERO+DXP*RIM
      XP(I)=1.E-10+XP(I)
      XPII=ABS(XP(I))
      RS=SQRT(XPII**2+YP(J)**2)
      IF(RS.GT.1.) GO TO 13
      THT=ATANM(YP(J),XP(I))
      IF(XPII.EQ.0.) THT=0.
      SIG=TAU-PIE/2.+THT
      IF(SIG.GT.PIE) SIG=SIG-TPIE
      IF(SIG.LT.MPIE) SIG=SIG+TPIE
      SIGI=SIG
      XS=RS*COS(SIG)
      IF(SIG.GE.1.) SIG=1.
      YS=RS*SIN(SIG)
      IF(DGN.GE.5) WRITE(6,44) SIG
   44 FORMAT(' ',E10.3)
      RI=I
      F=0.
      IF(DGN.GE.2.) WRITE(6,57) PHI,DELPHI,PSI,TAU,THT,SIG,SIGI,XS,YS
   57 FORMAT(' ANGLES=',10E10.3)
      WRITE(6,66) I
      CALL FUNCT(XS,YS,FA(I,J),NAF,DGN,NTWO)
      IF(MODE.EQ.1) CALL FUNCT(XS,YS,F,NOF,DGN,MONE)
      THEO(I,J)=F
      IF(NNN.GE.3) REWIND 3
      IF(NNN.GE.2) CALL FIELD (RS,SIGI,SOLN,NBD,BDA,DGN,KBD)
      IF(NNN.GE.1) CALL FIELD2 (RS,SIGI,SOLN,G,H,SCF,DGN)
      CA(I)=SOLN/BOX/HS
      CALC(I,J)=CA(I)-FA(I,J)
```

```
      RHO(I)=RHOINF*(CALC(I,J)+1.)                                   CAL02140
      ERR(I)=CA(I)                                                   CAL02150
   13 IF(MODE.EQ.1) ERR(I)=(CALC(I,J)-THEO(I,J))                     CAL02160
      IF(MODE.GT.1) THEO(I,J)=FA(I,J)                                CAL02170
      IF(LPT.EQ.0) GO TO 3                                           CAL02180
      LC=0                                                           CAL02190
      TTL=0                                                          CAL02200
      TL(1)=BL                                                       CAL02210
      IF((XP(I).GT.XPM).AND.(XP(I).LT.XPR)) TTL=1.                   CAL02260
      IF(IC.EQ.5) IC=0                                               CAL02270
      IF(IC.EQ.0) TL(1)=PL                                           CAL02280
      DO 2 L=2,62                                                    CAL02290
      IF((I.EQ.1).OR.(TTL.EQ.1.).OR.(I.EQ.NPTS)) TL(L)=PL           CAL02300
      IF(LC.EQ.10) LC=0                                              CAL02310
      IF((IC.EQ.0).AND.(LC.EQ.0)) TL(L)=PL                          CAL02320
      LC=LC+1                                                        CAL02330
    2 TL(2)=PL                                                       CAL02340
      TL(22)=PL                                                      CAL02350
      TL(62)=PL                                                      CAL02360
      IC=IC+1                                                        CAL02370
      RLW=(CA(I)+1.)*20.+2.5                                         CAL02380
      LW=RLW                          LW=62                          CAL02390
      IF(LW.GT.62) LW=62                                             CAL02400
      IF(LW.LT.2) LW=2                                               CAL02410
      TL(LW)=SC                                                      CAL02420
      RLY=(FA(I,J)+1.)*20.+2.5                                       CAL02430
      LY=RLY                          LY=62                          CAL02440
      IF(LY.GT.62) LY=62                                             CAL02450
      IF(LY.LT.2) LY=2                                               CAL02460
      IF(NAF.NE.0) TL(LY)=ST                                         CAL02470
      RLX=(THEO(I,J)+1.)*20.+2.5                                     CAL02480
      LX=RLX                          LX=62                          CAL02490
      IF(LX.GT.62) LX=62                                             CAL02500
      IF(LX.LT.2) LX=2                                               CAL02510
      IF(MODE.EQ.1) TL(LX)=OH                                        CAL02520
      RLZ=(CALC(I,J)+1.)*20.+2.5                                     CAL02530
      LZ=RLZ                          LZ=62                          CAL02540
      IF(LZ.GT.62) LZ=62                                             CAL02550
      IF(LZ.LT.2) LZ=2                                               CAL02560
      TL(LZ)=EX                                                      CAL02570
      WRITE(6,82)MOUT,KOUT,INDEX,THEO(I,J),ERR(I),CALC(I,J),RHO(I),  CAL02580
     1XP(I),(TL(L),L=1,62)                                           CAL02590
      IF((NPTS.LE.20).AND.(I.NE.NPTS)) WRITE (6,79)                  CAL02600
    3 CONTINUE                                                       CAL02610
      IF(LPT.NE.0) WRITE (6,81) (DH,I=1,54),(PL,I=1,13)
      TMAX=0.
      TMIN=0.
```

132

```
      IE=0
      BE=0.
      EB=0.
      DO 4 I=1,NPTS
      TH=THEO(I,J)
      IF(TH.GT.TMAX) TMAX=TH
      IF(TH.LT.TMIN) TMIN=TH
      ER=ABS(CALC(I,J)-TH)
      IF(ER.LE.BE) GO TO 4
      BE=ER
      IE=I
    4 CONTINUE
      TMM=TMAX-TMIN
      EB=RHOINF*(CALC(IE,J)-THEO(IE,J))
      IF(TMM.NE.0.) BE=(CALC(IE,J)-THEO(IE,J))*100./TMM
      IF((MODE.EQ.1).AND.(LPT.NE.0)) WRITE(6,75) EB,XP(IE),BE
      IF(DELPHI.NE.0.) YP(J)=PHI
    5 CONTINUE
      IF(BND) GO TO 14
      IF((LPT.EQ.0).OR.(LPT.GT.1)) WRITE(6,78) (ST,I=1,124)
      IF((LPT.GE.1).AND.(LPT.GT.1)) WRITE(6,74) (ST,I=1,95)
      IF(DGN.GE.1) WRITE(6,63) READ(5,79) ZZ
      CALL MAP,NLINS,CALC,NOF,Z,BND)
   14 IF(NAF.EQ.0) GO TO 10
      NAO=10*NOF+NAF
      IF((DGN.GE.1).AND.(NGP.EQ.-3)) WRITE(6,62)
      IF(NGP.EQ.-3) CALL GPUNCH(Z,XO,YO,PHISYM,NAO,IMAX,JMAX,G)
    7 DO 7 IJ=1,IJMX
    G(IJ)=G(IJ)-GA(IJ)
   10 IF(IPT.EQ.3) GO TO 11
      IF((IPT.EQ.1).OR.(IPT.GE.4)) WRITE(6,78) (ST,I=1,124)
      IF((IPT.EQ.2).OR.(IPT.GE.4)) WRITE(6,74) (ST,I=1,95)
      IF((CMS.EQ.1).AND.(IPT.GE.4)) READ(5,79) ZZ
      CALL GPRINT(G,MONE)
      IF(NGP.EQ.-1) CALL GPUNCH(Z,XO,YO,PHISYM,NOF,IMAX,JMAX,G)
      IF((IPT.EQ.3).OR.(IPT.GE.4)) WRITE(6,78) (ST,I=1,124)
      IF(IPT.GE.4) WRITE(6,74) (ST,I=1,95)
      IF((CMS.EQ.1).AND.(IPT.GE.4)) READ(5,79) ZZ
      CALL GPRINT(GA,NTWO)
   11 IF(KPT.EQ.3) GO TO 12
      IF((KPT.EQ.1).OR.(KPT.GE.3)) WRITE(6,78) (ST,I=1,124)
      IF((KPT.EQ.2).OR.(KPT.GE.4)) WRITE(6,74) (ST,I=1,95)
      IF((CMS.EQ.1).AND.(KPT.EQ.2).OR.(KPT.GE.4)) READ(5,79) ZZ
      IF(DGN.GE.1) WRITE(6,61)
   12 CALL GPLOT(G,GA,JMS)
      WRITE(6,78) (EX,I=1,124)
      AGAIN=ST
```

CAL02620
CAL02630
CAL02640
CAL02650
CAL02660
CAL02670
CAL02680
CAL02690
CAL02700
CAL02710
CAL02720
CAL02730
CAL02740
CAL02750
CAL02760
CAL02770
CAL02780
CAL02790
CAL02800
CAL02810
CAL02820
CAL02830
CAL02840
CAL02850
CAL02860
CAL02870
CAL02880
CAL02890
CAL02900
CAL02910
CAL02920
CAL02930
CAL02940
CAL02950
CAL02960
CAL02970
CAL02980
CAL02990
CAL03000
CAL03010
CAL03020
CAL03030
CAL03040
CAL03050
CAL03060
CAL03070
CAL03080
CAL03090

```
      IF (CMS.NE.1.) READ(5,60) AGAIN
      IF (AGAIN.EQ..BL) GO TO 20
      WRITE (6,77)
60    FORMAT (6F12.7)
87    FORMAT (/' THE INPUT DATA FOR ADD-ON FUNCTION NO.8 (',I3,
     1 ' POINTS) WAS:'/7(11F10.3/))
86    FORMAT (/' THE INPUT DATA FOR THE TEST FUNCTION NO.8, (',I3,
     1 ' POINTS) WAS:'/7(11F10.3/))
85    FORMAT (1H1/,'THE INVERTED CROSS SECTION FOR:'
     1 ' =',F8.3,' CM.'/10X,'PHI=',F8.3,' DEGREES'/10X,
      14HY- ,F8.3,' CM.= ORIGINAL FUNCTION'/
      270X,'ADD-ON FUNCTION.')
84    FORMAT (' ADJUST PAGE, HIT SPACE AND RETURN.')
83    FORMAT (' MAX ORIGINAL ABS.COMPUTED (MG/CC)'/'
     1 ' KTERM   FUNCTION  ERROR  FUNCTION DENSITY ',6H X' ,F4.1,
82    FORMAT (2X,I2,1X,I3,1X,I4,1X,F9.4,F7.3,1X,F9.4,1X,F7.3,
     1 26F10.1)
81    FORMAT (3X,54A1,2X,A1,12(4X,A1))
80    FORMAT (' K TERM',2X,'MAX',3X,'ADD-ON',6X,'THE',4X,'DENSITY
     1 62X,'LIMIT',2X,'FUNCTION',5X,'SUM',3X,'FUNCTION DENSITY ',
      M X- ,2X,'FUNCTION',
79    FORMAT (F4.1,6F10.3)
78    FORMAT (1X,124A1)
77    FORMAT (1X/)
76    FORMAT (4X,'INVERTED FUNCTION =(RHO/RHO-INFINITY)-1.0',33X,': = THE'
     1 ' =',4X,F10.2,'PERCENT.'//70X,'=COMPUTED FUNCTION:')
75    FORMAT (1X,47A1,'LARGEST ERROR:',F8.6,' GMS/CC:         AT ',3HX'=',F6.3
74    FORMAT (' INVERTED SUM'
      26H SET PAGE, HIT SPACE, RETURN ',48A1)
69    FORMAT (' CALL FREAD')
68    FORMAT (' CALL GARRAY.')
67    FORMAT (' LINE',I3,' DO LOOP')
66    FORMAT (' POINT',I3,' CALL FUNCT')
65    FORMAT (' CALL FIELD')
64    FORMAT (' CALL BDGEN.')
63    FORMAT (' CALL MAP.')
62    FORMAT (' CALL GPUNCH')
61    FORMAT (' CALL GPLOT')
60    FORMAT (80A1)
      STOP
      END
C00C001
C
```

```fortran
      SUBROUTINE BDGEN (G,H,SCF,DGN,NBD,BDA,KBD)                         SUB00030
C                                                                       SUB00040
C     BDGEN EVALUATES THE B AND D COEFFICIENTS FOR ALL M AND K, AND WRITESSUB00050
C     THE ARRAY LINEARLY ON DISK.                                       SUB00060
C                                                                       SUB00070
      COMMON      IMAX,JMAX,IIMX,JJMX,IJMX,ALPHA,SIZE,EPS,MODE,BOX,SD,IX,ZSUB00080
      COMMON /TAB/ INDEX,KEXTRA,MEXTRA,KLIMIT,MLIMIT,KOUT,MOUT          SUB00090
      COMMON /SYM/ ISYM,JSYM,MSYM,FCU,IMS,JMS,QSYM                      SUB00100
      DIMENSION G(IJMX),H(IIMX,5),SCF(JJMX,6),BDA(KBD)                   SUB00110
C     INITIALIZE THE VALUES:                                           SUB00120
      INDEX=0                                                          SUB00130
      KL2=NBD*KLIMIT                                                   SUB00140
      REWIND 3                                                         SUB00150
      JJMX6=JJMX*6                                                     SUB00160
      IIMX2=(IIMX+1)/2                                                 SUB00170
      PIE=3.14159265358979793                                         SUB00180
      RIMAX=IIMAX                                                      SUB00190
      KLMP=KLIMIT+1                                                    SUB00200
      DX=2./RIMAX                                                      SUB00210
      RJMAX=JMAX                                                       SUB00220
      DXI=2.*PIE/FCU                                                   SUB00230
C     INITIALIZE THE MODIFIED HERMITE POLYNOMIAL ARRAY:  VECTORS:      SUB00240
C     (1)=H1, (2)=H2,(3)=ALPHA*X(I), (4)=HM+2 STORED, (5)=HM+1 STORED  SUB00250
      DO 1 II=1,IIMX2                                                  SUB00260
      RII=II-1                                                         SUB00270
      H(II,3)=ALPHA*(RII*DX-DX-1.)                                     SUB00280
      IIM=IIMX-II+1                                                    SUB00290
      H(IIM,3)=-H(II,3)                                                SUB00300
      H(II,1)=2.*H(II,3)                                               SUB00310
      H(IIM,1)=-H(II,1)                                                SUB00320
      H(II,2)=(H(II,3)*H(II,1)-1.)/3.                                  SUB00330
      H(IIM,2)=H(II,2)                                                 SUB00340
      H(II,5)=H(II,1)                                                  SUB00350
      H(IIM,5)=H(IIM,1)                                                SUB00360
      H(II,4)=H(II,2)                                                  SUB00370
    1 H(IIM,4)=H(IIM,2)                                                SUB00380
C     INITIATE THE SIN/COS ARRAY:                                     SUB00390
      ISIGN=1                                                          SUB00400
      DO 2 J=1,JJMX                                                    SUB00410
      RJM=J-1                                                          SUB00420
      SCF(J,1)=0.                                                      SUB00430
      SCF(J,2)=1.                                                      SUB00440
      SCF(J,3)=SIN(RJM*DXI-PIE/2.)                                     SUB00450
      SCF(J,4)=COS(RJM*DXI-PIE/2.)                                     SUB00460
      SCF(J,5)=0.                                                      SUB00470
    2 SCF(J,6)=0.                                                      SUB00480
      MS=0                                                             SUB00490
C     COMMENCE THE M LOOP:                                            SUB00500
```

135

```
      DO 7 MP=1,MLIMIT                                                   SUB00510
      M=MP-1                                                            SUB00520
      RM=M                                                              SUB00530
      SIGN=-SIGN                                                        SUB00540
C                                                                       SUB00550
      IF(DGN.LE.-4) WRITE (6,88) SCF(1,1),SCF(2,1),SCF(1,2),SCF(2,2)    SUB00560
C TEST FOR SYMMETRY SKIPS:                                             SUB00570
      IF(MS.EQ.MSYM) MS=0                                              SUB00580
      TOTAL=0.                                                         SUB00590
      MS=MS+1                                                          SUB00600
      IF(MS.NE.1) GO TO 6                                              SUB00610
C COMMENCE THE K LOOP:                                                 SUB00620
      DO 5 KP=1,KLIMIT                                                 SUB00630
      K=KP-1                                                           SUB00640
      PK=KP                                                            SUB00650
      RK=K                                                             SUB00660
C                                                                       SUB00670
      INDEX=INDEX+1                                                    SUB00680
C CALL THE B & D COEFFICIENTS AND WRITE THEM ON DISK:                  SUB00690
      CALL BD (M,K,G,H,SCF,B,D,JJMX6)                                  SUB00700
      IF(DGN.EQ.3.) WRITE(6,89) M,K,B,D                                SUB00710
      IF(DGN.LE.-2) WRITE (6,89) M,K,B,D                               SUB00720
      IF(DGN.LE.-4) WRITE (6,88) H(1,1),H(1,2),H(1,4),H(1,5)           SUB00730
      KK=K*NBD+1                                                       SUB00740
      K2=K*KP*NBD                                                      SUB00750
      BDA(KK)=B                                                        SUB00760
      BDA(KK2)=D                                                       SUB00770
C GENERATE THE NEXT ORDER OF THE SET OF HERMITE POLYNOMIALS FOR NEW K: SUB00780
      ORDER=M+2*KP+1                                                   SUB00790
      HA=SQRT((PK+RM))/ORDER                                           SUB00800
      HB=2.*SQRT((PK+1.)*(RM+PK+1.))/(ORDER+1.)/(ORDER+2.)             SUB00810
      DO 5 II=1,IIMX2                                                  SUB00820
      IIM=I,II+1                                                       SUB00830
      H(IIM,1)=2.*(H(II,3)*H(II,1))                                    SUB00840
      H(IIM,1)=2.*SIGN*H(II,1)                                         SUB00850
      H(IIM,2)=HB*(H(II,3)*H(II,1)-ORDER*H(II,2))                      SUB00860
C ADVANCE THE SIN/COS ARRAY FOR THE NEXT M:                            SUB00870
      DO 3 J=1,JMX                                                     SUB00880
      IF(DGN.LE.-5) WRITE (6,87) (SCF(J,NT),NT=1,6)                    SUB00890
   87 FORMAT(' SIN/COS MXI:'8E10.3)                                    SUB00900
      STEMP=SCF(J,1)                                                   SUB00910
      SCF(J,1)=SCF(J,1)*SCF(J,4)+SCF(J,2)*SCF(J,3)                     SUB00920
      SCF(J,2)=SCF(J,2)*SCF(J,4)-STEMP*SCF(J,3)                        SUB00930
    3 DO 4 J=1,JMAX                                                    SUB00940
      SCF(J,5)=SCF(J+1,1)-SCF(J,1)                                     SUB00950
      SCF(J,6)=SCF(J+1,2)-SCF(J,2)                                     SUB00960
    4 WRITE(6,88) (BDA(I),I=1,10)                                      SUB00970
      IF(DGN.LE.-3) WRITE(6,88) (BDA(I),I=1,KBD)
    6 IF(JSYM.GT.JMAX) RETURN
      RM=RM+1
```

136

```
C     REGENERATE THE HERMITE ARRAY FOR NEW M, K=0:
      DO 7 II=1,IIMX2
      IIM=IIMX-II+1
      H(II,2)=H(II,4)*SQRT(RM)/(RM+1.)
      H(IIM,1)=-SIGN*H(II,1)
      H(II,2)=2.*H(II,1)
      H(II,2)=SQRT(RM+1.)*(H(II,3)*H(II,1)-(RM+1.)*H(II,2))
      H(II,1)=H(II,2)/(RM+3.)
      H(II,4)=H(II,2)
7     H(II,5)=H(II,2)
89    FORMAT(' M=',I4,',  K=',I4,',  B=',E10.4,',   D=',E10.4)
88    FORMAT(2X,10E10.3)
      RETURN
      END
C000002
C
      SUBROUTINE FIELD (RS,SIG,SOLN,NBD,BDA,DGN,KBD)
C
C     FIELD EVALUATES THE VALUE OF THE FIELD FUNCTION AT A PARTICULAR
C     POINT DESIGNATED IN CYLINDRICAL COORDINATES, BY USING THE INVERSION
C     EQUATION OF MALDONADO; ET.AL. FIELD USES THE ARRAY OF B & D
C     COEFFICIENTS GENERATED IN SUBROUTINE BDGEN.
C
      COMMON IMAX,JMX,IIMX,JJMX,ALPHA,SIZE,EPS,MODE,BOX,SD,IX,Z
      COMMON /TAB/ INDEX,KEXTRA,MEXTRA,KLIMIT,MLIMIT,KOUT,MOUT
      COMMON /SYM/ ISYM,JSYM,MSYM,FCU,IMS,JMS,QSYM
      DIMENSION BDA(KBD), STK(52), STM(52)
C     INITIALIZE THE VALUES:
      INDEX=0
      MTIMER=0
      KOUT=0
      MMAX=0
      KMAX=0
      TOTAL=0.
      JJMX6=JJMX*6
      REWIND 3
      AR=ALPHA*RS
      ARG=AR**2
      EXPON=EXP(-ARG)
      PIE=3.14159265358979793
      APP=ALPHA/PIE/PIE
      M=0
      RM=M
      RIMAX=IMAX
      DX=2./RIMAX
```

137

```
      RJMAX=JMAX
      SIGN=1.
      STK(1)=0..
      STM(1)=0..
      SMS=0..
      CMS=1..
      SMI=SIN(SIG)
      CMI=COS(SIG)
      MEP=MEXTRA+1
  16  DO 16 MB=1,MEP
      STM(MB)=0.
      FM=1.
C     COMMENCE THE M LOOP:
  2   SIGN=-SIGN
      K=0
      RK=K
      RM=M
      ARM=1.
      IF(M.NE.0) ARM=AR**M
      KTIMER=KEXTRA+1
      KEP=KEXTRA+1
  15  DO 15 KB=1,KEP
      STK(KB)=0.
      SIGNK=-1.
C     COMPUTE THE K=0 & K=1 ORDERS OF LAGUERRE POLYNOMIAL FOR GIVEN M:
      PM=0.*(1./FM)
      P=SQRT(1./FM)
      PP=(RM+1.-ARG)*SQRT(1./FM/(RM+1.))
C     TEST FOR SYMMETRY SKIPS:
      IF(MS+1.EQ.MSYM) MS=0
      MS=MS+1
      IF(MS.NE.1) GO TO 7
C     READ A LINE OF B & D COEFFICIENTS FOR GIVEN M:
      READ(3) (BDA(I),I=1,KBD)
      IF(DGN.LE.-6) WRITE(6,88) (BDA(I),I=1,10)
C     COMMENCE THE K LOOP:
      INDEX=INDEX+1
      SIGNK=-SIGNK
C     COMPUTE THE M,K SUMMATION TERM:
  3   KK=K*NBD+1
      B=BDA(KK)
      D=0.
      IF(NBD.EQ.2) D=BDA(KK+1)
      BRAKET=B
      IF(RM.EQ.0.) GO TO 4
      BRAKET=B*CMS+D*SMS
  4   ADD=SIGNK*BRAKET*P*ARM
```

```
      TOTAL=TOTAL+ADD
      IF (DGN.GT.-5) GO TO 5
      STOT=TOTAL*EXPON*APP/BOX/SIZE
      WRITE (6,89) M,K,STOT,ADD,BRAKET,P,ARM,B,CMS,D,SMS
C     ESTABLISH CHECK AS THE RELATIVE SIZE OF THE M,K TERM OF THE SERIES:
5     CHECK=ABS(ADD)
      IF (TOTAL.GT.EPS) CHECK=ABS(ADD/TOTAL)
C     ADVANCE THE K INDEX:
      K=K+1
      RK=K
      DO 10 KA=1,KEXTRA
      KB=KEXTRA-KA+1
      STK(KB+1)=STK(KB)
10    STK(2)=TOTAL
      ORDER=M+2*K+1
C     GENERATE THE NEXT ORDER OF LAGUERRE POLYNOMIAL FOR NEW K:
      PM=P
      P=PP
      PP=P*(ORDER-ARG)-PM*SQRT(RK*(RM+RK))
      PP=PP/SQRT((RK+1.)*(RM+RK+1.))
C     SET KTIMER TO PROVIDE EXTRA K TERMS AFTER CHECK < EPS:
      KTIMER=KTIMER+1
      IF(K.GE.KLIMIT) GO TO 6
      IF(CHECK.GE.EPS) KTIMER=0
      IF(KTIMER.LE.KEXTRA) GO TO 3
      GO TO 7
6     KOUT=KOUT+1
      IF (KEXTRA.EQ.0) GO TO 7
      DO 11 KA=1,KEXTRA
      TOTAL=TOTAL+STK(KA+1)
11    RKX=KEXTRA
      TOTAL=TOTAL/RKX
C     END OF K LOOP; ADVANCE M:
7     M=M+1
      RM=M
      STP=SMS
      SMS=SMS*CMI+CMS*SMI
      CMS=CMS*CMI-STP*SMI
      IF (K.GT.KMAX) KMAX=K
      FM=FM*RM
      DO 12 MA=1,MEXTRA
      MB=MEXTRA-MA+1
      STM(MB+1)=STM(MB)
12    STM(2)=TOTAL
C     SET M TIMER FOR EXTRA M TERMS:
      IF (MS.EQ.1) MTIMER=MTIMER+1
      IF (JSYM.GT.JMAX) GO TO 9
```

```
13    IF (K.GT.KEXTRA)  MTIMER=0
      IF (M.GE.MLIMIT) GO TO 13
      IF (MTIMER.LE.MEXTRA) GO TO 2
      IF (MEXTRA.EQ.0) GO TO 9
      TOTAL=C.
      DO 14 MA=1,MEXTRA
14    TOTAL=TOTAL+STM(MA+1)
      RMX=MEXTRA
      TOTAL=TOTAL/RMX
C9    END OF M LOOP;  COMPUTE OUTPUT SOLN.
      MOUT=M-1
      IF (KOUT.EQ.0) KOUT=KMAX-1
      SOLN=TOTAL*EXPON*APP/2.
89    FORMAT ('   M=',I4,'',  K=',I4,'',  SUBTOTAL=',9E10.3)
88    FORMAT (2X,10E10.3)
      RETURN
      END
C000003
C
      SUBROUTINE BD (M,K,G,H,SCF,B,D,JJMX6)
C
C     BD EVALUATES THE FIRST (B) AND SECOND (D) COEFFICIENTS IN THE
C     INVERSION EQUATION, FOR A PARTICULAR SET OF INDEXES M & K.
C     BD MAKES USE OF THE HERMITE POLYNOMIAL ARRAY GENERATED BY
C     SUBROUTINE FIELD AS M & K ADVANCE.
C
      COMMON IMAX,JMAX,IIMX,JJMX,ISYM,JJMX,ALPHA,SIZE,EPS,MODE,BOX,SD,IX,Z
      COMMON /SYM/ ISYM,JSYM,MSYM,FCU,IMS,JMS,QSYM
      DIMENSION G(IJMX),SCF(JJMX6),H(IIMX)
      PIE=3.14159265358979
      B=0.
      D=0.
      RM=M
      RK=K
      RJMAX=JMAX
      JJMX4=4*JJMX
      DXI=2.*PIE/FCU
      FORMAT(1IX,I10,/)
200   IF (M.NE.0) GO TO 2
      S=DXI
      DO 1 J=1,JMAX
      DO 1 I=1,IMAX
      II=I+1
      IJ=IMAX*(J-1)+I
```

SUB02400
SUB02410
SUB02420
SUB02430
SUB02440
SUB02450
SUB02460
SUB02470
SUB02480
SUB02490
SUB02500
SUB02510
SUB02520
SUB02530
SUB02540
SUB02550
SUB02560
SUB02570
SUB02580
SUB02590
SUB02600
SUB02610
SUB02620
SUB02630
SUB02640
SUB02650
SUB02660
SUB02670
SUB02680
SUB02690
SUB02700
SUB02710
SUB02720
SUB02730
SUB02740
SUB02750
SUB02760
SUB02770
SUB02780
SUB02790
SUB02800
SUB02810
SUB02820
SUB02830
SUB02840

```
      DH=H(II)-H(I)
1     B=B+G(IJ)*S*DH
      B=B*QSYM/2.
      RETURN
2     DO 3 J=1,JMAX
      JS=J+JMX4
      S=SCF(JS)/RM
      DO 3 I=1,IMAX
      II=I+1
      IJ=IMAX*(J-1)+I
      DH=H(II)-H(I)
3     B=B+G(IJ)*QSYM
      RETURN
4     IF(M.NE.0) GO TO 6
      S=DXI
      DO 5 J=1,JMAX
      DO 5 I=1,IMAX
      II=I+1
      IJ=IMAX*(J-1)+I
      DH=H(II)-H(I)
5     B=B+G(IJ)*S*DH
      B=B/2.
      RETURN
6     DO 7 J=1,JMAX
      JS=J+JJMX
      J2=JS+JJMX
      S=SCF(JS)/RM
      CC=SCF(J2)/RM
      DO 7 I=1,IMAX
      II=I+1
      IJ=IMAX*(J-1)+I
      DH=H(II)-H(I)
      B=B+G(IJ)*S*DH
7     D=D-G(IJ)*C*DH
66    FORMAT(' BD:',4I5,10F6.2)
      RETURN
      END
C000004
C
      SUBROUTINE FIELD2 (RS,SIG,SOLN,G,H,SCF,DGN)
C     FIELD2 COMPUTES THE SAME INVERSION AS SUBROUTINE FIELD, EXCEPT THAT
C     THE COEFFICIENTS B AND D ARE COMPUTED INDIVIDUALLY AS USED BY
C     CALLING BD. DISK STORAGE IS NOT REQUIRED, BUT COMPUTING TIME IS
C     MUCH GREATER. FIELD2 IS UTILIZED BY SPECIFYING A NEGATIVE MODE ON
```

```
SUB02850
SUB02860
SUB02870
SUB02880
SUB02890
SUB02900
SUB02910
SUB02920
SUB02930
SUB02940
SUB02950
SUB02960
SUB02970
SUB02980
SUB02990
SUB03000
SUB03010
SUB03020
SUB03030
SUB03040
SUB03050
SUB03060
SUB03070
SUB03080
SUB03090
SUB03100
SUB03110
SUB03120
SUB03130
SUB03140
SUB03160
SUB03170
SUB03180
SUB03190
SUB03200
SUB03210
SUB03220
SUB03230
SUB03240
SUB03250
SUB03260
SUB03270
SUB03280
SUB03290
SUB03300
```

```
C   THE INPUT PARAMETER.  VALUE OF THE FIELD FUNCTION AT A PARTICULAR
C   FIELD EVALUATES THE FIELD FUNCTION AT A PARTICULAR
C   POINT DESIGNATED IN CYLINDRICAL COORDINATES, BY USING THE INVERSION
C   EQUATION OF MALDONADO, ET AL.  FIELD CALLS SUBROUTINES BD & GARRAY.
C
      COMMON  IMAX,JMAX,IIMX,JJMX,IIJMX,ALPHA,SIZE,EPS,MODE,BOX,SD,IX,Z
      COMMON /TAB/ INDEX,KEXTRA,MEXTRA,KLIMIT,MLIMIT,KOUT,MOUT
      COMMON /SYM/ ISYM,JSYM,MSYM,FCU,IMS,JMS,QSYM
      DIMENSION G(IJMX,5),H(IIMX,5),SCF(JJMX,6)
C   INITIALIZE THE VALUES:
      INDEX=0
      MTIMER=0
      KOUT=0
      MOUT=0
      MMAX=0
      KMAX=0
      TOTAL=0.
      JJMX6=JJMX*6
      IIMX2=(IIMX+1)/2
      AR=ALPHA*RS
      ARG=AR**2
      EXPON=EXP(-ARG)
      PIE=3.141592653589793
      APP=ALPHA/PIE/PIE
      M=0
      RM=M
      RIMAX=IMAX
      DX=2./RIMAX
      RJMAX=JMAX
      DXI=2.*PIE/FCU
C   INITIALIZE THE MODIFIED HERMITE POLYNOMIAL ARRAY:  VECTORS:
C   (1)=H1, (2)=H2, (3)=ALPHA*X(I), (4)=HM+2 STORED, (5)=HM+1 STORED
      DO 1, II=1,IIMX2
      RII=IIMX-II+1
      H(III,3)=ALPHA*(RII*DX-DX-1.)
      H(IIM,3)=-H(III,3)
      H(III,1)=2.*H(III,3)
      H(IIM,2)=(H(III,1)*H(II,1)-1.)/3.
      H(III,2)=-H(III,1)
      H(IIM,5)=H(III,2)
      H(III,5)=H(III,2)
      H(IIM,4)=H(III,1)
      H(III,4)=H(IIM,1)
      SIGN=1.
    1 FM=1.
C   INITIATE THE SIN/COS ARRAY:
```

```
      DO 11 J=1,JJMX
      RJM=J-1
      SCF(J,1)=0.
      SCF(J,2)=1.
      SCF(J,3)=SIN(RJM*DXI-PIE)
      SCF(J,4)=COS(RJM*DXI-PIE)
      SCF(J,5)=0.
   11 SCF(J,6)=0.
C     COMMENCE THE M LOOP:
    2 SIGN=-SIGN
      K=0
      RK=K
      ARM=1.
      IF(M.NE.0) ARM=AR**M
      KTIMER=0
      SIGNK=-1.
C     COMPUTE THE K=0 & K=1 ORDERS OF LAGUERRE POLYNOMIAL FOR GIVEN M:
      PM=0.
      P=SQRT(1./FM)
      PP=(RM+1.-ARG)*SQRT(1./FM/(RM+1.))
C     ADVANCE THE SIN/COS ARRAY FOR NEW M:
      DO 12 J=1,JJMX
      SCF(J,1)=SCF(J,1)*SCF(J,4)+SCF(J,2)*SCF(J,3)
   12 SCF(J,2)=SCF(J,2)*SCF(J,4)-SCF(J,1)*SCF(J,3)
      DO 13 J=1,JMAX
      SCF(J,5)=SCF(J+1,1)-SCF(J,1)
   13 SCF(J,6)=SCF(J+1,2)-SCF(J,2)
C     TEST FOR SYMMETRY SKIPS:
      IF(MS.EQ.MSYM) MS=0
      TOTAL=0.
      MS=MS+1
      IF(MS.NE.1) GO TO 7
      RMS=RM*SIG
      CMS=COS(RMS)
      SMS=SIN(RMS)
C     COMMENCE THE K LOOP:
    3 INDEX=INDEX+1
      SIGNK=-SIGNK
C     CALL THE B & D COEFFICIENTS AND COMPUTE THE M,K SUMMATION TERM:
      CALL BD(M,K,G,H,SCF,B,D,JJMX6)
      IF(DGN.LE.-2.) WRITE(6,89) M,K,B,D
      BRAKET=B
      IF(RM.EQ.0.) GO TO 4
      BRAKET=B*CMS+D*SMS
      ADD=SIGNK*BRAKET*P*ARM
    4 TOTAL=TOTAL+ADD
C     ESTABLISH CHECK AS THE RELATIVE SIZE OF THE M,K TERM OF THE SERIES:
```

143

```
C     CHECK=ABS(ADD)                                                    SUB04270
      IF(TOTAL.GT.EPS) CHECK=ABS(ADD/TOTAL)                             SUB04280
C     ADVANCE THE K INDEX:                                              SUB04290
      K=K+1                                                             SUB04300
      RK=K                                                              SUB04310
      ORDER=M+2*K+1                                                     SUB04320
C     GENERATE THE NEXT ORDER OF LAGUERRE POLYNOMIAL FOR NEW K:         SUB04330
      PM=P                                                              SUB04340
      P=PP                                                              SUB04350
      PP=P*(ORDER-ARG)-PM*SQRT(RK*(RM+RK))                             SUB04360
      PP=PP/SQRT((RK+1.)*(RM+RK+1.))                                   SUB04370
C     GENERATE THE NEXT ORDER OF THE SET OF HERMITE POLYNOMIALS FOR NEW K: SUB04380
      HA=SQRT(RK*(RK+RM))/ORDER                                        SUB04390
      HB=2.*SQRT((RK+1.)*(RM+RK+1.))/(ORDER+2.)                        SUB04400
      DO 5 II=1,IIMX2                                                   SUB04410
      IIM=IIMX-II+1                                                     SUB04420
      H(II,1)=2.*(H(II,3)*H(II,2)-HA*H(II,1))                          SUB04430
      H(II,1)=SIGN*H(II,1)                                             SUB04440
    5 H(II,2)=HB*(H(II,3)*H(II,1)-ORDER*H(II,2))                       SUB04450
C     PROVIDE EXTRA K TERMS AFTER CHECK < EPS:                         SUB04460
C     SET K TIMER:                                                     SUB04470
      KTIMER=KTIMER+1                                                   SUB04480
      IF(K.GE.KLIMIT) GO TO 6                                          SUB04490
      IF(MTIMER.LE.MEXTRA) GO TO 2                                     SUB04500
      IF(CHECK.GE.EPS) KTIMER=0                                        SUB04510
      IF(KTIMER.LE.KEXTRA) GO TO 3                                     SUB04520
      GO TO 7                                                          SUB04530
C     END OF K LOOP:  ADVANCE M AND COMPUTE NEW TOTAL:                 SUB04540
    6 KOUT=KOUT+1                                                      SUB04550
    7 M=M+1                                                            SUB04560
      IF(K.GT.KMAX) KMAX=K                                            SUB04570
      RM=M                                                            SUB04580
      FM=FM*RM                                                        SUB04590
C     REGENERATE THE HERMITE ARRAY FOR NEW M, K=0:                    SUB04600
      DO 8 II=1,IIMX2                                                 SUB04610
      IIM=IIMX-II+1                                                   SUB04620
      H(II,2)=H(II,4)*SQRT(RM)/(RM+1.)                                SUB04630
      H(II,1)=-SIGN*H(II,5)*SQRT(RM+2.)                               SUB04640
      H(IIM,2)=2.*SQRT(RM+1.)*(H(II,3)*H(II,1)-(RM+1.)*H(II,2))       SUB04650
      H(IIM,2)=H(IIM,2)/(RM+2.)/(RM+3.)                               SUB04660
      H(II,4)=H(II,1)                                                 SUB04670
      H(II,2)=H(IIM,2)                                                SUB04680
C     SET M TIMER FOR EXTRA M TERMS:                                  SUB04690
    8 MTIMER=MTIMER+1                                                 SUB04700
      IF(MS.EQ.1) MTIMER=MTIMER+1                                     SUB04710
      IF(JSYM.GT.JMAX) GO TO 9                                        SUB04720
      IF(K.GT.KEXTRA) MTIMER=0                                        SUB04730
      IF(M.GE.MLIMIT) GO TO 9                                         SUB04740
C     END OF M LOOP:  COMPUTE OUTPUT SOLN.
```

144

```
9     MOUT=M-1
      IF(KOUT.EQ.0) KOUT=KMAX-1
      SOLN=TOTAL*EXPON*APP/2.                                            SUB04750
89    FORMAT('  M=',I4,',',  K=',I4,',',  B=',E10.4,',',  D=',E10.4)     SUB04760
      RETURN                                                            SUB04770
      END                                                               SUB04780
C000005                                                                 SUB04790
C                                                                       SUB04800
                                                                        SUB04810
      SUBROUTINE GARRAY (G,GA,NOF,DGN,NUMB,XO,YO,PHISYM)                SUB04820
C     GARRAY FILLS THE DATA ARRAY OVER AN ORTHOGONAL AREA WITH         SUB00010
C     THE REGULAR DATA OBTAINED BY THE METHOD CORRESPONDING TO THE     SUB00020
C     PARTICULAR MODE:                                                  SUB00030
C                                                                       SUB00040
C     MODE 1  -  DATA OBTAINED BY SAMPLING A KNOWN FUNCTION SUPPLIED    SUB00050
C                IN SUBROUTINE FUNCT AND SAMPLED IN SUBROUTINE GOLF.    SUB00060
C                                                                       SUB00070
C     MODE 2  -  DATA OBTAINED BY GENERATING A REGULAR ARRAY FROM       SUB00080
C                IRREGULAR EXPERIMENTAL INPUT DATA READ IN.  CALLS      SUB00090
C                SUBROUTINE EXPERIMENTAL.  SEE SHEET.)                  SUB00100
C                BE SIMULATED, SEE SHEET.)                              SUB00110
C                                                                       SUB00120
C     MODE 3  -  UTILIZES RAW DATA TAKEN AT THE PROPER INTERVAL,        SUB00130
C                OR PREVIOUSLY GENERATED, AND READ DIRECTLY INTO THE    SUB00140
C                GARRAY.  CALLS SUBROUTINE READ.                        SUB00150
C                                                                       SUB00160
      COMMON IMAX,JMAX,IIMX,JJMX,IJMX,ALPHA,SIZE,EPS,MODE,BOX,SD,IX,Z   SUB00170
      COMMON /SYM/ IISYM,JSYM,MSYM,FCU,IMS,JMS,QSYM                     SUB00180
      COMMON /IO/ CMS,IN1,IN2,IN4                                       SUB00190
      DIMENSION G(IMAX,JMAX),GA(IMAX,JMAX)                              SUB00200
      PIE=3.141592653589793                                            SUB00210
      HS=SIZE/2.                                                        SUB00220
      IF(MODE.GT.3) MODE=1                                              SUB00230
      RIMX=IMAX                                                         SUB00240
      RJMX=JMAX                                                         SUB00250
      DELR=SIZE/RIMX                                                    SUB00260
      DELXI=2.*PIE/FCU                                                  SUB00270
      IF(MODE.GT.1) GO TO 2                                             SUB00280
      DO 1 J=1,JMS                                                      SUB00290
      RJ=J                                                              SUB00300
      XI=(RJ-.5)*DELXI-PIE                                              SUB00310
      J2=J+2*(JMS-J)                                                    SUB00320
      J3=J+JMAX/2                                                       SUB00330
      J4=J2+JMAX/2                                                      SUB00340
```

```
      DO 1 I=1,IMS                                              SUB00390
      RI=I                                                      SUB00400
      II=IMAX+1-I                                               SUB00410
      R=(RI-.5)*DELR-HS                                         SUB00420
      CALL GOLF(R,XI,GIJ,NOF,DGN,NUMB)                          SUB00430
      G(I,J)=GIJ                                                SUB00440
      IF(ISYM.EQ.2) G(II,J)=GIJ                                 SUB00450
      IF(ISYM.EQ.2) GO TO 1                                     SUB00460
      G(II,J3)=GIJ                                              SUB00470
      IF(JSYM.EQ.0) GO TO 1                                     SUB00480
      G(II,J2)=GIJ                                              SUB00490
      G(II,J4)=GIJ                                              SUB00500
 1    CONTINUE                                                  SUB00510
      GO TO 4                                                   SUB00520
 2    IF(MODE.GT.2) GO TO 3                                     SUB00530
      CALL SHEET(G,GA,XO,YO,PHISYM,NOF)                         SUB00540
      GO TO 4                                                   SUB00550
 3    CALL READ (Z,XO,YO,PHISYM,NOF,IMAX,JMAX,G)                SUB00560
 4    IF(DGN.GE.2) WRITE (6,39)                                 SUB00570
      RETURN                                                    SUB00580
 39   FORMAT (' GARRAY RETURNS')                                SUB00590
      END                                                       SUB00600
C000006                                                         SUB00610
C                                                               SUB00620

      SUBROUTINE GOLF (R,XI,GIJ,NOF,DGN,NUMB)                   SUB00630
C                                                               SUB00640
C     GOLF COMPUTES THE FUNCTION G(R,XI) FOR A PARTICULAR LINE OF SIGHT SUB00650
C     FROM A KNOWN FUNCTION CONTAINED IN SUBROUTINE FUNCT.      SUB00660
C                                                               SUB00670
      COMMON IMAX,JMAX,IIMX,JJMX,IJMX,ALPHA,SIZE,EPS,MODE,BOX,SD,IX,Z SUB00680
      ZERO=0.                                                   SUB00690
      LMAX=IMAX*3                                               SUB00700
      RLMAX=LMAX                                                SUB00710
      DELXP=SIZE/RLMAX                                          SUB00720
      SXI=SIN(XI)                                               SUB00730
      CXI=COS(XI)                                               SUB00740
      DELXS=DELXP*CXI                                           SUB00750
      DELYS=DELXP*SXI                                           SUB00760
      XP=DELXP*.5-SIZE/2.                                       SUB00770
      XS=XP*CXI-R*SXI                                           SUB00780
      YS=XP*SXI+R*CXI                                           SUB00790
      GIJ=0.                                                    SUB00800
      DO 1 L=1,LMAX                                             SUB00810
      RL=L                                                      SUB00820
      CALL FUNCT(XS,YS,F,NOF,DGN,NUMB)                          SUB00830
      GIJ=GIJ+F                                                 SUB00840
```

146

```
      XS=XS+DELXS
      YS=YS+DELYS
      IF (GIJ.NE.0.) GIJ=GIJ*DELXP*BOX                          SUB00850
    1 IF ((SD.EQ.0.).OR.(NUMB.EQ.1)) GO TO 2                    SUB00860
      IF (DGN.GE.3) WRITE (6,28) IX                             SUB00870
      CALL GAUSS (IX,SD,ZERO,RV)                                SUB00880
      GIJ=GIJ+RV                                                SUB00890
      IF (DGN.GE.3) WRITE (6,29) R,XI,GIJ                       SUB00900
      RETURN                                                    SUB00910
   29 FORMAT (' '      R=',F8.3,'  XI=',F8.3,''    GIJ=',F8.3)  SUB00920
   28 FORMAT (' '      GAUSS, IX=',I8)                          SUB00930
      END                                                       SUB00940
C000007                                                         SUB00950
C                                                               SUB00960
                                                                SUB00970
      SUBROUTINE FUNCT (XS,YS,F,NOF,DGN,NUMB)                   SUB00980
C
CP67USERID 1095BOXJ                                             SUB00990
C                                                               SUB01000
C     FUNCT EVALUATES AS INPUT FUNCTION AT POSITION (X,Y) IN THE TEST
C     SECTION COORDINATE SYSTEM.  NOF IDENTIFIES THE EQUATION USED.
C                                                               SUB01020
      COMMON IMAX,JMAX,IIMX,JJMX,IJMX,ALPHA,SIZE,EPS,MODE,BOX,SD,IX,Z  SUB01030
      COMMON /EQPARA/ A,B,C,D,E,P,Q,S,T,U,V,W,RO,RA,RO,NA,N1,N2        SUB01040
      DIMENSION RO(101),RA(101)                                 SUB01050
      AA=A                                                      SUB01060
      BB=B                                                      SUB01070
      CC=C                                                      SUB01080
      DD=D                                                      SUB01090
      EE=E                                                      SUB01100
      PP=P                                                      SUB01110
      IF (NUMB.LE.1) GO TO 50                                   SUB01120
      AA=S                                                      SUB01130
      BB=T                                                      SUB01140
      CC=U                                                      SUB01150
      DD=V                                                      SUB01160
      EE=W                                                      SUB01170
      PP=Q                                                      SUB01180
   50 PIE=3.141592653589793                                     SUB01190
      HS=SIZE/2.                                                SUB01200
      R=SQRT(XS**2+YS**2)/HS                                    SUB01210
      F=0.                                                      SUB01220
      IF (R.GT.1.) GO TO 11                                     SUB01230
      IF (NOF.LE.0) GO TO 11                                    SUB01240
C                                                               SUB01250
C   1.  AXISYMMETRIC GAUSSIAN:                                  SUB01260
                                                                SUB01270
                                                                SUB01280
```

147

```
1     IF (NOF.GT.1) GO TO 2                                      SUB01290
      F=AA*EXP(-1.*(R*HS/BB)**2)                                 SUB01300
      GO TO 11                                                   SUB01310
C                                                                SUB01320
C2    ADJUSTABLE RECTANGULAR STEP FUNCTION:                      SUB01330
2     IF (NOF.GT.2) GO TO 3                                      SUB01340
      F=PP                                                       SUB01350
      IF ((ABS(XS-DD).LE.BB).AND.(ABS(YS-EE).LE.CC)) F=AA        SUB01360
      GO TO 11                                                   SUB01370
C                                                                SUB01380
C3    DISPLACABLE ELLIPTICAL GAUSSIAN:                           SUB01390
3     IF (NOF.GT.3) GO TO 4                                      SUB01400
      F=AA*EXP(-1.*(((XS-DD)/BB)**2+((YS-EE)/CC)**2))            SUB01410
      GO TO 11                                                   SUB01420
C                                                                SUB01430
C4    CONSTANT:                                                  SUB01440
4     IF (NOF.GT.4) GO TO 5                                      SUB01450
      F=AA                                                       SUB01460
      GO TO 11                                                   SUB01470
C                                                                SUB01480
C5    ADJUSTABLE AND DISPLACABLE ELLIPTIC RAMP FUNCTION:         SUB01490
5     IF (NOF.GT.5) GO TO 6                                      SUB01500
      RBC=SQRT(((XS-DD)/BB)**2+((YS-EE)/CC)**2)                  SUB01510
      F=0.                                                       SUB01520
      IF (RBC.LT.1.) F=AA*((1.-RBC)**PP)                         SUB01530
      GO TO 11                                                   SUB01540
C                                                                SUB01550
C6    DISPLACABLE ELLIPTIC STEP FUNCTION:                        SUB01560
6     IF (NOF.GT.6) GO TO 7                                      SUB01570
      RBC=SQRT(((XS-DD)/BB)**2+((YS-EE)/CC)**2)                  SUB01580
      F=0.                                                       SUB01590
      IF (RBC.LT.1.) F=AA                                        SUB01600
      GO TO 11                                                   SUB01610
C                                                                SUB01620
C7    CIRCULAR COSINE-SQUARED FUNCTION OF BB MAXIMA:             SUB01630
7     IF (NOF.GT.7) GO TO 8                                      SUB01640
      F=AA*COS((2.*BB-1.)*PIE*R/2.)**2                           SUB01650
      GO TO 11                                                   SUB01660
C                                                                SUB01670
C8    NUMERICAL FUNCTION:    REQUIRES AN INPUT ARRAY READ IN BY  SUB01680
C     SUBROUTINE FREAD; N    FOLLOWED BY N POINT VALUES. (101 MAX) SUB01690
C     A CONSTANT VALUE AA    IS ADDED TO THE FUNCTION.           SUB01700
8     IF (NOF.GT.8) GO TO 9                                      SUB01710
      IF (NUMB.LE.1) N=NO                                        SUB01720
      IF (NUMB.GT.1) N=NA                                        SUB01730
      NM=N-1                                                     SUB01740
      NMM=N-2                                                    SUB01750
      RN=N                                                       SUB01760
```

148

```
      RI=R*(RN-1.)+1.
      IR=INT(RI)
      RIR=FLOAT(IR)
      DI=RI-RIR
      IF(NUMB.LE.1) F=RO(IR)
      IF(NUMB.GT.1) F=RA(IR)
      IF((IR.NE.N).AND.(NUMB.LE.1))  F=F+DI*(RO(IR+1)-RO(IR))
      IF((IR.NE.N).AND.(NUMB.GT.1))  F=F+DI*(RA(IR+1)-RA(IR))
      F=F*AA+BB
      GO TO 11
C
C  9.  SPECIAL FUNCTION: MAY BE WRITTEN FOR THE OCCASION AND
C      INSERTED IN SUBROUTINE SPFUN
9     IF(NQF.GT.9) GO TO 10
      CALL SPFUN (XS,YS,F)
      GO TO 11
C
C 10   EQUATIONS NO. 10 AND BEYOND ARE SET TO ZERO.
10    F=0.
C
C 11   IF (DGN.GE.4) WRITE (6,99) XS,YS,F
99    FORMAT(' XS=',F8.3,', YS=',F8.3,',    F=',F8.3)
      RETURN
      END
C000008
C
      SUBROUTINE SPFUN (XS,YS,F)
C
C     SPFUN IS A SPECIAL ROUTINE FOR EQ'N NO. 9.  ANY FUNCTION MAY BE
C     ENTERED.
C
      COMMON /EQPARA/ A,B,C,D,E,P,Q,S,T,U,V,W,RO,RA,NO,NA,N1,N2
      DIMENSION RO(101),RA(101)
      F=0.
      IF((ABS(XS).LE.B).AND.(ABS(YS).LE.C))   F=A
      RETURN
      END
C000009
C
```

```
SUB01770
SUB01780
SUB01790
SUB01800
SUB01810
SUB01820
SUB01830
SUB01840
SUB01850
SUB01860
SUB01870
SUB01880
SUB01890
SUB01900
SUB01910
SUB01920
SUB01930
SUB01940
SUB01950
SUB01960
SUB01970
SUB01980
SUB01990
SUB02000
SUB02010
SUB02020
SUB02030
SUB02040
SUB02050
SUB02060
SUB02070
SUB02080
SUB02090
SUB02100
SUB02110
SUB02120
SUB02130
SUB02140
SUB02150
SUB02160
```

```
      SUBROUTINE SHEET (G,D,X0,Y0,PHISYM,NOF)                           SUB02170
C     SHEET READS IRREGULARLY SPACED VALUES OF THE LINE INTEGRAL, AS     SUB02180
C     OBTAINED FROM HOLOGRAPHIC INTERFEROGRAMS. THE INTEGRAL LINES MAY BE SUB02190
C     DEFINED EITHER BY GRID INTERCEPT POSITIONS, OR BY ANGLE AND RADIUS  SUB02200
C     ABOUT THE CENTER OF THE LABORATORY COORDINATE SYSTEM CENTER. LINES  SUB02210
C     MUST BE ENTERED IN CONSECUTIVE ORDER FROM LOWEST (NEG.) TO HIGHEST  SUB02220
C     (POS.) RADIUS. DATA MAY BE SIMULATED BY SPECIFYING NCODE=1, TO      SUB02230
C     FOLLOWED BY APERATURE POSITIONS FOR A FUNCTION NUMBER IN 'SUBFUNCT'.SUB02240
C                                                                         SUB02250
      COMMON IMAX,JMAX,IIMX,JJMX,IJMX,ALPHA,SIZE,EPS,MODE,BOX,SD,IX,Z    SUB02260
      COMMON /SYM/ISYM,JSYM,MSYM,FCU,IMS,JMS,QSYM                        SUB02270
      COMMON /IO/CMS,IN1,IN2,IN4                                         SUB02280
      DIMENSION G(303),XD(303),D(IMAX,JMAX),XI(303),RR(303)             SUB02290
      DIMENSION XG(303),YG(303),YD(303),YD(303),XY(303)                 SUB02300
      NAR=303                                                            SUB02310
      PIE=3.141592653589793                                             SUB02320
      MPIE=2*PIE                                                         SUB02330
      TPPIE=2.*PIE                                                       SUB02340
      PIET=PIE*PIE/2.                                                    SUB02350
C     ZERO THE ARRAYS:                                                   SUB02360
      DO 1 J=1,JMAX                                                      SUB02370
      DO 1 I=1,IMAX                                                      SUB02380
      G(I,J)=0.                                                          SUB02390
    1 D(I,J)=0.                                                          SUB02400
      DO 2 I=1,NAR                                                       SUB02410
      XG(I)=0.                                                           SUB02420
      YG(I)=0.                                                           SUB02430
      YD(I)=0.                                                           SUB02440
      XY(I)=0.                                                           SUB02450
      XI(I)=0.                                                           SUB02460
    2 RR(I)=0.                                                           SUB02470
C     READ THE BASIC DATA:                                               SUB02480
      IF(CMS.EQ.1.) REWIND 1                                             SUB02490
      READ(IN1,59) NOF,NCODE                                            SUB02500
      READ(IN1,58) Z,X0,Y0,PHISYM,XMX,XMN,YMX,YMN                        SUB02510
      READ(IN1,59) JM                                                    SUB02520
      RIMX=IMAX                                                          SUB02530
      DR=SIZE/RIMX                                                       SUB02540
      R=(-DR-SIZE)/2./RIMX                                               SUB02550
      RZO=SQRT(X0**2+Y0**2)                                              SUB02560
      GAM=ATANM(Y0,X0)                                                   SUB02570
      TP=3-ISYM                                                          SUB02580
      BT=JSYM                                                            SUB02590
      DAN=PIE*TP/BT                                                      SUB02600
      HS=SIZE/2.                                                         SUB02610
                                                                         SUB02620
                                                                         SUB02630
                                                                         SUB02640
```

```
      MXY=1
      IF((XMX.NE.0.).OR.(XMN.NE.0.).OR.(YMX.NE.0.).OR.(YMN.NE.0.))MXY=0     SUB02650
      IF(MXY.EQ.1) GO TO 3                                                  SUB02660
      XMX=XO++HS                                                            SUB02670
      YMX=YO++HS                                                            SUB02680
      XMN=XO-HS                                                             SUB02690
      YMN=YO-HS                                                             SUB02700
C     COMMENCE THE READ AND FILL LOOP:                                      SUB02710
    3 DO 12 J=1,JM                                                          SUB02720
      READ (IN1,59)IM                                                       SUB02730
      MN=0                                                                  SUB02740
      XH=0.                                                                 SUB02750
      YH=0.                                                                 SUB02760
C     READ THE LINES, DETERMINE CODE, CALCULATE RADIUS & ANGLE FOR CODE 1:  SUB02770
      DO 5 I=1,IM                                                           SUB02780
      IF(NCODE.LE.0)READ(IN1,58) XD(I),YD(I),XG(I),YG(I),D(I,J),RR(I),      SUB02790
     1XI(I),XY(I)                                                           SUB02800
      IF(NCODE.GE.1)CALL SIM(XD(I),YD(I),XG(I),YG(I),RR(I),XI(I),           SUB02810
     1XY(I),XO,YO,PHISYM,XMX,XMN,YMX,YMN,NOF,I,IM)                          SUB02820
      IF(XY(I).EQ.3.) GO TO 5                                               SUB02830
      IF((XY(I).NE.0.).OR.(YD(I).NE.0.)) XY(I)=1.                           SUB02840
      IF((XG(I).NE.0.).OR.(XI(I).NE.0.)) XY(I)=1.                           SUB02850
      IF((RR(I).NE.0.).AND.(XY(I).EQ.0.)) XY(I)=2.                          SUB02860
      IF((XY(I).EQ.0.).AND.(D(I,J).NE.0.)) XY(I)=2.                         SUB02870
      DEN=SQRT((XG(I)-XD(I))**2+(YG(I)-YD(I))**2)                           SUB02880
      IF(DEN.EQ.0.) XY(I)=4.                                                SUB02890
      IF(XY(I).EQ.4.) GO TO 4                                               SUB02900
      RR(I)=((YO-XD(I))*(YG(I)-YD(I))-(XG(I)-XD(I))*(YO-YD(I)))/DEN         SUB02910
      XIM=ATANM((YG(I)-YD(I)),(XG(I)-XD(I)))                                SUB02920
    4 XIM=XI(I)                                                             SUB02930
      IF(XY(I).EQ.2.) XIM=XI(I)                                             SUB02940
      XIN=XIM                                                               SUB02950
      IF(XY(I).EQ.2.) RR(I)=RR(I)+RZO*SIN(GAM-XI(I))                        SUB02960
    5 CONTINUE                                                              SUB02970
C     COMPUTE MAX AND MIN ANGLE INDEXES FOR APERATURE POSITION LOCATION:    SUB02980
      DO 6 I=1,IM                                                           SUB02990
      IF((XY(I).NE.1.).OR.(XY(I).NE.2.)) GO TO 6                            SUB03000
      IF((XI(I).GT.XIM) XIM=XI(I)                                           SUB03010
      IF((XI(I).GT.XIM) IMT=I                                               SUB03020
      IF((XI(I).LT.XIN) XIN=XI(I)                                           SUB03030
      IF((XI(I).LE.XIN) INT=I                                               SUB03040
    6 CONTINUE                                                              SUB03050
C     DETERMINE APERATURE LOCATION:                                         SUB03060
      LPR=0                                                                 SUB03070
      XID=XI(IMT)-XI(INT)                                                   SUB03080
      IF(ABS(XID).LT.0.0001) LPR=1                                          SUB03090
      XIH=(XI(IMT)+XI(INT))/2.                                              SUB03100
```

151

```
      RRH=10000.*COS(XIH)                                              SUB03130
      XH=RRH*COS(XIH)                                                  SUB03140
      YH=RRH*SIN(XIH)                                                  SUB03150
      IF (LPR.EQ.1) GO TO 7                                            SUB03160
      YTX=-RR(IMT)*SIN(XI(IMT))-YO                                     SUB03170
      YTN=-RR(INT)*SIN(XI(INT))-YO                                     SUB03180
      XTX=RR(IMT)*COS(XI(IMT))-XO                                      SUB03190
      XTN=RR(INT)*COS(XI(INT))-XO                                      SUB03200
      UA=TAN(XI(IMT))                                                  SUB03210
      UC=TAN(XI(INT))                                                  SUB03220
      UB=YTX-UA*XTX                                                    SUB03230
      UD=YTN-UC*XTN                                                    SUB03240
      XH=(UD-UB)/(UA-UC)                                               SUB03250
      YH=XH*UA+UB                                                      SUB03260
      RRH=SQRT((XH-XO)**2+(YH-YO)**2)                                  SUB03270
      XIH=ATANM((YH-YO),(XH-XO))                                       SUB03280
    7 CONTINUE                                                         SUB03290
C     FILL THE ANGLE AND RADIUS FOR ANY CODE 3 OR 4 LINES:            SUB03300
      DO 9 I=1,IM                                                      SUB03310
      IF(XY(I).NE.3.) GO TO 8                                          SUB03320
      BAS=SQRT(RRH**2-RR(I)**2)                                        SUB03330
      XI(I)=XIH-ATANM(RR(I),BAS)                                       SUB03340
      GO TO 9                                                          SUB03350
    8 XI(I)=ATANM((YH-YD(I)),(XH-XD(I)))                               SUB03360
      RR(I)=RRH*SIN(XI(I))-XIH                                         SUB03370
    9 CONTINUE                                                         SUB03380
C     ANGLES AND RADII ARE NOW FILLED FOR ALL POINTS IN THIS LINE.    SUB03390
C     VACATE THE SET OF VECTORS TO BE USED AS TEMPORARY STORAGE:      SUB03400
      DO 10 I=1,IM                                                     SUB03410
      XD(I)=0.                                                         SUB03420
      YD(I)=0.                                                         SUB03430
      XG(I)=0.                                                         SUB03440
      XY(I)=0.                                                         SUB03450
      RR(I)=RR(I)                                                      SUB03460
      D(I,J)=0.                                                        SUB03470
   10 XI(I)=0.                                                         SUB03480
C     CONVERT THE LINE TO REGULAR RADII USING INTERPOLATION:          SUB03490
      RR(1)=R+DR                                                       SUB03500
      CALL SPLINE(YG,XY,IM,RR(1),D(1,J))                              SUB03510
      DO 11 I=2,IMAX                                                   SUB03520
   11 RR(I)=R+DR*RI                                                    SUB03530
      CALL SPLINN(YG,XY,IM,RR(I),D(I,J))                              SUB03540
C     GENERATE THE VECTOR OF ANGLES FOR THIS COLUMN AND STORE IN G ARRAY: SUB03550
      DO 12 I=1,IMAX                                                   SUB03560
      BAS=SQRT(RRH**2-RR(I)**2)                                        SUB03570
      G(I,J)=XIH-ATANM(RR(I),BAS)                                      SUB03580
```

```
      YG(I)=0.
      D(I,J)=XY(I)
      XY(I)=0.
C     COLUMNS ARE NOW ALL REGULARLY FILLED.
C     NEXT,INTERPOLATE EACH ROW REGULARLY OVER THE ANGLES.
      DO 23 I=1,IMAX
C     EXPAND THE DATA TO 2 SETS TO ESTABLISH SMOOTH INTERPOLATION.
      JM3=3*JM
      II=IMAX+1-I
      IF(JSYM.NE.0) GO TO 14
      DO 13 J=1,JMS
      J2=J+JMS
      J3=J2+JMS
      XD(J2)=D(II,J)
      XD(J3)=D(I,J)
      XG(J2)=G(II,J)-TPIE-PHISYM
      XG(J3)=G(I,J)-PIE-PHISYM
   13 XG(J)=G(I,J)-PHISYM
      GO TO 16
   14 DO 15 J=1,JMS
      J1=JMS+J
      J2=JMS+1-J
      J3=JM3+1-J
      XD(J1)=D(II,J)
      XD(J2)=D(II,J)
      XD(J3)=D(II,J)
      XG(J1)=G(II,J)-2.*(G(I,J)-PHISYM)-PIE-PHISYM
      XG(J2)=PIE-PHISYM
      XG(J3)=G(II,J)+2.*(DAN+PHISYM-G(II,J))-PIE-PHISYM
   15 CONTINUE
   16 JM2=2*JMS
      JP=JMS/2
      DO 17 J=1,JM2
      XD(J)=XD(J+JP)
   17 XG(J)=XG(J+JP)
      JJS=JM2+1
      DO 18 J=JJS,JM3
   18 XD(J)=0.
C     FIND THE SMALLEST ANGLE
      XY(1)=1.
      SA=XG(1)
      DO 19 J=1,JM2
      IF(XG(J).GE.SA) GO TO 19
      SA=XG(J)
      XY(1)=J
   19 CONTINUE
```

```
C     FIND THA MAX ANGLE IN THE ROW:                              SUB04090
      XY(JM2)=JM2                                                 SUB04100
      SB=XG(JM2)                                                  SUB04110
      DO 20 J=1,JM2                                               SUB04120
      IF (XG(J).LE.SB) GO TO 20                                   SUB04130
      SB=XG(J)                                                    SUB04140
      XY(JM2)=J                                                   SUB04150
20    CONTINUE                                                    SUB04160
C     DETERMINE THE ORDER OF INCREASING ANGLE IN THE ROW          SUB04170
      JJ=2                                                        SUB04180
21    JSA=XY(JJ-1)                                                SUB04190
      SA=XG(JJ-1)                                                 SUB04200
      JTS=0                                                       SUB04210
      DO 22 J=1,JM2                                               SUB04220
      IF (XG(J).LE.SA) GO TO 22                                   SUB04230
      IF (XG(J).GT.SB) GO TO 22                                   SUB04240
      SB=XG(J)                                                    SUB04250
      JTS=J                                                       SUB04260
22    CONTINUE                                                    SUB04270
      IF (JTS.EQ.0) JM2=JJ                                        SUB04280
      JJ=JJ+1                                                     SUB04290
      IF (JJ.LE.JM2) GO TO 21                                     SUB04300
      DO 23 J=1,JM2                                               SUB04310
      JX=XY(J)                                                    SUB04320
      YD(J)=XD(JX)                                                SUB04330
C     INTERPOLATE:                                                SUB04340
      DXI(J)=2.*PIE/FCU                                           SUB04350
      XI(J)=DXI(J)/2.-PIE-PHISYM                                  SUB04360
      CALL SPLINE (XG,YD,JM2,XI(J),G(I,J))                        SUB04370
      DO 24 J=2,JMS                                               SUB04380
      XI(J)=XI(J-1)+DXI                                           SUB04390
      CALL SPLINN (XG,YD,JM2,XI(J),G(I,J))                        SUB04400
24    DO 25 J=1,JMS                                               SUB04410
      XIJ=XI(J)                                                   SUB04420
      XU=XMX                                                      SUB04430
      IF ((XIJ.GE.0.).AND.(XIJ.LT.PIE)) XU=XMN                    SUB04440
      YU=YMN                                                      SUB04450
      IF ((XIJ.GE.MPIT).AND.(XIJ.LT.PIT)) YU=YMX                  SUB04460
      XL=XMN                                                      SUB04470
      IF ((XIJ.GE.0.).AND.(XIJ.LT.PIE)) XL=XMX                    SUB04480
      YL=YMX                                                      SUB04490
      IF ((XIJ.GE.MPIT).AND.(XIJ.LT.PIT)) YL=YMN                  SUB04500
      SXIJ=SIN(XIJ)                                               SUB04510
      CXIJ=COS(XIJ)                                               SUB04520
      RMN=(XO-XL)*SXIJ-(YO-YL)*CXIJ                               SUB04530
      RMX=(XO-XU)*SXIJ-(YO-YU)*CXIJ                               SUB04540
```

```
      DO 25 I=1,IMAX
      IF(RR(I).LT.RMN) G(I,J)=0.
      IF(RR(I).GT.RMX) G(I,J)=0.
25    CONTINUE
C     EXPAND SYMMETRY SECTOR INTO AN ORTHOGONAL INTERVAL.
      IF (ISYM.EQ.2) GO TO 27
      DO 26 J=1,JMS
      J2=JMAX/2+1-J
      J3=JMAX/2+J
      J4=JMAX+1-J
      DO 26 I=1,IMAX
      II=IMAX+1-I
      G(I,J2)=G(I,J)
      G(II,J3)=G(I,J)
      G(II,J4)=G(I,J)
26    RETURN
C     FOR EVEN SYMMETRY, AVERAGE THE GARRAY COLUMNS.
27    IMS=(2*IMAX+1)/2
      DO 28 J=1,JMAX
      DO 28 I=1,IMS
      II=IMAX+1-I
      GST=(G(I,J)+G(II,J))/2.
      G(I,J)=GST
      G(II,J)=GST
28    RETURN
59    FORMAT (5I5)
58    FORMAT (10F7.3)
      END
C0000010
C
      FUNCTION ATANM(Y,X)
C     COMPUTES THE ARCTAN OF Y/X BETWEEN -PI AND +PI.
C
      PIE=3.141592653589793
      PI2=PIE/2.
      ATANM=SIGN(PI2,Y)
      IF(X.NE.0.) ATANM=ATAN(Y/X)
      IF(X.GE.0.) RETURN
      IF(Y.GE.0.) ATANM=PIE+ATANM
      IF(Y.LT.0.) ATANM=-PIE+ATANM
      RETURN
      END
C0000011
C
```

SUB04570
SUB04580
SUB04590
SUB04600
SUB04610
SUB04620
SUB04630
SUB04640
SUB04650
SUB04660
SUB04670
SUB04680
SUB04690
SUB04700
SUB04710
SUB04720
SUB04730
SUB04740
SUB04750
SUB04760
SUB04780
SUB04790
SUB04800
SUB04810
SUB04820
SUB04830
SUB04840
SUB04850
SUB04860
SUB04870
SUB04880
SUB04890
SUB04900
SUB04910
SUB04920
SUB04930
SUB04940
SUB04950
SUB04960
SUB04970
SUB04980
SUB04990
SUB05000
SUB05010

```
      SUBROUTINE SIM (XD,YD,XG,YG,D,R,XI,XY,XO,YO,PS,XM,XN,YM,YN,I,IM,       SUB05020
     1DG,NF)                                                                 SUB05030
C     SIM SIMULATES THE FRINGE NUMBER DATA ONE WOULD OBTAIN FROM THE         SUB05040
C     HOLOGRAPHIC INTERFEROGRAM PROCESS FOR A KNOWN FUNCTION AS              SUB05050
C     CONTAINED IN SUBROUTINE FUNCT. THE GRID BOX DIMENSIONS MUST            SUB05060
C     EXCEED THE INVERSION CIRCLE SIZE, AND APERATURE POINTS SPECIFIED       SUB05070
C     MUST FALL BETWEEN XI=-40 DEGREES, AND XI=+130 DEGREES.                 SUB05080
                                                                             SUB05090
      COMMON IMAX,JMAX,IIMX,JJMX,IJMX,ALF,SIZ,EPS,MOD,BOX,SD,IX,Z            SUB05100
      COMMON /IO/ CMS,INI,IN2,IN4                                            SUB05110
      READ (IN1,29) XH,YH                                                    SUB05120
      ZER=0.                                                                 SUB05130
      RIM=IM                                                                 SUB05140
      RI=I                                                                   SUB05150
      DX=(XM-XN)/(RIM-1.)                                                    SUB05160
      DY=(YM-YN)/(RIM-1.)                                                    SUB05170
      X1=XM-(RIM-1.)*DX                                                      SUB05180
      Y1=YM-(RIM-1.)*DY                                                      SUB05190
      XI1=ATANM (YH-Y1,XH-X1)-PS                                             SUB05200
      RRH=SQRT((XH-XO)**2+(YH-YO)**2)                                        SUB05210
      XIO=ATANM(YH-YO,XH-XO)-PS                                              SUB05220
      RI1=RRH*SIN(XI1-XIO)                                                   SUB05230
      IF ((I.GT.1).AND.(I.LT.IM)) GO TO 1                                    SUB05240
      IF (ABS(RI).LT.SIZ/2.) R1=SIGN(SIZ/2.,R1)                             SUB05250
      XY=3.                                                                  SUB05260
      GO TO 2                                                                SUB05270
    1 CALL GOLF (R,XI,D,NR,ZER,ZER)                                          SUB05280
      XD=XN                                                                  SUB05290
      YD=YN                                                                  SUB05300
      IF (XH.NE.X1)  YD=Y1-(X1-XN)*(YH-Y1)/(XH-X1)                           SUB05310
      IF (YS.GE.YN) GO TO 2                                                  SUB05320
      YD=YN                                                                  SUB05330
      IF (YH.NE.Y1) XD=X1-(Y1-YN)*(XH-X1)/(YH-Y1)                            SUB05340
   29 RETURN                                                                 SUB05350
   29 FORMAT (10F7.3)                                                        SUB05360
      END                                                                    SUB05370
                                                                             SUB05380

C000012

      SUBROUTINE FREAD (NO,RO,NF,ZZ)                                         SUB00010
C     FREAD READS THE NUMERIC ARRAY WHICH IS USED FOR EQUATION 8 OF          SUB00020
C     SUBROUTINE FUNCT. FIRST CARD IS NUMBER OF POINTS (N.GE.1),             SUB00030
C     FOLLOWED BY ONE POINT PER CARD.                                        SUB00040
                                                                             SUB00050
      DIMENSION RO(101)                                                      SUB00060
```

```
      READ (NF,89) NO,ZZ                                         SUB00100
      WRITE(6,90) NO,ZZ
      DO 10 I=1,NO
      READ(NF,88) RO(I)
      WRITE(6,88) RO(I)                                          SUB00120
   10 CONTINUE                                                   SUB00140
   89 FORMAT(I5,F9.3)                                            SUB00150
   88 FORMAT(F8.5)                                               SUB00160
   90 FORMAT(1X,I5,F9.3)                                         SUB00170
      RETURN
      END
C000013
C
      SUBROUTINE GPRINT (G,NUMB)                                 SUB00180
C                                                                SUB00190
C     GPRINT PRINTS THE DATA ARRAY 'G'  WHICH WAS INPUT TO       SUB00200
C     THE PROGRAM IN SUBROUTINE GARRAY.                          SUB00210
C                                                                SUB00220
      COMMON IMAX,JMAX,IIMX,JJMX,IJMX,ALPHA,SIZE,EPS,MODE,BOX,SD,IX,Z  SUB00230
      DIMENSION G(IJMX)                                          SUB00240
      DIMENSION X(15)                                            SUB00250
      DATA HYP,VERT/1H-,1HI/                                     SUB00260
      IF (NUMB.EQ.1) WRITE (6,99) MODE,Z                         SUB00270
      IF (NUMB.EQ.2) WRITE (6,92) Z                              SUB00280
      JM2=JMAX/2                                                 SUB00290
      RIMAX=IMAX                                                 SUB00300
      RJMAX=JMAX                                                 SUB00310
      DX=SIZE/RIMAX                                              SUB00320
      DXI=360./RJMAX                                             SUB00330
C     INTRVL SETS THE NUMBER OF TERMS PRINTED PER LINE.  IF IT IS ALTERED,  SUB00340
C     ONE MUST ALSO REDIMENSION X AND ALTER FORMATS 98, 97, AND 95.  SUB00350
      INTRVL=15                                                  SUB00360
      IB=1                                                       SUB00370
    1 IT=IB+INTRVL-1                                             SUB00380
      IF(IT.GT.IMAX) IT=IMAX                                     SUB00390
      IBT=IT-IB+1                                                SUB00400
      WRITE (6,98) (II,II=IB,IT)                                 SUB00410
      DO 2 I=1,IBT                                               SUB00420
      RI=IB-1+I                                                  SUB00430
      X(I)=-SIZE/2.+(RI-.5)*DX                                   SUB00440
      LM=7*IBT+1                                                 SUB00450
      WRITE (6,97) (X(I),I=1,IBT)                                SUB00460
      WRITE (6,96) (HYP,L=1,LM),VERT                             SUB00470
      JMH=JM2+1                                                  SUB00480
      DO 3 J=JMH,JMAX                                            SUB00490
      RJ=J                                                       SUB00500
```

157

```
      XI=-180.+DXI*(RJ-.5)
      IGB=(J-1)*IMAX+IB
      IGT=IGB-IB+IT
      WRITE (6,95) J,XI,(G(L),L=IGB,IGT)
      WRITE (6,94) (HYP,L=1,LM),VERT
    3 IB=IB+INTRVL
      ITOLD=IT
      IT=IT+INTRVL
      IF (ITOLD.LT.IMAX) GO TO 1
      WRITE (6,93)         THE ARRAY OF INPUT DATA (G), OBTAINED BY GARRAY,
    1 MODE
   99 FORMAT('1H1//' ' FOR Z=',F7.3,' CM:')
   98 FORMAT('1',//,15I7)
   97 FORMAT(11X,' X= ',15F7.3)
   96 FORMAT(11X, J= ',15F7.3)
   95 FORMAT(2X,I3,F9.2,' ',15A1)
   94 FORMAT(14X,' ',115A1)
   93 FORMAT(//5X)
   92 FORMAT('1H1//')      THE ADD-ON FUNCTION GARRAY FOR Z=',F7.3,' CM:')
      RETURN
      END
C000014
C
      SUBROUTINE GPUNCH (Z,XO,YO,PHS,NOF,IMX,JMX,G)
C
C  GPUNCH PUNCHES OUT THE FIRST NON-SYMMETRIC PORTION OF GARRAY
C  (OR WRITES IT ON FILE 7 IN CMS VERSION)
      COMMON /SYM/ ISM,JSM,MSM,FCU,IMS,JMS,QSM
      DIMENSION G(IMX,JMX)
      WRITE(7,39) NOF,IMX,JMX,ISM,JSM,IMS,JMS
      WRITE(7,38) ((G(I,J),I=1,IMS),J=1,JMS)
   39 FORMAT(10I5)
   38 FORMAT(10F7.3)
      RETURN
      END
C000015
C
      SUBROUTINE READ (Z,XO,YO,PHISYM,NOF,IMAX,JMAX,G)
C
C  READS THE NON-SYMMETRIC PORTION OF THE GARRAY AND EXPANDS IT TO AN
C  ORTHOGONAL SET. NOTE, INSURE SUFFICIENT DIMENSIONS IN MAIN PROGRAM.
C
      COMMON /SYM/ ISYM,JSYM,MSYM,FCU,IMS,JMS,QSYM
```

```
SUB00510
SUB00520
SUB00530
SUB00550
SUB00560
SUB00570
SUB00580
SUB00590
SUB00600
SUB00610
SUB00620
SUB00630
SUB00640
SUB00650
SUB00660
SUB00670
SUB00680
SUB00690
SUB00700
SUB00710
SUB00720
SUB00730
SUB00740
SUB00750
SUB00760
SUB00770
SUB00780
SUB00790
SUB00800
SUB00810
SUB00820
SUB00830
SUB00840
SUB00850
SUB00860
SUB00880
SUB00890
SUB00900
SUB00910
SUB00920
SUB00930
SUB00940
```

```
      COMMON /IO/ CMS,IN1,IN2,IN4
      DIMENSION G(IMAX,JMAX)
      READ(IN1,39) NQF,IMAX,JMAX,ISYM,JSYM,IMS,JMS
      READ(IN1,40) Z,XO,YO,PHISYM
   10 DO 10 J=1,JMS
      READ(IN1,38) (G(I,J),I=1,IMS)
      WRITE(6,37) NQF,Z,XO,YO,PHISYM,IMAX,JMAX,JSYM
      RJMX=JMAX
      MSYM=JSYM
      IF((ISYM*.EQ.0).OR.(MSYM.GT.JMAX)) MSYM=1
      FCU=ISYM*JSYM*JMAX
      IF(JSYM.GT.JMAX) FCU=JMAX
      QSYM=FCU/RJMX
    1 DO 4 J=1,JMS
      IF(ISYM.EQ.1) GO TO 2
      II=IMAX+1-I
      DO 1 I=1,IMS
    1 G(II,J)=G(I,J)
    2 GO TO 4
      J2=JMAX/2+1-J
      J3=JMAX/2+J
      J4=JMAX+1-J
      DO 3 I=1,IMAX
      II=IMAX+1-I
    3 G(III,J2)=G(I,J)
      G(III,J3)=G(I,J)
      G(III,J4)=G(I,J)
    4 CONTINUE
   39 FORMAT(10I5)
   40 FORMAT(4F7.3)
   38 FORMAT(10F7.3)
   37 FORMAT(//' MODE 3 READS GARRAY DIRECTLY; NQF=',I4/'
     1' XO=',F7.3,' YO=',F7.3,' Z=',F7.3,' IMAX=',I4/'
     2' JMAX=',I4,' JSYM=',I4,' PHISYM=',F7.3///)
      RETURN
      END
C000016
C
C
      SUBROUTINE MAP (IM,JM,A,N,Z,BAND)
C
C     MAP CALLS SUBROUTINE MIMPII AND PLOTS A CONTOUR MAP OF THE ARRAY
C
      DIMENSION A(IM,JM),T(24)
      DATA BL/1H /
      DO 1 I=1,24
    1 T(I)=BL
```

```
      ICON=1
      IF(BAND.LT.0.) ICON=0
      IF(BAND.LT.0.) BAND=-BAND
      AMIN=0.
      IJT=0
      AZ=1.
      BZ=0.
      WRITE(6,49) N,Z
      CALL MTMPII (A,IM,JM,T,BAND,AZ,BZ,AMIN,IJT,ICON)
   49 FORMAT(1H1//' THE FUNCTION SURFACE, TEST NO.'I3,'   Z='F5.3//)
      RETURN
      END
C000017
C
      SUBROUTINE GPLOT (G,GA,JMS)
C
C  GPLOT PRINTS A ROUGH PLOT OF THE LINE INTEGRAL FUNCTIONS IN GARRAY.
C
      COMMON IMAX,JMAX,IIMX,JJMX,IJMX,ALPHA,SIZE,EPS,MODE,BOX,SD,IX,Z
      COMMON /TAB/ INDEX(7),JSYM,ISYM
      COMMON /TAB2/ IPT,KPT,LPT,MPT,REST(5)
      DIMENSION G(IMAX,JMAX),GA(IMAX,JMAX),ROW(101)
      DIMENSION A(201),B(101),C(201),D(101)
      JM=101
      DATA BL,PL,ST,DH,EX/1H ,1H+,1H*,1H-,1HX/
      JMS2=JMAX/2+1
      IF(ISYM.EQ.2)JMS2=1
      JMS3=JMS2+JMS-1
      DO 8 J=JMS2,JMS3
      WRITE(6,67) (ST,I=1,120)
      DO 1 I=1,IMAX
      A(I)=G(I,J)
    1 C(I)=GA(I,J)
      AS=.5
      BS=.0
      CALL INTERP (A,IMAX,AS,B,JM,BS)
      CALL INTERP (C,IMAX,AS,D,JM,BS)
      WRITE(6,69) J
      BIG=0.
      SMALL=0.
      DO 2 I=1,IMAX
      IF(A(I).GT.BIG)  BIG=A(I)
      IF(C(I).GT.BIG)  BIG=C(I)
      IF(A(I).LT.SMALL) SMALL=A(I)
    2 IF(C(I).LT.SMALL) SMALL=C(I)
      RANGE=BIG-SMALL
```

```
      RINK=RANGE/80.
      TOP=BIG+RINK
      CEN=BIG
      BOT=BIG-RINK
      KC=0
      DO 7 K=1,41
      IC=0
      DO 6 I=1,101
      ROW(I)=BL
      IF((I.EQ.1).OR.(I.EQ.51).OR.(I.EQ.101))ROW(I)=PL
      IF((K.EQ.1).OR.(K.EQ.41))ROW(I)=PL
      IF((TOP.GE.C.).AND.(BOT.LE.0.)) ROW(I)=DH
      GO TO 3
    3 IC=0
      ROW(I)=PL
      IF(KC.EQ.10) GO TO 5
    4 IF(KPT.LE.2) ROW(I)=PL
      IF((D(I).LE.TOP).AND.(D(I).GE.BOT)) ROW(I)=ST
      IF((B(I).LE.TOP).AND.(B(I).GE.BOT)) ROW(I)=EX
    5 IC=IC+1
      IF(KC.EQ.5) KC=0
    6 IF(KC.NE.0) WRITE (6,65) (ROW(I),I=1,101)
      IF(KC.EQ.0) WRITE (6,68) CEN.,(ROW(I),I=1,101)
      TOP=TOP-2.*RINK
      CEN=CEN-2.*RINK
      BOT=BOT-2.*RINK
      KC=KC+1
    7 WRITE (6,66)  (ST,I=1,120)
    8 FORMAT (//,I=.,i3//)
   69 FORMAT (1X,F8.3,/i12iA1//)
   68 FORMAT (1H1,/i12iA1//)
   67 FORMAT (//,i21A1//)
   65 FORMAT (10X,101A1)
      RETURN
      END
COC0018
C
      SUBROUTINE INTERP (A,IM,AS,B,JM,BS)
C
C     INTERP CONVERTS A REGULAR VECTOR A OF IM POINTS TO A REGULAR VECTOR
C     B OF JM POINTS. OS=.5 FOR A VECTOR WITH POINTS DEFINED IN THE
C     CENTER OF THE INTERVAL, AS AND BS ARE THE % OF AN INTERVAL FROM THE
C     EDGE OF THE FIELD TO THE FIRST POINT (.0 OR .5 FOR EDGE OR CENTER
C     DEFINED POINTS)
C
      DIMENSION A(IM),B(JM)
```

SUB01850
SUB01860
SUB01870
SUB01880
SUB01890
SUB01900
SUB01910
SUB01920
SUB01930
SUB01940
SUB01950
SUB01960
SUB01970
SUB01980
SUB01990
SUB02000
SUB02010
SUB02020
SUB02030
SUB02040
SUB02050
SUB02060
SUB02070
SUB02080
SUB02090
SUB02100
SUB02110
SUB02120
SUB02130
SUB02140
SUB02150
SUB02160
SUB02170
SUB02180
SUB02190
SUB02200
SUB02210

SUB02220
SUB02230
SUB02240
SUB02250
SUB02260
SUB02270
SUB02280
SUB02290
SUB02300

```
      RIM=IM                                                      SUB02310
      RJM=JM                                                      SUB02320
      RAT=(RIM-1.+2.*AS)/(RJM-1.+2.*BS)                           SUB02330
      DO 2 I=1,JM                                                 SUB02340
      BI=I                                                        SUB02350
      AI=RAT*(BI+BS)-AS                                           SUB02360
      IA=AI                                                       SUB02370
      F=AI-FLOAT(IA)                                              SUB02380
      IF((IA.EQ.0).OR.(IA.EQ.JM)) GO TO 1                         SUB02390
      B(I)=A(IA)+F*(A(IA+1)-A(IA))                                SUB02400
      GO TO 2                                                     SUB02410
    1 IF(IA.EQ.0) B(I)=A(1)*(F-AS)/(1.-AS)                        SUB02420
      IF(IA.EQ.JM) B(I)=A(JM)*F/(1.-AS)                           SUB02430
    2 CONTINUE                                                    SUB02440
      RETURN                                                      SUB02450
      END                                                         SUB02460
                                                                  SUB02470

C000019
C                                                                 SPL00010
      SUBROUTINE SPLINE                                           SPL00020
C                                                                 SPL00030
C     PURPOSE                                                     SPL00040
C        PROVIDES INTERPOLATED VALUE USING "CUBIC SPLINE FITTING" SPL00050
C                                                                 SPL00060
C     USAGE                                                       SPL00070
C        FIRST CALL TO SUBROUTINE:                               SPL00080
C        CALL SPLINE(X,Y,M,XINT,YINT)                            SPL00090
C                                                                 SPL00100
C        SUBSEQUENT CALLS:                                       SPL00110
C        CALL SPLINN(X,Y,M,XINT,YINT)                            SPL00120
C                                                                 SPL00130
C     DESCRIPTION OF PARAMETERS                                   SPL00140
C        X:   MONOTONICALLY INCREASING ABSCISSA ARRAY            SPL00150
C        Y:   ONE-FOR-ONE CORRESPONDING ORDINATE ARRAY           SPL00160
C        M:   NUMBER OF X AND Y VALUES SUPPLIED ( OR = 300       SPL00170
C        XINT:  VALUE OF ABSCISSA FOR WHICH CORRESPONDING ORDINATE SPL00180
C               IS TO BE INTERPOLATED (OR EXTRAPOLATED)          SPL00190
C        YINT:  INTERPOLATED (OR EXTRAPOLATED) ORDINATE VALUE    SPL00200
C                                                                 SPL00210
C     REMARKS                                                     SPL00220
C        IF SPECIFIED X FALLS OUTSIDE OF RANGE, AN EXTRAPOLATED   SPL00240
C        VALUE WILL BE SUPPLIED                                   SPL00250
C                                                                 SPL00260
C     SUBROUTINES AND FUNCTION SUBPROGRAMS REQUIRED              SPL00270
C        SUBROUTINE SPLICO IS INCLUDED IN SUBROUTINE SPLIN PACKAGE SPL00280
C                                                                 SPL00290
C                                                                 SPL00300
C                                                                 SPL00310
```

```
C      MATHEMATICAL METHOD                                              SPL00320
C      UPON FIRST ENTRY TO SPLIN, A CALL TO SPLICO IS MADE TO           SPL00330
C      DETERMINE THE COEFFICIENTS TO BE USED IN PERFORMING THE          SPL00340
C      INTERPOLATIONS.  SEARCH FOR BRACKETING ABSCISSA VALUES IS        SPL00350
C      ALWAYS MADE FROM THE REFERENCE LAST USED IN INTERPOLATING.       SPL00360
C                                                                       SPL00370
C                                                                       SPL00380
C      REFERENCE                                                        SPL00390
C      PENNINGTON, RALPH H., "INTRODUCTORY COMPUTER METHODS AND         SPL00400
C      NUMERICAL ANALYSIS", THE MACMILLAN COMPANY, NEW YORK, 1965       SPL00410
C                                                                       SPL00420
C                                                                       SPL00430
       SUBROUTINE SPLINE(X,Y,M,XINT,YINT)                               SPL00440
       DIMENSION X(M),Y(M),C(4,300)                                     SPL00460
       CALL SPLICO(X,Y,M,C)                                             SPL00470
       K=1                                                              SPL00480
       ENTRY SPLINN(X,Y,M,XINT,YINT)                                    SPL00490
       IF(XINT-X(1)) 70,1,2                                             SPL00500
       K=1                                                              SPL00510
 3     GO TO 7                                                          SPL00520
 70    YINT=Y(1)                                                        SPL00530
 1     RETURN                                                           SPL00540
 2     IF(XINT-X(K+1)) 6,4,5                                            SPL00550
 4     YINT=Y(K+1)                                                      SPL00560
       RETURN                                                           SPL00570
 5     K=K+1                                                            SPL00580
       IF(M-K) 71,71,3                                                  SPL00590
 71    K=M-1                                                            SPL00600
       GO TO 7                                                          SPL00610
 6     IF(XINT-X(K)) 13,12,11                                           SPL00620
 12    YINT=Y(K)                                                        SPL00630
       RETURN                                                           SPL00640
 13    K=K-1                                                            SPL00650
       GO TO 6                                                          SPL00660
 7     PRINT 101,XINT                                                   SPL00670
 101   FORMAT(8HOXINT = E18.9,32H, OUT OF RANGE FOR INTERPOLATION)      SPL00680
       YINT=(X(K+1)-XINT)*(C(1,K)*(X(K+1)-XINT)**2+C(3,K))              SPL00690
 11    YINT=YINT+(XINT-X(K))*(C(2,K)*(XINT-X(K))**2+C(4,K))             SPL00700
       RETURN                                                           SPL00710
       END                                                              SPL00720
```

```
      SUBROUTINE SPLICO(X,Y,M,C)                                         SPL00730
      DIMENSION X(M),Y(M),C(4,300),D(300),P(300),E(300),A(300,3),B(300), SPL00740
     1Z(300)                                                             SPL00750
      MM=M-1                                                             SPL00760
      DO 2 K=1,MM                                                        SPL00770
      D(K)=X(K+1)-X(K)                                                   SPL00780
      P(K)=D(K)/6.                                                       SPL00790
    2 E(K)=(Y(K+1)-Y(K))/D(K)                                           SPL00800
      DO 3 K=2,MM                                                        SPL00810
    3 B(K)=E(K)-E(K-1)                                                   SPL00820
      A(1,3)=-1.-D(1)/D(2)                                               SPL00830
      A(1,2)=D(1)/D(2)                                                   SPL00840
      A(2,3)=P(2)-P(1)*A(1,3)                                            SPL00850
      A(2,2)=2.*(P(1)+P(2))-P(1)*A(1,2)                                  SPL00860
      A(2,3)=A(2,3)/A(2,2)                                               SPL00870
      B(2)=B(2)/A(2,2)                                                   SPL00880
      DO 4 K=3,MM                                                        SPL00890
      A(K,2)=2.*(P(K-1)+P(K))-P(K-1)*A(K-1,3)                            SPL00900
      B(K)=B(K)-P(K-1)*B(K-1)                                            SPL00910
      A(K,3)=P(K)/A(K,2)                                                 SPL00920
    4 B(K)=B(K)/A(K,2)                                                   SPL00930
      Q=D(M-2)/D(M-1)                                                    SPL00940
      A(M,1)=1.+Q+A(M-2,3)                                               SPL00950
      A(M,2)=-Q-A(M,1)*A(M-1,3)                                          SPL00960
      B(M)=B(M-2)-A(M,1)*B(M-1)                                          SPL00970
      Z(M)=B(M)/A(M,2)                                                   SPL00980
      MN=M-2                                                             SPL00990
      DO 6 I=1,MN                                                        SPL01000
      K=M-I                                                              SPL01010
    6 Z(K)=B(K)-A(K,3)*Z(K+1)                                            SPL01020
      Z(1)=-A(1,2)*Z(2)-A(1,3)*Z(3)                                      SPL01030
      DO 7 K=1,MM                                                        SPL01040
      Q=1./(6.*D(K))                                                     SPL01050
      C(1,K)=Z(K)*Q                                                      SPL01060
      C(2,K)=Z(K+1)*Q                                                    SPL01070
      C(3,K)=Y(K)/D(K)-Z(K)*P(K)                                         SPL01080
    7 C(4,K)=Y(K+1)/D(K)-Z(K+1)*P(K)                                     SPL01090
      RETURN                                                             SPL01110
      END                                                                SPL01120
C000020                                                                  MET000010
C                                                                        MET000020
C**********************************************************************  MET000030
C      SUBROUTINE MTMPII                                                 MET000040
C                                                                        MET000050
C      PURPOSE                                                           MET000060
```

164

```
      MTMPII WILL PRODUCE ON THE PRINTER, A CONTOUR MAP            METO0070
      OF ANY SINGLE PRECISION TWO DIMENSIONAL ARRAY.              METO0080
                                                                  METO0090
   USAGE                                                          METO0100
                                                                  METO0110
      CALL MTMPII(Y,N,M,T,BND,AZ,BZ,AMIN,IJT,ICON)                METO0120
                                                                  METO0130
   DESCRIPTION OF PARAMETERS                                      METO0140
                                                                  METO0150
      Y    - THE ARRAY TO BE CONTOURED. DIMENSIONED Y(N,M)        METO0160
      N    - NUMBER OF ROWS IN Y.                                 METO0170
      M    - NUMBER OF COLUMNS IN Y.                              METO0180
      T    - ARRAY FOR PLOT TITLE. REAL*4. T(24).                 METO0190
      BND  - A BANDWIDTH FOR THE CONTOURING. IF BND IS ZERO       METO0200
             BND=(MAX(Y)-MIN(Y))/15. WILL BE CALCULATED AS FOLLOWS METO0210
                                                                  METO0220
      AZ   - A LINEAR TRANSFORMATION MAYBE PERFORMED ON           METO0230
             THE ARRAY Y OF THE FOLLOWING FORM AZ*Y+BZ.           METO0240
             IF AZ=0 THEN AZ WILL BE COMPUTED SUCH THAT           METO0250
             MAX(IMAX(Y),),IMIM(Y),) WILL BE LESS THAN 1,         METO0260
             AND BZ WILL BE LEFT AS INPUT.                        METO0270
      BZ   - SEE UNDER AZ                                         METO0280
      AMIN - THE LEVEL AT WHICH COUTOURING WILL BEGIN. IF         METO0290
             AMIN > MIN(Y) THEN AMIN WILL BE CALCULATED           METO0300
             TO BE ,WITH REFERENCE AT ZERO, THE NEXT LOWER        METO0310
             CONTOUR LEVEL FROM MIN(Y) AS DETERMINED BY           METO0320
             BND.                                                 METO0330
      IJT  - IF IJT=0 AMIN WILL BE CALCULATED AS DESCRIBED        METO0340
             ABOVE.                                               METO0350
      ICON - IF ICON=0 NO CONTOURING WILL BE DONE BUT THE         METO0360
             ARRAY Y WILL BE PRINTED IN THE PLOT FORMAT.          METO0370
                                                                  METO0380
   REMARKS                                                        METO0390
      MTMPII REQUIRES A PRINTER WITH 132 PRINT POSITIONS.         METO0400
      IF NECESSARY THE MAP WILL BE SEGMENTED COLUMNWISE. SOME     METO0410
      THE ROWS AND COLUMNS ARE NUMBERED ALONG THE EDGES.          METO0420
      THAT A SEGMENT MAYBE EASILY JOINED TOGETHER.                METO0430
      ONLY THREE SIGNIFICANT FIGURES WILL BE PRINTED AT           METO0440
      EACH POINT. THE POSITION OF THE FIRST SIGNIFICANT           METO0450
      DIGIT WILL BE DETERMINED BY MAX(IMAX(Y),),IMIN(Y),).        METO0460
      THE PLOT WILL BE PRODUCED ON A INCH GRID. IT                METO0470
      WILL BE ASSUMED THAT THE SPACING BETWEEN POINTS IN          METO0480
      BOTH DIRECTIONS IS THE SAME AND EQUAL FOR ALL POINTS        METO0490
                                                                  METO0500
   SUBROUTINES REQUIRED                                           METO0510
      NONE                                                        METO0520
                                                                  METO0530
   METHOD                                                         METO0540
      THE CONTOUR LEVELS ARE DETERMINED BY SIMPLE LINEAR
```

```
C     INTERPOLATION FROM THE FOUR SURROUNDING PIONTS.                 MET00550
C     ************************************************************    MET00560
C     ************************************************************    MET00570
C                                                                     MET00580
C     MTMPII SUBROUTINE FOR ONE-INCH GRID SPACING                     MET00590
C     OAKES CODE 5105   15 JAN 69                                     MET00600
                                                                      MET00610
                                                                      MET00620

      SUBROUTINE MTMPII(Y,N,M,T,BND,AZ,BZ,AMIN,IJT,ICON)              MET00630
      REAL*4 IH,KG,ITJZ                                               MET00640
      DIMENSION A(140),B(140),C(140),D(140),IH(20),Y(N,M),TP(10),TPX(10) MET00650
     Z,TPM(10),XMT(10),BTM(10),BTX(10),BT(10),KG(10),T(24)           MET00660
      DIMENSION E(140),F(140),G(140),H(140)                          MET00670
C                                                                     MET00680
C                                                                     MET00690
      DATA DUE /4H    /,EPL/4H+   /,EMI/4H-   /,IH/1H0,1H ,1H1,1H2,   MET00700
     1 1H ,1H3,1H ,1H4,1H ,1H5,1H ,1H6,1H ,1H7,1H ,1H8,1H ,1H9,1H ,  MET00710
     2 1H0,1H1,1H2,1H3,1H4,1H5,1H6,1H7,1H8,1H9/,BLK/4H    /          MET00720
C                                                                     MET00730
      YMIN=Y(1,1)                                                     MET00740
      YMAX=Y(1,1)                                                     MET00750
      DO 20 I=1,M                                                     MET00760
      DO 10 J=1,N                                                     MET00770
      YMIN=AMIN1(YMIN,Y(J,I))                                         MET00780
      YMAX=AMAX1(YMAX,Y(J,I))                                         MET00790
   10 CONTINUE                                                        MET00800
   20 CONTINUE                                                        MET00810
      DELY=YMAX-YMIN                                                  MET00820
      IF(BND) 25,25,30                                                MET00830
   25 BND=DELY/15.0                                                   MET00840
   30 IF (AMIN-YMIN) 31,31,32                                         MET00850
   31 IF (IJT) 33,32,33                                               MET00860
   32 PD=YMIN/BND                                                     MET00870
      PF=ABS(PD-INT(PD))                                              MET00880
      IF (YMIN) 2,1,1                                                 MET00890
    1 AMIN=YMIN-PF*BND                                                MET00900
      GO TO 33                                                        MET00910
    2 AMIN=YMIN-(1.0-PF)*BND                                          MET00920
   33 AHLD=AZ                                                         MET00930
      IF(AZ) 55,35,55                                                 MET00940
   35 SM=AMAX1(ABS(YMIN),ABS(YMAX))                                   MET00950
      NS=0                                                            MET00960
   40 NS=NS+1                                                         MET00970
      SM=10.0*SM                                                      MET00980
      IF(SM-1.0) 40,50,45                                             MET00990
   45 NS=NS-1                                                         MET01000
```

```
      SM=SM/10.0
   50 IF(SM-1.0)50,50,45                                          METO1010
   55 AHLD=10.0**NS                                               METO1020
      HBND=BND/2.0                                                METO1030
      PRINT 70,T                                                  METO1040
    6 FORMAT(5X,24A4,//)                                          METO1050
      PRINT 57,AHLD,BZ                                            METO1060
   57 FORMAT(1H0,65HTHE FOLLOWING TRANSFORMATION WAS PERFORMED ON THE INMETO1070
     1PUT MATRIX /5X,1H(,E12.5,8H*Y(I,J)+,E12.5,5,1H)//2X,73HAND THREEMETO1080
     2 DIGITS TO THE RIGHT OF THE DECIMAL POINT ARE PRINTED IN THE MAP )METO1090
C                                                                 METO1100
      PRINT 54,YMAX,YMIN                                          METO1110
   54 FORMAT(/4X,5HYMAX=,E15.7,5X,5HYMIN=,E15.7)                  METO1120
      IF(ICON)5,58,5                                              METO1130
    5 PRINT 11,BND                                                METO1140
   11 FORMAT(2X,17HTHE BAND WIDTH IS,E12.5,6H UNITS //4X,14HCONTOUR LEVEMETO1150
     1LS )                                                        METO1160
      I=0                                                         METO1170
      YTOP=AMIN                                                   METO1180
      IF(ABS(YMIN-YMAX)-100.0*BND)53,53,58                        METO1190
   53 YB=YTOP                                                     METO1200
      YTOP=YTOP+BND                                               METO1210
      I=I+1                                                       METO1220
      J=MOD(I,20)                                                 METO1230
      ITJZ=IH(J)                                                  METO1240
      IF(YB-YMAX)59,58,58                                         METO1250
   59 PRINT 61,YB,YTOP,ITJZ                                       METO1260
   61 FORMAT(/4X,E10.3,4H TO ,E10.3,2H =,1X,A1)                   METO1270
      GO TO 53                                                    METO1280
   58 NCCP=0                                                      METO1290
      NCP=0                                                       METO1300
   60 PRINT 70                                                    METO1310
   70 FORMAT(1H1)                                                 METO1320
      PRINT 6,T                                                   METO1330
      NLINE=0                                                     METO1340
      NCCP=NCP+1                                                  METO1350
      NCP = NCP + 13                                              METO1360
   73 IF(NCP-M)80,80,75                                           METO1370
   75 NCP=M                                                       METO1380
   80 CONTINUE                                                    METO1390
      J=-2                                                        METO1400
      NLINE=NLINE+1                                               METO1410
      LLINE=N-NLINE+1                                             METO1420
C SET UP HEADING                                                  METO1430
   85 IF(NCCP-1) 85,85,90                                         METO1440
   90 DO 100 I = 1,135                                            METO1450
                                                                  METO1460
                                                                  METO1470
                                                                  METO1480
```

```
      A(I)=BLK
      B(I)=BLK
      H(I)=BLK
100   CONTINUE
110   DO 160 L=NCCP,NCP
      J=J+8
      KI=L
      IF(KI-100) 130,120,120
120   LL=KI/100
      A(J)=KG(LL+1)
      KI=KI-100*LL
      GO TO 135
130   A(J)=KG(1)
135   J=J+1
      IF(KI-10) 150,140,140
140   LL=KI/10
      A(J)=KG(LL+1)
      KI=KI-10*LL
      GO TO 155
150   A(J)=KG(1)
155   J=J+1
      A(J)=KG(KI+1)
160   CONTINUE
C     SETUP FIRST ROW OF ARRAY
      GO TO 260
170   NLINE=NLINE+1
      LLINE=N-NLINE+1
      IF(NLINE-N) 180,180,380
180   DO 190 I=1,135
      A(I)=BLK
      B(I)=BLK
      C(I)=BLK
      D(I)=BLK
      E(I)=BLK
      F(I)=BLK
      G(I)=BLK
      H(I)=BLK
190   CONTINUE
      IF(ICON)195,260,195
195   NCY=NCCP-1
      J=4
      IF(NCY)200,200,210
200   J=5
210   NCY=NCY+1
      IF(NCY-NCP) 220,220,260
220   IF(NCY-M) 230,260,260
230   NLINE = NLINE - 1
      YD1 = Y(NLINE,NCY) - Y(NLINE+1,NCY)
```

METO1490
METO1500
METO1510
METO1520
METO1530
METO1540
METO1550
METO1560
METO1570
METO1580
METO1590
METO1600
METO1610
METO1620
METO1630
METO1640
METO1650
METO1660
METO1670
METO1680
METO1690
METO1700
METO1710
METO1720
METO1730
METO1740
METO1750
METO1760
METO1770
METO1780
METO1790
METO1800
METO1810
METO1820
METO1830
METO1840
METO1850
METO1860
METO1870
METO1880
METO1890
METO1900
METO1910
METO1920
METO1930
METO1940
METO1950
METO1960

```
      YD2=Y(NLINE+1,NCY+1)-Y(NLINE+1,NCY+1)                      METO1970
      TP(1)=Y(NLINE,NCY+1)-0.125*YD1                             METO1980
      TPX(1)=Y(NLINE,NCY+1)-0.250*YD1                            METO1990
      TPM(1)=Y(NLINE,NCY+1)-0.375*YD1                            METO2000
      XMT(1)=Y(NLINE,NCY+1)-0.500*YD1                            METO2010
      BTM(1)=Y(NLINE,NCY+1)-0.625*YD1                            METO2020
      BTX(1)=Y(NLINE,NCY+1)-0.750*YD1                            METO2030
      BT(1)=Y(NLINE,NCY+1)-0.875*YD1                             METO2040
      TP(10)=Y(NLINE,NCY+1)+0.125*YD2                            METO2050
      TPM(10)=Y(NLINE,NCY+1)+0.375*YD2                           METO2060
      XMT(10)=Y(NLINE,NCY+1)+0.500*YD2                           METO2070
      BTM(10)=Y(NLINE,NCY+1)+0.625*YD2                           METO2080
      BTX(10)=Y(NLINE,NCY+1)+0.750*YD2                           METO2090
      BT(10)=Y(NLINE,NCY+1)+0.875*YD2                            METO2100
      NLINE=NLINE+1                                              METO2110
      D1=(TP(10)-TP(1))/9.                                       METO2120
      D2=(TPX(10)-TPX(1))/9.                                     METO2130
      D3=(TPM(10)-TPM(1))/9.                                     METO2140
      D4=(XMT(10)-XMT(1))/9.                                     METO2150
      D5=(BTM(10)-BTM(1))/9.                                     METO2160
      D6=(BTX(10)-BTX(1))/9.                                     METO2170
      D7=(BT(10)-BT(1))/9.                                       METO2180
      DO 240 I=2,9                                               METO2190
      TP(I)=TP(I-1)+D1                                           METO2200
      TPX(I)=TPX(I-1)+D2                                         METO2210
      TPM(I)=TPM(I-1)+D3                                         METO2220
      XMT(I)=XMT(I-1)+D4                                         METO2230
      BTM(I)=BTM(I-1)+D5                                         METO2240
      BTX(I)=BTX(I-1)+D6                                         METO2250
      BT(I)=BT(I-1)+D7                                           METO2260
  240 CONTINUE                                                   METO2270
      DO 250 I=1,10                                              METO2280
      J=J+1                                                      METO2290
      I1=MOD(IFIX((TP(I)-AMIN)/BND),20)+1                        METO2300
      I2=MOD(IFIX((TPX(I)-AMIN)/BND),20)+1                       METO2310
      I3=MOD(IFIX((TPM(I)-AMIN)/BND),20)+1                       METO2320
      I4=MOD(IFIX((XMT(I)-AMIN)/BND),20)+1                       METO2330
      I5=MOD(IFIX((BTM(I)-AMIN)/BND),20)+1                       METO2340
      I6=MOD(IFIX((BTX(I)-AMIN)/BND),20)+1                       METO2350
      I7=MOD(IFIX((BT(I)-AMIN)/BND),20)+1                        METO2360
      A(J)=IH(I1)                                                METO2370
      B(J)=IH(I2)                                                METO2380
      C(J)=IH(I3)                                                METO2390
      D(J)=IH(I4)                                                METO2400
      E(J)=IH(I5)                                                METO2410
      F(J)=IH(I6)                                                METO2420
      G(J)=IH(I7)                                                METO2430
                                                                 METO2440
```

169

```
250   CONTINUE                                                          METO2450
      GO TO 210                                                         METO2460
260   NCY=NCCP-1                                                        METO2470
      J=-2                                                              METO2480
265   IF(NCY) 265,265,270                                              METO2490
      J=-1                                                              METO2500
      GO TO 330                                                         METO2510
270   NCY=NCY+1                                                         METO2520
      IF(NCY-NCP) 280,280,310                                          METO2530
280   J=J+7                                                             METO2540
      THLD=AHLD*Y(NLINE,NCY)+BZ                                         METO2550
      IF(THLD) 285,290,290                                             METO2560
285   H(J)=EMI                                                          METO2570
      GO TO 295                                                         METO2580
290   H(J)=EPL                                                          METO2590
295   NUM=INT(ABS(THLD-INT(THLD))*1000.0+0.5)                          METO2600
      NDS=100                                                           METO2610
      DO 300 KK=1,3                                                     METO2620
      J=J+1                                                             METO2630
      KI=NUM/NDS                                                        METO2640
      H(J)=KG(KI+1)                                                     METO2650
      NUM=NUM-KI*NDS                                                    METO2660
      NDS=NDS/10                                                        METO2670
300   CONTINUE                                                          METO2680
      GO TO 270                                                         METO2690
310   IF(NCP-M) 360,320,320                                            METO2700
320   IF(J-127)330,330,360                                             METO2710
330   J=J+3                                                             METO2720
      KI=NLINE                                                          METO2730
      IF(KI-100) 340,335,335                                           METO2740
335   LL=KI/100                                                         METO2750
      KI=KI-100*LL                                                      METO2760
      GO TO 343                                                         METO2770
340   H(J)=KG(1)                                                        METO2780
343   J=J+1                                                             METO2790
      IF(KI-10) 350,345,345                                            METO2800
345   LL=KI/10                                                          METO2810
      H(J)=KG(LL+1)                                                     METO2820
      KI=KI-10*LL                                                       METO2830
      GO TO 355                                                         METO2840
350   H(J)=KG(1)                                                        METO2850
355   J=J+1                                                             METO2860
      H(J)=KG(KI+1)                                                     METO2870
      J=J+5                                                             METO2880
      IF(NCY-1) 270,270,360                                            METO2890
360   IF(NLINE-1)362,362,368                                           METO2900
362   PRINT 370,(A(I),I=1,132),(B(IP1),IP1=1,132),(H(IP2),IP2=1,132)   METO2910
                                                                        METO2920
```

170

```
368   GO TO 170
      PRINT 370,(A(I),I=1,132),(B(IP1),IP1=1,132),(C(IP2),IP2=1,132),   METO02930
     1(D(IP3),IP3=1,132),(E(IP4),IP4=1,132),(F(IP5),IP5=1,132),         METO02940
     2(G(IP6),IP6=1,132),(H(IP7),IP7=1,132)                             METO02950
370   FORMAT(132A1)                                                     METO02960
      GO TO 170                                                         METO02970
380   DO 390 I=1,135                                                    METO02980
      A(I)=BLK                                                          METO02990
      B(I)=BLK                                                          METO03000
      C(I)=BLK                                                          METO03010
      D(I)=BLK                                                          METO03020
390   CONTINUE                                                          METO03030
      J=-2                                                              METO03040
      IF(NCCP-1) 395,395,400                                            METO03050
395   J=-1                                                              METO03060
400   DO 430 L=NCCP,NCP                                                 METO03070
      J=J+8                                                             METO03080
      KI=L                                                              METO03090
      IF(KI-100) 410,405,405                                            METO03100
405   LL=KI/100                                                         METO03110
      C(J)=KG(LL+1)                                                     METO03120
      KI=KI-100*LL                                                      METO03130
      GO TO 412                                                         METO03140
410   C(J)=KG(1)                                                        METO03150
412   J=J+1                                                             METO03160
      IF(KI-10) 420,415,415                                             METO03170
415   LL=KI/10                                                          METO03180
      C(J)=KG(LL+1)                                                     METO03200
      KI=KI-10*LL                                                       METO03210
      GO TO 422                                                         METO03220
420   C(J)=KG(1)                                                        METO03230
422   J=J+1                                                             METO03240
      C(J)=KG(KI+1)                                                     METO03250
430   CONTINUE                                                          METO03260
      PRINT 370,(B(IP1),IP1=1,132),(C(IP2),IP2=1,132)                   METO03270
      IF(NCP-M)60,500,500                                               METO03280
500   RETURN                                                            METO03290
      END                                                               METO03300

C000021
C
C
      SUBROUTINE GAUSS                                                  GAUS  10
C                                                                       GAUS  20
C     PURPOSE                                                           GAUS  30
C        COMPUTES A NORMALLY DISTRIBUTED RANDOM NUMBER WITH A GIVEN     GAUS  40
C                                                                       GAUS  50
C                                                                       GAUS  60
C                                                                       GAUS  70
```

171

```
C     MEAN AND STANDARD DEVIATION                                    GAUS  80
C                                                                    GAUS  90
C     USAGE                                                          GAUS 100
C        CALL GAUSS(IX,S,AM,V)                                       GAUS 110
C                                                                    GAUS 120
C     DESCRIPTION OF PARAMETERS                                      GAUS 130
C        IX -IX MUST CONTAIN AN ODD INTEGER NUMBER WITH NINE OR      GAUS 140
C             LESS DIGITS ON THE FIRST ENTRY TO GAUSS. THEREAFTER    GAUS 150
C             IT WILL CONTAIN A UNIFORMLY DISTRIBUTED INTEGER RANDOM GAUS 160
C             NUMBER GENERATED BY THE SUBROUTINE FOR USE ON THE NEXT GAUS 170
C             ENTRY TO THE SUBROUTINE.                               GAUS 180
C        S  -THE DESIRED STANDARD DEVIATION OF THE NORMAL            GAUS 190
C             DISTRIBUTION.                                          GAUS 200
C        AM -THE DESIRED MEAN OF THE NORMAL DISTRIBUTION             GAUS 210
C        V  -THE VALUE OF THE COMPUTED NORMAL RANDOM VARIABLE        GAUS 220
C                                                                    GAUS 230
C     REMARKS                                                        GAUS 240
C        THIS SUBROUTINE USES RANDU WHICH IS MACHINE SPECIFIC        GAUS 250
C                                                                    GAUS 260
C     SUBROUTINES AND FUNCTION SUBPROGRAMS REQUIRED                  GAUS 270
C        RANDU                                                       GAUS 280
C                                                                    GAUS 290
C     METHOD                                                         GAUS 300
C        USES 12 UNIFORM RANDOM NUMBERS TO COMPUTE NORMAL RANDOM     GAUS 310
C        NUMBERS BY CENTRAL LIMIT THEOREM. THE RESULT IS THEN        GAUS 320
C        ADJUSTED TO MATCH THE GIVEN MEAN AND STANDARD DEVIATION.    GAUS 330
C        THE UNIFORM RANDOM NUMBERS COMPUTED WITHIN THE SUBROUTINE   GAUS 340
C        ARE FOUND BY THE POWER RESIDUE METHOD.                      GAUS 350
C                                                                    GAUS 360
C     ...................................................            GAUS 370
C                                                                    GAUS 380
      SUBROUTINE GAUSS(IX,S,AM,V)                                    GAUS 390
      A=0.0                                                          GAUS 400
      DO 50 I=1,12                                                   GAUS 410
      CALL RANDU(IX,IY,Y)                                            GAUS 420
      IX=IY                                                          GAUS 430
   50 A=A+Y                                                          GAUS 440
      V=(A-6.0)*S+AM                                                 GAUS 450
      RETURN                                                         GAUS 460
      END                                                            GAUS 470

C000022                                                              RAND  10
C     .................................................              RAND  20
C                                                                    RAND  30
```

172

```
C     SUBROUTINE RANDU                                          RAND  40
C                                                               RAND  50
C     PURPOSE                                                   RAND  60
C        COMPUTES UNIFORMLY DISTRIBUTED RANDOM REAL NUMBERS     RAND  70
C        BETWEEN 0 AND 1.0 AND RANDOM INTEGERS BETWEEN ZERO     RAND  80
C        AND 2**31. EACH ENTRY USES AS INPUT AN INTEGER         RAND  90
C        RANDOM NUMBER AND PRODUCES A NEW INTEGER AND REAL      RAND 100
C        RANDOM NUMBER.                                         RAND 110
C                                                               RAND 120
C     USAGE                                                     RAND 130
C        CALL RANDU(IX,IY,YFL)                                  RAND 140
C                                                               RAND 150
C     DESCRIPTION OF PARAMETERS                                 RAND 160
C        IX - FOR THE FIRST ENTRY THIS MUST CONTAIN ANY ODD     RAND 170
C             INTEGER NUMBER WITH NINE OR LESS DIGITS. AFTER     RAND 180
C             THE FIRST ENTRY, IX SHOULD BE THE PREVIOUS VALUE   RAND 190
C             OF IY COMPUTED BY THIS SUBROUTINE.                 RAND 200
C        IY - A RESULTANT INTEGER RANDOM NUMBER REQUIRED FOR     RAND 210
C             THE NEXT ENTRY TO THIS SUBROUTINE. THE RANGE OF    RAND 220
C             THIS NUMBER IS BETWEEN ZERO AND 2**31              RAND 230
C        YFL- THE RESULTANT UNIFORMLY DISTRIBUTED, FLOATING      RAND 240
C             POINT, RANDOM NUMBER IN THE RANGE 0 TO 1.0         RAND 250
C                                                               RAND 260
C     REMARKS                                                   RAND 270
C        THIS SUBROUTINE IS SPECIFIC TO SYSTEM/360 AND WILL     RAND 280
C        PRODUCE 2**29 TERMS BEFORE REPEATING. THE REFERENCE    RAND 290
C        BELOW DISCUSSES SEEDS (65539 HERE), RUN PROBLEMS       RAND 300
C        CONCERNING MACLAREN AND RANDOM DIGITS USING THIS       RAND 310
C        GENERATION SCHEME. MARSAGLIA AND MARSAGLIA, JACM 12,   RAND 320
C        P. 83-89, DISCUSS CONGRUENTIAL GENERATION METHODS,     RAND 330
C        AND THE USE OF TWO GENERATORS OF THE RANDU TYPE. ONE   RAND 340
C        BENEFIT WHICH HAS BEEN NOTED IS THE GENERATION OF A    RAND 350
C        TABLE, WHILE FILLING A TABLE. A BETTER STATISTICAL     RAND 360
C        CASE. A BETTER DEVIATE PROPERTIES                      RAND 370
C        SUGGESTED AS A BENEFIT IN ACCORDANCE WITH THE          RAND 380
C        FOR HIGH ORDER BITS OF THE GENERATED DISCUSSION        RAND 390
C        SEEDS SHOULD BE CHOSEN IN ACCORDANCE IT SHOULD BE      RAND 400
C        GIVEN IN THE REFERENCE BELOW. ALSO, NOTED THAT         RAND 410
C        AVAILABLE FROM RANDU. THE RANDOM NUMBERS ARE           RAND 420
C        FLOATING POINT DEVIATES ARE MODIFIED DESIRED, AS ARE   RAND 430
C        DEVIATES HAVE HIGH PROBABILITY OF IN FACT THESE        RAND 440
C        ORDER ZERO BIT IN THEIR FRACTIONAL HAVING A TRAILING   RAND 450
C        PART. LOW                                              RAND 460
C                                                               RAND 470
C     SUBROUTINES AND FUNCTION SUBPROGRAMS REQUIRED             RAND 480
C        NONE                                                   RAND 490
C                                                               RAND 500
C     METHOD                                                    RAND 510
C        POWER RESIDUE METHOD DISCUSSED IN IBM MANUAL C20-8011,
C        RANDOM NUMBER GENERATION AND TESTING
```

173

```
C .....................................................
C .....................................................                    RAND 520
                                                                          RAND 530

      SUBROUTINE RANDU(IX,IY,YFL)                                         RAND 540
      IY=IX*65539                                                        RAND 550
      IF(IY)5,6,6                                                        RAND 560
    5 IY=IY+2147483647+1                                                 RAND 570
    6 YFL=IY                                                             RAND 580
      YFL=YFL*.4656613E-9                                                RAND 590
      RETURN                                                             RAND 600
      END
```

BIBLIOGRAPHY

1. Caulfield, H. J. and Lee, Sun, <u>The Applications of Holography</u>, John Wiley and Sons, 1970.

2. Ellis, B. K. and Furey, R. J., <u>Wing-Body Interactions at a Mach Number of 9.5.</u>, Naval Ship Research and Development Center Report 2564, Aerodynamics Laboratory Research and Development Report 1133, September 1967.

3. Jagota, R. C., <u>The Application of Holographic Interferometry to the Determination of the Flow Field Around a Right Circular Cone at Angle of Attack</u>, Aeronautical Engineer Thesis, Naval Postgraduate School, December 1970.

4. Jagota, R. C. and Collins, D. J., "Finite Fringe Holographic Interferometry Applied to a Right Circular Cone at Angle of Attack", to be published in <u>Journal of Applied Mechanics</u>.

5. Kaufman, L. G. II and Meckler, L., <u>Pressure and Heat Transfer Measurements at Mach 5 and 8 for a Fin-Flat Plate Model</u>, Technical Documentary Report No. ASD-TDR 63-235, April 1963.

6. Kaufman, L. G. II, <u>Pressure Distributions and Oil Film Photographs for Mach 5 Flows Past Fins Mounted on a Flat Plate</u>, Technical Documentary Report No. ASD-TDR-63-755, September 1963.

7. Landenberg, R. W., et. al., ed., <u>Physical Measurements in Gas Dynamics and Combustion</u>, Princeton University Press, 1954.

8. Liepmann, H. W., and Roshko, A., <u>Elements of Gas Dynamics</u>, p. 165, John Wiley and Sons, Inc., 1957.

9. Maldonado, C. D., Caran, A. P., and Olsen, H. N., "New Method for Obtaining Emission Coefficients from Emitted Spectral Intensities. Part I--Circularly Symmetric Light Sources.", <u>Journal of the Optical Society of America</u>, Vol. 55, No. 10, pp. 1247-1254, October 1965.

10. Maldonado, C. D., "Note on Orthogonal Polynomials Which Are 'Invariant in Form' to Rotations of Axis", <u>Journal of Mathematical Physics</u> Vol. 6, No. 12, pp. 1935-1938, December 1965.

11. Maldonado, C. D. and Olsen, H. N., "New Method for Obtaining Emission Coefficients from Emitted Spectral Intensities. Part II--Asymmetrical Sources", <u>Journal of the Optical Society of America</u>, Vol 56, No. 10, pp. 1305-1313, October 1966.

12. Matulka, R. D., <u>The Application of Holographic Interferometry to the Determination of Asymmetric Three-Dimensional Density Fields in Free Jet Flow</u>, Ph. D. Thesis, Naval Postgraduate School, June, 1970.

13. Matulka, R. D. and Collins D. J., "Determination of Three-Dimensional Density Fields from Holographic Interferograms", <u>Journal of Applied Physics</u>, Vol. 42, No. 3, March 1971.

14. Okayama, H. and Emori, Y., "Polarization Effects in Holography", _Applied Physics Letters_, Vol. 19, No. 9, pp. 359-360, 1 November 1971

15. Olsen, H. N., Maldonado, C. D., Duckworth, G. D., and Caron, A. P., _Investigation of the Interaction of an External Magnetic Field with an Electric Arc_, Aerospace Research Laboratories Report ARL 66-0016, January 1966.

16. Olsen, H. N., Maldonado, C. D., and Duckworth, G. D., "A Numerical Method for Obtaining Internal Emission Coefficients from Externally Measured Spectral Intensities of Asymmetrical Plasmas", _J. Quant. Spectrosc. Radiat. Transfer_, Vol. 8, pp. 1419-1430, 1968.

17. Ragent, B. and Brown, R. M., editors, Holographic Instrumentation Applications, Conference held at Ames Research Center, Moffett Field, California, NASA Sp-248, January 13-14, 1970.

18. Roe, P. L., _Exploratory Flow Measurements in the Wing-Body Junction of a Possible Mach Four Vehicle_, Royal Aircraft Establishment Technical Report No. 65257, November 1965.

19. Polutchko, R. J., _Hypersonic Flow Field About a Blunt Slab Wing at Angle of Attack: Phase I_, Aerospace Research Laboratories 64-213, December 1964.

20. Stewartson, K. and Treadgold, D. A., "Wing-Body Interference at Supersonic Speeds", Transonic Aerodynamics, AGARD Conference Proceedings No. 35, pp. 19-1--19-9, September 1968.

21. Stewartson, K., _On Wing-Body Interference in Supersonic Flow_, Aeronautical Research Council 27-715, 9 February 1966.

22. Stollery, J. K., _Hypersonic Viscous Interaction--An Experimental Investigation of Flow over Flat Plates at Incidence and Around an Expansion Corner_, Aerospace Research Laboratories 70-0125, July 1970.

23. Thomas, J. P., _Investigation of the Pressure Distribution on a Blunt-F: Blunt-Plate Combination at a Mach Number of 11.26_, Aerospace Research Laboratories 66-0142, July 1966.

24. Thomas, J. P., _Flow Investigation About a Fin-Plate Model at a Mach Number of 11.26_, Aerospace Research Laboratories 67-0188, September 1!

25. Weirich, R. L. and Vahl, W. A., _Flow-Field Properties Near an Arrow-Wing-Body Model at Mach Numbers of 1.60, 2.36, and 2.96_, NASA Technical Note D-4809, October 1968.

26. Winkelmann, A. E., "Flow Visualization Studies of a Fin Protuberance Partially Immersed in a Turbulent Boundary Layer at Mach 5", United Sta Naval Ordinance Laboratory NOLTR-70-93, 20 May 1970.

27. Winkelmann, A. E., "Aerodynamic Interaction Phenomena Produced by a Fin Protuberance Partially Immersed in a Turbulent Boundary Layer at Mach AGARD Conference Proceedings No. 71, September 1970.

INITIAL DISTRIBUTION LIST

		No. Copies
1.	Defense Documentation Center Cameron Station Alexandria, Virginia 22314	2
2.	Library, Code 0212 Naval Postgraduate School Monterey, California 93940	2
3.	Chairman, Department of Aeronautics Naval Postgraduate School Monterey, California 93940	1
4.	Professor D. J. Collins, Code 57Co Department of Aeronautics Naval Postgraduate School Monterey, California 93940	1
5.	LT Robert W. Heyer, USN 10811 Spring Lane Lemoore, California 93245	1

DOCUMENT CONTROL DATA · R & D

(Security classification of title, body of abstract and indexing annotation must be entered when the overall report is classified)

1. ORIGINATING ACTIVITY *(Corporate author)*	2a. REPORT SECURITY CLASSIFICATION
Naval Postgraduate School Monterey, California 93940	Unclassified
	2b. GROUP

3. REPORT TITLE

Holographic Interferometry of The Flow Field Between a Fin And Flat Plate

4. DESCRIPTIVE NOTES *(Type of report and, inclusive dates)*

Master's Thesis; (March 1972)

5. AUTHOR(S) *(First name, middle initial, last name)*

Robert Ward Heyer

6. REPORT DATE	7a. TOTAL NO. OF PAGES	7b. NO. OF REFS
March 1972	178	27

8a. CONTRACT OR GRANT NO.	9a. ORIGINATOR'S REPORT NUMBER(S)
b. PROJECT NO.	
c.	9b. OTHER REPORT NO(S) *(Any other numbers that may be assigned this report)*
d.	

10. DISTRIBUTION STATEMENT

Approved for public release; distribution unlimited.

11. SUPPLEMENTARY NOTES	12. SPONSORING MILITARY ACTIVITY
	Naval Postgraduate School Monterey, California 93940

13. ABSTRACT

This study was an attempt to map the density field in a fin-flat plate junction three-dimensionally using holographic interferometry. This investigation has extended the density studies by Matulka [12, 13] and Jagota [3, 4] to include, for the first time, interferometric fringe information obtained through a transparent model in supersonic flow. The fringe information was then inverted by a FORTRAN computer program to produce a plot of the density field around the model. The feasibility of the method was demonstrated.

The factors which are thought to have limited the success of the experiment include vibration of the model, fluctuations of the tunnel flow and the fact that the model was somewhat too large in relation to the size of the wind tunnel test section. Schlieren photography was used to look through and around the model and to verify that the same flow was established as was reported by Thomas [23, 24] and Winkelmann [26, 27].

The data reduction of holographic interferograms was, for the first time, accomplished using photographic enlargements. This technique is considered to be much easier and more accurate than the one used in the previous investigations. However, the data reduction step, because of the time and labor involved, is considered to be the rate controlling process of the whole analysis.

DD FORM 1473 (PAGE 1)
1 NOV 65

S/N 0101-807-6811

178

UNCLASSIFIED
Security Classification

A-31408

14 KEY WORDS	LINK A		LINK B		LINK C	
	ROLE	WT	ROLE	WT	ROLE	WT
fin-flat plate flow field						
wing-root flow field						
holography						
three-dimensional density field						
three-dimensional flow field						
fin						
flat plate						
interferogram						
flow field						
fin flat plate junction						
wing root junction						
holographic interferometry						
supersonic flow						

DD FORM 1473 (BACK)
1 NOV 65
S/N 0101-807-6921

179

UNCLASSIFIED
Security Classification

A-31409